Genome-wide identification of virulence-associated genes in *Staphylococcus aureus* using Transposon insertion-site deep sequencing

Genomweite Identifizierung Virulenz-assoziierter Gene in *Staphylococcus aureus* mittels Transposon-Sequenzierung

Dissertation

for

Doctoral degree at the Graduate School of Life Sciences

Julius-Maximilians-Universität Würzburg

Section: Infection and Immunity

Author:

Sudip Das

from Kolkata, India

Würzburg, 2016

Submitted on:

Members of *Promotionskomitee*:

Chairperson: Prof. Dr. Thomas Dandekar, Chair of Bioinformatics, Biocenter, Julius-Maximilians-Universität Würzburg, Germany.

Primary Supervisor: Prof. Dr. Thomas Rudel, Chair of Microbiology, Biocenter, Julius-Maximilians-Universität Würzburg, Germany.

Supervisor(Second): Prof. Dr. Dr. Bhanu Sinha, Department of Medical Microbiology, University Medical Center Groningen, Netherlands.

Supervisor(Third): PD Dr. Knut Ohlsen, Institute for Molecular Infection Biology, Julius-Maximilians-Universität Würzburg, Germany.

Date of Public Defence:

Date of Receipt of Certificates:

Abstract

Staphylococcus aureus asymptomatically colonises one third of the healthy human population, finding its niche in the nose and on skin. Apart from being a commensal, it is also an important opportunistic human pathogen capable of destructing tissue, invading host cells and killing them from within. This eventually contributes to severe hospital- and community-acquired infections. Methicillin-resistant *Staphylococcus aureus* (MRSA), resistant to commonly used antibiotics are protected when residing within the host cell.

This doctoral thesis is focused on the investigation of staphylococcal factors governing intracellular virulence and subsequent host cell death. To initiate an unbiased approach to conduct this study, complex *S. aureus* mutant pools were generated using transposon insertional mutagenesis. Genome-wide infection screens were performed using these *S. aureus* transposon mutant pools *in vitro* and *in vivo*, followed by analysis using Transposon insertion site deep sequencing (Tn-seq) technology.

Amongst several other factors, this study identified a novel regulatory system in *S. aureus* that controls pathogen-induced host cytotoxicity and intra-host survival. The primary components of this system are an AraC-family transcription regulator called Repressor of surface proteins (Rsp) and a virulence associated non-coding RNA, SSR42. Mutants within *rsp* exhibit enhanced intra-host survival in human epithelial cells and delayed host cytotoxicity. Global gene-expression profiling by RNA-seq demonstrated that Rsp controls the expression of SSR42, several cytotoxins and other bacterial factors directed against the host immune system. Rsp enhances *S. aureus* toxin response when triggered by hydrogen peroxide, an antimicrobial substance employed by neutrophils to destroy pathogens. Absence of *rsp* reduces *S. aureus*-induced neutrophil damage and early lethality during mouse pneumonia, but still permits blood stream infection. Intriguingly, *S. aureus* lacking *rsp* exhibited enhanced survival in human macrophages, which hints towards a Trojan horse-like phenomenon and could facilitate dissemination within the host.

Hence, Rsp emerged as a global regulator of bacterial virulence, which has an impact on disease progression with prolonged intra-cellular survival, delayed-lethality but allows disseminated manifestation of disease. Moreover, this study exemplifies the use of genome-wide approaches as useful resources for identifying bacterial factors and deduction of its pathogenesis.

Zusammenfassung

Staphylococcus aureus ist ein fakultativ pathogener Kommensale des Menschen und besiedelt bei etwa einem Drittel der Bevölkerung überwiegend den Nasen-Rachenraum sowie die Haut ohne klinische Symptome auszulösen. Darüber hinaus zählen diese Bakterien zu den wichtigsten Vertretern der Krankenhauskeime, die schwerwiegende Infektionen besonders im Bereich der Intensivstationen in Krankenhäusern hervorrufen können. Methicillin-resistente *Staphylococcus aureus* (MRSA) sind dabei resistent gegen übliche Antibiotika und daher schlecht therapierbar. Neuere Forschungsarbeiten zeigten, dass *S. aureus* von Zellen des Wirts aufgenommen wird und diese von innen heraus abzutöten vermag. Über die zugrunde liegenden molekularen Mechanismen dieser Zelltoxizität ist jedoch nicht viel bekannt.

In der vorliegenden Arbeit sollten daher Faktoren von *S. aureus* identifiziert und charakterisiert werden, die die intrazelluläre Virulenz des Bakteriums und das darauf folgende Absterben der Wirtszelle beeinflussen. Dafür wurden mittels Transposon-Insertionsmutagenese *S. aureus* Mutanten-Bibliotheken erstellt, welche für genomweite Infektionsscreens *in vitro* und *in vivo* genutzt wurden. Die Auswertung dieser Analysen erfolgte dabei durch Hochdurchsatz-Sequenzierung der Transposon-Insertionsstellen (Tn-seq). In diesen Studien wurde neben zahlreichen bakteriellen Faktoren ein neuartiges Virulenzregulator - System identifiziert. Dieses System besteht aus dem Transkriptionsregulator der AraC-Familie Repressor of surface proteins (Rsp) und einer nicht-kodierenden RNA, SSR42. *rsp*-Mutanten zeigten eine erhöhte intrazelluläre Überlebensrate in menschlichen Epithelzellen sowie eine verzögerte Cytotoxizität im Wirt. Durch RNA-Sequenzierung (RNA-seq) wurde der Einfluss von Rsp auf die globale Genexpression ermittelt. Dabei zeigte sich, dass Rsp die Expression von SSR42, sowie Cytotoxinen und anderen immunmodulatorischen Faktoren von *S. aureus* kontrolliert. Wasserstoffperoxid, ein Molekül, welches durch Neutrophile zur Bekämpfung von Pathogenen gebildet wird, führt dabei Rsp-abhängig zu einer Erhöhung der bakteriellen Toxinproduktion. Die Abwesenheit von Rsp in bakteriellen Mutanten resultiert in einer Reduktion *S. aureus*-induzierter Zerstörung von Neutrophilen sowie zum Überleben von Versuchstieren im Lungeninfektionsmodell. Eine systemische Infektion ist dabei jedoch weiterhin möglich. Interessanterweise führt ein Fehlen des *rsp* zu einer erhöhten Überlebensrate von Makrophagen, welches auf eine Verbreitung der Bakterien im Organismus in diesem Zelltyp hindeuten könnte.

Rsp ist demnach ein neuartiger globaler Regulator bakterieller Virulenz, der zwar die infektionsbedingte Letalität verzögert, jedoch damit eine Disseminierung der Infektion mit *S. aureus* begünstigt.

Contents

List of Figures

List of Tables

Dedicated to my father…

Dr. Debkrishna Das (1957-2013)

"Work hard without bothering about the outcome" - Your words.

Chapter 1

Introduction

1.1 *Staphylococcus aureus* is an important human pathogen

1.1.1 Taxonomy and Discovery

Staphylococcus aureus subsp. *aureus* is a Gram-positive bacterium. The name *Staphylococcus* is derived from the Greek words- 'staphyle', meaning bunch of grapes and 'kokkos', meaning berry. Staphylococci are round cocci-shaped bacteria with characteristic clusters giving it a grape bunch-like appearance (See Figures 1.1A and 1.1B), due to a distinct pattern of binary fission. A detailed classification according to taxonomy is mentioned in Table 1.1.

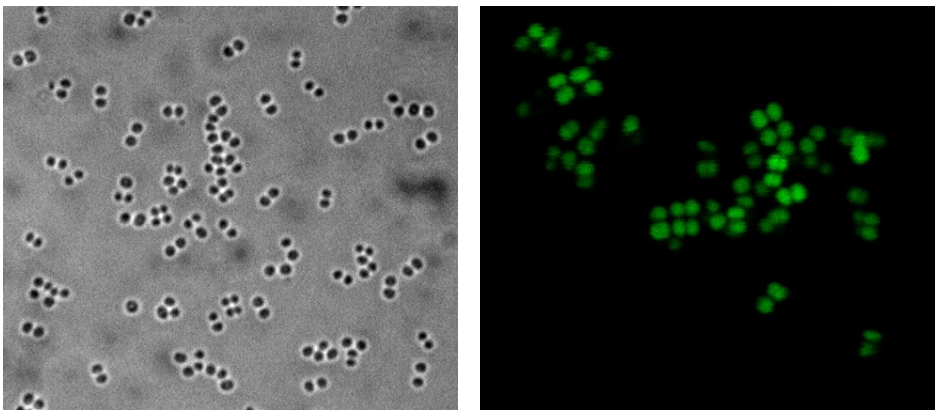

(A) **(B)**

Figure 1.1: (**A**) *S. aureus* exhibit typical cocci shape, as illustrated by Phase-contrast bright field microscopy; Magnification = 100x. (**B**) The arrangement of cells is clustered due to a distinct pattern of binary fission, which is visualized by bacteria expressing Green fluorescent protein (GFP) under fluorescence microscope; Magnification = 63x.

S. aureus was first identified as a pathogen by Scottish surgeon Sir Alexander Ogston, while working at the Aberdeen Royal Infirmary, United Kingdom. He discovered it during microscopic examination of pus from surgical abscesses of a patient's knee joint [1] and tested it by injecting the pus in mice to observe

the occurrence of new abscesses. In 1882, Sir Ogston coined the term staphylococci and also elaborately described different manifestations staphylococcal diseases and its role in sepsis formation[2].

Table 1.1: Taxonomic lineage of *Staphylococcus aureus* subsp. *aureus*

Domain	*Bacteria*
Phylum	*Firmicutes*
Class	*Bacilli*
Order	*Bacillales*
Family	*Staphylococcaceae*
Genus	*Staphylococcus*
Species	*aureus*
Subspecies	*aureus*

In 1884, German physician Friedrich Julius Rosenbach isolated two species of staphylococci and named them according to the pigmentation of colonies. One of them was named *Staphylococcus aureus*, 'aureus' from the Latin word 'aurum', meaning gold, which was due to its orange-yellow colour[3]. Hence, the subspecies name was given after Rosenbach.

1.1.2 Colonisation and Epidemiology

S. aureus is a human commensal primarily residing in human anterior nares and colonising 25-30% of the healthy population. It can also be found on extra-nasal sites such as skin, throat, vagina and gastro-intestinal tract[4,5]. Humans are natural asymptomatic reservoirs but individuals colonised with *S. aureus* are always at a higher risk of ensuing infections[1,6,7]. Since in all reported cases, over 90% of the invasive infections were caused by the same strain residing in nares and/or on skin[8,9]. Apart from healthy individuals, elevated colonisation of *S. aureus* is common amongst patients undergoing surgery[6], haemodialysis[8], with diabetes[10] or in-dwelling devices[11], intravenous drug abusers[12] and in HIV-positive individuals[13].

S. aureus carriage is a dynamic process and can differ variedly between individuals. Longitudinal studies suggest three major categories of colonisation: non-carriers, intermittent and persistent[9,14]. Persistent carriage has been observed in 20% of the cases, where *S. aureus* is usually detected throughout lifetime based on consecutive sampling. These individuals exhibit higher anti-staphylococcal antibodies with considerable increase in bacterial load. Intermittent carriers are usually found in 60% of the cases, where bacteria could be detected but with long or short offsets in time period that can be anywhere between 70 days to 8 years. Along with the non-carriers, which makes upto 20% of the observations, intermittent carriers show lower antibody production[15]. Transmission of *S. aureus* can occur by direct skin contact, neonates while birth or from contaminated fomites. However, contact does not guarantee colonisation due to differences in host, which are yet to be fully understood. The most alarming problem is the emergence of antibiotic-resistant *S. aureus* strains amongst human reservoirs. Apart from colonising humans, *S. aureus* can also colonise other animals such as pigs, dogs, horses and cattle[16–18] and can consequently result in zoonoses[19].

An important step in colonisation is attachment to host surfaces. To achieve this *S. aureus* uses adhesins, extra-cellular martix binding proteins and surface structures[20–22], which have been associated with facilitating adhesion to nasal and skin cells. Apart from colonisation, *S. aureus* can also be a versatile opportunistic pathogen, which upon breach in natural barriers like skin or mucosal surfaces can access the underlying tissue or bloodstream leading to severe infections.

A large majority of staphylococcal infections and outbreaks are caused by drug resistant strains, standing over 50%[23] of all reported cases in the last decade. MRSA has spread to pandemic proportions globally (ECDC 2012), colonising healthy individuals and at a higher rate amongst nosocomial residents (approx. 60- 70%)[11]. Hospital acquired (HA)-MRSA has been prevalent in nosocomial infections due to inclining risk factors but Community-acquired (CA)-MRSA is impeding more with the capability to infect healthy individuals[24]. In recent years, outbreaks of CA-MRSA has risen over 40% in disease cases[25] and children are being more affected with 81.5% of all MRSA isolates. Therefore, the focus of *S. aureus* epidemiology and demography has shifted towards the community[26] with the identification of similar lineages to that of nosocomial settings.

In recent times, genome-based definitions are being encouraged more and location-based segregation is becoming less relevant[27]. Genotyping of *S. aureus* isolates is performed primarily with three methodologies, namely Single-locus sequence typing (SLST), Multi-locus sequence typing (MLST) and Pulse Field Gel electrophoresis (PFGE).

SLST allows classification of *S. aureus* isolates by evaluating polymorphisms in a single gene. The most widely used determinant is the gene encoding staphylococcal protein A; *spa* and hence commonly termed as *spa*-typing. This method recognizes differences in a 24-nucleotide variable region called 'X' in otherwise highly conserved *spa* and[28,29], and segregate isolates accordingly. Another locus used for typing is the staphylococcal cassette chromosome *mec* (SCC*mec*)[30], a mobile genetic determinant of MRSA, carrying the *mec*A[31]. SCC*mec* typing classifies isolates according to genetic variations in *mec* and *ccr*, and till date 11 types identified[32,33].

MLST method takes multiple events of polymorphisms into account by analyzing sequences of several genes at a single time[34]. This is particularly useful for classifying large collection of isolates in global epidemiological studies[35]. In this procedure, gene fragments from constitutive loci with variable sequences are analyzed, which are called distinct alleles. *S. aureus* isolates can be segregated according to the allelic variation into Sequence types (ST). The ones with same allelic profile are considered to clones and classified under the same Clonal Complex (CC).

In contrast to MLST, Pulse field gel electrophoresis (PFGE) based genotyping is more useful for local epidemiological studies[33]. This method relies on the differential DNA restriction patterns produced by *S. aureus* isolates. A common or outbreak pattern is identified by analysing DNA fragments produced by isolates with agarose gel electrophoresis and subsequently matched to assess similarities. Isolates showing distinct patterns with less than 50% of fragments in common are considered to be unrelated and patterns with differences in only 2-3 fragments are considered to be subtypes[36].

Consequently, a number outbreak PFGE types were identified and are now being used to classify isolates. One such example is the MRSA USA300 in North America, which had a distinct PFGE pattern named as the USA type. It emerged within CC8, when ST-8 Methicillin-sensitive *Staphylococcus aureus* (MSSA) underwent a series of horizontal gene transfers to acquire SCC*mec* type IV, arginine catabolic mobile element (ACME) and *pvl*.

Beginning of the second millennium saw increasing prevalence of CA-MRSA in the United States of America (USA), with up to 64% within the community. Most demographically abundant CA-MRSA genotypes worldwide are ST-8, ST-80, ST-59, ST-1 and ST-772. In the USA, the most common genotype is ST-8, especially USA300, which has meanwhile spread globally with up to 20 descendant lineages[5]. By contrast, population structure of MRSA in Europe was dissimilar with the most prominent genotype being ST-80, commonly known as the European clone[5] and had comparably low frequencies of 39% within the community. Although in recent years, occurences of CA-MRSA has escalated to 59% and interestingly ST-8 (USA300) accounted for 40%, pushing back ST-80 to 28% of all reported cases[37]. ST-59, known as the Taiwan clone, is most common in Taiwan, China and other Asian countries[27], but was also reported in 15% of the demographic isolates in Europe[37]. ST-1, within which USA400 belongs, is much more virulent than USA300 but occurs more rarely. It is mostly found within native Americans, in Alaska and tribal Australia[27]. ST-772, also known as the Bengal Bay clone, is a variant of ST-1 that has recently emerged in Bangladesh and Indian subcontinent. It has also been reported from United Kingdom and Europe[27].

1.1.3 Staphylococcal infections and diseases

Both HA-MRSA and CA-MRSA can cause a broad array of infections leading to severe diseases or exacerbation of pre-existing clinical conditions (See Figure 1.2). These manifestations include severe skin and soft-tissue infections (SSTIs)[38], surgical-site infections (SSIs)[39], Atopic dermatitis[40], Osteomyelitis[41], Septic arthritis[42], lower respiratory tract infections[1] leading to life-threatening conditions such as endocarditis[43], bacteraemia[1] and Toxic-shock syndrome (TSS)[44].

SSTIs are presented by recurrent necrotising skin lesions associated with abscesses and cellutis[38]. More complicated SSTIs could lead to systemic inflammation, fever, possibility of bacteraemia and could require complex intra-venous multi-drug therapy[38,45]. The occurrence of *pvl* was found to be prevalent in SSTIs and were primarily caused by CA-MRSA[38,46].

Another exuberant skin condition effecting mostly children is Atopic dermatitis, which is a chronic and recurring inflammatory disease characterised by perivascular leukocyte infiltration and skin barrier dysfuntion[40]. Strikingly, almost 90% of individuals with this condition harbour *S. aureus*, which can gain access to skin lesions and thereby aggravating it[47].

Other conditions such as surgical site infections (SSIs) and blood stream infections (BSIs), also known as Bacteraemia are amongst the leading causes of *S. aureus*-related morbidities. Upto 20% of all hospital-acquired cases reported were *S. aureus* infections, with over 50% of them caused by MRSA. Frequent pre-

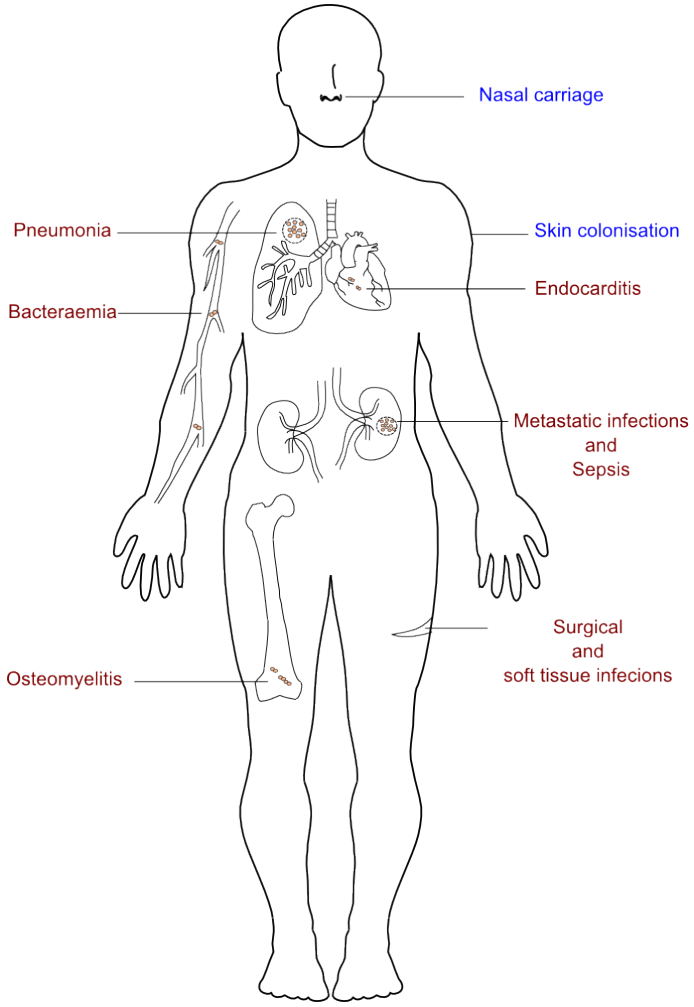

Figure 1.2: *S. aureus* is a commensal of human skin and nares (blue). But it is also an opportunistic pathogen that can cause an array of hospital-acquired and community-associated infections at different sites of the human body (red).

disposing conditions include intra-vascular devices and orthopaedic implants[39,48]. While both SSTIs and SSIs can lead to deep non-removable foci with massive tissue damage and spreading to the vascular system, BSIs can even lead to life threatening endocarditis and osteomyelitis[43].

Osteomyelitis is a common invasive bone infection caused by *S. aureus* , leading to severe inflammation in the marrow and destruction of the bone[41]. In bacterial septic arthritis the joints develop haematogenous seeding in the synovial membrane with bacterial growth. Conditions that expose to infection risks can be diabetes, open fracture or prosthetic implants[49,50], post joint-trauma infection without any skin breach or due to BSIs[42].

S. aureus-mediated lower respiratory tract infection and acute pneumonia are common in nosocomial settings[1], including cases of cystic fibrosis, where it is one of the earliest pathogens detected in children[51]. *S. aureus* pore-forming toxins have been shown to cause lung epithelium injury disrupting alveolar air-blood barrier and release of pro-inflammatory cytokines[51–53].

Last but not the least, *S. aureus* is capable of inducing Toxic Shock Syndrome (TSS), which is mostly

associated with post-BSI and Osteomyelitis. TSS symptoms include fever, drop in blood pressure and multi-organ failure[54]. Staphylococcal superantigens are primarily responsible for TSS, which include enterotoxins[44,55,56] and TSS toxin 1 (TSST-1)[54] causing large scale inflammatory response in the human body[56].

1.2 Staphylococcal virulence factors and their role in pathogenesis

The plethora of clinical manifestations caused by *S. aureus* is attributed to several virulence factors, which can broadly classified into two types: surface-associated factor and secreted proteins. *S. aureus* cell wall forms a major exoskeletal organelle for the interaction with external environment and host inflammatory responses in an infection condition. The cell wall function is augmented with a wide variety of surface-associated proteins and structures. Apart from the immobilized ones, a large proportion of virulence factors are secreted including adhesive macromolecules, toxins and immune evasion factors that together provide the resource for confounding the host.

1.2.1 Surface structures & Adhesive molecules

The cellular envelope of *S. aureus* is furbished with various proteinaceous and non-proteinaceous surface macromolecules and adhesins. These structures aid in bacterial attachment to host surfaces, immune evasion and acquisition of factors needed for establishing proper infection. Non-proteinaceous surface macromolecules in *S. aureus* include the cell wall itself and surface-associated glycopolymers such as Teichoic acids.

Surface proteins can be either covalently anchored to the peptidoglycan layer, hence named as cell wall-anchored (CWA) proteins, or non-covalently associated by means of ionic or hydrophobic interactions[57], which can be released into the vicinity complying to functions in adhesion and virulence . All staphylococcal CWA proteins are translocated to the membrane by SecYEG pathway[58] and contain a hydrophobic domain followed by a series of positively charged amino acids, which facilitate anchoring to membrane. These proteins also possess a sorting signal made up of the LPXTG (Leu-Pro-Any amino acid-Thr-Gly) amino acid motif[59]. The enzyme Sortase A recognizes this motif and proteolytically cleaves, and subsequently tethers the proteins to cell wall[60].

1.2.1.1 Staphylococcal cell wall

S. aureus cellular envelope comprises of a single lipid bilayer membrane surrounded by a peptidoglycan-rich, dense and rigid cell wall[61], which is characteristic of Gram-positive bacteria. Peptidoglycan is a cross-linked polymer made up of repeated units of the disaccharide: *N*-acetylmuramic acid (MurNAc) β(1-4) *N*-acetylglucosamine (GlcNAc)[62] (See Figure 1.3). The distinctive feature of *S. aureus* cell wall is the covalent linkage of peptidoglycan strands by a pentaglycine cross-bridge (MurNAc-D-Ala-$[Gly]_5$-L-Lys-MurNAc)[63]. In addition to this, the cell wall also contains covalently anchored teichoic acid poly-

mers.

Staphylococcal cell wall components are potent virulence factors. Peptidoglycan, in synergy with other components, can induce septic shock and inflammatory responses via Toll-like receptor (TLR) 2 in the host[64,65]. Apart from protecting the bacterial cell from mechanical and osmotic pressure, *S. aureus* cell wall also defends against antibiotics by accelerated peptidoglycan synthesis resulting in wall thickening[66,67].

1.2.1.2 Surface Teichoic Acids

Teichoic acids (TAs) are negatively charged polymers containing polyol repeating units linked by phosphodiester bonds, found on the cell surface of several Gram-positive bacteria[68], which has been linked to pro-inflammatory immune response and staphylococcal disease in host[64]. There are two types of TAs on bacterial surfaces: Lipoteichoic acids (LTAs), which are anchored to membrane lipid bilayer extending into the peptidoglycan layer and Wall teichoic acids (WTAs), which are covalently linked to the cell wall and externally exposed[69] (See Figure 1.3).

LTAs are usually made up of simple chains of polyglycerol 3-phosphate (PGP) attached to the plasma membrane by a glycolipid anchor[70]. The LTA anchor is made up of the glycolipid: glucosyl (β1-6), glucosyl (β1-3) Diacylglycerol (Glc2-DAG), which is synthesized by the staphylococcal glycosyltransferase YpfP or UgtP. This process primarily takes place in the cytoplasm and then the precursors are transported to the outer leaflet by permease LtaA[71] and extra-cellularly polymerized by the enzyme LtaS[72].

Mutants deficient in different components of LTA biosynthesis machinery show specific phenotypes. The lack of YpfP and LtaS reduces biofilm formation and ability to the blood brain barrier in the host[73,74], and leads to deformed bacterial morphology[72] respectively. Whereas, the lack of LtaA did not interrupt LTA biosynthesis and its role in infection is still elusive[72,75].

In *S. aureus* , wall teichoic acids (WTAs) are also made up of two main units: the cell wall linkage unit and the main polymer chain. The construction of WTAs is a highly conserved mechanism undertaken by consorted actions of different Teichoic acid of ribitol/glycerol (Tar/Tag) enzymes, both group being functionally similar. The linkage unit is initiated by transfer of *N*-acetylglucosamine (GlcNAc) onto the membrane lipid moeity Undecaprenyl phosphate, by the enzyme TarO. Lack of this enzyme completely abolishes WTA production, which results in decreased bacterial colonisation and occurence of endocarditis in the host[20]. Consequently, GlcNAc forms glycosyl linkage with ManNAc, in a reaction catalysed by the enzyme TarA, to produce the disaccharide: *N*-acetylmannosamine β(1-4) *N*-acetylglucosamine 1-phosphate[68]. TagB, a glycerolphosphotransferase primes chain polymerization by adding the first Glycerol 3-phosphate (GroP) monomer to the ManNAc. The main polymer is initiated with GroP monomers and extended using Ribitol 5-phosphate (RboP) by the enzyme TarL[68]. The completed molecule is transfered out of the cell membrane by TarGH transporter system, where it is coupled with MurNAc by phosphodiester linkage catalysed by TagTUV. In both LTAs and WTAs, the polyol backbone also consists of D-alanine modifications catalysed by the enzymes encoded from the *dlt* operon.

This modification is vital for resistance against host antimicrobial peptides, phagocytic killing and establishing infection in a murine model of septic arthritis[76].

1.2.1.3 Microbial surface component recognizing adhesive matrix molecules (MSCRAMMs)

The most abundant class of CWA proteins on *S. aureus* surface belongs to the family of microbial surface component recognizing adhesive matrix molecules (MSCRAMMs). These molecules are crucial for interaction with the extra-cellular matrix (ECM) of the host, which is a pioneering step in colonisation[77]. MSCRAMMs contain Immunoglobulin G (IgG)-like folded domains, which bind ligands by a 'dock, lock and latch' mechanism[78]. There are several MSCRAMMs, such as Protein A (SpA), Fibronectin-binding proteins (FnBPs), Collagen adhesin (Cna), Clumping factors (Clf) and Serine-Aspartate repeat (Sdr) proteins that has extensively studied and shown to play major roles in *S. aureus* virulence (See Figure 1.3).

SpA is a versatile and abundant MSCRAMM on the bacterial surface that binds host immunoglobulins and its widely used in *S. aureus* epidemiology (See section 1.1.2). Crystallographic studies have shown that this 56 kDa protein has an unique arrangement of five homologous triple-helical structures that enables it to bind several ligands[79]. Protein A is considered as a 'superantigen' that binds the Fc part of human IgG[80] and also the Fab domains of human Immunoglobulin M (IgM)[81]. This enables bacteria to escape opsonisation and block B-cell receptors, hence evading the host immune system. In addition, SpA influences a multitude of other host-pathogen interactions such as skin lesions and invasive disease[82], inflammation of airway epithelia by stimulating TNF receptor 1[83], bacterial manipulation of host cell trafficking by activating RhoA-GTPases and facilitaing invasion[84].

FnBPs have central role during staphylococcal invasion of host cells and bind the glycoproteins Fibronectin, which are abundantly found in the host ECM. This interaction allows bridging with host $\alpha_5\beta_1$ Integrins and thereby, promoting invasion[85]. FnBPA and FnBPB, are two major FnBPs of approx. 112 kDa and contain multiple fibronectin-bindings repeats (FnBRs) each made up of 40 amino acid residues. These FnBRs bind the N-terminal domain of Fibronectin, forming a tandem β-zipper[86]. The amount of FnBPs expressed on the surface of staphylococci dictates the degree of invasiveness in non-professional phagocytes, as evidenced by adequate expression on *S. aureus* clinical isolates[85]. FnBPs have also been shown to elicit platelet aggregation[87] and invoke pro-inflammatory response in the host.

Cna binds host collagen and has been associated with septic arthritis[88]. It is a 133 kDa protein, that has three N-terminal IgG-like folded sub-domains connected by linkers and stabilized by hydrophobic interactions. Unlike the 'dock, lock and latch' mechanism, it forms a conformation that binds the ligand by embracing it and hence is known as a 'Collagen Hug'[89]. Although, Cna has been concurrently detected in invasive *S. aureus* isolates from orthopaedic implants, surgical reconstruction-associated infections and osteomyelitis, it has been contradicted for being a major virulence determinant of *S. aureus* bone infections[90]. Nevertheless, there is sufficient evidence in specific animal models of experimental osteomyelitis[91], keratitis[92] and endocarditis[93], to suggest its role in *S. aureus*-related bone infections.

Clumping factors (Clf) and Serine-Aspartate repeat (Sdr) proteins are prototypical MSCRAMMs that have structural similarities to each other and are abundantly decorated on the bacterial surface [78]. Both proteins have three classical N-terminal IgG-folded ligand binding sub-domains and Serine-Aspartate (SD) repeats, with Sdr proteins having additional B-repeats linkers in between. Two major clumping factors in *S. aureus* are ClfA and ClfB, with cognate domain organization can bind different ligands to mediate *S. aureus* adhesion and immune-evasion [78]. ClfA facilitates *S. aureus* binding to the γ-chain of fibrinogen (Fg) and human platelets [78]. Prevention of ClfA-Fg binding by peptide antagonists can potentially ameliorate staphylococcal infection severity [94]. On the other hand, ClfB primarily binds human type 1 cytokeratin 10, but also binds human αC fibrinogen. It promotes adherence to human nasal epithelium by binding the most abundant cornified envelope protein, Loricrin and thereby promoting bacterial colonisation of the human nares [95–98]. Sdr family of proteins consists of SdrC, D and E are present on *S. aureus* surface in differential combinations between clinically isolated MRSA and MSSA [99]. Sdr proteins have been associated with invasive osteomyelitis due to its affinity towards bone sialoproteins [100,101].

1.2.1.4 Secretable expanded repertoire adhesive molecules (SERAMs)

In addition to MSCRAMMs, *S. aureus* possesses a collection of proteins that are associated with the cell envelope by hydrophobic or ionic interactions. These proteins can dissociate and recruited to target broad range of host proteins belonging to immune system and ECM. Amongst the most widely studied secretable adhesive molecules are host fibrinogen binding proteins such as Staphylocoagulase (SC), von Willebrand-factor binding protein (vWbp) and Extracellular fibrinogen binding protein (Efb).

SC is a 75 kDa conserved protein encoded by *coa* gene, which activates human prothrombin and promote blood coagulation [102,103]. It is detected as part of routine microbial diagnosis to identify *S. aureus* species [104] in clinical settings. SC has an archetypal structure common with most SERAMs, containing two topologically similar N-terminal D1 and D2 domains made up of α-helical bundles [102]. Co-crystallization studies have demonstrated the binding of D1/D2 domains to human α-thrombin and its precursor [102]. Although, SC has been shown to facilitate fibrinogen cleavage and contribute to cardiac valve abscesses, its precise role during infection in experimental animal models is still dubious.

Similar to SC, vWbp also exhibits N-terminal domain-mediated interaction with human prothrombin resulting in coagulase activity [103]. On the contrary, Extracellular fibrinogen binding protein (Efb) of *S. aureus* binds Aα chain of fibrinogen and impairs would healing process by preventing the aggregation of platelets [103].

Unlike *S. aureus* SpA, a second binding protein of immunoglobulin (Sbi) shows dual association with the bacterial surface. It is non-covalently associated on the cell surface due to the lack of LPXTG motif but also exist bound to LTAs on the bacterial surface. Sbi contains four triple helical bundles D1-D4, with two having sequence similar to SpA. It also displays affinity towards the Fc region of IgG preventing opsonophagocytosis of bacteria by human leukocytes [105]. Sbi also has a complement C3 binding do-

main that interacts with both C3b/d and Factor H to form a ternary complex leading to inhibition of the complement system and interference with host immune recognition [106].

1.2.1.5 Haeme-acquisition proteins

Iron-regulated surface determinants (Isd) of *S. aureus* are part of protein system encoded by 5 operons, *isd*A, *isd*B, *isd*CDEF*srt*B*isd*G, *isd*H, *isd*I [107]. Almost every Isd protein can bind haeme and are associated with the bacterial surface via different interactions, and fulfill various roles in haemoglobin capture, iron uptake and intra-host survival [78,108]. IsdA, B, H are CWA proteins anchored via Sortase A action, on the contrary IsdC is processed by Sortase B and embedded within the cell wall without direct attachment with peptidoglycan [108]. These proteins have been specifically shown to bind haeme via one or two N-terminal Near iron transporter (NEAT) motifs - D1/D2 or D1&D2. Furthermore, IsdDEF forms an ABC transporter for haeme across the bacterial membrane [107,109,110]. IsdA is vital for *S. aureus* survival on human skin providing resistance to skin fatty acids [111] and IsdB helps scavenging iron by acting as a haemoglobin receptor [107]. Both proteins also provide *S. aureus* protection from antimicrobial superoxide and neutrophil-mediated killing [112].

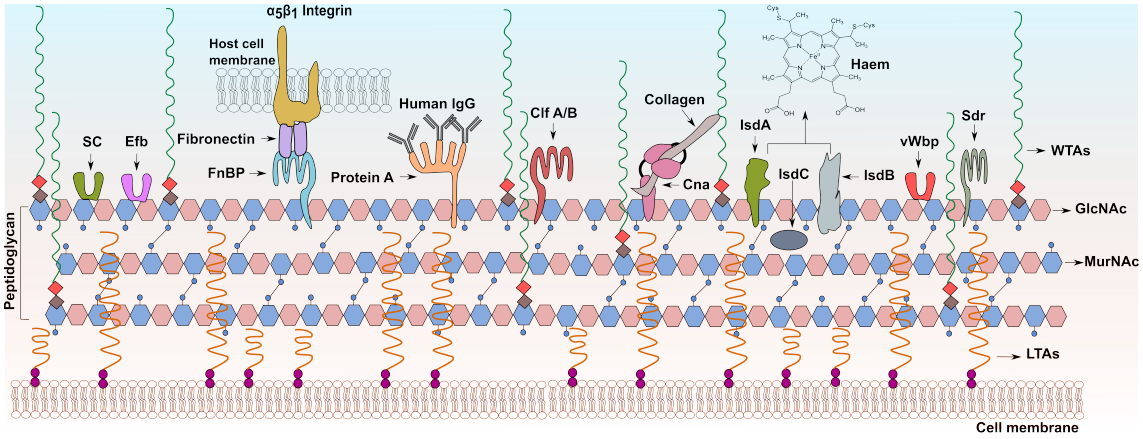

Figure 1.3: A graphical representation of *S. aureus* cell wall decorated with an array of proteins and glycopolymers *S. aureus* cell surface harbors several important structures that serve different purposes in making it a successful coloniser and a dangerous human pathogen. The building block of the peptidoglycan chains is MurNAc -β(1-4)-GlcNAc, with the occasional linkage to the adjacent chains by a pentaglycine bridge (Blue ball and stick). WTAs and LTAs are covalently linked to MurNAc and the cell membrane respectively. The cell wall is decorated several different proteins, which are either covalently anchored or non-covalently associated or embedded. For details on individual components refer to Section 1.2.1.

1.2.2 Secreted cytolytic toxins and peptides

Along with cell surface molecules, a broad variety of exotoxins and small peptides secreted by *S. aureus*, together provide the resource for eliciting cytotoxicity in the host and evade the immune system. These secretions include pore-forming toxins and small membrane active cytolytic peptides.

1.2.2.1 Pore-forming toxins

S. aureus secretes several potent pore-forming toxins (PFTs) that attack different host cell types, by forming membrane pores and compromising cellular integrity. One of the most widely studied PFTs is α-toxin also called α-haemolysin. It has been associated with *S. aureus*-induced exfoliating skin disease [113] and pneumonia [114]. It also causes rupture of erythrocytes [115] (haemolysis), which is presented either by characteristic clear zones around the colonies on blood agar or by visible release of haeme. α-toxin is secreted as 33 kDa single chain monomers encoded by *hla*, which attacks the membrane of almost all cell types in two stages. At first the hydrophilic monomers come in contact with the host membrane by lateral diffusion and stoichiometric oligomerization to form a homo-heptameric pre-pore. This is followed by a major conformational change and insertion its amphiphatic β-barrel domain into the membrane forming a transmembrane pore of approx. 1-2 nm in diameter [116,117], which results in a heavy influx of extra-cellular Calcium ions and necrotic cell death [118]. α-toxin can attack host membranes in both receptor-dependent manner and by non-specific adsorption requiring higher number of molecules [119]. In the former case, the low-toxin and high-affinity binding sites were later found out to be ADAM10 metalloproteases on the eukaryotic cell surface [120]. Although the catalytic site of ADAM10 was not essential, the disintegrin pro-domain is required for toxin-mediated membrane damage [121]. However, this mechanism still requires membrane lipids [120] and the presence of sphingomyelin synthesis machinery [122]. The association of α-toxin and ADAM10 has been shown to promote the cleavage of cellular junction protein E-cadherin in lung epithelial cells and *S. aureus*-induced lethal pneumonia [123]. Recent studies have made the versatility of α-toxin more apparent. In co-infection of lower-respiratory passages, α-haemolysin prevents acidification of macrophage phagosomes and assists in successful dissemination of co-infections [124]. Furthermore, α-toxin also enhances bacterial invasion and survival within Mast cells by augmenting the presentation of β1 integrins [125].

In addition to α-toxin, *S. aureus* secretes bicomponent hetero-oligomeric PFTs that consist of two polypeptides called S (slow) or F (fast) subunits, with approx. 70% sequence similarity. S subunits are primarily responsible for cell targeting and are recruited first followed by the F subunit [126]. This group of pore complexes primarily include Haemolysin-γ (Hlg) and Leukotoxins (Luk). Similar to α-toxin these proteins are produced as water-soluble monomers and self-assemble on the target membrane [127]. From structural studies, the monomers of Luk and Hlg are known to be prolate ellipsoids that comprises an anti-parallel β-sheet sandwich that is largely similar to that of α-toxin, an extended β-sheet pre-stem region that is held in vicinity of β-sandwich with hydrophobic interactions and a rim domain with exposed aromatic residues [128]. A functional pore complex is a hetero-octamer made of different combinations of S and F subunits, from both Hlg and Luk. A combination of LukF+LukS forms leukotoxic pore and LukF+Hlg shows haemolytic activity [128].

Haemolysin-γ corresponds to two combinations: HlgA or C, which are the S subunits and the F subunit HlgB [127]. These are produced by most *S. aureus* strains [129] and exhibit haemolytic activity against rabbit and human erythrocytes [130]. These are also cytolytic towards mammalian leukocytes [130,131] and

is shown to bind the membrane lipid-derivative Monoganglioside (G_{M1})[126]. In addition, γ-haemolysins are important for bacterial survival in human blood[132] and concomitantly with α-haemolysin promote septic arthritis[133]. These toxins are all expressed from the cluster of γ-haemolysin has 60%-80% sequence homology[131].

Leukocidins exist in different variants: LukAB (GH), Panton-Valentine Leukocidin (PVL); LukSF-PVL, LukED and are expressed differentially in *S. aureus* strains and clinical isolates. LukAB also referred to as LukGH, shares 30%-40% homology with other bicomponent toxins and shows no haemolytic activity[134]. On the other hand, LukAB exhibit cytotoxicity towards human leukocytes in particular[126] and contributes substantially to staphylococcal disease[135]. LukAB binds the A-domain of CD11b subunit in Integrin αM/β2 (Mac-1) specifically on the surface of human polymorphonuclear cells to promote toxin-mediated membrane damage both intra- and extra-cellularly[136,137]. Furthermore, it also targets CD11b on human monocytes and induces necrotic cell death by activating the human NLRP3 inflammasome[138]. LukSF-PVL is more potent than LukAB[127] towards against human and rabbit neutrophils[139]. It specifically targets human chemokine receptors C5aR and C5L2 to disrupt neutrophil cell membrane. LukSF-PVL is only found in strains with a pro-phage carrying *luk*S-PV and *luk*F-PV structural genes[53,140]. Similar to LukAB, it induces inflammatory response in human phagocytes[141], elicits dermonecrotic effects in humanized mice[142] and rabbits[143] but unlike α-toxin, its role in staphylococcal lethal pneumonia is highly debated[53,140].

Similar to γ-haemolysins but to a lesser extent, Leukocidin ED can target both erythrocytes[129] and leukocytes[126]. Although feebly leukotoxic, *luk*E and D are present in 87% of the clinical isolates and have been associated with necrotic skin infections[144]. LukED is strikingly homologous to γ-haemolysins and have a rather broad range of species specificity[126]. It mediates killing of human lymphocytes, macrophages and dendritic cells by targeting the chemokine receptor CCR5, but also humans in a CCR5 independent manner[145].

1.2.2.2 Secreted virulence-associated small peptides

In addition to the exotoxins, *S. aureus* also secretes small peptides ranging from 20 to 44 amino acids in length. Most well studied cytolytic peptides belong to the Phenol-soluble modulin (PSM) family, which were first identified in hot phenol extracts of *S. epidermidis* secretions[146]. These are amphiphatic, alpha-helical and membrane-active peptides found in several staphylococcal species[147] and are remarkably cytolytic towards human neutrophils, monocytes and erythrocytes[148].

PSMs are classified into α and β types, which are of varied lengths encoded from three different genetic locations in *S. aureus*[146] and are important for community-acquired staphylococcal disease[148]. α-type PSMs are approx. 20-25 amino acids long and comprises PSMα1-PSMα4 and δ-toxin, while β-type PSMs are approx. 44 amino acid in length and have two variants: PSMβ1 and PSMβ2[148]. PSMs are exported out of the cell by the Phenol-soluble modulin transporter (Pmt), which is encoded by four genes: *pmt*A-D[149]. The Pmt exporter system is made of PmtB and D, which forms a membrane ABC

transporter, and two ATPases PmtA and C. Absence of this system leads to accumulation of PSMs in bacterial cytoplasm and decrease in viability[149]. Apart from its leukotoxic activity, PSMs have been shown to activate neutrophils[150], stimulated TLR2 response[151], cause neonatal entercolitis[152], elicit mast cell degranulation in allergic skin reactions[47] and promote bacterial escape from phagolysosomes into host cytoplasm[153].

1.2.3 Virulence-associated exoproteins and enzymes

S. aureus secretions also contain various other proteins and enzymes that either bind to host receptors, cleave host surface proteins or augment biofilm formation. *S. aureus* neutral sphingomyelinase (SaNSMase) or β-toxin is found in both bovine isolates and human isolates. It has a unique haemolytic activity, where it binds erythrocytes at 37°C but only lyse them at lower temperatures[154], a phenomenon known as 'hot cold' haemolysis that can be observed on sheep blood agar plates. SaNSMase is a 35 kDa protein that forms a four-layer β-sandwich with a long β duplex that interacts with the *N*-acyl chain of sphingomyelin[154]. It has been shown to be cytotoxic towards human monocytes[155], lymphocytes[154] and cross-links with extra-cellular DNA of bacteria to promote biofilm formation[156].

Furthermore, *S. aureus* has acquired strategies to evade disinfection by host innate immune cells. Chemotaxis-inhibitory protein of *S. aureus* (CHIPS) and Staphopain A (ScpA) contribute to this process by inhibiting inter-neutrophil communication and chemotaxis. CHIPS is a 14.1 kDa protein encoded by *chs* from a prophage and is found in more than 87% of clinical isolates. It specifically obstructs Formyl peptide receptor 1 (FPR1) and C5a receptor (C5aR)-mediated chemotaxis, and neutrophil recruitment *in vivo*[157]. It binds directly to these receptors blocking the interaction with natural ligands: fMLP and C5a, which are produced during neutrophil recruitment and host chemokine response[158].

Similarly, the papain-like cysteine protease ScpA also inhibits chemokine-dependent neutrophil activation and chemotaxis. Unlike CHIPS, it binds and cleaves the N-terminus of chemokine receptor CXCR2, thereby inhibiting neutrophil activation and migration towards a number of known chemoattractants, with exception of C5a and fMLP[159]. This indicates selective substrate specificity existing between CHIPS and ScpA, hence justifying the preservation of both functionally similar proteins by the bacteria.

In addition to this, *S. aureus* are vicious producers of nucleases. The staphylococcal nuclease (Nuc), also called micrococcal nuclease encoded by *nuc* gene, is a phospdiesterase that has endonucleolytic activity towards both DNA and RNA[160]. *S. aureus* uses Nuc to degrade Neutrophil Extracellular Traps (NETs) and the enzyme adenosine synthase A (AdsA) to convert the degraded product deoxyadenosine monophosphate into 2'-deoxyadenosine, which triggers caspase-3 mediated apoptosis in immune cells[161].

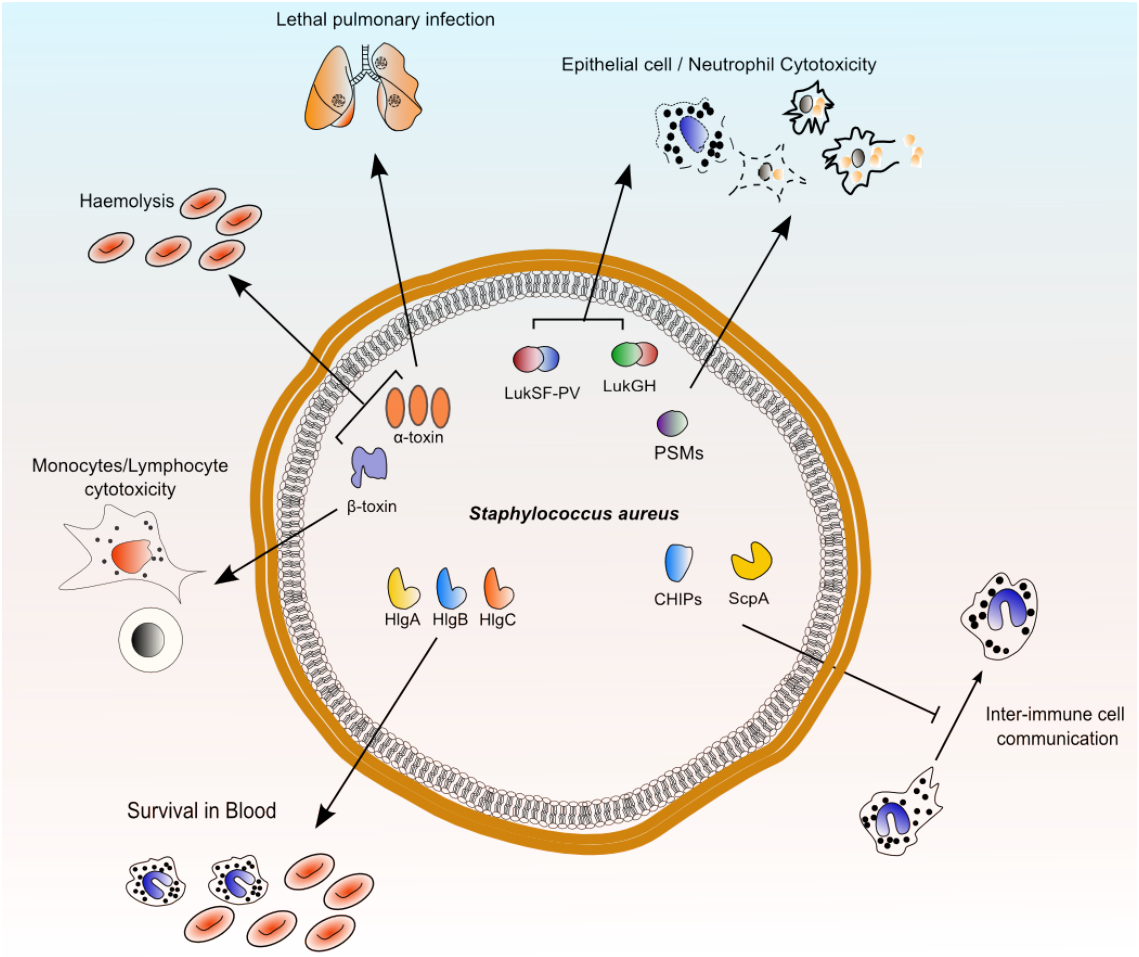

Figure 1.4: A graphical representation of major toxins, virulence associated secreted proteins of *S. aureus* and their role in infection. A broad array of secreted proteins and toxins are employed by *S. aureus* to perform specific roles, engaging various host cells and tissues. PFTs are released to target a number of host cells. α-toxin induces lethal pneumonia and β-toxin target monocytes and lymphocytes. Both of them also cause haemolysis. Leukotoxins (LukSF-PV, LukGH) and PSMs have cytolytic acivity towards epithelial cells and neutrophils. γ-haemolysins (HlgA, B and C) mediate survival in blood, aid in immune evasion and haemolysis. CHIPS and ScpA hinder immune cell communications. The culmination of these actions significantly contribute to the being a successful pathogen. For details on individual components refer to Section 1.2.2

1.3 Regulation of Staphylococcal virulence

Apart from the basic processes in a bacterial cell, signal transduction systems regulate genes involved in accessory functions such as quorum sensing, nutrient stress, chemical and host immune stress. All staphylococcal virulence factors and host-pathogen interactions are very intricately controlled by concerted action of regulatory proteins and non-coding RNAs. Regulatory proteins comprise of mostly transcription factors, which bind to DNA and function either unaccompanied or in cohort with functionally co-dependent proteins or RNA. *S. aureus* regulatory systems are broadly classified into two major categories: two-component regulatory systems (TCRS) and SarA protein family[162,163]. Also, *S. aureus* regulation alters significantly between exponential and post-exponential growth phases and there are reg-

ulators, which reorganise cellular functions accordingly.

1.3.1 Two-component regulatory systems (TCRS)

Accessory gene regulator (Agr) proteins constitute one most important TCRS responsible for controlling several staphylococcal genes including surface and secreted proteins [164,165]. Agr constitutes the major quorum-sensing system in *S. aureus* and the genetic locus comprises an operon with two divergent transcriptional units driven by two separate promoters - P2 and P3 [166,167] (See Figure 1.5). P2 controls production of the single polycistronic RNAII harbouring the open reading frames (ORFs) *agr*BDCA in tandem. AgrC and AgrA form the sensor kinase and DNA-binding response regulator respectively, in this TCRS [168]. AgrD is the precursor of quorum-sensing activator thiolactone molecules called auto-inducing peptides (AIPs) [167]. The pro-peptides undergo cleavage by a transmembrane endopeptidase AgrB to form mature hepta-peptides with a single thiol-linkage [169,170]. The AIPs are maintained at basal levels by each cell in the population and cell density determines the abundance of AIPs, which upon reaching critical concentration lead to enhanced *agr* transcription. The transmembrane domain of AgrC detects the threshold of both homologous/heterologous AIPs, then autophosphorylates by its cytoplasmic histidine kinase domain [171]. Subsequently, AgrC then transphosphorylates the regulator AgrA(See Figure 1.5) that binds target DNA. *agr*A is driven by an independent promoter of its own called P1 [165] and codes for a 27 kDa LytTR-family transcriptional regulator with a β-stranded C-terminus, which includes a helix-turn-helix DNA-binding domain and forms dimers before binding successive major grooves [172] on the target DNA sequence of imperfect direct repeats-[TA][AC][CA]GTTN[AG][TG] [173]. However upon phosphorylation, AgrA specificity changes from P2 to P3 promoter [174] leading to increased production of the effector RNAIII and subsequent virulence factors. RNAIII is a 514 nucleotides long regulatory non-coding RNA that harbours δ-toxin gene and promotes the production of exoproteins and toxins, but represses surface proteins. [164,166,175,176]. The mechanisms by which RNAIII acts involves either gene expression modification by binding to transcription factors or translational interference by complementarity to Shine-Dalgarno sequence or activation of genes by post-transcriptional stabilization of mRNA [167,175,177].

Consequently, *agr* operon commands global gene expression in *S. aureus* on two levels, by RNAIII-dependent and independent ways to positively regulate exoproteins such as α-toxin [176],β-toxin [175], δ-toxin [166], TSST-1 [167], PSMs [178], extra-cellular proteases [179] and negatively regulate coagulase [180], Repressor of toxin (Rot) protein [181], protein A and Sbi [182]. Absence of *agr* genes have also been attributed to reduced biofilm formation [183] and severe attenuation of pathogenicity in a number infection models [184–186].

Besides Agr, another TCRS also constitute one of the major virulence regulatory pathways in *S. aureus* and the expression of *sae* genes are maximum at the post-exponential growth phase [187]. *sae* operon consists of four open reading frames; *sae*P, Q, R and S (See Figure 1.6) expressing four overlapping transcripts driven by three distinct promoters P1, P2 and P3 [188,189]. P1 drives the expression of the entire operon, but can also produce only SaeP and whereas, P2 drives the expression of SaeQ, R and S.

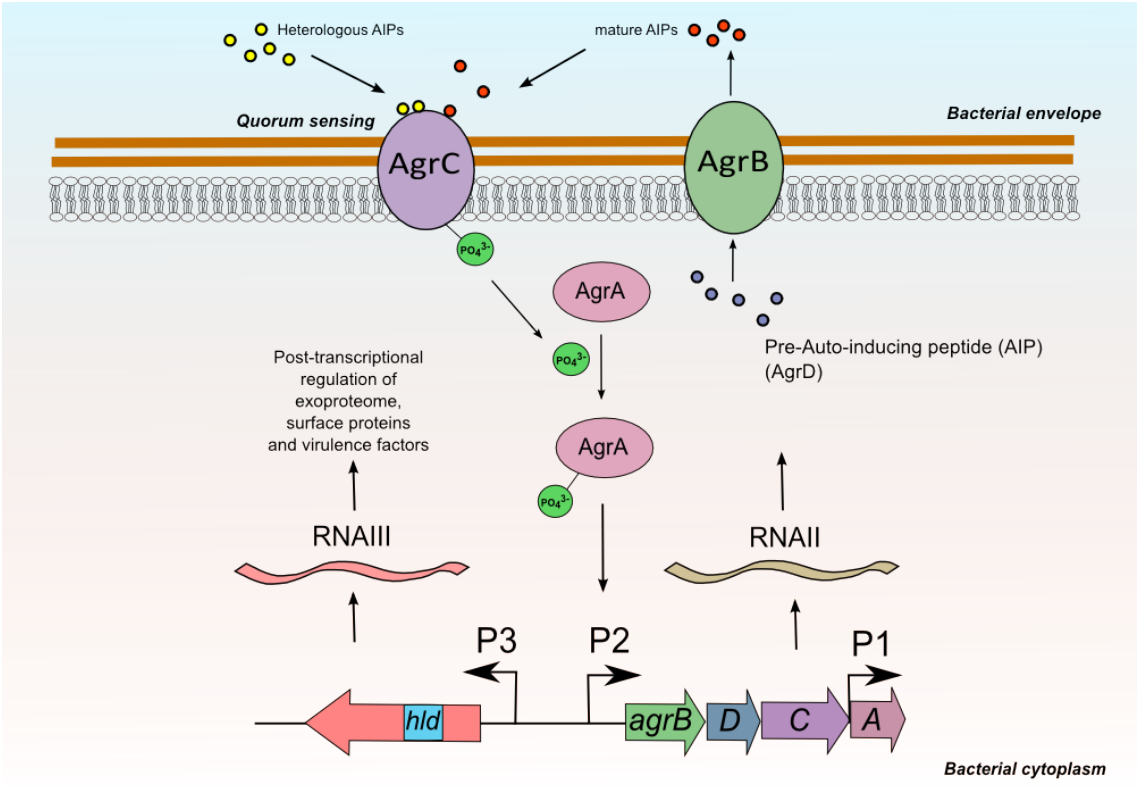

Figure 1.5: Graphical representation of the *S. aureus* accessory gene regulator (*agr*) operon structure and gene regulation. This operon is primarily under the control of two divergent promoters - P2 that drives the expression of RNAII i.e. the mRNA for *agr*BDCA and P3 that makes RNAIII. AgrD (blue) is the precursor for autoinducing peptides (AIPs), which undergoes maturation and transported out of cell (red), both by the action of transmembrane protein AgrB (). Both homologous and heterologous AIPs are sensed by a transmembrane sensor kinase AgrC (purple), which then concedes auto-phosphorylation. AgrC subsequently trans-phosphorylates and activates the DNA-binding response regulator AgrA (pink), which binds the promoters P2 and P3. This eventually promotes the transcription of *agr* genes.

*sae*Q harbors an internal promoter P3 that is responsible for the production of only SaeR and SaeS, which form the sensor histidine kinase and response regulator respectively [187]. SaeS is a 39.7 kDa intramembrane sensor kinase that autophosphorylates upon environmental cue [187] resulting in transphosphorylation of the N-terminal regulatory site of SaeR, which is a 26.8 kDa transcriptional regulator with a C-terminal DNA-binding domain. Phosphorylated SaeR undergoes conformation changes, which is critical for binding to its DNA recognition sequence ($GTTAAN_6TTTAA$) at -35 region of the promoter P1, thereby driving the expression of targets [190]. The *sae* operon has a feedback system controlled by the SaeP and SaeQ, which enforces conformational change of SaeS and exposes its phosphatase activity. SaeS can hence dephosphorylate and abolish SaeR target gene expression [191]. Sae TCRS is stimulated by host innate immune stress [112,192] and is required for the expression a number of virulence genes such as *hla, spa,efb, vwbp, hlg*ACB, *sbi, emp, chs, luk*AB, *fnb*AB and *luk*ED [189–193].

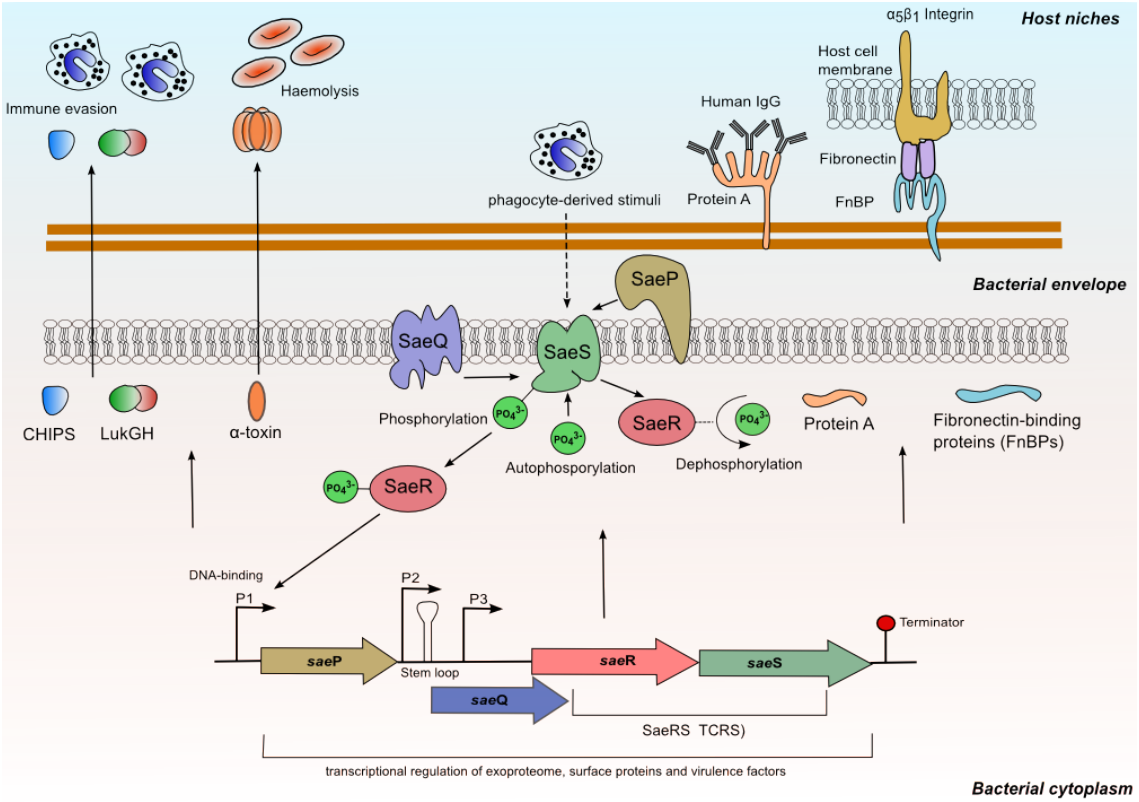

Figure 1.6: A graphical illustration of the cellular signaling governed by *S. aureus* Sae regulatory system. SaeRS TCRS, is a part of an operon structure consising of four ORFs - *sae*PQRS, which are transcribed by three promoters - P1, P2 and P3 (For details refer to Section 1.3.1). SaeS is a transmembrane sensor kinase that senses host immune system and undergoes autophosphorylation. Consequently, SaeS reversibly phosphorylates the response regulator SaeR, which binds P1 to promote the transcription of the entire operon. The accessory proteins SaeP and Q are involved in a feedback mechanism. These proteins trigger conformational changes in SaeS converting it to a phosphatase, which leads to subsequent dephosphorylation and inactivation of SaeR. SaeRS promotes the production of secreted virulence proteins like α-toxin, LukGH, CHIPS and surface proteins like Protein A, FnBPs.

1.3.2 SarA protein family

Staphylococcal accessory regulator (Sar) A is an exemplary member of a group of proteins, collectively called Sar homologs. These proteins can be broadly classified into 3 major subfamilies: single-domain proteins, double-domain proteins and MarR homologs.

The single domain proteins consist of SarA, SarR, SarT, SarV, SarX and Repressor of toxins (Rot). SarA is a 14.7 kDa protein with a helix-turn-helix DNA binding domain [194]. It is transcribed from the *sar* locus consisting of three distinct transcripts driven by promoters - P1, P2 and P3 [195,196]. SarA binds *agr* and as well as other promoters, and significantly contributes to virulence by regulating expression of over 100 effector proteins [162,197]. SarA promotes the formation of biofilms [198], positively regulates FnBPA and B, and α-toxin but negatively regulates protein A and extra-cellular proteases [162,163].

SarR is 13.6 kDa DNA binding protein [199] that binds and represses the expression *sar*A [200]. It also binds the *agr* promoter, thereby regulating the expression virulence genes [201]. SarA and SarR are a dimeric winged helix DNA-binding transcriptional regulator [163]. SarR DNA-binding protein forming homodimers and abrogates SarA production by binding to P1 promoter in the *sar* locus [200]. Interestingly,

these two proteins compete for the same region on the *agr* promoter[201], however SarR possesses higher affinity towards *agr* P2, therefore during the transition to late-exponential phase displaces SarA and binds *agr* P2[202]. SarT and V are repressed by SarA facilitating toxin production[162] and contributing to autolysis[203] respectively. Whereas, SarX represses *agr* to reduce toxin production[204].

Rot is a transcriptional factor that regulates the expression of nearly 168 genes, primarily repressing toxins and enhancing surface proteins[205]. RNAIII has been suggested to obstruct the translation of *rot* mRNA[206].

The double domain proteins consist of SarS, SarU and SarY. SarS has two non-identical SarA homologous domains[163]. It activates protein A transcription and is activated by SarT. SarU on the other hand is repressed by SarT and its an activator of *agr* expression[163]. Whereas, SarY is yet to be assigned with any function in *S. aureus* .

MarR homologs consists of MgrA and SarZ, these SarA homologs show higher sequence similarity to MarR protein in *Escherichia coli* , rather the aforementioned SarA family proteins[207]. MgrA has emerged as a crucial transcription regulator in *S. aureus* , influencing the expression of 355 genes[208]. It positively regulates *agr*, *sar*S and *sar*X and enhances toxin production simultaneously decreasing surface proteins[207]. In addition, MgrA translation in directly influenced by RNAIII through mRNA stabilization[177]. MgrA can activate signaling pathways upon sensing oxidation by Reactive Oxidation Species (ROS) and turns on antibiotic resistance in *S. aureus*[209]. SarZ on the other hand, has been shown to important for haemolysis and virulence in mice[210].

1.4 Host-pathogen interactions during *Staphylococcus aureus* infections

In the host-pathogen tug of war, the series of events during *S. aureus* intra-cellular infection begins with invasion into the host cell, which is followed by escaping the phago-lysosomal enclosure, then replication in the host cytoplasm and ultimately killing the host cell to release bacterial progeny that are capable of infecting the next host cell.

1.4.1 Adhesion and Invasion into host cells

Staphylococcal invasion is mediated by cumulative actions of a number of surface adhesive molecules (See Section 1.2.1), which binds host ECM and mediates bacterial entry into the host cell (See Figure 1.7A, B). Besides active phagocytosis by immune cells, *S. aureus* can be internalisedin mammalian epithelial and endothelial cells by a process resembling receptor-mediated endocytosis. A number of specific bacterial surface structures have been shown to be involved adhesion and invasion of different host cell types (See Section 1.2.1). FnBPA and FnBPB, are the most important *S. aureus* factors that aid in adhesion by binding the N-terminal F1 module of Fibronectin, via the direct repeats on its C-terminal domain[211]. Subsequently, the fibronectin present in host ECM forms the bridge with host cell $\alpha_5\beta_1$,

which triggers Src kinase-mediated cytoskeletal rearrangement[212] and internalisation of bacteria by a 'zipper type' mechanism[85]. This process may be assisted by fibronectin-binding Extracellular adherence protein (Eap)[213] and β3-integrin binding IsdB[214]. Furthermore, WTAs have been shown to play an important role in bacterial adherence to the mammalian nasal mucosa by directly interacting with the F-type scavenger receptor, SREC-1, thereby facilitating colonisation[215].

On the contrary, *S. aureus* tend to evade internalisation by phagocytes; neutrophils and macrophages. Phagocytosis depends highly on opsonisation, a process by which opsonins, such as complement proteins or IgG, decorate the surface of bacteria. *S. aureus* employs both MSCRAMMs and SERAMs to hinder this process thereby evading phagocytosis[78]. However in some cases, *S. aureus* deliberately invades phagocytes specifically Mast cells (MCs) to avoid degranulation-mediated bacterial killing. Upon encountering MCs, *S. aureus* increases the expression of α-toxin and FnBPs. The interaction between α-toxin and ADAM10 promotes the production of more β3-integrin, to which FnBPs can bind and hence, enhancing bacterial adhesion and internalisation[125].

1.4.2 Intra-cellular survival of *S. aureus*

S. aureus can thrive within a variety of host cells including epithelial cells, neutrophils and macrophages for long time periods without damaging the host, masking itself from antibiotic-mediated killing, facilitating dissemination, which may lead to recurrent and chronic disease in humans[216–220]. *S. aureus* can also exhibit dynamic phenotype switching and convert to slow-growing persistent form called small colony variants (SCVs) to survive inside the host phagolysosomes for weeks[220,221]. SCVs exhibit altered and sluggish metabolism as a consequence of either thymidine auxotrophy or a defective electron transport system[220]. This phenotype is characterised by small-sized colonies on semi-solid medium that appears to be less virulent in animal models, has lower toxin production due to inactive *agr* operon, higher expression of surface adhesins and can revert back to normal phenotype upon addition of menadione, haemin and/or CO_2 or upon leaving the intra-cellular location[220–222]. Although in this form, *S. aureus* can survive relatively less in professional phagocytes like macrophages[221].

Besides SCVs, metabolically active *S. aureus* can replicate in phagolysosomes within macrophages[223] and survive for up to 6 days when infected with a higher multiplicity of infection, before lysing out from the host cell[217]. In neutrophils however, metabolically active *S. aureus* has been observed to survive for up to 24 hours post phagocytosis, preventing cytokine production during this time[216]. In both professional and non-professional phagocytes, *S. aureus* intra-cellular proliferation is dependent of major virulence regulators like *sar*[216], *agr*[224], although low-toxin producers and mutants of *agr*A could survive longer within host cells[219,224].

1.4.3 Escape from phago-lysosomal compartment

Post-internalisation into host cells, *S. aureus* is initially maintained in phagolysosomes/phagosomes but ultimately escapes out into the cytoplasm[225] (See Figure 1.7C). On the contrary, there are also natural *S.*

aureus strains that do not escape but remain within the phago-lysomal compartment [153]. To escape from the phagosomes, bacteria needs to extirpate the surrounding membrane, therefore pore-forming toxins are thought to be the prime candidates responsible for this phenomenon. Although, its a relatively naive area of investigation and role of different PFTs in phagosomal escape has been argued and individual factors responsible for this event have emerged in several studies.

In airway epithelial cells, *S. aureus* requires α-toxin to escape phagosomes, when the Cystic Fibrosis Transmembrane Conductance Receptor (CFTR) [226] is absent, although it is not exclusively sufficient when CFTR is present [227]. Furthermore, *S. aureus* can also employ β-toxin and δ-toxin acting in synergy to mediate phagosomal escape [228]. Within the host phagosome, staphylococcal quorum sensing and expression of *agr* operon is triggered and required for efficient escape [229]. Quite recently, the role of Phenol soluble modulins (PSMs) in phagosomal escape has been made apparent. Unlike PSMβ and PSMγ, PSMα has been shown to exclusively contribute to phagosomal escape in non-professional and professional phagocytes [153,224].

1.4.4 Intra-cellular replication of *S. aureus*

In epithelial cells, after exiting the phagosomes, *S. aureus* rapidly proliferate to increase its numbers in the cytoplasm before lysing the host cell (See Figure 1.7D). This property of bacteria may differ between strains and isolates [230]. Within the host cell, *S. aureus* is protected from antibiotics and can hence replicate unhindered [231]. Several factors have been shown to influence intra-host replication and some that are involved in phagosomal escape, such as *agr*-dependent PSM operon, are also required for efficient intra-cellular replication [153]. Host cytoplasm presents some stress on residing or proliferating bacteria. Therefore, *S. aureus* adapts to this environment by undergoing significant changes gene expression and protein stability. *S. aureus* 6850 strain upon internalisation shuts down genes involved in cell division and regulatory processes but simultaneously upregulating genes related to iron-scavenging and toxin production [232]. However later, the genes responsible for major metabolic functions were increased. Furthermore, *S. aureus* also undergo proteomic remodelling to tackle stresses conferred by the host cytoplasm. This phenomenon is governed by molecular chaperone and proteolytic systems such as Clp ATPases, and the lack of it can heavily influence intra-cellular replication [233].

Contrastingly, *S. aureus* can proliferate not only within membrane bound vacoules in bovine mammary cells [234] but also inside mature phagolysosomes of human and murine macrophages [223]. On the other hand, there is little evidence of exponential intra-cellular replication of *S. aureus* inside neutrophils [216], although *agr* expression is important for resisting disinfection by professional phagocytes [235]. Therefore with regards to bacterial replication, metabolically active *S. aureus* can have two fates inside the host cell, depending on the presence of vital regulatory systems. It can either proliferate avidly after phagosomal escape or be eliminated by the host lysosomal degradation system and hence, cannot replicate.

1.4.5 Host cell death induced by *S. aureus*

Most often similar *S. aureus* factors are involved in escape, proliferation and ultimately for triggering host cell death. Efficient escape from the phagosome is often the prerequisite for successful killing of the host cell [153,225], with few exceptions. *S. aureus*-mediated host cytotoxicity is a multi-factorial process and can be apoptotic and/or necrotic, in a variety of professional and non-professional phagocytes [230]. Staphylococcal PFTs and cytolytic peptides are usually the perpetrators in host cellular damage, and can act via both extra-cellular and intra-cellular manner. *S. aureus* induces selective killing of peripheral blood mononuclear cells (PBMCs) either by α-toxin, which activates caspases leading to apoptosis and partially triggering caspase-independent necrotic cell death in T-lymphocytes [236,237 238], or by β-toxin that specifically target monocytes triggering the release of Interleukin-1β (IL-1β), shedding of Interleukin–6 receptors (IL-6R) and plasma membrane damage [155]. In addition, extra-cellular bacterial secretions activate caspase-1 associated NLRP3 inflammasome formation and induction of pyroptosis [239].

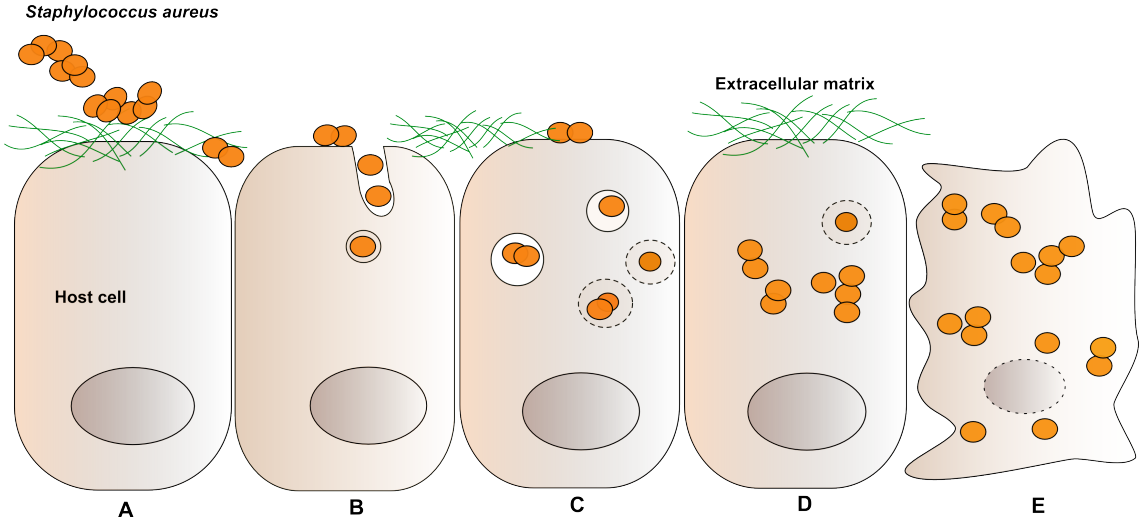

Figure 1.7: A graphical representation of the series of events during intra-cellular infection *S. aureus*. (**A**) Initiation of infection occurs with adhesion of *S. aureus* (orange) to the host extra-cellular matrix (green) , which is followed by (**B**) internalisation. (**C**) Within the host cell, *S. aureus* can either survive in phagolysosomes (solid hollow circles) or disrupt the surrounding membrane (dotted circle) escape into the cytoplasm. (**D**) If escaped, bacteria can proliferate inside the host and (**E**) eventually kills it from within.

Furthermore, *S. aureus* induces host cell death by both receptor-dependent and independent manner. It employs several cytotoxins that target host cell receptors to cause membrane damage such as ADAM10 via α-toxin [123], CD11b using LukAB [136], CXCR1/2 and CCR5 via LukED [145,240], C5aR by PVL [241]. Extra-cellularly present LukAB and PVL can induces cell death by triggering the NLRP3 inflammasome [138] and Bax-independent apoptosis by targeting mitochondria [242], respectively. *S. aureus* also employs PSMs that have high affinity towards membrane and induce damage, independent of any known receptors [146]. However, PSMs are inhibited by serum [243] and certain cell types are resistant to extra-cellular addition of α-toxin despite being susceptible to intra-cellular bacteria. These facts advocate for existence of an exclusive intracellular pathogen-mediated host cell death mechanism and factors regulating the

same. PSMs and LukAB are important during intra-cellular cytotoxicity both in epithelial and immune cells[137,153], which are regulated by *agr*A and stringent response[146,244]. Previous studies have shown the activation of *agr* regulatory system within the host cells[231].

1.5 Aim of the study

Although now a widely accepted fact, little is known about the factors that govern these processes of bacterial survival or intra-cellular pathogen-mediated host cytotoxicity. Therefore, this study aims to use genome-wide Himar1 transposon mutagenesis to generate pooled mutant libraries in the β-lactam resistant *S. aureus* 6850 strain[245]. These mutant libraries will provide with an efficient method for unbiased and simultaneous identification of virulence factors that are important for intra-cellular infection in human epithelial cells. These findings will be correlated to screening experiments in murine models, to assess the relevance in disease progression. High throughput sequencing will be employed to analyse transposon insertion sites throughout the bacterial genome and their relative abundances in each infection model. Furthermore, the identified genes will be characterised for its role in virulence and mechanisms.

Chapter 2

Genome-wide identification of *S. aureus* virulence factors by Tn-seq

2.1 Mariner transposon-mediated random insertional mutagenesis in *Staphylococcus aureus*

To generate high density random mutant libraries of *S. aureus* with maximum genome-wide coverage, random insertional mutagenesis with eukaryotic Himar1 transposon-based mobile element was employed. A single plasmid system; pBTn[246] that comprised of an erythromycin resistance gene (*erm*B) with its own promoter and terminator in place, flanked by the Himar1 Inverted Terminal Repeats (ITRs). Furthermore, it also harbours the Himar1 transposase gene (*tnp*), which is driven by a Xylose repressor system. Under normal circumstances, the xylose-inducible promoter (P_{xyl}) is repressed by the Xylose Regulator (XylR), encoded by *xyl*R gene on the same plasmid (See Figure 2.1). However, addition of D-(+) Xylose induces the release of XylR and thereby, leading to the production of Tnp. The transposase then recognises the ITRs and cleaves to release the transposable element, which randomly jumps onto insert within any "TA" dinucleotide present in the genome (See Figure 2.1).

2.1.1 Generation of pooled mutant libraries in *Staphylococcus aureus* 6850

S. aureus 6850 was transformed with plasmid pBTn[246] by electroporation (See Section 5.4). The plasmid pBTn has a size of 10 kb (See Figure 2.2A) and harbors the 1.3 kb long Himar1 transposon-based mobile element (See Figure 2.2B), a gene coding the transposase enzyme and a chloramphenicol-resistance gene as a selection marker for the plasmid backbone. Bacteria were selected for dual resistance i.e. Erythromycin and Chloramphenicol post transformation. The transposase gene in pBTn is driven by a Xylose inducible promoter (See Chapter 2.1 and has a temperature sensitive origin of replication, which can replicate only ≤30°C. The protocol for generation of mutant pool was adapted from Min Li et al.

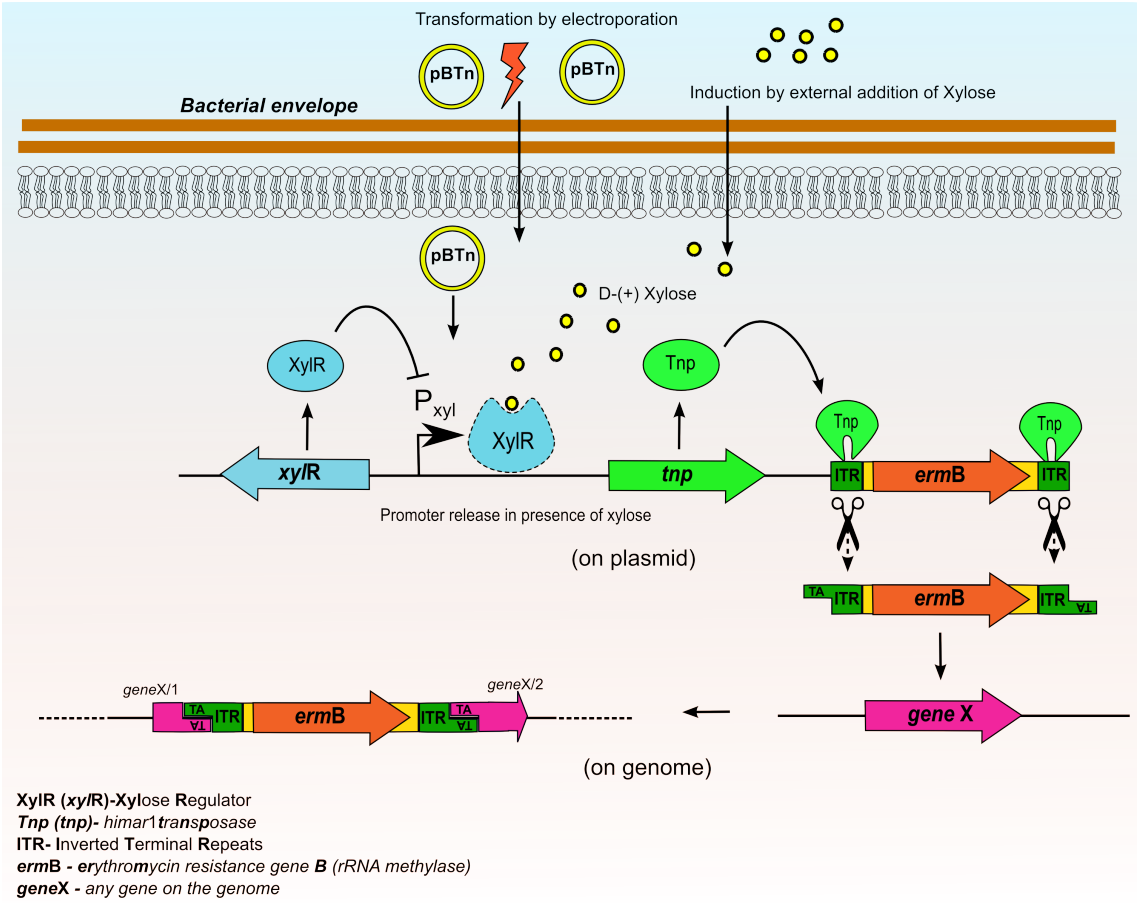

Figure 2.1: Schematic illustration of Himar1 transposon-based insertional mutagenesis in *S. aureus* utilizing the plasmid pBTn. The plasmid was introduced in *S. aureus* by electroporation. In the absence of inducer, the XylR protein (light blue) binds the promoter P_{xyl} and thereby blocking the production of transposase; Tnp (light green). Upon external addition, D-(+) Xylose (yellow circles) binds XylR inducing a conformational change resulting in promoter release. This promotes the production of Tnp, which in turn recognises the ITR (dark green) of the transposable element consisting of an erythromycin resistance gene; *erm*B (orange). This genetic element eventually jumps onto any genomic location (gene X, pink) in the bacteria, thereby disrupting its function.

2009. This protocol required induction of the promoter by addition of Xylose in liquid medium at 30°C for mutagenesis, followed by raising the temperature to 43°C. The latter was done three times by diluting in fresh medium, to get rid of the plasmid. Prior to creation of the libraries, mock tests were performed to optimise the experiment for most suitable medium and also the loss of plasmid after temperature elevation was tested.

To test for a suitable medium, replication of *S. aureus* 6850 including the effect of temperature shift was checked using three different medium; Luria-Bertani broth (LB), Nutrient Broth (NB) and Tryptic Soy Broth (TSB). Optical density of overnight cultures grown at 30°C, the starter sub-culture for induction of mutagenesis and all three steps at 42°C were checked. The temperature elevation steps were extended upto six for examination of the precise number of cycles required for complete plasmid loss. In LB and TSB, bacteria had similar growth rates at 30°C, upon elevation of temperature the bacterial growth reduced drastically until the 2nd 42°C step followed by a sudden increase in growth during the 3rd

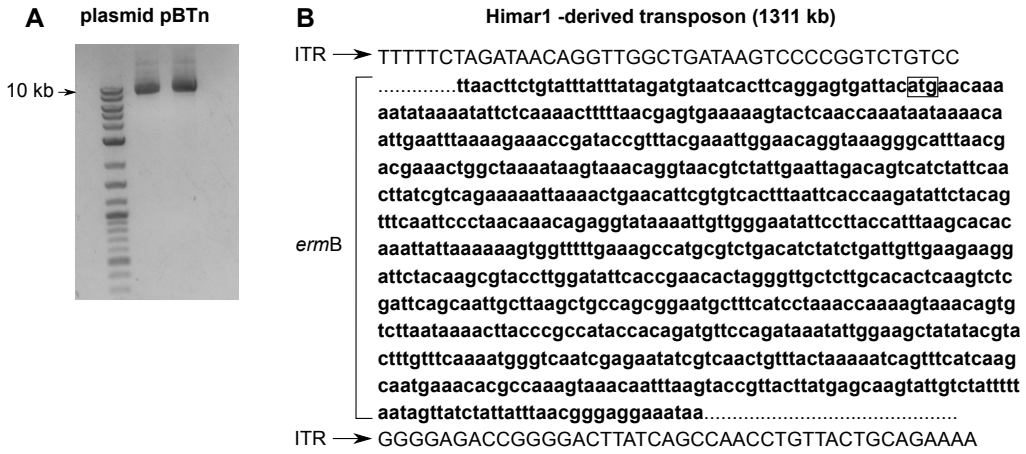

Figure 2.2: The plasmid pBTn carrying a Himar1-derived mobile element was used to mutagenesis. (**A**) Isolation of plasmid after transformation of *S. aureus* followed by agarose gel electrophoresis determined the size of pBTn to be approx. 10 kb. (**B**) A sequence map of the 1311 kilobases (kb) mobile genetic element harboured on the plasmid pBTn, shows an erythromycin resistance gene (*erm*B, bold letters) with its ORF marked by a start codon (black box), flanked by Himar1 inverted terminal repeats (ITR, capital letters).

(See Figure 2.3A, C). From hereon, the growth rates were stable until the 6^{th} 42°C. On the other hand, *S. aureus* grown in NB had slower growth rate but did not show large fluctuations regardless of temperature elevation (See Figure 2.3B). In all medium tested, viability of bacteria were also determined by CFU enumeration at crucial steps; overnight culture, 3^{rd} (Final) step at 42°C and extended step of 6^{th} 42°C step (See Figure 2.3D). There were no large differences between individual steps in each medium tested.

To determine the number of 42°C steps required to completely eradicate the plasmid, chloramphenicol sensitivity was determined by enumeration of colonies obtained on NB agar supplemented 10 µg/ml Chloramphenicol, when compared to enumeration CFUs on NB agar with and without 5 µg/ml Erythromycin, after each round of incubation. The difference in viable CFU showed that plasmid loss was efficient in all media (See Figure 2.3E), with maximum accuracy obtained when using NB agar; 99.99%. Furthermore, it was also evident that 3 rounds of incubation at 42°C was sufficient to ensure maximum plasmid loss, especially in case of NB medium (See Figure 2.3E). Hence for generation pooled transposon mutant libraries in *S. aureus* 6850, NB was chosen as the most suitable propagation medium. Bacteria were treated with 0.5% D-(+) Xylose at 30°C overnight to allow for mutagenesis, followed by 3 times dilution steps at 42°C (See Figure 2.3F). The bacteria were stored at high densities of $1x10^{10}$ CFUs/ml, as master libraries.

2.1.2 Arbitrary PCR shows successful and random transposon mutagenesis

To determine whether the mutagenesis experiment was successful and that there were randomly inserted transposons in the bacterial genome, the master library was plated and several colonies were picked randomly. Genomic DNA from these colonies were isolated and transposon ends were amplified by arbitrary PCR method[246] (See Section 5.6.1), which is a combinatorial PCR involving both linear and exponential amplification. This approach requires two sets of primers; 3 tandem transposon specific

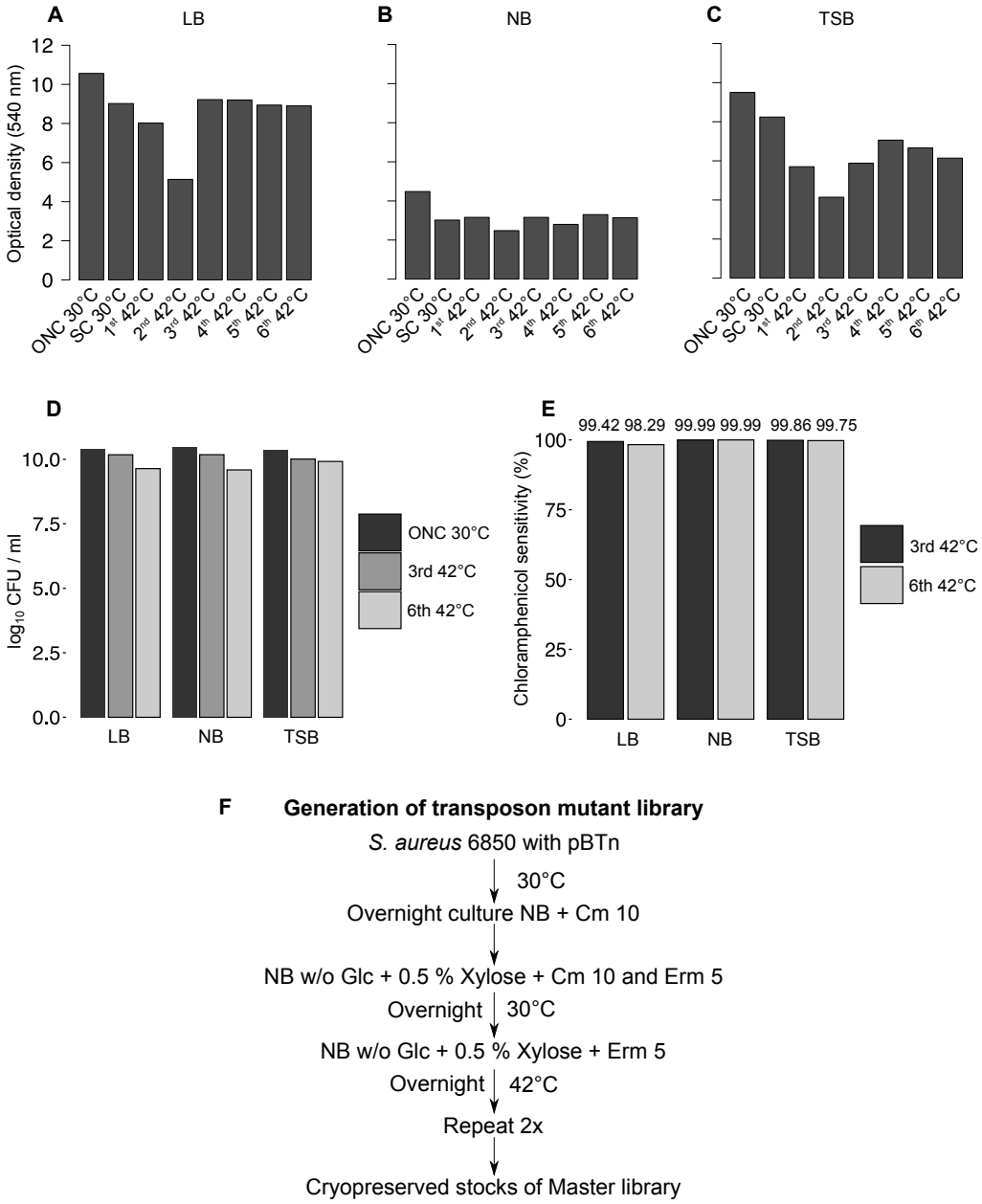

Figure 2.3: Optimisation of mutant library generation conditions in strain 6850 and induction of transposon mutagenesis. Prior to mutant library generation the *S. aureus* 6850 strain with plasmid pBTn was grown in Luria-Bertani broth (LB, **A**), Nutrient Broth (NB, **B**) and Tryptic Soy Broth (TSB, **C**). Growth rates were measured by determination of optical density at 540 nm of overnight cultures (ONC) and sub-cultures (SC) at 30°C, and all 6 steps at 42°C. (**F**) A flow diagram showing the steps used to generate transposon mutant library, which began with introduction of pBTn into *S. aureus* 6850. Overnight cultures of bacteria were grown, diluted in TSB without (w/o) Glucose supplemented with antibiotics 10 µg/ml Chloramphenicol (Cm 10) and 5 µg/ml Erythromycin (Erm 5) and incubated overnight for mutagenesis to take place. The plasmid was eliminated by shifting to higher temperatures and repeating the step 2 more times. Finally, the bacteria were cryopreserved as stocks

primers binding to both 5′ and 3′ ends of the erythromycin gene in the transposon (See Figure 2.4A) and arbitrary primers that bind the genome of bacteria at regular intervals. Depending on the primer set used and proximity of the arbitrary primer, a precise combination will amplify the genetic locus either at the 5′ or 3′ of transposon insertion site (See Figure 2.4B), in a two step PCR reaction (See Section

5.9.1.5).

The nucleotide composition of amplification products from the arbitrary PCR reactions were determined by Sanger sequencing. The sequences were aligned with plasmid pBTn and the 6850 genome (NCBI Genbank Accession ID CP006706.1.) and were found to originate from different genetic location. Some exemplary genetic locations are displayed in Table 2.1.

2.1.3 Development of a DNA fragment library preparation strategy for Transposon insertion-site deep sequencing (Tn-seq)

To track transposon insertion site from individual bacteria in the entire pool of mutants, a massively parallel sequencing approach tailored for Illumina® platform, was adapted. This pipeline involved isolation and fragmentation of genomic DNA from the mutant pool to be analysed. Fragment DNA library preparation included end repair and size selection modules, ligation of Illumina® flow cell compatible adapters, high-sensitive quality control and enrichment of Transposon insertion sites by PCR (See Figure 2.5A). DNA was sheared by ultrasonics to a range of 100 - 500 base pairs (bp) (See Figure 2.5B) and fragment ends were repaired before proceeding to size selection process (See Sections 5.9.1.1 and 5.9.1.2). A gel-free procedure was adapted using a precise ratio paramagnetic beads and DNA solution[247], which extracted the desired range of fragments with a mode length of approx. 217 (± 10) bp (See Figure 2.5C).

This combination of ultrasonication and bead-based size selection procedure was highly reproducible and produced similar fragment distribution (R^2= 0.967) under standardized conditions (See Figure 2.5D, E). Deoxyadenosine triphosphate (dATP) molecules was added to the polished ends of the fragments to accommodate the adapters (See Figure 5.9.1.3). Illumina® flow cell compatible adapters were assembled by annealing two separate oligonucleotides; Multiplex-Y-Adapt_f (33 nt) with 5′ phosphorylated end and Multiplex-Y-Adapt_r (20 nt) with a phosphorothioate linkage at 3′ end (See Section 5.9.1.4, Appendix B, and Table B.1). This resulted in a 33 nt Y-shaped adapter, due to partial complementation (See Figure 2.5F). Successful ligation of adapters was evident by a size shift in the fragments with the mode changing from 217 (± 10) bp to 278 (± 13) bp, detected by high sensitivity on-chip electrophoresis (See Figure 2.5G).

Prior to deep sequencing, enrichment of the transposon insertion sites (TIS) was done by PCR, which also introduced barcodes for multiplexing and flow cell complementary sequences. The first PCR step was to enrich the loci at both 5′ and 3′ of the transposon by two separate short PCR cycles using the primers Himar-5-PCR or Himar-3-PCR as one of the primer (See Appendix B and Table B.1), which bound beyond the ITRs within the mobile element (See Figure 2.6A). This design was intentional since the mosaic were identical and the amplification would otherwise not be bidirectional. The MP-Index primers, were used as the second oligonucleotide (See Appendix B and Table B.1), which was complementary to the adaptor sequence and introduced a 7 nt unique barcode, which facilitated identification of sequences from a precise library during data analysis (See Figure 2.6B). Each reaction generated fragments of similar range between 200-400 bp, enriching for the TISs (See Figure 2.6C).

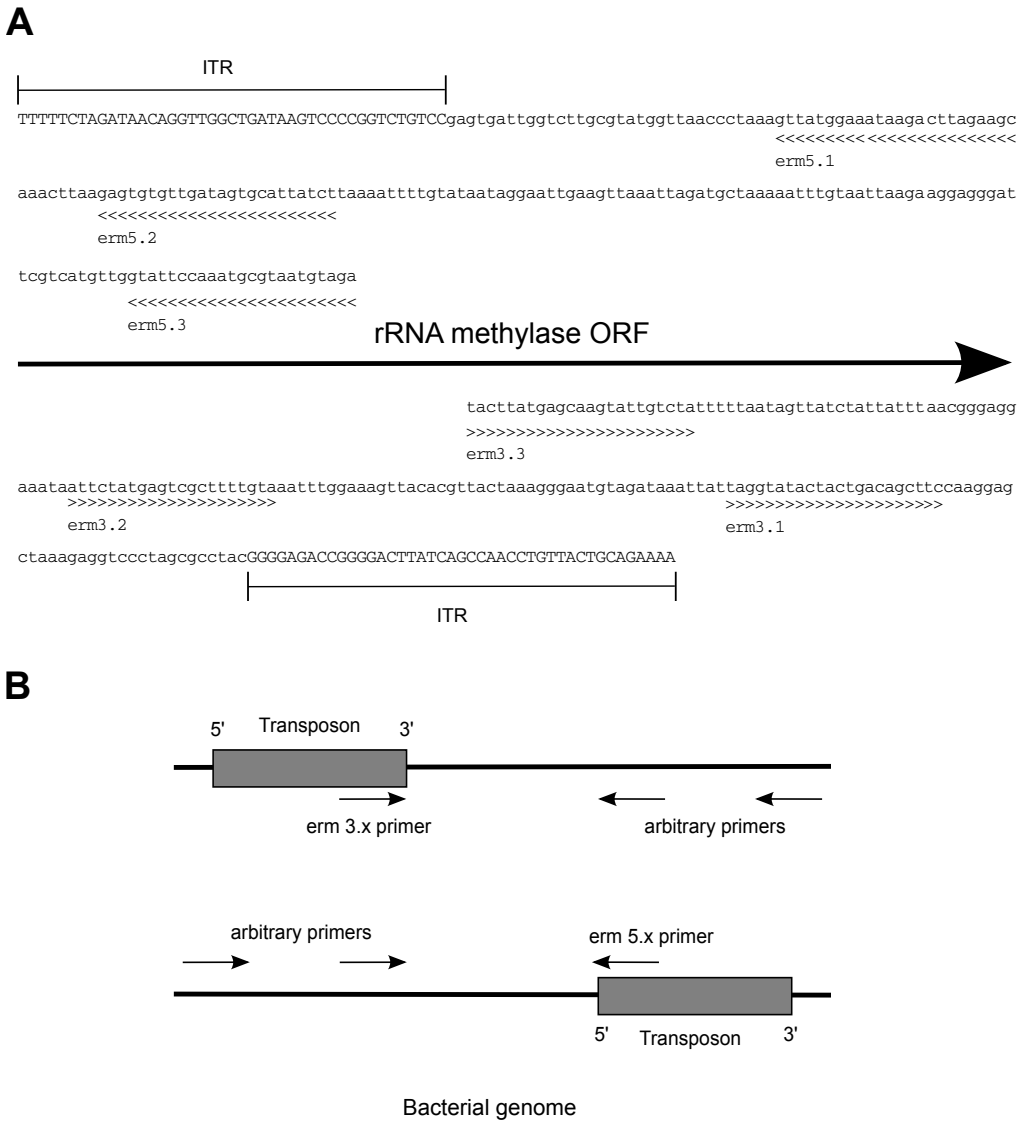

Figure 2.4: Detailed outline of Arbitrary PCR strategy for amplification of Himar1 transposon ends and confirmation of successful insertion in randomly picked *S. aureus* mutants. (**A**) Two sets of primers were used, transposon specific primers sets; erm 5.1, 5.2, 5.3 and erm 3.1, 3.2, 3.3 recognises the 5′ and 3′ ends of the transposon respectively and bind beyond the inverted terminal repeats (ITR) within the erythromycin gene. (**B**) These two primer sets were used in two consequential PCR steps along with the arbitrary primers to amplify out of the transposon into flanking region of the insertion site, in both 5′ or 3′ direction.

In the second PCR step, the two separate 5′ and 3′ PCR reaction products were mixed at equimolar ratios and further amplified with Tn-seq_HimarPCR_v2_PT, that consisted adaptor and flow cell specific sequences, and recognises the ITR region and IS-BC-Reverse, which is shorter derivative of MP-Index primer (See Figure 2.6D, Appendix B, Table B.1). The final fragment product contained the TIS flanked by adaptor-flow cell combinatorial sequences carrying the barcode region (See Figure 2.6E) and had the desired size range of 200-400 bp (See Figure 2.6F).

These PCR products were sequenced on the Illumina® HiSeq 2500 platform$^{\epsilon}$ (See Section 5.9.1.5). For sequencing the Himar1 seq primer recognizing the ITR was used (See Appendix B, Table B.1) and at least 10 million 100 bp single reads were obtained from each sample. This oligonucleotide recog-

Table 2.1: Amplification of insertion site from 10 randomly sampled individual transposon mutants by Arbitrary PCR.

Serial no.	Gene[a]	Function[b]
1	Dehydrosqualene desaturase	Staphyloxanthin biosynthesis
2	Intergenic	Unknown
3	conserved hypothetical protein (61.1 kDa)	Unknown
4	putative alpha-acetolactate decarboxylase	acetoin biosynthesis
5	glycolipid permease *lta*A	Lipotechoic acid biosynthesis
6	Selenocysteine lyase	Breakdown of L-selenocysteine into L-alanine and H2Se
7	putative ABC transporter family protein	Drug resistance
8	Putative Copper-translocating P-type ATPase	detoxification of heavy metals
9	alcohol dehydrogenase, zinc-containing	anaerobic metabolism
10	Triacylglycerol lipase	Fatty acid catabolism

[a]NCBI Genbank Accession ID CP006706.1.
[b]As indicated by data mining from NCBI or EBI

nised the distal end of the ITR with reference to the TIS in bacterial genome, instead of the proximal end (See Figure 2.6G). This enabled the recognition of a particular stretch of nucleotides, as the transposon end instead of the classical approach of TA duplication caused by a mariner transposon insertion. The pipeline for data analysis involved checking for transposon ends containing the search sequence 'CAACCTGT' on the positive strand and its complementary sequence on the negative strand (See Figure 2.6G). This was followed by mapping of the sequences to *S. aureus* 6850 genome and determining the number of TIS per gene/genome (See Section 5.9.1.6)[ϱ].

2.2 Tn-seq screens identify diverse genes vital for *S. aureus* virulence

2.2.1 Development of infection screens with *S. aureus* transposon mutant pools

Tn-seq data analysis showed that the bacterial mutant libraries comprised of approx. 25,000 unique TIS, evenly distributed across the genome. This library was used for further screening experiments, to investigate bacterial genes associated with host cytotoxicity, the mutant library was screened in human epithelial cells and mouse pneumonia model. To screen for blood stream infection related bacterial factors the mutant library was used in a mouse model of osteomyelitis.

In vitro non-cytotoxicity model was developed where HeLa cells were infected with *S. aureus* mutant pools and bacterial genes associated with intra-cellular *S. aureus*-mediated host cell were investigated collectively using Tn-seq. To avoid obfuscating effects, an 'one cell vs. one bacteria' approach was necessary, which in terms of infection is multiplicity of infection (MOI) 1. Hence prior to screening, HeLa

For details on data analysis refer to Materials and Methods 5.9.1.6.
[ϵ] Sequenced on Illumina® HiSeq platform was performed by the group of Prof. Dr. Richard Reinhardt at the Max Planck Genome Center, Cologne, Germany.
[ϱ] Post Tn-seq data processing, filtering, mapping and partial statistical analysis including DESeq2, was done by Christian Remmele and Dr. Dr. Marcus Dittrich, Chair of Bioinformatics, University of Würzburg, Germany

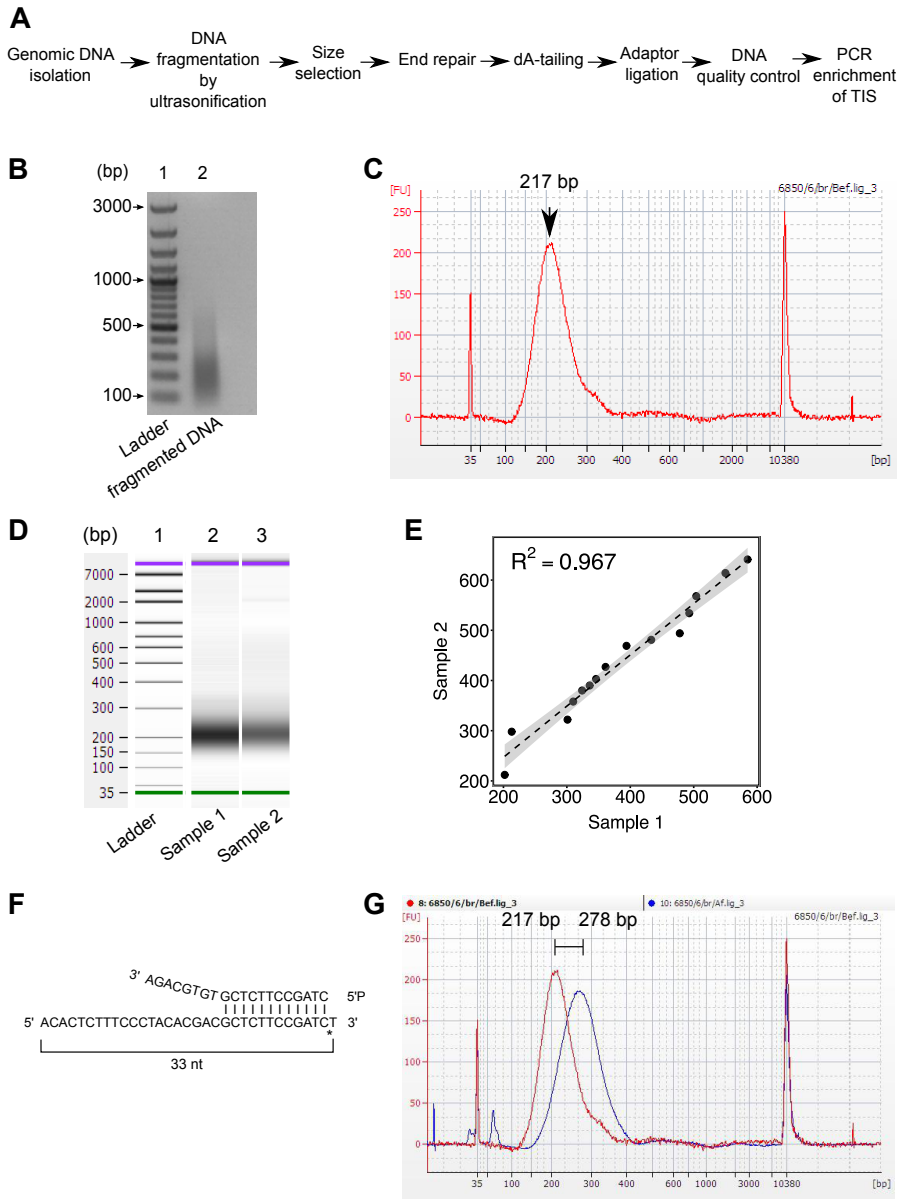

Figure 2.5: Development of DNA fragment library preparation strategy for Tn-seq. (**A**) The general workflow of this approach starts with isolation of genomic DNA to enrichment of TIS by PCR. (**B**) Agarose gel electophoresis (1%) shows the marker; Generuler 100 bp Plus DNA ladder (Lane 1) and DNA fragmented using a Bioruptor, ranging from 100 to 500 bp (Lane 2) under standardized setting; 20kHz, 320W (High), shear cycle: 30 seconds 'ON' and 30 seconds 'OFF'. (**C**) Electrophoretogram from on-chip DNA electrophoresis on Bioanalyzer, show precise range of DNA fragments obtained after size selection post sonication by using AMPure XP magnetic beads, with maximum number of fragments at 217 bp. The x-axis shows DNA size and y-axis shows quantity determined by Fluorescent Units [FU]. (**D**) Computer-generated image simulating agarose gel electrophoresis shows that the this approach generated highly reproducible results across multiple samples and (**E**) DNA fragment size range were consistently similar between samples when determine by linear modeling and Pearson's correlation co-efficient(R^2= 0.967). (**F**) After dA-tailing, a 33 nt Y-shaped adapter with a phosphate (P) at the 5′ end and last nucleotide at the 3′ end has a phosphorothioate bond (∗), were ligated to the fragments. (**G**) This resulted in shift of fragment size and mode changed from 217 bp to 278 bp, shown by the electrophoretogram. Fragment distributions are shown by red and blue histograms representing before and after adapter ligation respectively.

cells were infected with *S. aureus* 6850 at MOI 1 to examine infection rates and host cytotoxicity. Invasion rates were checked by lysostaphin-gentamicin protection and were observed to be efficient; 0.52

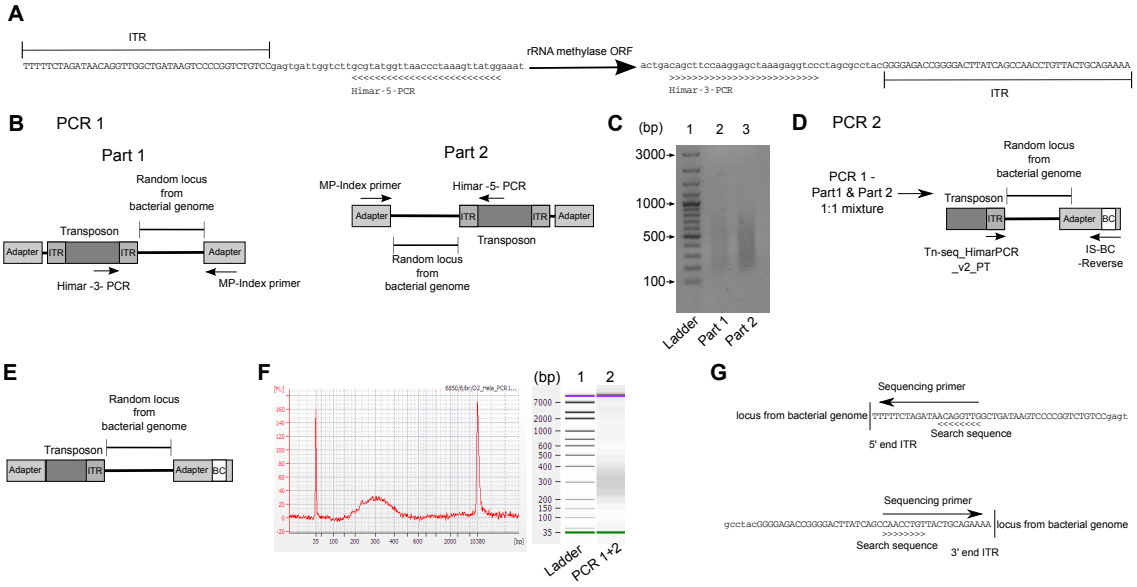

Figure 2.6: Two step PCR based enrichment of TISs and deep sequencing on Illumina® platform. (**A**) In the first PCR (PCR1) step, the loci adjacent to the 5′ and 3′ ends of the transposon, Himar-3-PCR and Himar-5-PCR primers were used. These primers have binding sites beyond the mosaic ends (ITR), within the erythromycin gene. (**B**) Two reactions were performed separately (Part 1 and Part 2) in combination with MP-Index primers containing the barcode sequence, which binds the adapter and (**C**) the products were examined by agarose gel electrophoresis. The fragment size ranged from 200-400 bp. (**D**) In the second PCR, equimolar ratio of the 5′ or 3′ products were used as template. The primer Tn-seq_HimarPCR_v2_PT re-introduces the adaptor and flow cell-specific sequence and amplified Transposon containing sequence by binding the ITRs. IS-BC-Reverse binds the distal end of the sequence introduced by MP-Index maintaining the 7 nt barcode (BC). (**E**) This resulted in fragments containing the Transposon with either of the ITRs and random locus from the bacterial genome, flanked by the adaptor-flow cell combinatorial sequences and (**F**) contained the required size range between 200-400 bp, as shown by the electrophoretogram and computer-generated image simulating agarose gel electrophoresis. (**G**) The sequencing was performed on a Illumina® 2500 machine with sequencing primers binding to the distal end of the ITR with reference to the adjacent loci, which proved advantageous during data analysis since it provided with an extended search sequence and hence indicated the transposon ends.

fold, 95% CI (0.16- 0.88), with more that 50% of the inoculum recovered shortly after infection (See Figure 2.7A). Furthermore, time required for intra-cellular bacteria to induce significant host cell death at MOI 1, was investigated. HeLa cells started dying already at 4h p.i; 13.4% and was comparatively higher at 8h p.i; 24% (See Figure 2.7B).

In addition to this, the mutant libraries were also to be tested in two different mouse models of infection: *S. aureus*-induced pneumonia[⊥] and osteomyelitis[♮]. To determine bacterial dosage required for establishing severe pneumonia in mice, *S. aureus* USA300 LAC at three different concentrations were intra-nasally administered and mice survival was monitored upto 72 hours p.i. Kaplan-Meier survival analysis showed an increase in lethality with increasing bacterial dosage and time (n=5, P= 0.009; Log rank test). After 72 hours, the lowest dosage; 0.5 x 10^8 CFUs, (Expected = 2.0, Observed = 0.0) showed the maximum survival, followed by the medium dosage; 1.0 x 10^8 CFUs (Expected = 2.0, Observed = 1.0). Whereas, the highest dosage; 2.0 x 10^8 CFUs (Expected = 2.0, Observed = 3.0) proved to be lethal (See Figure 2.7C). Although in case of strain 6850, the lower dosage; 0.7 x 10^8 CFUs (Expected = 7.58, Observed = 9.0) and the highest dosage; 2.0 x 10^8 CFUs (Expected = 7.58, Observed = 10.0) both proved

to be lethal (See Figure 2.7D).

With this prior knowledge, the mutant library in strain 6850 was tested for bacterial recovery from lungs in mouse pnemonia model at a sub-lethal concentration of 0.5 x 10^8 CFUs. Interestingly, the bacteria were eliminated from the mouse lung, indicating a possible due to lower survival rates of different mutants. Hence, mice were infected with 2.0 x 10^8 CFUs and bacteria could be recovered from the lungs after 24 hour post infection, although lower than the inoculate (See Figure 2.7E). In addition to this, bacteria were also detectable in kidney, liver and tibia 24 hours after intra-venous administration approx. 2.0 x 10^6 CFUs and were similarly lower than the inoculate used (See Figure 2.7F).

Finally to complete the screening experiments, HeLa cells were infected with *S. aureus* transposon mutant library for 8 hours during which the bacteria were kept strictly intra-cellular by supplementation with antibiotics after internalisation. During this time, some mutants were unable to either invade or survive the host cell hence would have been depleted at the end. Also, some could kill the host and were eradicated after being released into the medium, thereby enriching for the non-cytotoxic bacteria inside the host cell within the given time. The inoculate was considered as input library and the bacteria harvested by rupturing the HeLa cells, were considered as the output (See Figure 2.7G). This infection cycle was repeated three times with the output of previous cycle being used as input of the next to ensure magnification of either enrichment or depletion of mutant population. Similarly, mice were infected with the same mutant library and bacteria were recovered from organs, 24 hours post infection[♭♮] (See Figure 2.7G). All input and output libraries were analysed by Tn-seq (See Section 5.9.1), which quantified the number of TIS present in both input and output, with coverage and frequencies (See Figure 2.7F). The differences in TIS reads across all samples were analysed using DESeq2 computer algorithm[ϱ] (See Section 5.9.1.6).

[⊥] Experiments performed in collaboration with Dr. Babett Österreich and Martina Selle, Institute for Molecular Infection Biology, University of Wuerzburg, Germany.
[♮] Experiments performed by Dr. Sarah Horst, Helmholtz Centre for Infection Research, Braunschweig, Germany.
[ϱ] Post Tn-seq data processing, filtering, mapping and partial statistical analysis including DESeq2, was done by Christian Remmele and Dr. Dr. Marcus Dittrich, Chair of Bioinformatics, University of Würzburg, Germany

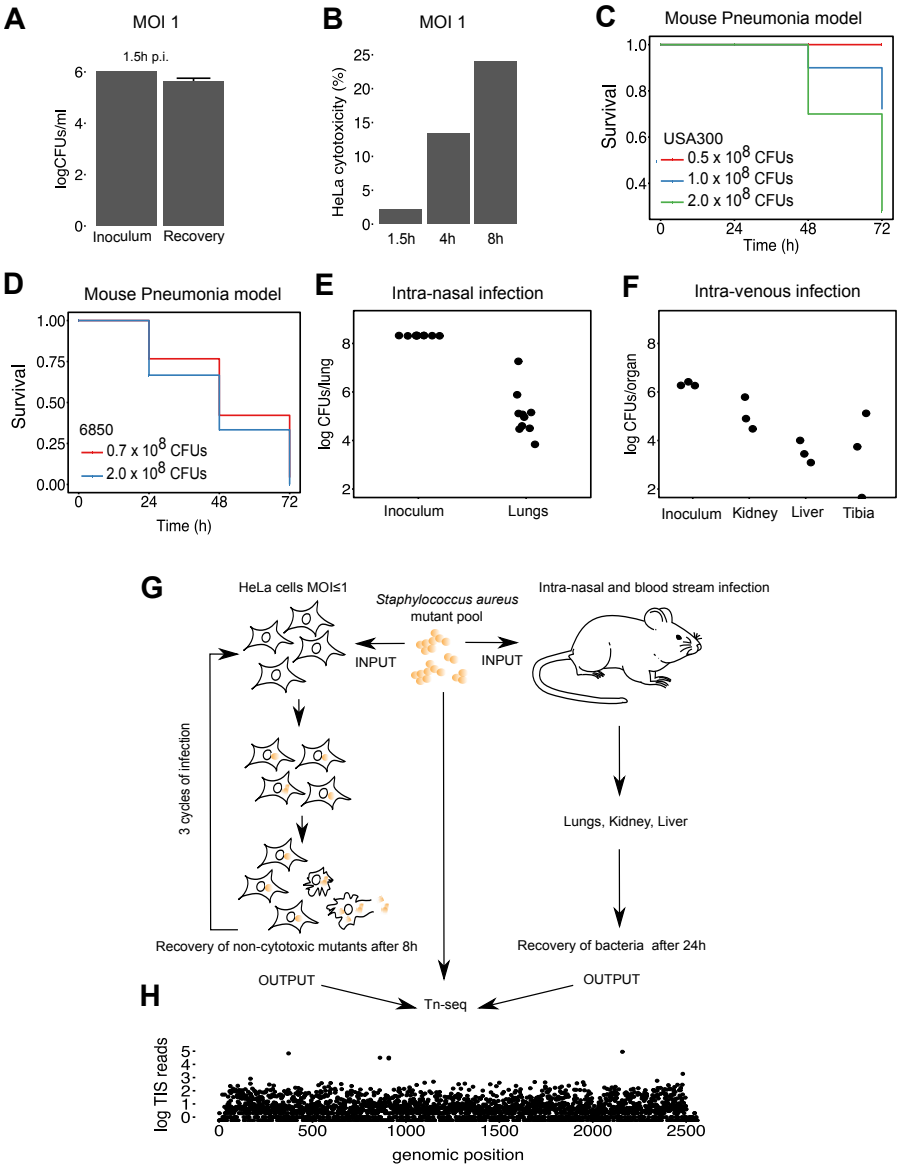

Figure 2.7: Successful implementation of infection screens *in vitro* and *in vivo* using *S. aureus* transposon mutant library and detection of global differences using Tn-seq. (**A**) HeLa cells were infected with the mutant library at MOI 1 and tested for bacterial recovery after 1.5h p.i. to assess infectivity. Bar graphs compares the mean log CFU per ml (n=3) in inoculum and recovery. (**B**) The ability of intra-cellular bacteria to kill HeLa cells after invasion at MOI 1 was assessed over time, which was to be used for the screening experiment. Bar graphs compare the percentage of HeLa cytotoxicity measured by Propidium Iodide staining, over 1.5, 4 and 8h p.i.(n=1). (**C**) Lethal and sub-lethal bacterial dosage were titrated in a mouse pneumonia model for both (**C**) USA300 LAC and (**D**) 6850 strains (n=5). Kaplan-Meier estimation curves show mice survival (y-axis) after 24, 48 and 72 hours (x-axis). The recovery of mutant library was compared to inoculum by enumeration of CFUs after 24h p.i from (**E**) mice lung after intra-nasal infection in the pneumonia model and (**F**) from Kidney, Liver and bones (Tibia) after intra-venous infection. (**G**) In an epithelial cell non-cytotoxicity model, *S. aureus* mutant library was used to infect HeLa cells at an MOI of less than equal to 1 (INPUT) and bacteria were recovered after 8 hours (OUTPUT). This infection cycle was repeated 3 times for enriching the effects. Mutant libraries were also administered intra-nasally[b] and intra-venously[h] in mice (INPUT) and bacteria were recovered from organs after 24 hours (OUTPUT). All inputs and outputs including the master library source were analysed by Tn-seq. (**H**) An exemplary manhattan plot shows reads obtained from Tranposon insertion sites and genome-wide coverage demonstrated by the sequencing results.

2.2.2 Tn-seq analyses show differential abundance of TIS reads in infection screens

Tn-seq analysis of two independently created *S. aureus* mutant library demonstrated the randomness of transposon insertion. In the aforementioned experiments Library number 6 was used, but it was also compared to a later created mutant Library number 7, which showed some similarity but were also noticeably different (See Figure 2.8A, R^2= 0.49) in frequencies and distribution of TIS.

From the HeLa cell time course experiment, the first output pool was largely similar to the inoculate (See Figure 2.8B, R^2= 0.86), indicating no abrupt changes in library complexity. Moreover, all the output libraries were perfectly co-linear with each other (See Figure 2.8C, D, R^2= 1) and also the final output to the input (See Figure 2.8E, R^2= 1). Hence, indicating that the mutants recovered during each step and at the end belong to the same population of mutants and had similar TIS distribution.

Furthermore, mutant population recovered from mouse lungs[♭] was largely similar to the inoculate (See Figure 2.8F, R^2= 0.6), although the correlation decreased when compared to that of HeLa cell experiments. Mutant libraries recovered from the mouse osteomyelitis model[♮] show similar characteristics. The bacterial populations from kidney, liver and tibia were similar to the input (See Figure 2.8G, H, I, R^2= 0.52, 0.53, 0.52) but with decreased co-linearity.

For the gene-wise analysis of TIS, all reads originating from transposon insertion sites were counted for each gene and each library. All three infection models used the same inoculum but ensure any bottleneck effects arising due to dilution of input library, median TIS read values for each gene was calculated and only TIS that were detected in two out three input libraries (median > 0) were considered to be true. TIS reads from 1924 genes out of 2559 in strain 6850 were consistently present in the inocula (See Figure 2.9A).

Taking 1924 genes into consideration, TIS read frequencies from the corresponding outputs were subtracted from the input creating difference datasets. To reduce the background noise, Interquartile range (IQR) normalisation was applied, which forces the distributions to be more even[248]. Different IQR values were obtained for outputs from *in vitro* and *in vivo* screens, and any gene with read differences more or less than the IQR cut-off were considered to be true alterations within that dataset. In the HeLa cell non-cytotoxicity model, TIS read abundances from 614 genes were increased/enriched (See Figure 2.9B) hence indicating role in host cytotoxicity or intra-host survival. Whereas, reads from 290 genes remained unchanged and 1020 gene had decreased reads.

Furthermore, TIS reads from 1746 genes seemed to be important for survival in lungs and 119 genes had possible advantages (See Figure 2.9C) in a mouse pneumonia model. Similarly, during blood stream infection in a mouse osteomyelitis model, 1580 genes had decreased TIS reads and 241 had increased read counts (See Figure 2.9D). Interestingly, in the liver and tibia most of the genes were observed to required for efficient infection and bacterial survival in these organs (See Figure 2.9E, F).

To compare genes that had altered TIS reads in one model compared to another, the difference datasets were fitted into linear models and similarities were calculated by Pearson's correlation co-efficient (R). Most of the genes that were enriched in the HeLa cells were depleted in the lungs, shown by a strong

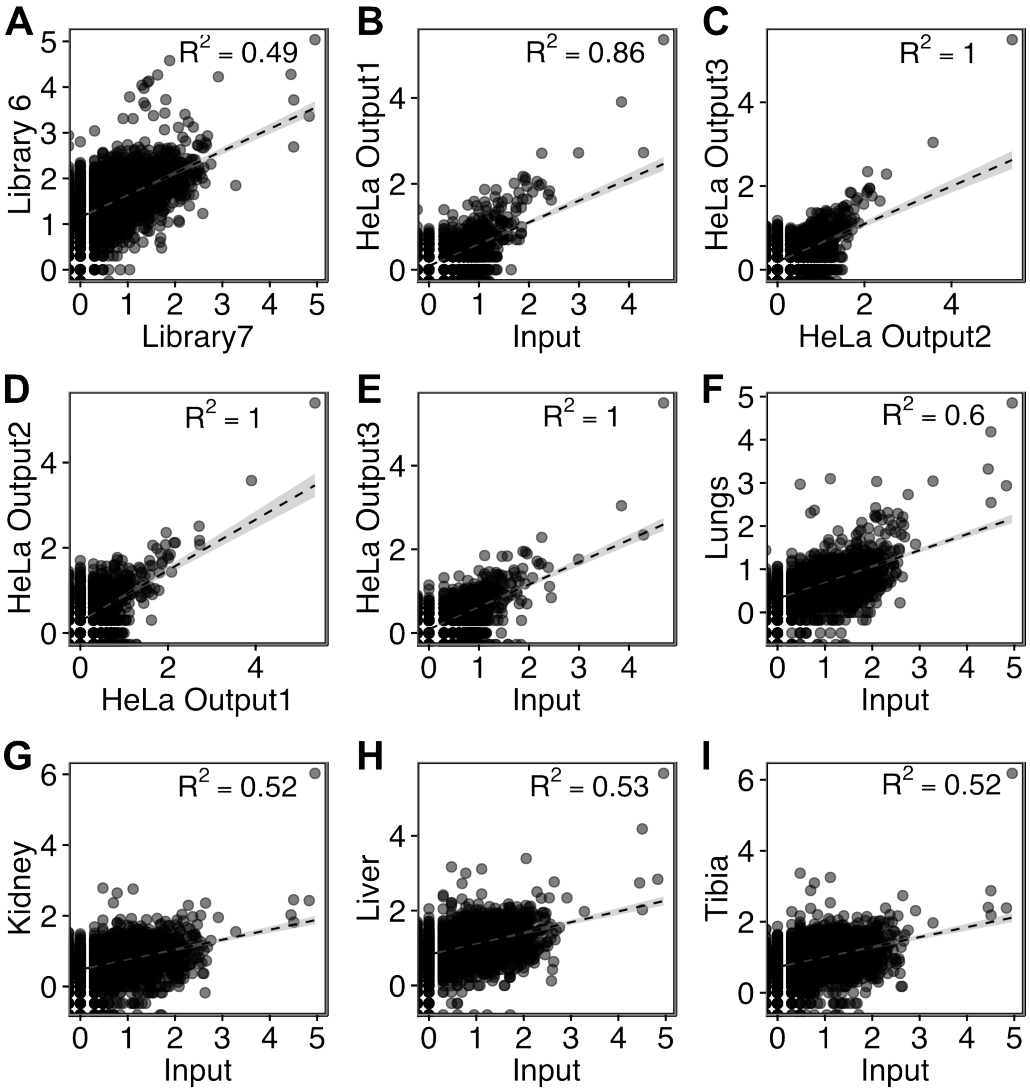

Figure 2.8: Pairwise comparison of different *S. aureus* input mutant libraries created and recovered libraries from screening experiments by determination of Pearson's correlation coefficient (R). Two independently created mutant libraries; Library 6 and 7 (**A**) show co-linearity but slightly deviating from each other in gene-wise TIS read and complexity (R^2=0.49). During the HeLa cell non-cytotoxicity screen, the input representing the master library and the output libraries were highly similar to each other (**B-E**, R^2=0.86, 1, 1, 1) indicating no drastic change in TIS composition. Whereas during *in vivo* experiments, although largely co-linear the outputs from Lung (**F**, R^2=0.6), Kidney (**G**, R^2=0.52), Liver (**H**, R^2=0.53) and Tibia (**I**, R^2=0.52), also deviated from the input in TIS composition

correlation and a negative slope (See Figure 2.10A, m= -5.37, adj. R^2= 0.88).In addition to this, most of the mutations that were enriched in HeLa were increased in mouse kidneys determined by a marginally positive slope, with exception of a few genes (See Figure 2.10A, m= 0.183, adj. R^2= 0.89). This effect was similar in liver and tibia, although in liver the mutants that were increased had decreased correlation with those enriched in HeLa (See Figure 2.10C, m= 0.25, adj. R^2= 0.53), thus indicating a mixed effect. However, the bacteria obtained from tibia highly correlated with that of HeLa, although with marginally positive slope (See Figure 2.10D, m= 0.13, adj. R^2= 0.95). The discrepancies between positive correlation and slope values very close to zero was due to some genes like *gua*A, *ssr*42, RSAU000852 and *rsp* , which exhibited significantly large differences. More details about individual genes in the following Section

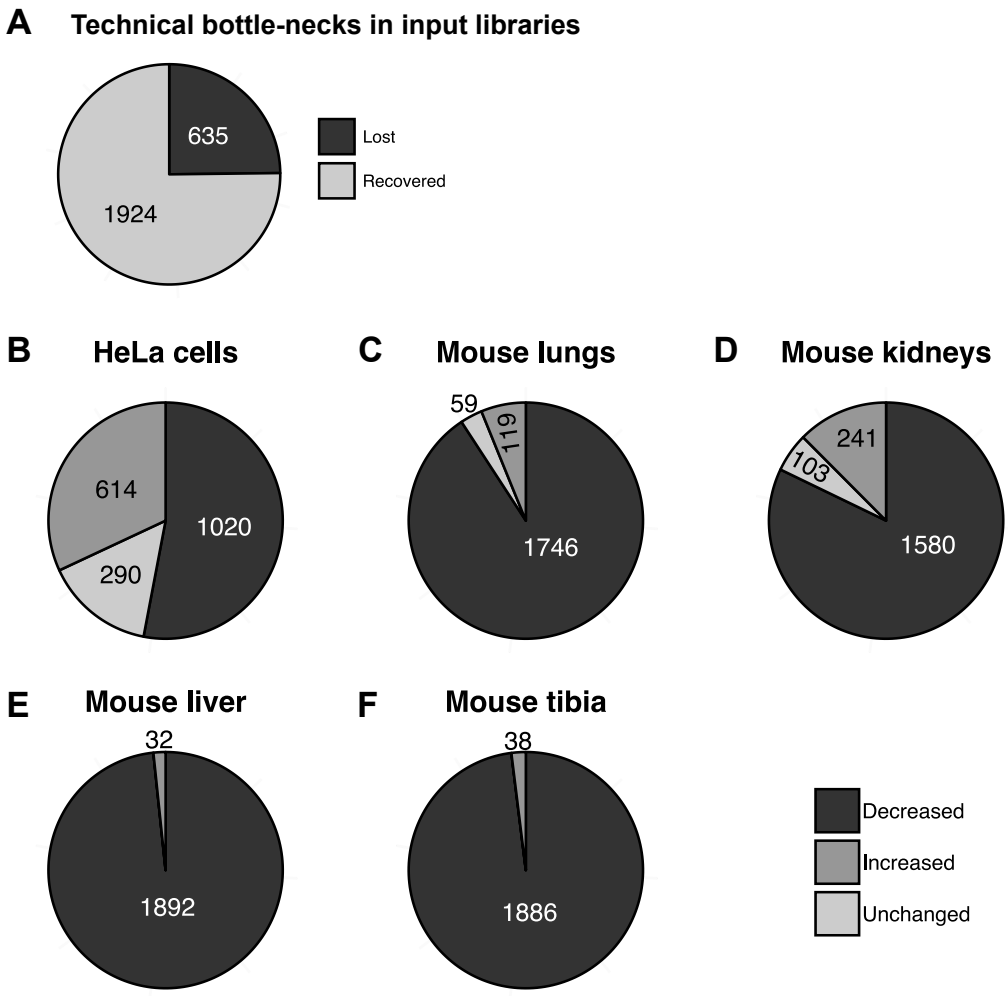

Figure 2.9: Changes in TIS reads from each gene, across different host niches and infection models analysed by Tn-seq. Prior to evaluating all genes, for TIS read frequencies the input library was examined for technical bottle-neck effects arising due to dilution of inocula. All 3 inputs were compared to each and (**A**) the result is displayed as a pie chart showing that 1924 out of 2559 genes in *S. aureus* 6850, were present in 2 out 3 inputs. Within those genes, alteration in TIS read numbers were calculated with IQR normalisation and represented as pie charts, which shows changes in gene-wise comparison TIS read abundances from (**B**) HeLa cells , (**C**) Mouse lungs, (**D**) kidneys, (**E**) liver and (**F**) tibia.

2.2.3.

2.2.3 Non-cytotoxicity screen in HeLa cells identify novel bacterial factors for intracellular virulence

Gene-wise analysis of Tn-seq data obtained from the HeLa cell non-cytotoxicity screen identified several factors that were significantly enriched or depleted inside the host cell (See Table 2.2, G.1). There were several mutations that rendered *S. aureus* either unable to invade or survive the host cells. Most prominently, the genes involved in *de novo* purine salvage and biosynthesis axis, and the genes belonging to the *pur* operon. *gua*A (adj. P<0.001) encoding for a bi-functional guanosine monophosphate (GMP) synthetase, which is an important part of the *de novo* purine biosynthesis and has been reported to be

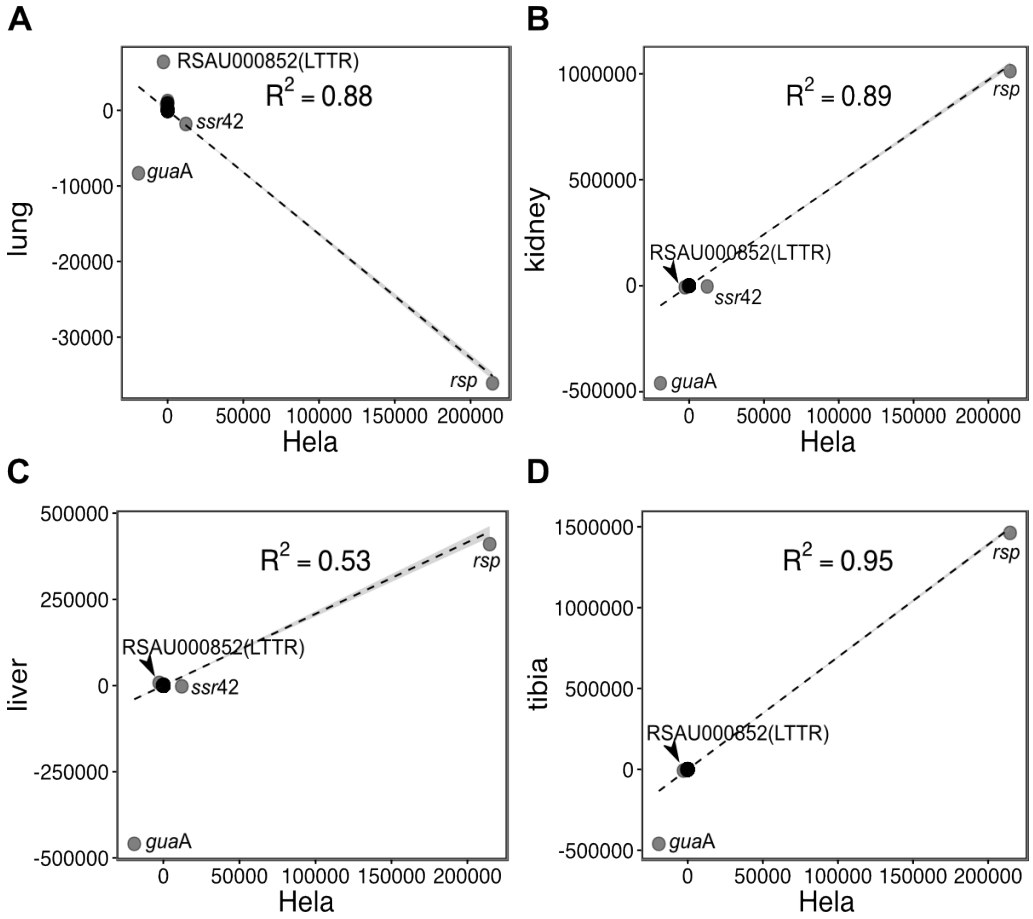

Figure 2.10: Multi-infection model gene-wise comparison of TIS show differential behavior of genes. Difference datasets generated by comparing the output from various infection models to the input mutant library. HeLa cell dataset was fitted to a linear regression model with either (**A**) mouse lungs dataset, (**B**) kidney, (**C**) liver or (**D**) tibia datasets. Scatter plots show difference in TIS frequency distribution of genes on HeLa compared to input (x-axis) against differences in mice organs, where each dot represent a gene and co-linearity was expressed as Pearson's correlation co-efficient (R)

important for stringent stress response and bacterial survival *in vivo*[249–251]. Belonging to the same pathway, the genes *pur* operon; *pur*R (adj. *P*= 0.01) and *pur*M (adj. *P*= 0.002) encode *pur* operon repressor and phosphoribosylformyl cyclo-ligase respectively. Similarly, *pbu*X (adj. *P*<0.001) coding for xanthine permease is an important part of purine salvage in *S. aureus*.

In addition to this, mutants of genes involved in sugar metabolism, such as a sucrose uptake enzyme[252] (*scr*A, adj. *P*= 0.035) and an excreted glycolytic aldolase (*fba*A, adj. *P*= 0.035), were depleted in the screen. Although roles of the aforementioned genes in bacterial physiology and in animal infection models are known, this screen identifies their new role in *S. aureus* intra-cellular virulence.

Transposon mutants that were significantly enriched included insertions in gene coding a lipase, DNA helicase, a haem metabolism enyzme, non-coding RNA and a transcription regulator. Staphylococcal Lipase or glycerol ester hydrolase encoded by *geh* (adj. *P*= 0.03), is secreted by the bacteria and has been implicated in interference with host functions and virulence[253]. Furthermore, the gene *ruv*A (adj. *P*= 0.044) produces an important DNA resolving enzyme; RuvA that takes part in genetic recom-

Table 2.2: Gene-wise analyis of Tn-seq screening results from *S. aureus* Himar1 transposon mutant library non-cytotoxic screen in HeLa cells

Gene/Locus ID[a]	Trend[b]	*P* value[c]	Product
*ssr*42	Increasing	$<1.0 \times 10^{-3}$	Small stable RNA (SSR) 42
*gua*A	Decreasing	3.0×10^{-4}	bifunctional GMP synthetase
rsp	Increasing	4.0×10^{-4}	AraC-type transcriptional regulator
RSAU_000220	Decreasing	4.0×10^{-4}	transmembrane efflux pump protein, putative
*pbu*X	Decreasing	4.0×10^{-4}	xanthine permease
*pur*M	Decreasing	2.9×10^{-3}	phosphoribosylformylglycinamidine cyclo-ligase; PurM
RSAU_001920	Decreasing	8.1×10^{-3}	ATP-dependent RNA helicase, DEAD box family
RSAU_002160	Decreasing	8.1×10^{-3}	phosphosugar-binding transcriptional regulator
*pur*R	Decreasing	1.2×10^{-2}	pur operon repressor; PurR
RSAU_001914	Decreasing	1.8×10^{-2}	putative membrane protein
*def*2	Decreasing	2.9×10^{-2}	polypeptide deformylase
RSAU_000132	Decreasing	3.5×10^{-2}	hypothetical protein
RSAU_000181	Decreasing	3.5×10^{-2}	putative membrane protein
*scr*A	Decreasing	3.5×10^{-2}	PTS system sucrose-specific IIBC component
*fba*A	Decreasing	3.5×10^{-2}	fructose-bisphosphate aldolase
geh	Increasing	3.6×10^{-2}	glycerol ester hydrolase
*ruv*A	Increasing	4.4×10^{-2}	Holliday junction DNA helicase; RuvA
RSAU_002327	Decreasing	4.6×10^{-2}	transposase IstA, putative
*hem*L	Increasing	4.9×10^{-2}	glutamate-1-semialdehyde aminotransferase

[a] NCBI Genbank Accession ID CP006706.1.

[b] Intracellular abundance and trend followed by transposon mutant in the corresponding loci, throughout the course of HeLa non-cytotoxicity screening.

[c] *P* values were corrected for multiple comparisons. In this table, only genes/loci with $P < 0.05$ are shown. For further details see Appendix G

bination[254] and *hem*L (adj. $P = 0.044$) codes for a glutamate-1-semialdehyde transferase that is part of haem biosynthesis pathway in *S. aureus*.

Two most significantly enriched mutants were within the Small stable RNA (SSR) 42 (*ssr*42, $P<0.001$), a non-conding regulatory RNA that positively influences the production of α-haemolysin[255] and the gene encoding Repressor of surface proteins (*rsp*, $P<0.001$) that has been reported to negatively influence surface protein and biofilm formation in *S. aureus*[256]. Site-wise analysis of Tn-seq not only provided with high resolution information of every single TIS, but also the significant changes in frequency during the HeLa cell screen (See Figure 2.11). This also revealed the juxtaposition of *rsp* and *ssr*42 in the *S. aureus* genome, and the sites within them that had the largest significant changes during the HeLa cell screen (See Figure 2.11 (inset), $P< 0.05$) after statistical evaluation using DESeq2. For detailed site-wise analysis refer to Table G.2.

Although, gene-wise analysis did not allot a significant *P* value to the locus RSAU_000852 coding for a LysR-type transcription regulator (LTTR), but site-wise analysis showed 4 TIS recovered from this gene and were depleted in the HeLa cell fraction. Amongst those 2 TIS at position 921654 ($P= 0.018$), 921655 ($P< 0.001$) were significantly depleted (See Table G.2).

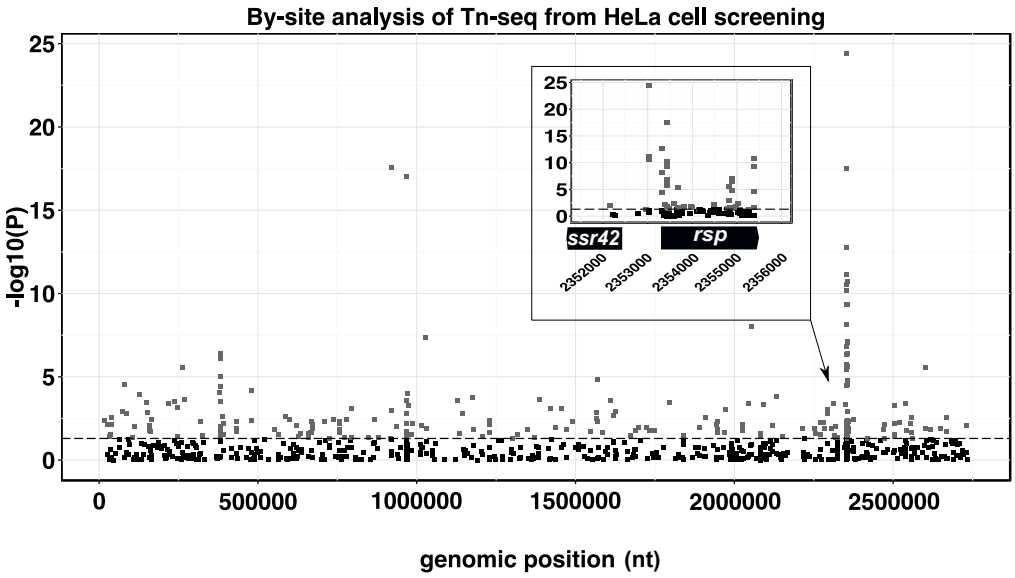

Figure 2.11: Site-wise statistical analysis of Tn-seq screen in HeLa cell non-cytotoxicity model. A manhattan plot showing the *P* values (y-axis), represented as negative logarithms (-log10 P), associated with every TIS (x-axis) after evaluation of differences in read frequencies obtained after screening in HeLa cells, throughout the genome of *S. aureus* 6850. -log10 P value threshold was set to 1.3 (α= 0.05, dotted line). Inset shows a magnified view of TIS originating from *rsp* and *ssr*42 , which were significantly enriched in HeLa cell non-cytotoxicity screen analysed by Tn-seq.

2.2.4 Multi-infection model comparison shows differential behavior of identified bacterial factors

Mutant library screening in mouse lungs also identified several insertions for which were either enriched or depleted in Tn-seq analysis (See Table 2.3). There were several genes that were common to both HeLa and lungs. But majority of genes that were enriched in HeLa cells were depleted in the mouse lung (See Figure 2.10A).

Similar to the HeLa screen, *gua*A (adj. *P*<0.001) was one of the top genes required for survival in the lung and the mutants were severely depleted in both screens (See Figure 2.10A). Unlike in the HeLa cells, there were some exclusively depleted TIS in lungs, originating from genes coding for glutamine amidotransferase (adj. *P*<0.001), which is crucial for glutamine usage in protein translation, CorA magnesium transporter (adj. *P*<0.001) and *ure*D (adj. *P*= 0.008), which is a component of the Urease operon that has been previously reported to be important *in vivo*[257].

Furthermore, the gene *aus*A (adj. *P*= 0.008) coding for one component of a non-ribosomal peptide synthetase (NRPS), was identified for the first time to be crucial for lung pneumonia. In addition to this, there were several TIS from genes of unknown functions, which were depleted in the lungs (See Table 2.3). On the other hand, there were genes producing nucleosidase and proteins in RNA metabolism that did not seem to be required for bacterial survival in lungs. Increasing trend in TIS frequency was observed for a gene; RSAU000802 (adj. *P*= 0.007) with putative 5′-nucleotidase function. A protein of similar function; AdsA has been shown to produce an extracellular adenosine-derivative for modu-

Table 2.3: Gene-wise analyis of Tn-seq screening results of *S. aureus* Himar1 transposon mutant library from mouse lungs

Gene /Locus ID[a]	Trend[b]	*P* value[c]	Product
*gua*A	Decreasing	$<1.0 \times 10^{-3}$	bifunctional GMP synthetase
RSAU_001762	Decreasing	$<1.0 \times 10^{-3}$	type 1 glutamine amidotransferase
RSAU_002181	Decreasing	$<1.0 \times 10^{-3}$	CorA-like Mg^{2+} transporter
RSAU_002354	Decreasing	4.0×10^{-3}	hypothetical protein
RSAU_000347	Decreasing	4.0×10^{-3}	hypothetical protein
RSAU_000919	Decreasing	4.0×10^{-3}	hypothetical protein
RSAU_002284	Decreasing	4.0×10^{-3}	drug transporter, putative
RSAU_002139	Decreasing	5.0×10^{-3}	hypothetical protein
RSAU_000898	Decreasing	6.0×10^{-3}	hypothetical protein
RSAU_000034	Decreasing	7.0×10^{-3}	putative transposase
RSAU_000802	Increasing	7.0×10^{-3}	5'-nucleotidase
*que*F	Increasing	7.0×10^{-3}	7-cyano-7-deazaguanine reductase
*ure*D	Decreasing	8.0×10^{-3}	urease accessory protein UreD
*aus*A	Decreasing	8.0×10^{-3}	non-ribosomal peptide synthetase
*rpo*E	Increasing	8.0×10^{-3}	DNA-directed RNA polymerase, delta subunit
*sbn*C	Decreasing	9.0×10^{-3}	IucC-family siderophore biosynthesis protein
hps	Decreasing	1.0×10^{-2}	hexulose-6-phosphate synthetase
*ylm*G	Decreasing	1.0×10^{-2}	YlmG membrane protein
*ssr*42	Decreasing	1.0×10^{-2}	ssr42
rsp	Decreasing	9.7×10^{-1}	AraC-family transcription regulator

[a] NCBI Genbank Accession ID CP006706.1.

[b] Intra-organ abundance and trend followed by transposon mutant in the corresponding loci, after 24 hours in mice lung.

[c] *P* values were corrected for multiple comparisons. In this table, only genes/loci with $P < 0.05$ are shown. For further details see Appendix G

lation of host immune defense[258]. Similarly, *que*F (adj. $P = 0.007$) producing 7-cyano-7-deazoguanine reductase, which is involved in tRNA-queuosine biosynthesis was also enriched. Interestingly, the gene *rpo*E (adj. $P = 0.008$) coding for an additional subunit of DNA-dependent RNA polymerase in *S. aureus* , which has been shown to control toxin production, was not required for survival in lungs. TIS from RSAU000852 were also increased in the lungs as opposed to being depleted in the HeLa cell screen (See Figure 2.10A).

The two most crucial *S. aureus* genes that were important for intra-cellular cytotoxicity; *ssr*42 (adj. $P = 0.007$) and *rsp* (adj. $P = 0.9$) unlike HeLa cell screen, were depleted in lungs (See Figure 2.10A, 2.3). Gene-wise analysis did not confer a good *P* value to overall TIS from *rsp*, but site-wise analysis could show significant TIS depletion in case of *ssr*42 and a total of 26 TIS from *rsp* to be significantly depleted up to 3-fold ($P < 0.05$, See Figure 2.12, Table G.2).

S. aureus genes identified to be important in HeLa cell non-cytotoxicity model and the mouse pneumonia model were compared with the Tn-seq results from mouse kidneys, liver and bones. Similar to the effect observed in lungs, *gua*A mutants were severely attenuated in all three organs (See Figure 2.10B, C, D). Interestingly, TIS from locus encoding the LTTR were depleted in kidneys and tibia (See

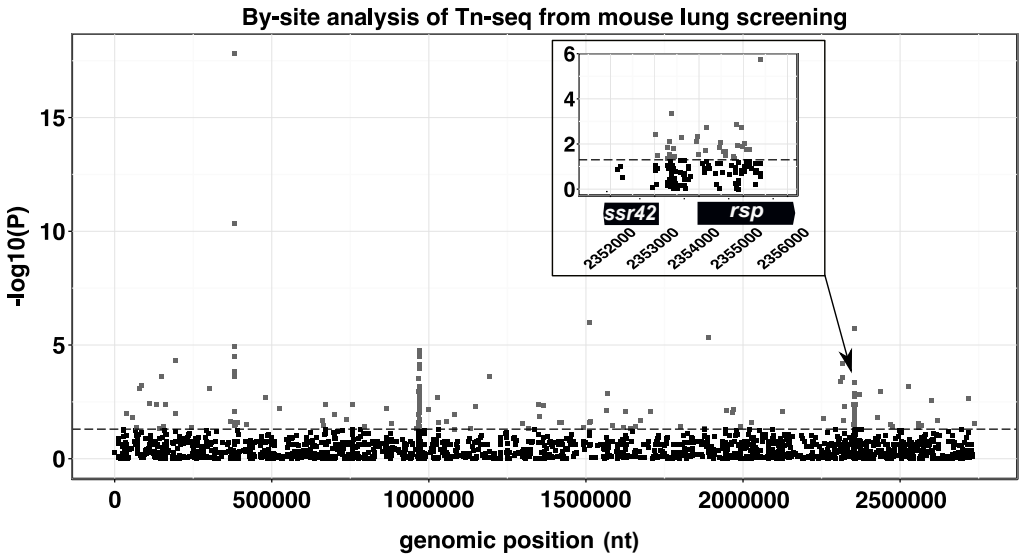

Figure 2.12: Site-wise statistical analysis of Tn-seq screen in mouse pneumonia model 24 hours post infection. A manhattan plot showing the *P* values (y-axis) represented as negative logarithms (-log10P), associated with every TIS (x-axis) after evaluation of differences in read frequencies obtained after screening in mouse lungs, throughout the genome of *S. aureus* 6850. -log10P value threshold was set to 1.3 (α= 0.05, dotted line). Inset shows a magnified view of TIS originating from *rsp* and *ssr*42, which were depleted in lungs analysed by Tn-seq.

Figure 2.10B, D), but not in liver (See Figure 2.10C). On the contrary, *ssr*42 seemed to be important for infection in kidneys and liver (See Figure 2.10B, C). Although, TIS from *rsp* were enriched in kidneys, liver and tibia unlike the lungs, indicating that either its not required for invasive blood stream infection or enhances the same.

Chapter 3

Repressor of surface proteins (Rsp) is a major regulator of *S. aureus* virulence

3.1 Rsp is vital for staphylococcal haemolysis

Pore-forming toxins of *S. aureus* can lyse erythrocytes efficiently causing haemolysis and *S. aureus* strains are routinely tested for haemolysis of sheep blood for characterisation. Rupture of erythrocytes leads to the release of haemoglobin, which imparts a bright red color and can be quantified spectrophotometrically at 540 nm or visualized on blood agar. Haemolytic activity is defined as the quantity haemoglobin release over a given time. On agar supplemented with sheep blood, complete haemolysis is presented by formation of a typical bright and clear yellow zone around the bacterial colony. To investigate the haemolytic potential of *rsp* mutants, experiments were performed in suspension and on semi-solid medium.

3.1.1 *S. aureus rsp* mutant secretions show attenuated haemolytic activity

Prior to testing the mutant, haemolytic activity of USA300 JE2 wild type was examined to optimize the concentration of intoxication. Overnight culture filtrates from *S. aureus* wild type caused haemolysis in a dose-dependent manner at 37°C and was co-linear with increasing percentage of culture filtrates (R^2 = 0.96, See Figure 3.1A), after 1 hour post intoxication. Unconditioned TSB medium showed negligible haemolysis; OD 0.04, 95% CI (0.034 - 0.057) compared to haemolysis caused by sterile water; OD 0.608, 95% CI (0.59 - 0.61), $P< 0.001$, which was accounted for 100% or total haemolysis. No significant increase in haemolysis observed at 0.5%; OD 0.056, 95% CI (0.04- 0.06), $P= 0.186$, but increased steadily from 1%; OD 0.067, 95% CI (0.05 - 0.07), $P= 0.009$, reaching half-maximum at 5%; OD 0.3, 95% CI (0.29 - 0.31), $P< 0.001$, which was accounted for the 50% Lethal Dose (LD_{50}). Interestingly, further increase in concentration of culture filtrates at 10% ($P = 0.29$) and 20% ($P = 0.99$) (See Figure 3.1B), did not result in more haemolysis when compared to LD_{50}. Haemolysis caused by phosphate buffer (1X PBS) and 20%

Triton X-100 treatment were observed, as additional controls.

Haemolysis due to the *rsp* insertional mutant, NE1304 (See Appendix Table A.1) was similar to wild type at lower concentrations of 0.5% ($P = 0.99$), 1% ($P = 0.99$) and 2% ($P = 0.12$). However, haemolytic activity of the mutant plummeted significantly at LD_{50} i.e. 5%; OD 0.1, 95% CI (0.08 - 0.11), $P< 0.001$) and was significantly low throughout, even at higher concentrations of 10% ($P < 0.001$) and 20% ($P < 0.001$)(See Figure 3.1B). Although, it should be noted that haemolysis due to the mutant increased at 10% ($P < 0.001$), when compared to its value at LD_{50}.

3.1.2 *rsp* mutants lack complete haemolysis

On blood agar, *S. aureus* mutants in *rsp* lacked complete haemolysis. The diameter of haemolysis zones were measured after spotting bacteria on sheep blood agar and incubation at 37°C. Prominent haemolysis was observed for wild type *S. aureus* USA300 LAC*; 5.39 mm, 95% CI (5.20 - 5.58) and 6850; 6.91 mm, 95% CI (6.72 - 7.10). However, the haemolysis zone around *rsp* mutants were significantly smaller, for both genetic backgrounds of USA300; 2.08 mm, 95% CI (1.89 - 2.27), $P< 0.001$ and 6850; 1.65 mm, 95% CI (1.46 - 1.84), $P< 0.001$ (See Figure 3.1C). The haemolysis phenotype was rescued upon reintroduction of *rsp in trans* on the plasmid pS2217 (For construction details see Materials and Methods, Section 5.8), reaching wild type levels in both USA300; 6.46 mm, 95% CI (6.28 - 6.65) and 6850; 6.52 mm 95% CI (6.34 - 6.71). Upon further incubation of the plates at lower temperatures (4°C), haemolysis due to β-haemolysin appeared in case of 6850 *rsp* mutant. Hence, indicating the loss of α-haemolysin (See Figure 3.1C).

3.1.3 Rsp-mediated haemolysis is dependent on the *agr* quorum sensing system

To further investigate the role of *rsp* in haemolysis, the multi-copy plasmid pS2217 was introduced into *S. aureus* RN4220 (*agr*$^+$), with dysfunctional *agr* quorum sensing system[164] and RN6911 (*agr*$^-$), which lacks the *agr* operon[165]. Both of these strains did not produce measurable haemolysis zone; 0 mm, 95% CI (-0.64 - +0.64) (See Figure 3.1D). But interestingly in presence of excess *rsp* , visible and significant haemolysis was produced around RN4220 pS2217; 2.2 mm, 95% CI (1.55 - 2.85), $P= 0.0023$. Hence, this indicates that *rsp* alone can promote haemolysis. However, the diameter of *rsp*-mediated haemolysis in RN4220 still appeared significantly smaller than in 6850 or USA300 wild type bacteria ($P = 0.029$) and no visible haemolysis was observed in case of RN6911 pS2217; 0 mm, 95% CI (-0.64 - +0.64).

In addition, in an *agr* mutant, the relative expression of *rsp* analysed by quantitative real time PCR, was found to be lower at stationary growth phase; 0.42, 95% (CI -0.05 - +0.9), when the expression *agr* is usually higher (See Figure 3.1E). This hints towards the presence of a functional *agr* system for *rsp* expression and consequent haemolysis.

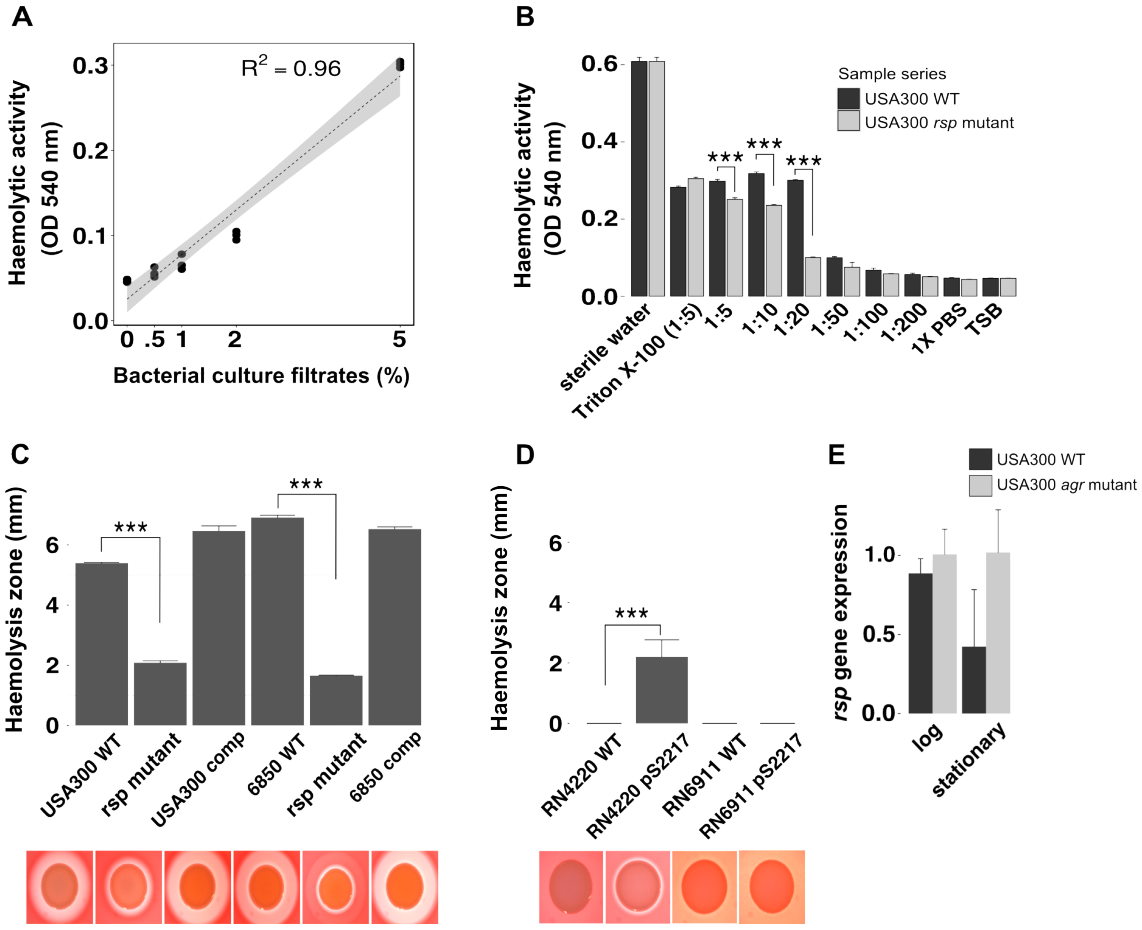

Figure 3.1: Rsp is indispensable for *S. aureus* mediated haemolysis. Staphylococcal haemolysis was investigated using two different methods. (**A**) Haemolytic activity of wild type USA300 JE2 strain in sheep blood measured at 540 nm (y-axis), was dose dependent and had increasing co-linearity with doses of bacterial overnight culture filtrates (x-axis), R^2 = 0.96. (**B**) Varying ratios of culture filtrates from wild type *S. aureus* (USA300 WT, black bars) and insertion mutant NE1304 (USA300 *rsp* mutant, gray), were tested for haemolytic activity, and were compared to sterile water, Triton X-100 (1:5), 1X PBS and unconditioned TSB medium. Bar plots show mean optical density at 540 nm and SEM as error bars. Statistical analysis was done by pairwise t-test. ***; P< 0.001. (**C**, **D**) Haemolysis examined on sheep blood agar and diameter of haemolysis zones plotted (y-axis) for wild type bacteria (USA300 WT and 6850 WT), isogenic *rsp* mutants and complemented bacteria (USA300 comp and 6850 comp). Also in case of *rsp* over-expression from plasmid pS2217, in *S. aureus* strains RN4220 and RN6911. Bar plots show mean diameter of haemolysis zone in millimeters (mm) and SEM as error bars. Statistical analysis was performed by one-way ANOVA and Tukeyś HSD test for individual comparisons. ***; $P < 0.001$. (**E**) Relative expression of *rsp* (y-axis) was performed by quantitative real time PCR, in wild type *S. aureus* (USA300 WT, black) and isogenic insertion mutant in *agr*A (USA300 *agr* mutant, gray), during logarithmic and stationary growth phase (x-axis). Bar plots show mean RQ with SEM as error bars.

3.2 Rsp influences *S. aureus* -mediated intra-cellular virulence and host cytotoxicity *in vitro.*

The significant abundance of *rsp* mutants in the non-cytotoxic fraction recovered from HeLa cells and its role in α-toxin production (See Figure 3.1), indicate its precedence in *S. aureus* -mediated intra-cellular virulence in the host cell.

3.2.1 Rsp does not influence bacterial proliferation, invasion and escape from host phagolysosomes

Prior to investigating the role of Rsp in host cell death, the influence of Rsp on bacterial proliferation and invasion, was investigated. The growth rate of *rsp* mutants from both USA300 and 6850 genotypes *in vitro* was investigated by culturing in TSB medium for 24 hours and comparing it to wild type bacteria. Optical densities was measured in an automated fashion every 30 minutes (See Figure 3.2A). Growth of both wild type strains did not differ significantly ($P = 0.5129$). More importantly, mutants in *rsp* and its respective wild type counterparts did not show any noticeable contradiction in growth.

Invasion into the host cell can determine the intra-cellular abundance of bacteria, which was assessed by Lysostaphin-gentamicin protection assay (See Section 5.13.1). HeLa cells were infected with 6850 *rsp* mutants, isogenic wild type and complemented mutants. Enumeration of CFUs recovered 90 minutes post infection, did not show any significant difference between all three groups (See Figure 3.2B). Therefore indicating similar bacterial abundances in the host cell at initial stages of infection.

Furthermore, the influence of *rsp* mutation on *S. aureus* phagosomal escape was analysed[⊛], since this event has significant effect on bacterial survival within host cells [153,213]. HeLa YFP-CWT cells (See Appendix A, Table A.3) were infected with *S. aureus* USA300 JE2 wild type, *rsp* mutant (NE1304) and *agr* mutant (NE1532), and escape rates were quantified by automated fluorescence microscopy (See Section 3.2.1). Whereas USA300 JE2 wild type escaped efficiently from the host phagolysosome; 83.96%, 95% CI (63.14 - 104.78) and NE1532 was highly attenuated; 3.98%, 95% CI (-16.83 - +24.80), P= 0.0013 (See Figure 3.2C), a phenomenon that has also been described previously [153]. On the contrary, *rsp* mutants translocated to the host cytoplasm with similar escape efficiency as the wild type; 70.24%, 95% (CI 49.42-91.07), P= 0.52.

Phagosomal escape precedes replication of *S. aureus* in the host cytoplasm, which is followed by host cell death [213]. Since there was no remarkable effect of *rsp* mutation on this intra-cellular event, the ability of mutants to proliferate within the host cell was investigated by fluorescence accumulation over time. Increase in fluorescent signal over time could be attributed to bacterial replication inside the host cell and was quantified by flow cytometry at 607 nm. Lysostaphin-Gentamicin protection assay was performed (See Section 5.13.1), where HeLa cells were infected with *S. aureus* 6850 wild type and *rsp* mutants, expressing monomeric red fluorescent protein (mRFP) *in trans* [259] and fluorescence was measured at 90 and 180 minutes post infection. A linear increase in fluorescence over time indicated by a positive difference in slope (m) = 5671, successfully demonstrated bacterial replication inside the host. The slopes obtained for both wild type and *rsp* mutants did not show any significant difference ($P = 0.38$).

[⊛] Experiments performed by Sebastian Blättner, Chair of Microbiology, University of Würzburg, Germany.

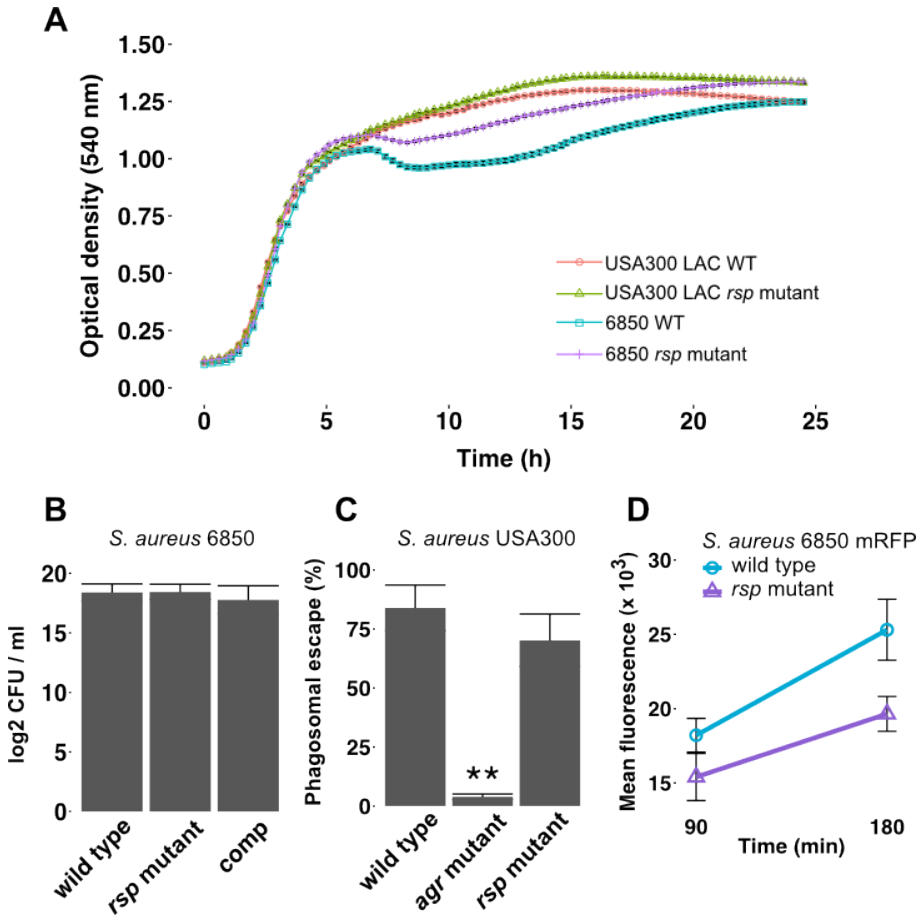

Figure 3.2: Rsp does not influence *S. aureus* invasion, phagosomal escape and proliferation in the host cell. (**A**) Bacterial growth in TSB was expressed in terms of optical density at 540 nm (y-axis) over time (x-axis). Wild type *S. aureus* ; USA300 WT (red) and 6850 WT (blue) were compared to *rsp* mutants (green, purple), with data recorded every 30 minutes. Line graph shows comparison of mean optical density as points and SEM as error bars. (**B**) Invasion potential of *S. aureus* 6850 *rsp* mutant was compared to isogenic wild type and complemented mutant (comp). Bacteria were recovered from HeLa cells 90 minutes post infection and CFUs were enumerated by plating on agar. Bar plots show mean CFU per milliliter expressed in logarithmic scale (y-axis).(**C**) Post-invasion, the ability of *rsp* mutant in *S. aureus* USA300 to escape from host phagolysosomes, was tested via confocal microscopy and compared to isogenic wild type and *agr*A mutant. Bar plots show mean relative escape (y-axis) and SEM as error bars. Statistical analysis was performed by one-way ANOVA and Tukey's HSD test for individual comparison. (**D**) Proliferation of monomeric red fluorescent protein (mRFP) expressing wild type and *rsp* mutant in the host cytoplasm post invasion, was tested by quantification of increase in fluorescence (y-axis) with given time (x-axis). Line graph shows mean fluorescence quantified by flow cytometry as points and SEM as error bars. Statistical analysis was performed by two-way ANCOVA, assessing difference in slopes. **; $P<0.01$

3.2.2 Rsp specifically influences intra-cellular pathogen-induced host cell death

Considering the results from HeLa cell screening and the influence on other intra-cellular events, it was hypothesized that Rsp could have a role in host cell death after escaping into the cytoplasm. To investigate this further, a kinetics experiment determining intra-cellular *S. aureus*-induced host cell death over time, was performed. HeLa cells were infected as previously described (See Section 5.13.1), either with USA300 LAC* wild type, isogenic *rsp* mutant, complemented *rsp* mutant, *agr*A mutant (NE1532) and *sae*R mutant (NE1622) or left uninfected. Cell death was determined at 1.5, 4, 8 and 24 hours post infection for all samples, by quantifying the cellular uptake of Propidium Iodide (PI) by flow cytometry (See Section 5.14.1).

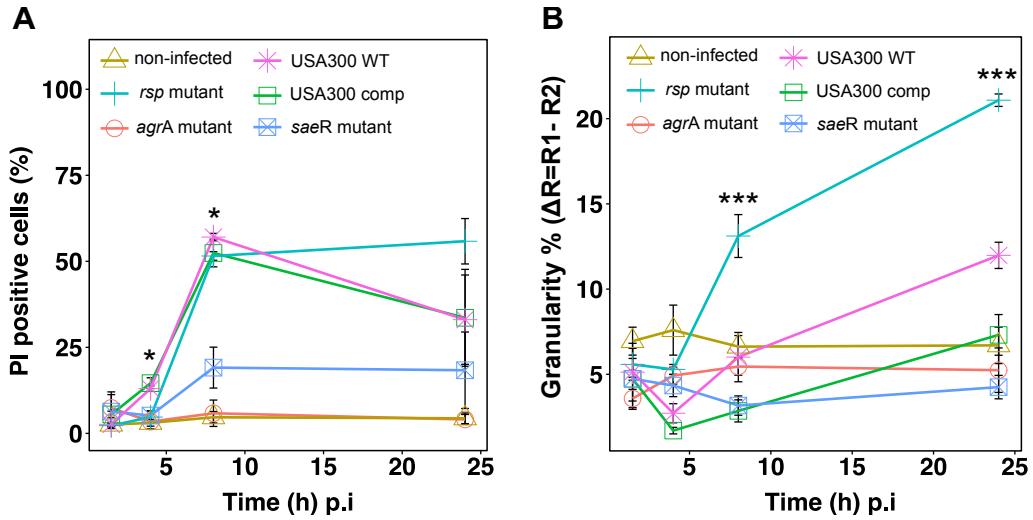

Figure 3.3: *S. aureus rsp* mutants show reduced but delayed host cytotoxicity. **(A)** Plot depicting a kinetics experiment, by quantifying the percentage of dying HeLa cells that took up the stain Propidium Iodide (PI, y-axis) over time (x-axis). The cells were either left uninfected or infected with *S. aureus* strain USA300 LAC* wild type (USA300 WT), its isogenic *rsp* mutant and complemented mutants (USA300 comp). Cytotoxicity was compared to mutants in *agr*A and *sae*R. (**B**) Simultaneously the cellular granularity was examined, which could indicate the cytoplasmi presence of bacteria. Percentage Granularity (ΔR) (y-axis) was calculated over time (x-axis), by gating the side scatter of the non-infected (R1) and compared to that of infected samples (R2) *; P<0.05, ***; P<0.001 for wild type vs *rsp* mutant

At 4 hours post infection, host cell death caused by *rsp* mutants; 4.75%, 95% CI (-5.88 - +15.38) was significantly less when compared to the wild type bacteria; 13.01%, 95% CI (2.38 - 23.64), P= 0.0147 (See Figure 3.3A). This effect was recovered after complementation of the *rsp in trans* from an episomal location; 14.6%, 95% CI (3.96 - 25.23) . Cytotoxicity of *rsp* mutants was comparable to that of *agr*A; 3.41%, 95% CI (-7.21 - +14.04) and *sae*R; 5.18%, 95% CI (-5.44 - +15.81). Interestingly, *rsp* mutants gained cytotoxic potential later at 8 hours; 51.55%, 95% CI (40.91 - 62.18) but still significantly lower than the wild type (P = 0.028), whereas *agr*A and *sae*R mutants remain attenuated throughout the course of experiment. Furthermore, cytotoxicity due to *rsp* mutants reached wild type levels only after 24 hours post infection; 55.83%, 95% CI (45.20 - 66.46, P= 0.84)(See Figure 3.3A). Therefore, demonstrating that the bacteria remained within the cells and induced of host cell death at a later time point.

Further indication came from examining host cell granularity during the course of infection. In the

context of infection, increased abundance of cytoplasm granularity when compared to an uninfected cell, indicates the presence of multiplying bacteria inside. Cytoplasmic granularity can be adjudged by the side-scatter (SSC) of light detected by the flow cytometer (See Section 5.14.2). During the cell death experiment, SSC threshold was set by applying a gate to select cell population in question and any increase over this threshold was taken into account. The percentage difference in granularity (ΔR) was calculated for each infection group at every time point. Obscurely, cells infected with *rsp* mutants displayed significantly enhanced SSC (ΔR) at 8 hours; 13.11%, 95% CI (11.23 - 14.99), $P< 0.001$, and 24 hours; 21.08%, 95% CI (19.20 - 22.96), $P< 0.001$ (See Figure 3.3B).

3.2.3 Mutation in *rsp* did not alter Gentamicin susceptibility of *S. aureus*

The non-cytotoxic mutant screen as well as experimental validations were done in presence of the antibiotic Gentamicin in the culture medium to maintain only intra-cellular *S. aureus*. Hence, susceptibilities of both USA300 and 6850 genotypes used in these infection models, towards Gentamicin was tested (See Section 5.3) to refute any effect of the antibiotic on selection of *rsp* mutants. Minimum inhibitory concentration (MIC) of Gentamicin was similar in wild type, *rsp* mutants and the complemented mutants were found to be similar; 0.5 µg/ml (See Figure 3.4), indicating no influence of Rsp on gentamicin resistance.

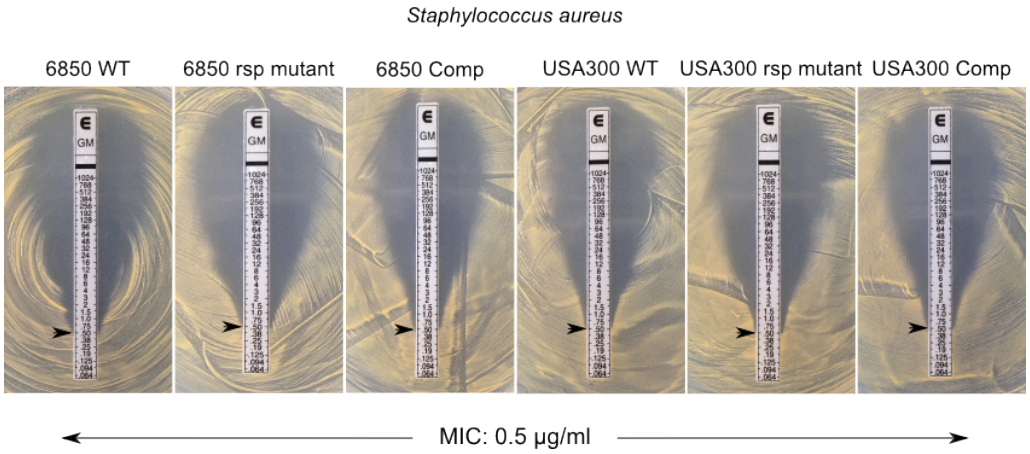

Figure 3.4: Rsp does not influence susceptibility of *S. aureus* to the antibiotic gentamicin Gentamicin MIC was found to be similar for *S. aureus* 6850 and USA300 wild types (WT), *rsp* mutants, complemented mutants (Comp). Antibiotic strips were placed on MH agar containing bacteria and MIC was determined by the point where the clear zone starts

3.3 Rsp influences *S. aureus* -induced infection *in vivo*

S. aureus α-haemolysin is known to elicit severe and fatal pneumonia in mice[53], which is lacking in case of an *rsp* mutant (See section 3.1). Moreover, in the Tnseq screen from mouse lungs *rsp* mutants performed weakly whereas, in other organs its numbers were increased when compared to its enrichment in the non-cytotoxicity model (See Figure 2.10). Based on these observations, a mouse pneumonia

model was chosen for further *in vivo* experiments.

3.3.1 Rsp is vital for *S. aureus* -induced acute pneumonia and lethality

For investigating the influence of Rsp in *S. aureus*-induced lethal pneumonia, 6 weeks old female Balb/c mice were intra-nasally administered with both wild type, *rsp* mutants and complemented bacteria from both USA300 and 6850 backgrounds[⊥]. The bacterial numbers were titrated for lethal and sub-lethal dosage for both strains, before continuing with the actual experiments. For testing pneumonia related mortality, lethal dosage were administered and mice survival were monitored over a period of 72 hours, using Kaplan-Meier (KM) estimation model. All mice infected with *rsp* mutants survived when compared to isogenic wild type and complemented mutants (See Figure 3.5A and B). Log-rank test for equal survival function demonstrated unequal estimates within infection groups in both genetic backgrounds (6850; P= 5.92 x 10^{-5} and USA300 LAC*; P= 6.6 x 10^{-16} and survival estimates were significantly better for the *rsp* mutants in both genetic backgrounds; 6850 (Expected = 7.33, Observed = 0.0), P= 3.94 x 10^{-3} and USA300 LAC* (Expected= 18.7, Observed = 0.0), P= 4.57 x 10^{-10} (See Figure 3.5A and B).

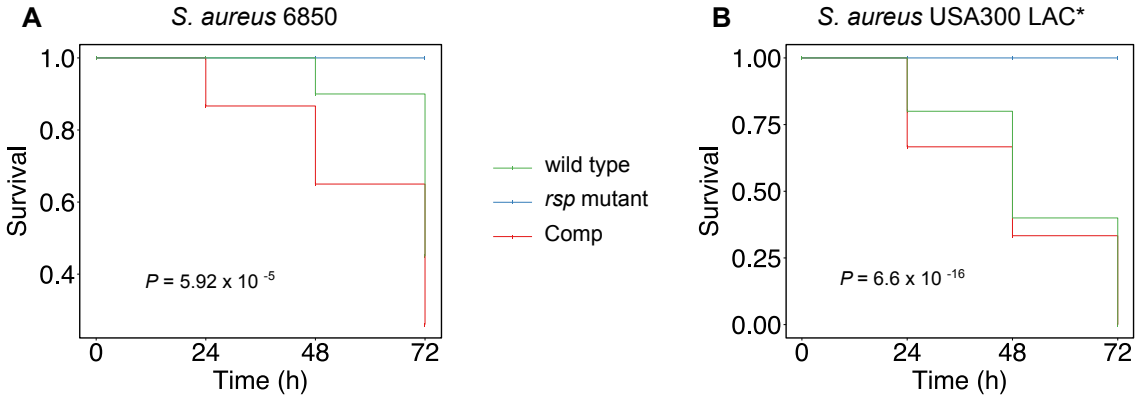

Figure 3.5: *rsp* mutants were non-lethal during *S. aureus* -induced acute pneumonia in mice. Kaplan-Meier (KM) estimation of mouse survival after intranasal administration of *S. aureus* at lethal dosage. KM plots show survival index (y-axis) of mice groups infected with *S. aureus rsp* mutants (blue) when compared to isogenic wild type (green) and complemented mutants (Comp, red) over the course of 72 hours post administration (x-axis), in both genetic backgrounds i.e. 6850 and USA300 LAC*. Statistical analysis was performed by Log-rank test for equal survival function within infection groups for both genetic backgrounds.

3.3.2 Mutants in *rsp* did not alter bacterial numbers and inflammation in mouse lung

Owing to the drastic attenuation of *rsp* mutants in lethal pneumonia model, bacterial numbers from mice lungs were enumerated to further assessment. 6 week old Balb/c mice were intra-nasally administered with sub-lethal doses[⊥] of 6850 wild type, *rsp* mutants and complemented mutants, followed by

[⊥] Experiments performed in collaboration with Dr. Babett Österreich and Martina Selle, Institute for Molecular Infection Biology, University of Wuerzburg, Germany.
[⫛] Histopathological evaluation was conducted in collaboration with Melanie Schott and Prof. Dr. Alma Zernecke, Institute for Experimental Biomedicine, University of Wuerzburg, Germany.

enumeration of CFUs from lungs after 24 hours. The mean bacterial numbers obtained from *rsp* mutants group; $\log_{10}$ 4.87, 95% CI (4.13 - 5.60) (See Figure 3.6A), were similar to that of group infected with wild type; $\log_{10}$ 5.08, 95% CI (4.43 - 5.75) and complemented mutants; $\log_{10}$ 5.17, 95% CI (4.48 - 5.86), hence indicating no change in bacterial CFU loads in lungs (P= 0.81). Histopathological analysis$^{\text{ⴖ}}$ of fixed and paraffin embedded lung sections by Haematoxylin and Eosin (H&E) staining showed no difference in severity of inflammation and leukocyte infiltration (See Figure 3.6B). Furthermore, immunohistochemical analysis$^{\text{ⴖ}}$ of the sections were performed where granulocyte infiltration was assessed by using an anti-Ly6G monoclonal primary antibody (clone 1A8) and detected by Alexa Fluor 488 conjugated secondary antibody. Neutrophil densities were found to be similar across all samples irrespective of infection groups (See Figure 3.6C).

3.3.3 Mutants in *rsp* influenced cytokine production in mouse lung

Lung homogenates were also examined for the changes in inflammatory cytokines, which was assessed by flow cytometry-based cytokine bead arrays$^{\Psi}$. In case of both wild type and *rsp* mutants, elevated levels of inflammatory cytokines were observed 24 hours post infection with were no changes in the levels of Interferon (IFN)-γ, Interleukin (IL)-10, Monocyte Chemoattractant Protein (MCP)-1 (See Figure 3.6D-F).

3.4 Rsp is a global regulator *S. aureus* gene expression

Rsp is transcription regulator, which is primarily important for intra-cellular pathogen-mediated host cytotoxicity and haemolysis (See Section 3.2,3.1). To investigate whether Rsp has a role in *S. aureus* gene expression, MRSA strain USA300 JE2 and its isogenic *rsp* mutant, NE1304 were analysed for global transcriptional changes by RNA deep sequencing (RNA-seq). This technology commands some significant advantages over other existing methods for analysis of gene expression. Total RNA from bacteria was converted to cDNA libraries$^{\Pi}$, which was then is analysed by deep sequencing$^{\epsilon}$. Transcript detection is not limited by prior knowledge of genome sequence and it has an impeccable signal-to-noise ratio[260].

3.4.1 Mutation in *rsp* leads to genome-wide alterations in *S. aureus* gene expression

RNA-seq was performed with exponentially growing bacteria and statistical analysis was done using DESeq2[261] $^{\text{ʊ}}$. This approach demonstrated that mutation in *rsp* leads to massive genome-wide changes in gene expression, with 113 genes significantly altered when compared to the wild type (See Figure 3.7, log P> 1.30). Although, overall transcription was similar for both mutant and wild type (R^2= 0.99), in-

$^{\Psi}$ Cytokine quantification was performed by Natarajaswamy Kalleda, Center for Experimental Molecular Medicine, University of Würzburg, Germany

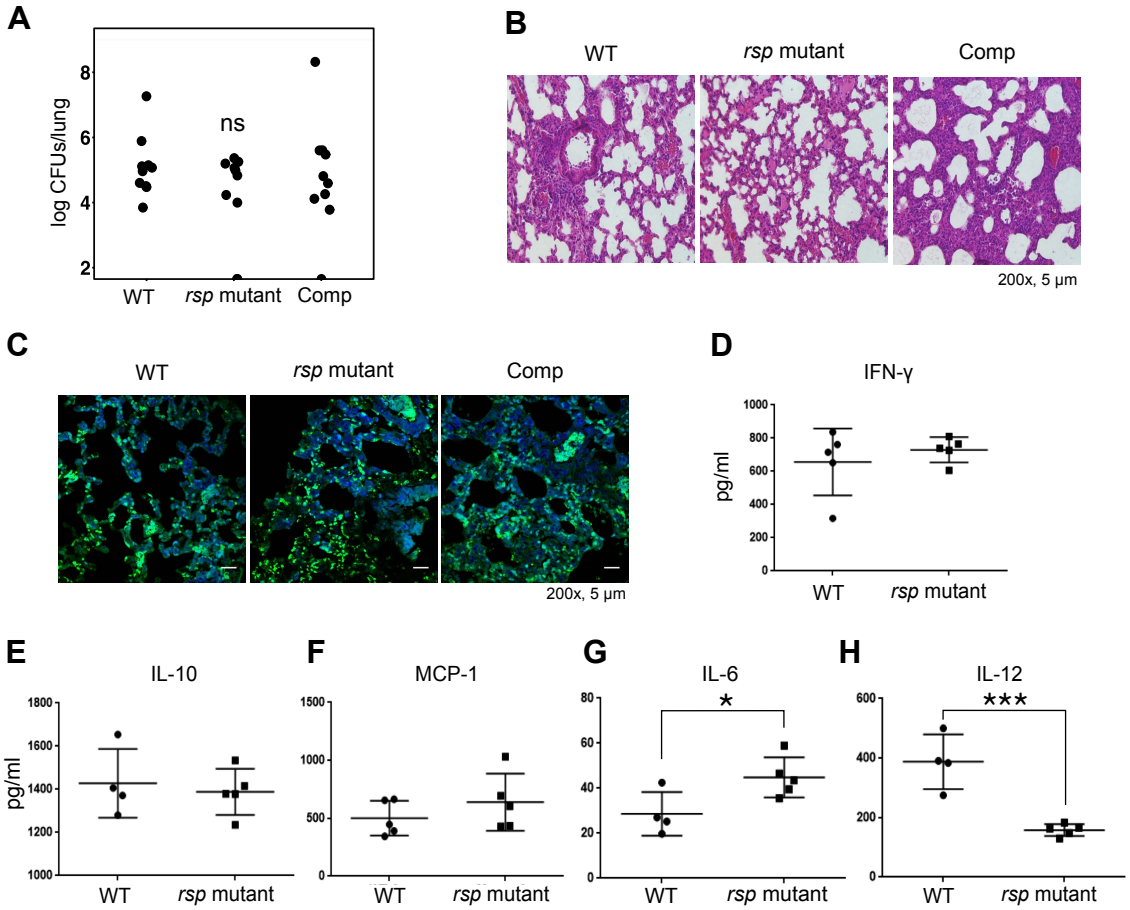

Figure 3.6: ***S. aureus rsp*** **mutants did not influence bacterial load and inflammation in lungs but resulted in changed levels of specific cytokines** Mice were intra-nasally infected with sub-lethal dosage of *S. aureus* 6850 wild type (WT), *rsp* mutants and mutants complemented with pS2217 (Comp). After 24 hours, mice lungs were homogenized for bacterial enumeration and cytokine analysis. In addition to this, lungs were also fixed in 1% PFA, embedded in paraffin and sections (thickness: 5 µm) were made for histopathological and immunohistochemical analysis. (**A**) Scatter plot shows $\log_{10}$ CFUs (y-axis) obtained from each mouse lung from all infection groups (x-axis). Statistical analysis was done using one-way ANOVA and Tukey's HSD test for individual comparisons (n=10). ns; not significant. (**B**) H&E staining show tissue inflammation and (**C**) fluorescence images show granulocyte infiltration in all three infection groups. Neutrophils were detected using anti-Ly6G primary antibody (mAb, clone 1A8) and Alexa Fluor 488 (Green) secondary antibody. Nuclei were stained using DAPI (Blue). Images (Magnification: 200x) are representation of 10 blinded observations made for each infection group, which included sections of upper and lowers lobes from both lungs. Lungs homogenates were examined for levels of inflammatory cytokines using CBA kit, which simultaneously detected (**D**) IFN-γ, (**E**) IL-10, (**F**) MCP-1, (**G**) IL-6 and (**H**) IL-12. Scatter plots show levels of cytokines measured in picograms per milliliter (pg/ml, y-axis) from groups infected with wild type and *rsp* mutant (x-axis). Statistical analysis was done by pairwise t-test (n=5). *; $P< 0.05$, **; $P< 0.01$, ***; $P< 0.001$

dicating genetic similarity. Amongst the 45 genes significantly down-regulated, were known important virulence genes of *S. aureus* (See Table 3.1, $P< 0.05$). These included the genes encoding for virulence-associated ncRNA SSR42 (*ssr*42 ; $2^{-7.76}$), staphylocoagulase (*coa*; $2^{-4.32}$); neutrophil chemotaxis inhibitors (*chs*; $2^{-4.06}$, *scp*A; $2^{-2.32}$), pore-forming toxins such as Leukocidin AB (*luk*A; $2^{-1.89}$, *luk*B; $2^{-2.32}$) and α-haemolysin (*hla*; $2^{-1.06}$), surface adhesive molecules and heme-acquisition proteins (*sbi*; $2^{-1.40}$, *empbp*; $2^{-2.00}$, *isd*H; $2^{-2.32}$, *isd*A ; $2^{-2.18}$). This also included staphylococcal accessory regulator (*sar*R; $2^{-2.84}$) and transposase from the SCC*mec* chromosomal cassette in MRSA (*IS431mec*; $2^{-4.06}$).

Furthermore, 68 genes were shown to be significantly over-expressed upon mutation in *rsp* , which

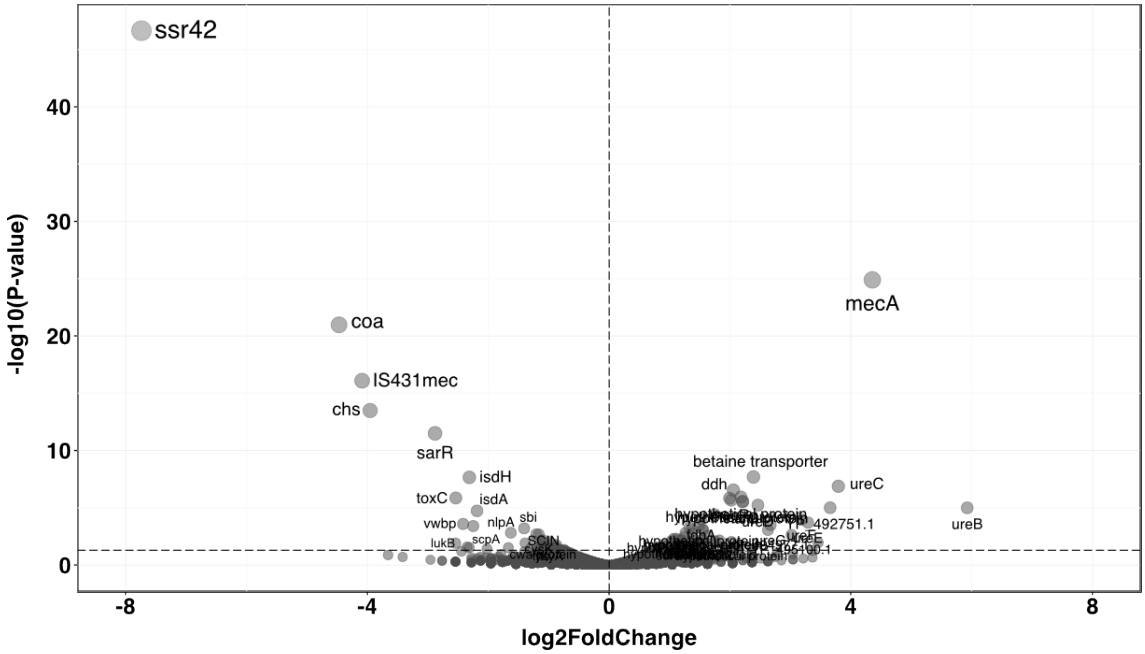

Figure 3.7: RNA deep-sequencing (RNA-seq) reveals Rsp as a global regulator of *S. aureus* gene expression. Total RNA from *S. aureus* insertion mutant within *rsp*, NE1304 was compared to isogenic wild type USA300 JE2 by genome-wide RNA deep sequencing (RNA-seq). Differential expression and statistical analysis was done by DEseq2 package in R. The volcano plot shows the changes in relative abundance of mRNAs, with negative logarithm of *P* values (-log10(P-value)) on the y-axis and logarithmic of fold change (log2FoldChange) represented by the x-axis, on either side of zero denoted by the vertical dotted line. Circles represent each gene/RNA. Lighter and bigger circles denote larger relative differences with lesser *P* values, the cut-off for which was kept at *P*= 0.05 i.e. -log(P-value)> 1.30, denoted by the horizontal dotted line.

included: genes belonging to the Urease operon (*ure*B; $2^{5.93}$, *ure*C; $2^{3.79}$, *ure*A; $2^{3.46}$), genes encoded from the *SCCmec* type IV responsible for methicillin-resistance (*mec*A; $2^{4.36}$, *mec*R1; $2^{1.99}$, *mec*I; $2^{1.75}$, *SAUSA300_0031*; $2^{3.65}$) and gene coding for D-lactate dehydrogenase (*ddh*; $2^{2.06}$).

Detailed table containing all significantly altered genes in *rsp* mutant during exponential growth phase, has been published[262] and can be accessed from the article's supplementary information. Furthermore, all data from RNA-seq and dRNA-seq experiments was deposited in NCBI Gene Expression Omnibus (GEO) and can be found under the Accession number GSE67424.

3.4.2 Primary transcriptome analysis by differential RNA deep sequencing (dRNA-seq) reveals global transcription start sites in *S. aureus*

RNA-seq experiments can be tailored to specific analysis such as detection of primary transcripts on a global scale, thereby determining genome-wide transcription start sites (TSS). Such a method utilizes an enzyme called 5′-phosphate dependent RNA terminal exonuclease (TEX), which eliminates transcripts

[Π] Enzymatic processing and library preparation was done at Vertis Biotechnology AG, Germany.
[ϵ] Sequenced on Illumina® HiSeq platform was performed by the group of Prof. Dr. Richard Reinhardt at the Max Planck Genome Center, Cologne, Germany.
[ʊ] RNA-seq and dRNA-seq data processing, application of DESeq2 and statistical analyses were performed by Dr. Konrad Förstner, Institute for Molecular Infection Biology, University of Wuerzburg, Germany.

Table 3.1: Top 30 genes down regulated upon *rsp* mutation during exponential growth phase detected by RNA-seq

RefSeq ID [a]	log2FoldChange	*P* value[b]	Gene/Locus/Product[c]
undefined	-7.738	2.26 x 10^{-47}	small stable RNA (ssr) 42
YP_493473.1	-4.468	1.07 x 10^{-21}	Staphylococcus coagulase
YP_492748.1	-4.086	8.12 x 10^{-17}	IS431mec
YP_494571.1	-3.953	3.21 x 10^{-14}	chemotaxis-inhibiting protein (CHIPS)
YP_494880.1	-2.879	3.18 x 10^{-12}	sarR
YP_495088.1	-2.541	1.22 x 10^{-2}	antibiotic protection permease
YP_493121.1	-2.536	1.39 x 10^{-6}	superantigen-like protein
YP_493475.1	-2.415	2.57 x 10^{-4}	vWbp
YP_494626.1	-2.348	2.60 x 10^{-2}	LukB subunit
YP_494961.1	-2.324	1.55 x 10^{-4}	rsp
YP_494542.1	-2.313	2.98 x 10^{-2}	staphopain A
YP_493122.1	-2.312	2.20 x 10^{-8}	Heme uptake protein IsdH
YP_492834.1	-2.248	3.94 x 10^{-4}	SirA
YP_493727.1	-2.185	1.86x 10^{-5}	isdA
YP_493474.1	-2.020	3.80 x 10^{-2}	emp
YP_494625.1	-1.910	7.25 x 10^{-4}	LukA subunit
YP_493422.1	-1.666	3.04 x 10^{-2}	amino acid uptake permease
YP_493498.1	-1.626	1.51 x 10^{-3}	NlpA
YP_494999.1	-1.405	6.26 x 10^{-4}	IgG-binding protein Sbi
YP_492944.1	-1.388	1.22 x 10^{-2}	prsW
YP_494772.1	-1.304	3.77 x 10^{-2}	Heme uptake permease
YP_492929.1	-1.233	8.79 x 10^{-3}	hypothetical protein
YP_494570.1	-1.206	2.01 x 10^{-3}	Staphylococcal complement inhibitor (SCIN)
YP_494069.1	-1.174	4.76 x 10^{-2}	DNA binding hypothetical protein
YP_493200.1	-1.162	2.03 x 10^{-3}	cysK
YP_494308.1	-1.136	2.11 x 10^{-2}	AbrB
YP_494372.1	-1.126	9.56 x 10^{-3}	tetrahydrofolate ligase (fhs)
YP_492853.1	-1.093	6.41 x 10^{-3}	LPXTG cell wall anchor protein
YP_493241.1	-1.075	2.32 x 10^{-2}	NAD-dependent epimerase
YP_493756.1	-1.065	4.51 x 10^{-2}	alpha haemolysin (hla)

[a] NCBI RefSeq Accession for USA300 FPR3757: NC_007793.1
[b] only genes/loci with $P < 0.05$ are shown
[c] Identified by NCBI BLAST/EBI UniProt

with 5′-monophosphate that is mostly found in processed transcripts. In a living cell rRNA precursors and naive / primary transcripts have a 5′-triphosphate, which when processed ends up with 5′-monophosphate end, which can be recognised by endogenous enzymes that carry out RNA decay (See Figure 3.8). Taking advantage of this phenomenon *in vitro*, total RNA was treated with TEX and primary transcripts were enriched[Π]. The treated and untreated samples were then sequenced[ϵ], to determine genome-wide primary transcripts and transcription start sites. This approach is known as differential RNA deep sequencing (dRNAseq) (See Figure 3.8).

Gene expression profiling by RNA-seq uncovered the difference in RNA abundances when *rsp* is

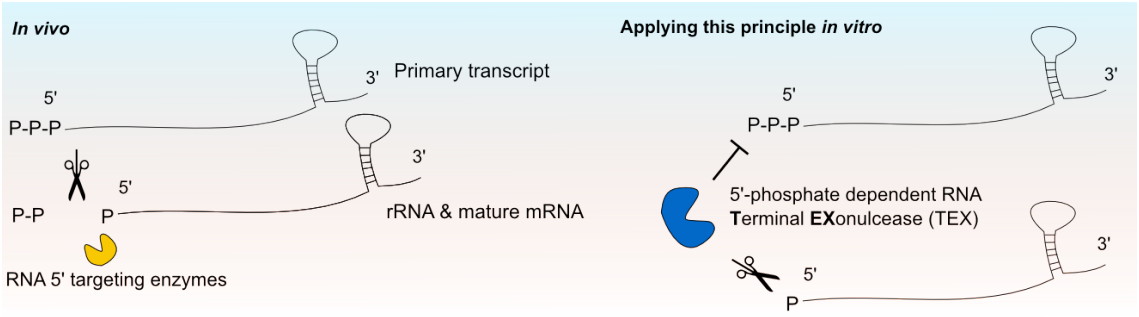

Figure 3.8: Graphical illustration of the principle of differential RNA-seq aided by TEX treatment, to detect primary transcripts In a cell, naive genes transcript and precursor rRNAs usually consist of 5′-triphosphate and the mature forms usually have 5′-monophosphate ends. Taking advantage of this principle *in vitro*, RNA can be subjected to 5′-phosphate dependent RNA terminal exonuclease (TEX) treatment that specifically removes RNA species with 5′-monophosphate and analysed by deep sequencing to detect genome-wide primary transcripts, in a process called Differential RNA deep sequencing (dRNA-seq).

non-functional. Apart from mRNA, there were also changes found in intergenic region/non-coding RNA for e.g. SSR42. But genome-wide information on transcriptional start sites, analysed by a sensitive approach was still lacking in case of pathogenic *S. aureus* . To gain more insights on characteristics of *rsp* and *ssr42* gene products amongst others, differential RNA sequencing (dRNA-seq) was performed aided by 5' phosphate-dependent terminal exonuclease (TEX) treatment.

Total RNA from exponentially growing MRSA USA300 JE2 was sequenced after TEX treatment and analysed in increasing order of sensitivity (Default, Higher and Highest). This strategy revealed the global primary transcriptome of USA300 elucidating the total number of transcription start sites (TSS), gene length, length and sequence of 5′- untranslated regions (UTRs), presence of antisense RNA. In total 696 transcripts were detected using default parameters and were categorized depending on the location (See Figure 3.9A). Amongst all, 64% mapped to existing mRNAs (46% preceding ORF, 16% Internal, 2% Secondary), 26% were antisense RNA (asRNA) and 13% were orphan TSS that did not match to a known mRNA or ORF. In analyses with more sensitive parameters, the number of asRNAs increased and the composition of mapped mRNAs varied (See Figure 3.9B, C). In addition to this, there were 328 5′- UTRs of varied lengths (Figure 3.9D) found in MRSA USA300. The average 5′- UTR length was found to be 94 nucleotides, with smallest being 7 and largest being 300 nucleotides long. The size distribution and frequency of 5′- UTRs varied with prediction sensitivity (Figure 3.9E, F).

Single nucleotide resolution of the TSS detection method, revealed the gene length of *rsp* to be 2185 nucleotides, which included a 5′- UTR of 79 nucleotides. SSR42, which was the most significantly depleted transcript upon *rsp* mutation is situated upstream of *rsp*, on the opposite strand of the DNA (See Figure 3.10A). SSR42 primary transcript was observed to be 1232 nucleotides long, which is longer that previously reported[255]. Furthermore, both genes are transcribed bidirectionally and has divergent transcription start sites. The predicted -10 and -35 regions of both *rsp* and *SSR42* were found to be distinct from each other (See Figure 3.10B) indicating the existence of independent promoters.

Full data from this experiment was deposited in NCBI Gene Expression Omnibus (GEO) and can be

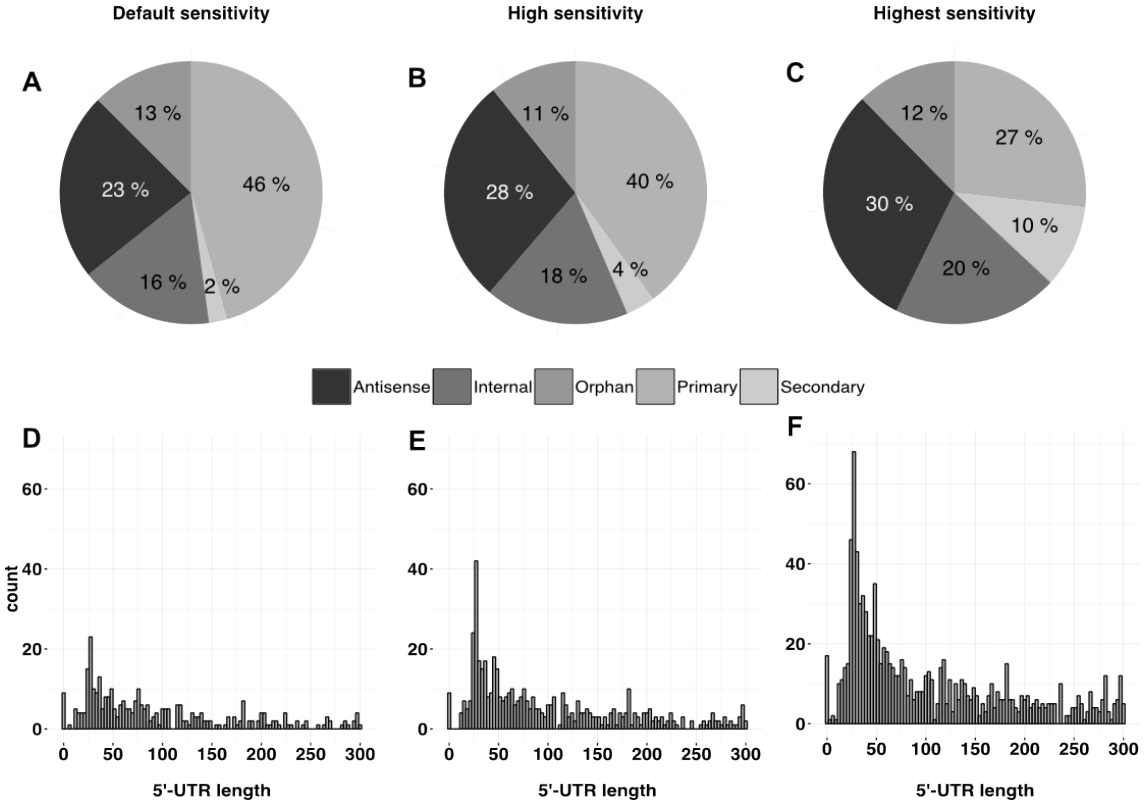

Figure 3.9: Analysis of transcription start sites (TSS) in *S. aureus* USA300 (MRSA) by differential RNA deep sequencing (dRNA-seq). 5′- Phosphate-dependent Terminal Exonuclease (TEX) treatment of *S. aureus* RNA followed by deep sequencing, identified genome-wide start sites of transcription and adjoining 5'- untranslated region (5′-UTR) with putative promoters. Pie charts show overall percentage of different transcript types detected and analysed in increasing order of sensitivities - default (**A, D**), high sensitivity (**B, E**) and the most sensitive (**C, F**). Histograms show the overall size distribution (x-axis) and count (y-axis) of the 5′-UTRs, corresponding to the sensitivity of transcript start site detection.

found under the Accession number GSE67424.

3.4.3 Validation of *rsp* -dependent gene expression reveals its targets and its regulatory effects on *S. aureus* virulence

To validate the results obtained from RNA-seq experiments (See Section 3.4.1, 3.4.2), the expression of each putative target gene was individually examined in the presence and absence of *rsp*, by qPCR. To demonstrate *rsp*-dependency, the complemented mutant was included in the analysis. These experiments were performed using both genotypes of 6850 and USA300 LAC, and bacteria were harvested from exponential and stationary phases of growth. This was done to observe any alteration in expression profile due to increased quorum sensing.

Upon complementation of mutants with multi-copy pS2217 plasmid both in 6850 and USA300 strains, expression of *rsp* was recovered significantly, when compared to the wild type. In exponentially growing bacteria, the relative expression levels of *rsp* were 23.99, 95% CI (21.64 - 26.34) in 6850 (See Figure 3.11A) and 17.45, 95% CI (11.18 - 23.71) in USA300 LAC* (See Figure 3.12A). Furthermore, during stationary

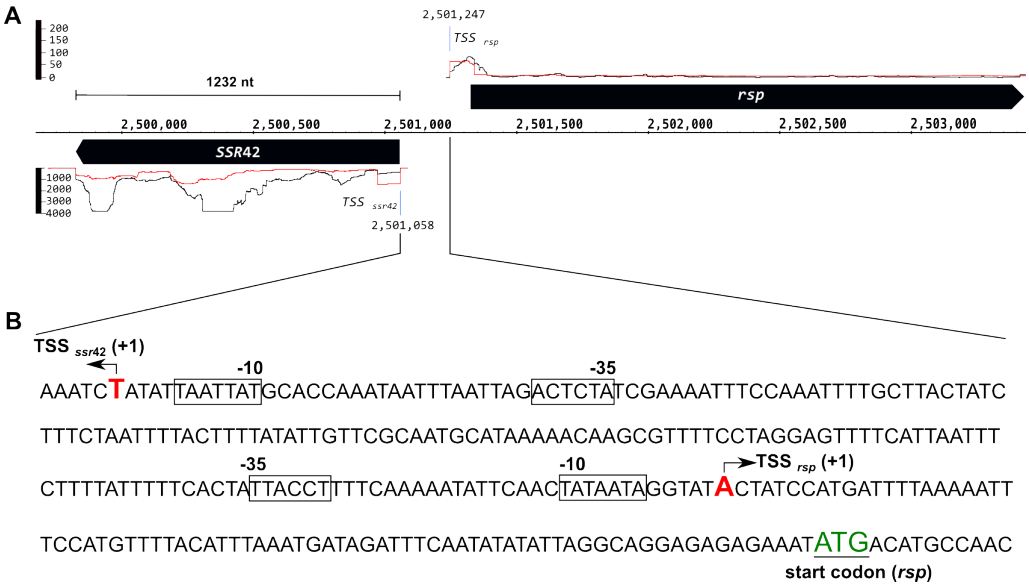

Figure 3.10: dRNA-seq reveals precise transcription start sites and transcript length of *rsp* and SSR42. Differential RNA-seq revealed the bi-directional nature of *rsp* and *ssr*42 transcription, shown by black horizontal bars. Overlaid lines show the genomic location and transcripts upon TEX treatment (red) compared to no treatment (black) (**A**). This approach comprehensively detected transcription sites up to single-nucleotide resolution. (**B**) Shows detailed nucleotide composition of the intergenic region between *ssr*42 and *rsp*. Transcription starts are shown as red letters with directional arrows, translation initiation codon (start codon) is shown in green. The promoter elements: -35 and -10 sequences are shown enclosed in bordered rectangles.

phase of growth the expression was similarly excess with 11.99, 95% CI (9.39 - 14.59) in 6850 (See Figure 3.13A) and 17.45, 95% CI (11.18 - 23.71) in USA300 LAC* (See Figure 3.14A).

Individual assessment of *rsp* target genes was first performed in exponentially growing *S. aureus* , which showed similar effects of *rsp* mutation as observed in the RNA-seq. In *S. aureus* 6850, targeted deletion of the complete *rsp* ORF lead to significant decrease in the relative quantification (RQ) of virulence genes such as *ssr*42 ; 0.01, 95% CI (-0.24 - +0.27), $P< 0.001$ (See Figure 3.11B), *luk*AB ; 0.83, 95% CI (0.60 - 1.06), $P= 0.01$ (See Figure 3.11H), *chs*; 0.60, 95% CI (0.26 - 0.94), $P= 0.03$ (See Figure 3.11I), *scp*A; 0.47, 95% CI (0.17 - 0.77), $P< 0.001$ (See Figure 3.11J), *hla*; 0.78, 95% CI (0.48 - 1.08), $P= 0.039$ (See Figure 3.11K).

Interestingly, in addition to these toxins and virulence factors, the expression of another global regulator, *sar*R[201]; 0.63 95% CI (0.32 - 0.94), $P= 0.04$, was significantly decreased (See Figure 3.11F). Consequently the expression of *sar*A, which is repressed by *sar*R[163], was significantly increased; 2.18, 95% CI (1.69 - 2.66), $P= 0.008$ (See Figure 3.11D). Furthermore, there was no influence of *rsp* mutation on other regulatory proteins and RNA, such as the *agr*-quorom sensing system (*agr*A , *RNA*III), alternate sigma factor *sig*B and the two-component virulence regulatory system (*sae*S) (See Figure 3.11). To exclude any adverse effect of *rsp* deletion on adjacent genes, the expression of RSAU002216 and RSAU002218 were investigated, which remained unaltered (See Figure 3.11M, N).

In USA300 LAC* strain, the effects of *rsp* mutation were largely similar to 6850 and could confirm RNA-seq results, with addition of new targets (See Figure 3.12). However, there were some exceptions

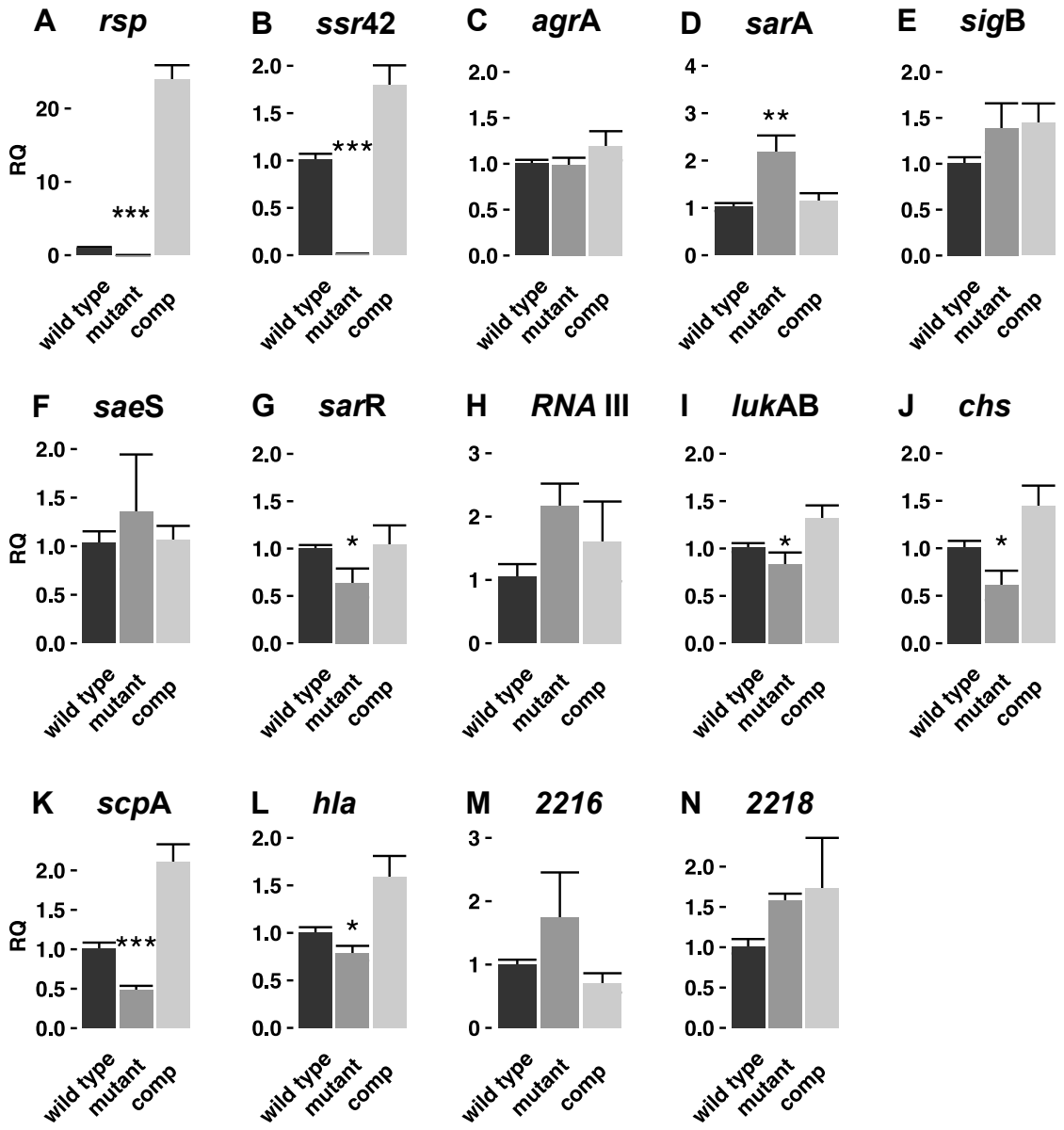

Figure 3.11: Validation of *rsp* -dependent gene expression in *S. aureus* strain 6850 (MSSA) during logarithmic growth phase. Individual gene expression in exponentially growing *Staphylococcus aureus* i.e. OD_{540nm} = 0.6, were assessed by quantitative real time PCR. Vertical axes show the relative quantification (RQ) of mRNA abundance in *rsp* mutants (dark grey) and complemented bacteria (comp, light grey), with reference to the wild type (black). Sample sizes for all experiments were n=6, with exceptions in case of *luk*AB (n=10) and *2128*, *RNA* III (n=4). Bar plots show mean RQ levels and SEM as error bars. Insets show zoomed plots to illustrate comparisons wherever not visible. Statistical analysis was done by one-way ANOVA and individual comparisons were done by Tukeyś HSD test.*; $P< 0.05$, **; $P< 0.01$, ***; $P< 0.001$

that showed discrepancies, such as *sae*S; 0.60, 95% CI (0.30 - 0.91), $P= 0.02$ (See Figure 3.12E) and *sar*A; 0.50, 95% CI (-0.00 - 1.00), $P= 0.007$, showed decreased expression despite *sar*R being similarly down regulated; 0.37, 95% CI (-0.11 - +0.87) (See Figure 3.12C, F). In case of the *agr* quorum sensing system, whereas there was no notable change in *agr*A expression observed in *rsp* mutants, there was a significant up-regulation of *RNA* III; 2.94, 95% CI (-6.71 - +12.60), $P= 0.01$, showing similar trend in case of 6850 (See Figure 3.12L, 3.11H). Paradoxically upon *rsp* complementation, the expression of *agr*A ; 5.81,

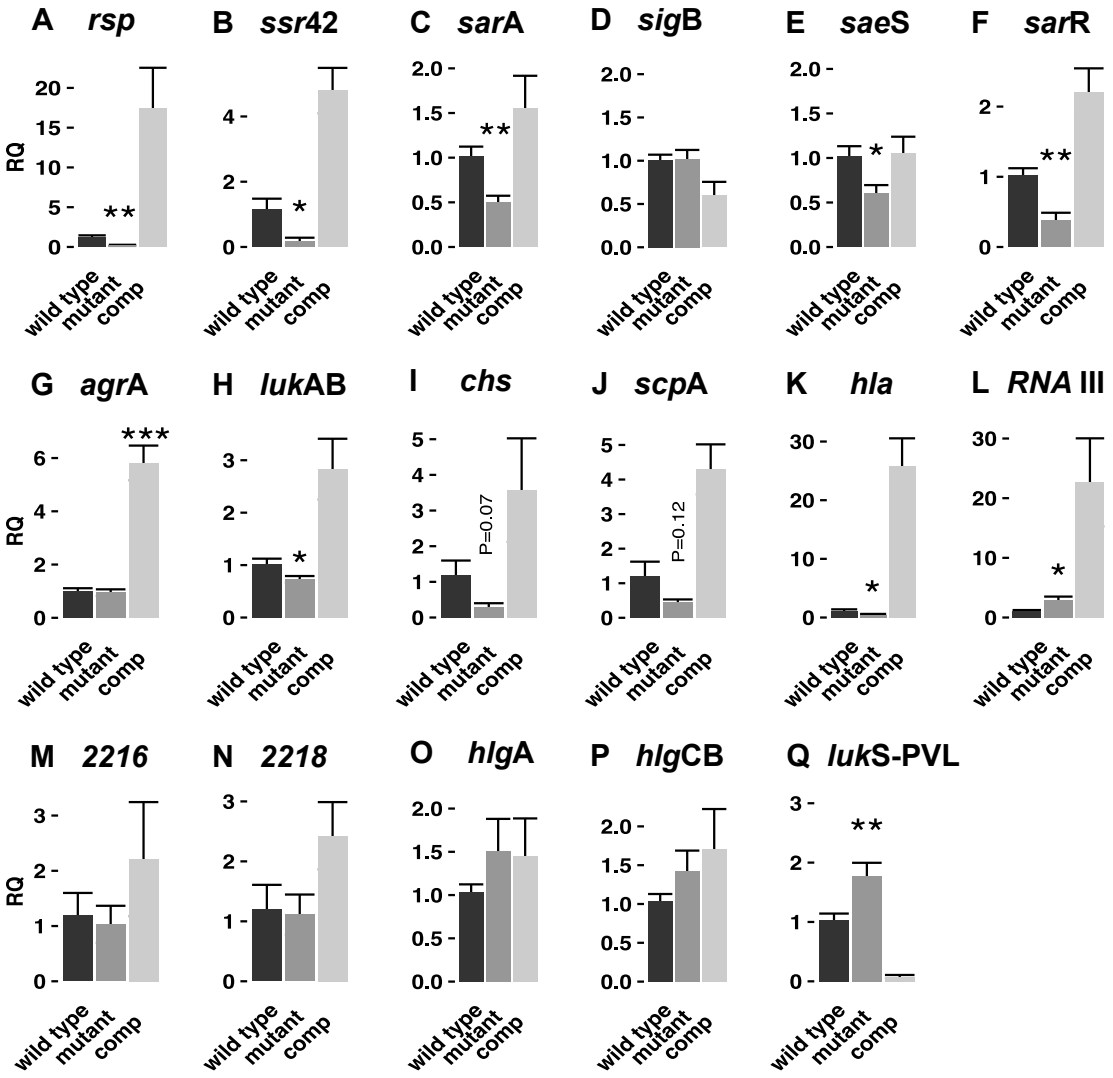

Figure 3.12: Validation of *rsp* -dependent gene expression in *S. aureus* strain USA300 LAC* (LAC star) (MRSA) during logarithmic growth phase. Individual gene expression in exponentially growing *Staphylococcus aureus* i.e. OD_{540nm} = 0.6, were assessed by quantitative real time PCR. Vertical axes show the relative quantification (RQ) of mRNA abundance in *rsp* mutants (dark grey) and complemented bacteria (comp, light grey), with reference to the wild type (black). Sample sizes for all experiments were n=6, with exceptions in case of *luk*AB (n=8) and *sar*A, *sig*B, *sae*S, *agr*A , *chs*, *2126*, *2128*, *RNA* III (n=4). Bar plots show mean RQ levels and SEM as error bars. Statistical analysis was done by one-way ANOVA and individual comparisons were done by Tukeyś HSD test.*; $P< 0.05$, **; $P< 0.01$, ***; $P< 0.001$

95% CI (4.93 - 6.69), $P< 0.001$ and *RNA* III; 22.65, 95% CI (12.98 - 32.31), $P= 0.014$, increased further when compared to the wild type (See Figure 3.12G, L). This resembled the phenomenon where haemolysis appeared upon increased *rsp* expression in agr^+ background (See Figure 3.1.3).

Furthermore, the genes encoding γ-haemolysins; *hlg*A , *hlg*CB and Panton-Valentine Leukocidin; *luk*S-PVL, were introduced as news target. The expression of *hlg*A and *hlg*CB was a bit higher, although did not change significantly in absence of *rsp* (See Figure 3.12O, P). But unlike Leukocidin AB (See Figure 3.12H) in the absence of *rsp* , USA300 LAC specific *luk*S-PVL transcripts increase in abundance 1.77, 95% CI (1.44 - 2.10), $P= 0.009$ and plummeting to negligible expression when *rsp* in overexpressed; 0.076, 95%

CI (-0.38 - +0.54), *P*= 0.006 (See Figure 3.12Q)

At stationary growth phase the effects of *rsp* mutation on virulence gene expression of *S. aureus* remained largely similar to that of exponential phase (See Figure 3.11, 3.12), with a few exceptions. In strain 6850, decreased expression upon *rsp* mutation was evident for *ssr*42 ; 0.01, 95% CI (-1.41 - +1.44), *P*< 0.001, *sar*R; 0.49, 95% CI (0.22 - 0.76), *P*< 0.001, *luk*AB ; 0.71, 95% CI (0.50 - 0.92), chs; 0.54, 95% CI (0.25 - 0.82), *P*= 0.0016 and *scp*A; 0.44, 95% CI (0.006 - 0.88), *P*< 0.001, and were successfully recovered by *rsp* complementation (See Figure 3.13B, G, I, J and K). However, unlike exponential phase, the expression of *sar*A; 0.85, 95% CI (0.64 - 1.07), *P*= 0.38 and *hla*; 0.86, 95% CI (0.34 - 1.39), did not alter significantly. Interestingly, although no change in case of *rsp* mutant, the expression of *agr*A ; 1.51, 95% CI (1.28 - 1.75), *P*= 0.029 and *hla*; 2.47, 95% CI (1.95 - 2.99), *P*= 0.003, were significantly higher upon *rsp* complementation (See Figure 3.13C and K), resembling the effect in USA300 LAC during exponential phase (See Figure 3.12G), where the effect was only observed in case of *agr*A .

Furthermore, in USA300 LAC* at stationary phase of growth, mutation is *rsp* lead similar and significant decrease in *ssr*42; 0.004, 95% CI (-1.24 - 1.25), *P*= 0.008, *sar*R; 0.31, 95% CI (-0.47 - 1.11), *P*= 0.04, *chs*; 0.47, 95% CI (-0.14 - 1.09), *P*= 0.05, *hla*; 0.47, 95% CI (-35.99 - 36.92), *P*= 0.008 (See Figure 3.14B, G, J, K), as in the exponential phase. Although, the expression some genes were differentially regulated at stationary phase. Unlike in the log phase, the expression of scpA; 0.69, 95% CI (0.18 - 1.20), *P*= 0.14, was not significantly altered. However, in *rsp* complemented mutant *scp*A; 37.38, 95% CI (-23.80 - 98.57) expression was observed to really high (See Figure 3.14K). Surprisingly, the over expression of *rsp* in complemented mutants lead to depletion of *sae*S; 0.16, 95% CI (-0.45 - +0.78), *P*= 0.07 and RNAIII; 0.15, 95% CI (-0.45 - +0.76), *P*= 0.11, transcripts but did not reach significance (See Figure 3.12F and H). Lastly, particularly in this growth phase and unlike in the exponential phase, the expression of RSAU002216; 0.12, 95% CI (-0.57 - +0.83), the gene upstream of *rsp* was decreased and could not be rescued upon complementation (See Figure 3.12M). Whereas the expression of *luk*AB and *sae*S did not change in *rsp* mutants, the genes *hlg*A ; 0.39, 95% CI (0.17 - 0.61), *P*< 0.001 and *hlg*B; 0.46, 95% CI (0.12 - 0.80), *P*< 0.001 had contradicting and significant decrease in expression (See Figure 3.14O and P), unlike in the exponential phase of growth (See Figure 3.12O and P)

3.5 Rsp influences *S. aureus* and host immune cell interactions

Rsp positively regulates the expression of several virulence factors such as Leukocidins, CHIPS, Staphopain that are targeted against host innate immune system, specifically neutrophils. To check the phenotypic effects of *rsp* mutation on *S. aureus* -neutrophil interactions were examined with wild type bacteria, *rsp* mutants and complemented mutants from both USA300 and 6850 genotypes, along with 6850 *hla* mutant, USA300 *agr*A mutant and laboratory strain RN4220. Effects on exoprotein induced cytotoxicity, intra-cellular pathogen-mediated neutrophil cytoxicity and intra-phagocytic survival of bacteria were assessed at several time points post infection.

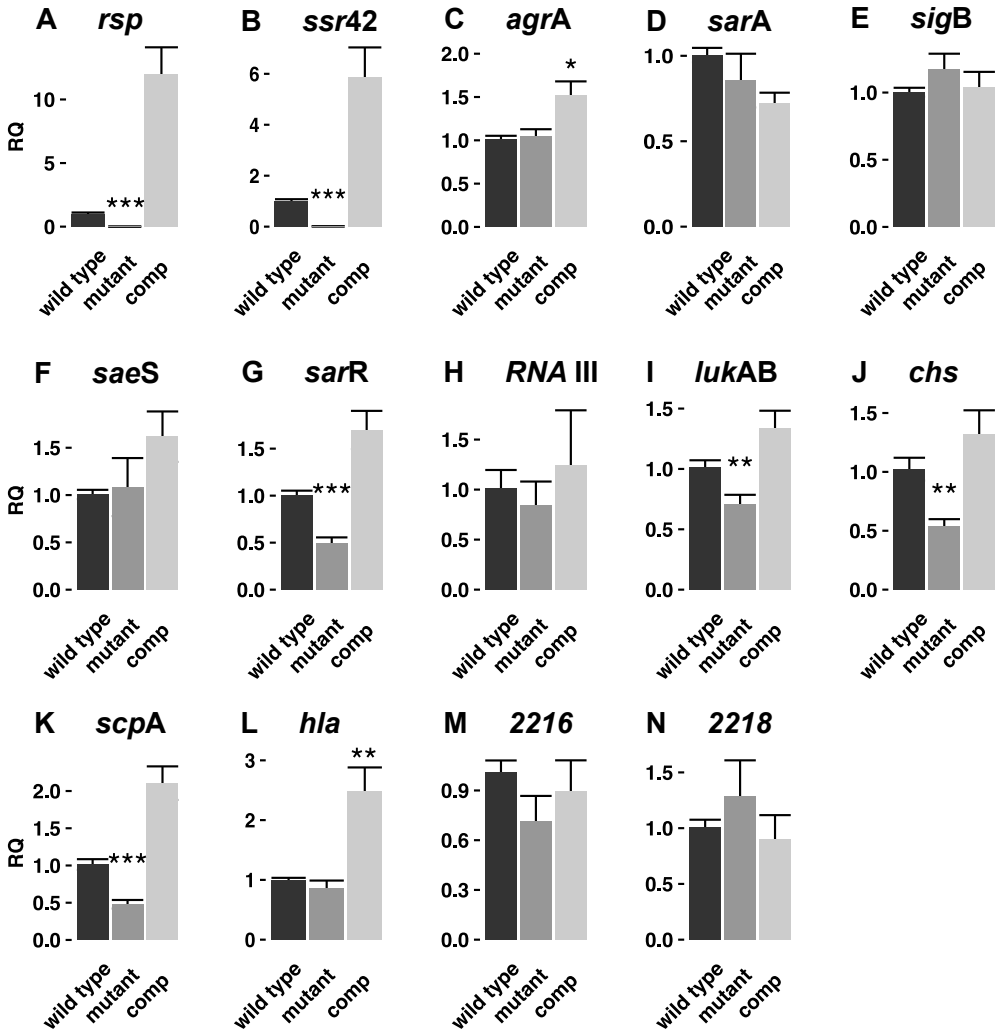

Figure 3.13: Validation of *rsp* -dependent gene expression in *S. aureus* strain 6850 (MSSA) during stationary growth phase. Individual gene expression in *Staphylococcus aureus* at stationary phase i.e. OD_{540nm} = 5.0, were assessed by quantitative real time PCR. Vertical axes show the relative quantification (RQ) of mRNA abundance in *rsp* mutants (dark grey) and complemented bacteria (comp, light grey), with reference to the wild type (black). Sample sizes for all experiments were n=6, with exceptions in case of *luk*AB (n=12), *RNA* III (n=2). Bar plots show mean RQ levels and SEM as error bars. Insets show zoomed plots to illustrate comparisons wherever not visible. Gene names are stated as titles of individual plots. Statistical analysis was done by one-way ANOVA and individual comparisons were done by Tukey's HSD test.*; $P< 0.05$, **; $P< 0.01$, ***; $P< 0.001$

3.5.1 Rsp positively influences neutrophil cytotoxicity induced by *S. aureus* exo-proteome

The extra-cellularly secreted protein repertoire of *S. aureus rsp* mutants is deficient of alpha toxin (See Section 3.1) and cytoplasmic abundance of *luk*AB and *hla* mRNAs were depleted (See Section 3.4), both indicating possible attenuation of toxin-mediated host cell damage. Hence, primary human neutrophils were intoxicated with bacterial culture supernatants and toxicity was quantified at 120 and 240 minutes p.i., by measuring release of cytoplasmic lactate dehydrogenase (LDH) (See Materials and Method Section 5.14.3. Neutrophil damage elicited by secretions from wild type bacteria were evident at 120 minutes, with 6850; 23.47%, 95% CI (16.31 - 30.63) showing higher toxicity than USA300; 10.87%, 95% CI (3.71 -

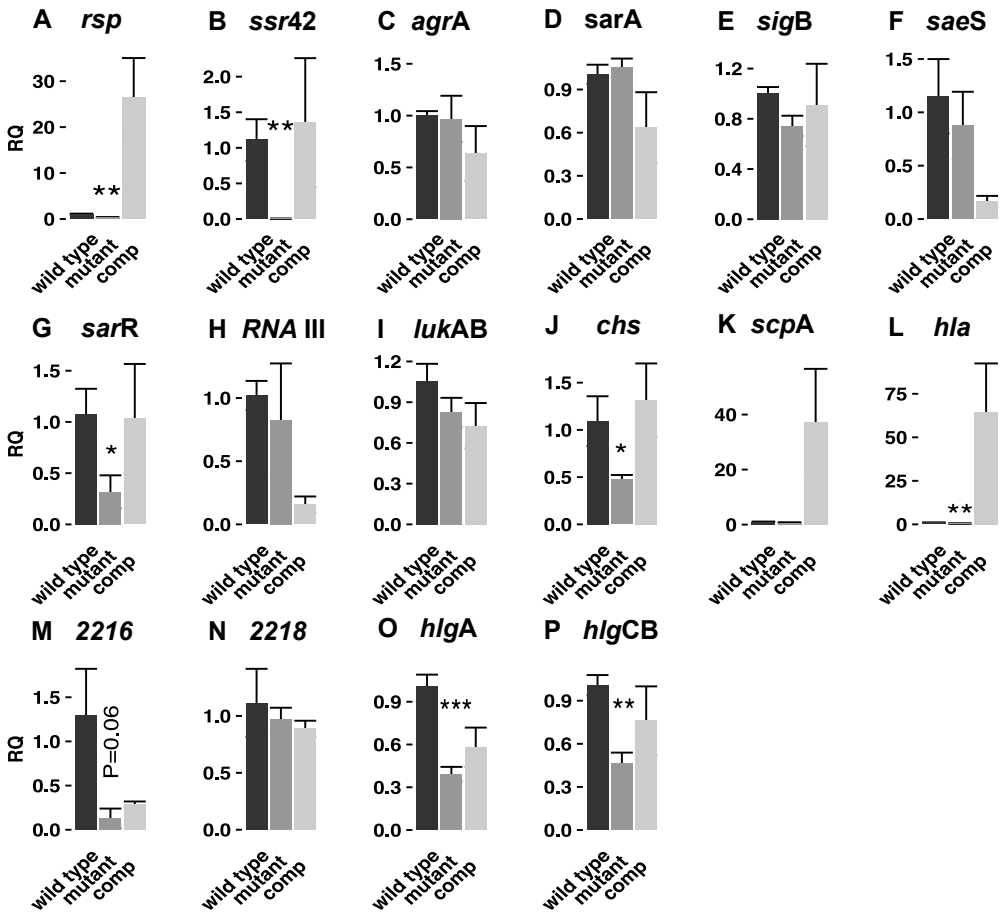

Figure 3.14: Validation of *rsp* -dependent gene expression in *S. aureus* strain USA300 LAC* (LAC star) (MRSA) during stationary growth phase. Individual gene expression in *Staphylococcus aureus* at stationary phase i.e. OD_{540nm} = 5.0, were assessed by quantitative real time PCR. Vertical axes show the relative quantification (RQ) of mRNA abundance in *rsp* mutants (dark grey) and complemented bacteria (comp, light grey), with reference to the wild type (black). Sample sizes for all experiments were n=4, with exceptions in case of *luk*AB (n=8). Bar plots show mean RQ levels and SEM as error bars. Insets show zoomed plots to illustrate comparisons wherever not visible. Statistical analysis was done by one-way ANOVA and individual comparisons were done by Tukeyś HSD test.*; $P<$ 0.05, **; $P<$ 0.01, ***; $P<$ 0.001

18.03), when compared to TSB treatment. Whereas, culture supernatant from *rsp* mutants showed significantly low toxicity for both 6850; 11.49%, 95% CI (4.33 - 18.65), P= 0.03 and USA300; 1.49%, 95% CI (-5.65 - +8.65), P= 0.05 (See Figure 3.15A). The effect was recovered in case of *rsp* complementation in both 6850; 25.42%, 95% CI (18.27 - 32.58) and USA300; 15.97%, 95% CI (8.81 - 23.13). As expected, the exoproteome of *agr* mutant; 1.65%, 95% CI (-5.50 - +8.81), P= 0.05, was less potent when compared to its isogenic USA300 wild type. But on the contrary, absence of α-toxin in 6850 *hla* mutant; 22.27%, 95% CI (15.12 - 29.43), P= 0.70, secretions did not alter neutrophil damage and was similar to that of its wild type counterpart (See Figure 3.15A).

Furthermore at 240 minutes post intoxication, there was substantial increase in neutrophil damage in case of both wild type 6850; 40.83%, 95% CI (27.08 - 54.58) and USA300 28.65%, 95% CI (14.90 - 42.40), whereas *rsp* mutant secretions were heavily attenuated in eliciting toxicity, with more pronounced difference in case of USA300; 5.00%, 95% CI (-8.74 - +18.75), P= 0.007, than 6850; 15.79%, 95% CI (2.04 -

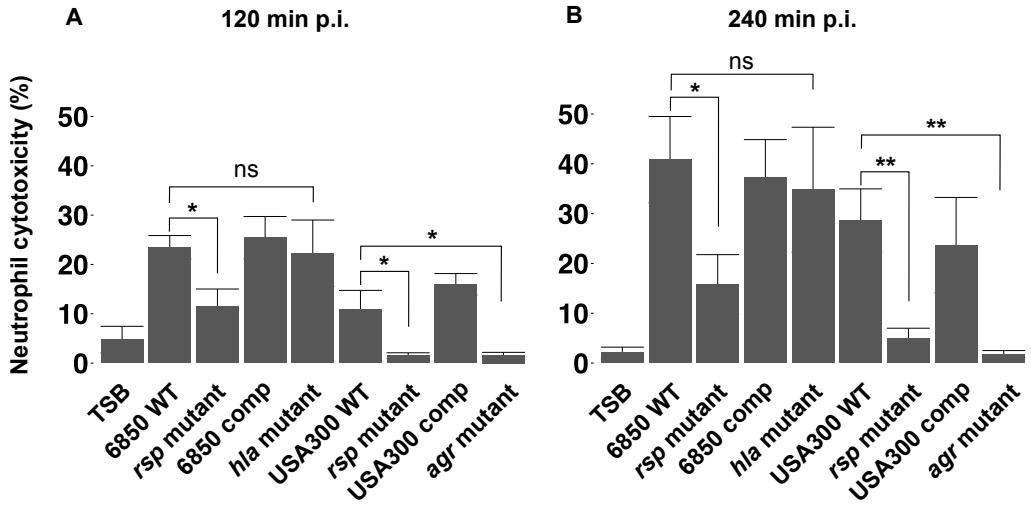

Figure 3.15: Extra-cellular secretions of *S. aureus rsp* mutants exhibit reduced neutrophil killing. Human neutrophils were intoxicated with sterile culture supernatant from *S. aureus rsp* mutants in both strains USA300 LAC* and 6850, isogenic wild types (6850 WT and USA300 WT), complemented mutants (6850 comp and USA300 comp), 6850 *hla* mutant, USA300 *agr* mutant (NE1532) and fresh sterile TSB medium. Bar plots show mean percentage of neutrophil cytotoxicity (y-axes) quantified at 120 (A) and 240 (B) minutes post intoxication, with SEM as error bars. Statistical analysis was performed by one-way ANOVA and individual comparisons were done by Tukeyś HSD test.*; $P< 0.05$, *; $P< 0.05$

29.54), $P= 0.04$ (See Figure 3.15B). These results were congruent with the observations during transcriptional profiling of *rsp* mutant (See Section 3.4).

3.5.2 Intra-cellular *rsp* mutants do not kill human neutrophils efficiently

Apart from culture supernatants, bacterial cells can also induce host killing from within by expression of virulence factors post internalization, an effect that has been observed previously in epithelial cells (See Section 3.2.2). To further investigate the role of *rsp* in intra-cellular pathogen-mediated neutrophil cytotoxicity post-phagocytosis, PMNs were infected with *S. aureus* , which were kept strictly intra-cellular by washing away extra-cellular bacteria (See Materials and Method Section 5.16.1) and host cytotoxicity was quantified at various time points by measuring release of cytoplasmic lactate dehydrogenase (LDH) in the spent medium. Initially, PMN death was minimal at 30 minutes post infection (See Figure 3.16A) with marginal but not significant increase at 60 minutes post infection ($P = 0.12$) (See Figure 3.16B).

However, at 120 minutes post infection accelerated neutrophil cytotoxicity was observed when compared to the initial time point ($P = 0.014$), induced similarly by both 6850; 29.83%, 95% CI (20.65 - 39.02) and USA300; 30.40%, 95% CI (19.80 - 41.01). Moreover, similar to the intoxication experiments (See Section 3.5.1), *rsp* mutant bacteria were inefficient in inducing neutrophil killing post-phagocytosis in case of both 6850; 16.52%, 95% CI (7.33 - 25.70), $P= 0.06$ and USA300; 15.89%, 95% CI (5.28 - 26.49), $P= 0.024$ and this phenotype was rescued upon re-introduction of *rsp in trans* (6850 comp, USA300 comp, See Figure 3.16C). Also, 6850 *hla* mutant; 30.09%, 95% CI (20.27 - 39.91), $P= 0.88$, did not have any defect in intra-cellular bacteria-induced neutrophil induce cell death. However, the laboratory strain RN4220; 15.63%, 95% CI (5.02 - 26.24), $P= 0.032$, was similarly attenuated as the *rsp* mutants (See Figure 3.16C).

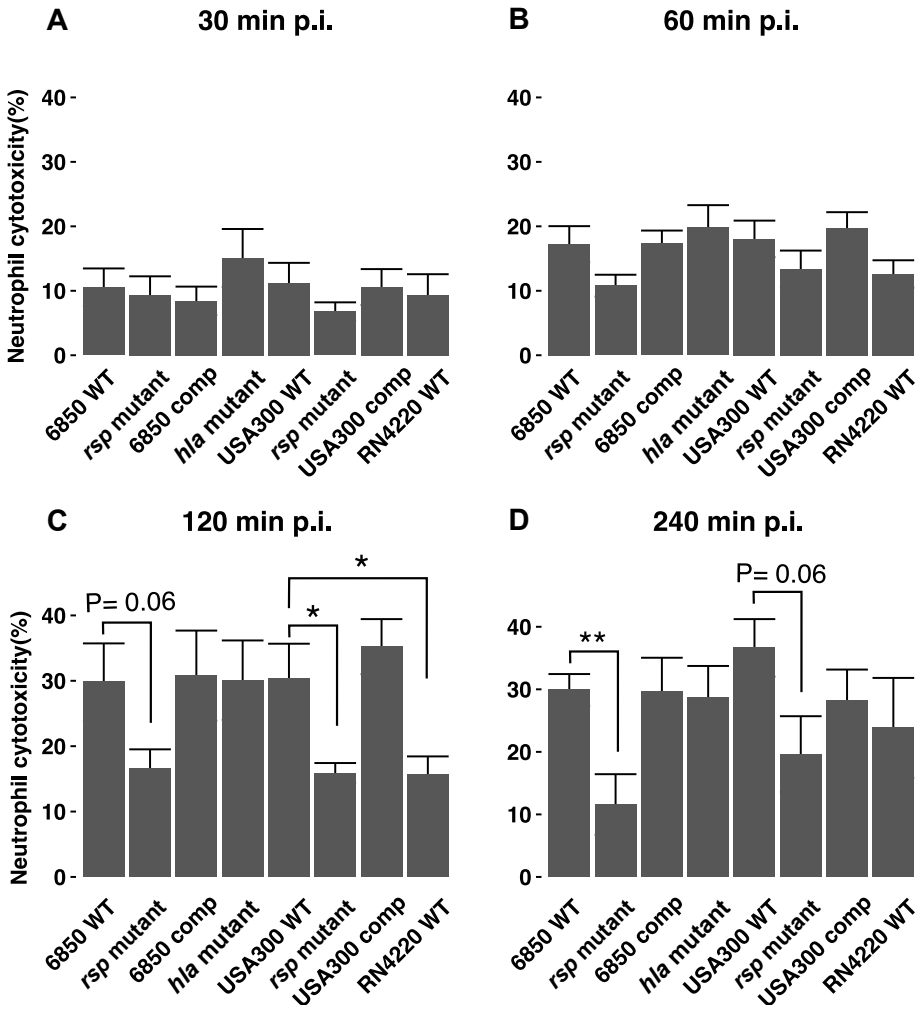

Figure 3.16: Intra-cellular *S. aureus* -induced neutrophil killing is influenced by Rsp. Cytotoxicity in primary human neutrophils (y-axes) was assessed by quantification of released lactate dehydrogenase (LDH), after infection with *S. aureus rsp* mutants in both strains USA300 LAC* and 6850 were compared to isogenic wild types, complemented mutants, 6850 lacking alpha toxin (*hla* mutant) and RN4220 with dysfunctional *agr* quorom sensing system. Neutrophil cytotoxicity was measured after 30 (A), 60 (B), 120 (C) and 240 (D) minutes post infection. Bar plots show mean percentage of neutrophil cytotoxicity and SEM as error bars. Statistical analysis was done by one-way ANOVA and individual comparisons were done by Tukeyś HSD test.*; $P< 0.05$, *; $P< 0.05$

Furthermore at 240 minutes post infection, although there was marginal increase in overall cytotoxicity for both wild type bacteria, when compared to the previous time point (See Figure 3.16D), *rsp* mutants remained attenuated in both 6850; 11.58%, 95% CI (1.66 - 21.49), $P= 0.06$ and USA300; 19.65%, 95% CI (7.50 - 31.80), $P= 0.007$ strain backgrounds (See Figure 3.16D). However, at this time point RN4220; 23.83%, 95% CI (12.96 - 34.69) showed increased cytotoxicity compared to the previous and had no more significant attenuation of PMN cell death.

3.5.3 *S. aureus rsp* mutants exhibit stunted intra-cellular proliferation in human neutrophils

During intra-cellular *S. aureus* -mediated PMN death, the survival of bacteria within PMNs over time were also simultaneously analysed by enumeration of intra-PMN CFUs, since neutrophils can destroy bacteria post-phagocytosis as an innate defence mechanism. Prior to testing *rsp* mutants, the enumeration of intra-phagocytic CFUs for all wild type bacteria at different times, showed the precise dynamics of *S. aureus* survival within neutrophils. Immediately after phagocytosis i.e. 10 minutes post infection, the bacteria were enumerated for assessing the initial number of internalized CFUs. Intriguingly until 60 minutes post infection, there was rapid destruction of bacteria by the neutrophils resulting in severe plunge in CFU numbers for USA300 LAC* strain (0.87 fold) and RN4220 (0.44 fold), but 6850 (0.39 fold) performed better when compared to its initial CFU counts (See Figure 3.17A). However at 120 minutes post infection, the surviving bacteria start replicating inside the neutrophil and notably, the laboratory strain RN4220 showed similar recovery as 6850. Finally after 240 minutes post infection, bacteria were found to be rapidly replicating inside the PMNs. At this time point, USA300 LAC* strain CFUs were 5.33 fold and 6850 CFUs were 6.54 fold higher CFUs than that at 60 minutes post infection. Although RN4220 did show evident replication (3.25 fold), it had significantly less replicative potential than 6850 (P = 0.0046).

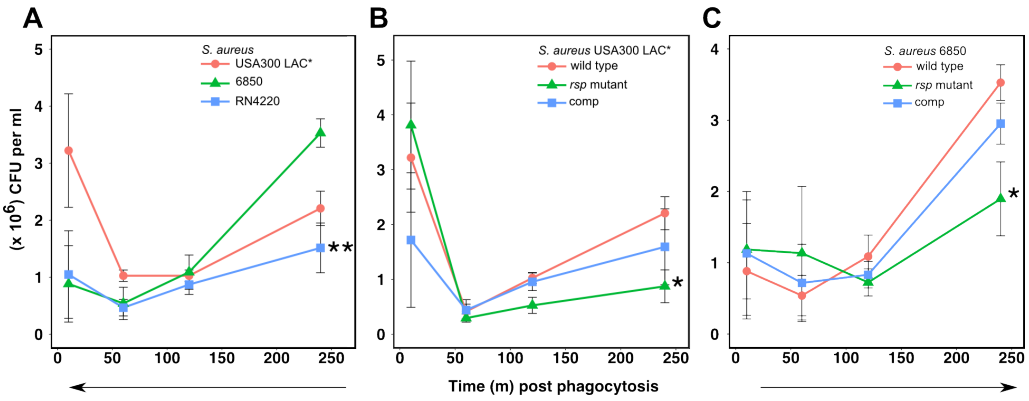

Figure 3.17: Intra-neutrophil survival and proliferation of *S. aureus* is influenced by Rsp. *S. aureus* survival within primary human neutrophils is shown in terms of viable CFUs recovered from within neutrophils after 10, 60, 120, 240 minutes post phagocytosis. (**A**) Intra-neutrophil survival of wild type *S. aureus* USA300 LAC* (red) and 6850 (green) were compared to each other and RN4220 (blue) with dysfunctional *agr* quorom sensing system, over given time course. (**B**) Survival of *S. aureus* USA300 *rsp* insertion mutant (green) was compared to its isogenic wild type (red) and complemented (comp, blue) counterparts. Similarly, (**C**) *rsp* deletion mutants (green) in strain 6850 was compared to its wild type (red) and complemented strain (comp, blue). Line graphs show mean enumeration of CFUs recovered from neutrophils over given time course and SEM as error bars. Statistical analysis was done by Studentś t-test at individual time points. *; P< 0.05, *; P< 0.05

rsp mutants and complemented mutants also followed similar dynamics as the wild type strain over the given time period. However, *rsp* mutants showed stunted proliferation ability after 240 minutes post infection, with significantly low number of CFUs in case both 6850 (0.53 fold, P= 0.031, See Figure 3.17B) and USA300 (0.39 fold, P= 0.034, See Figure 3.17C), when compared to isogenic wild type and

complemented bacteria. Therefore, *rsp* mutants perform weakly within neutrophils, which is congruent to its cytotoxic ability.

3.5.4 *S. aureus rsp* mutants exhibit prolonged intra-cellular survival in human macrophages

Apart from human neutrophils, *S. aureus* can infect human macrophages, which are also an important part of host innate immune response. To investigate the role of rsp during infection macrophages, these cells were challenged with monomeric red fluorescent protein-expressing wild type *S. aureus* 6850 and its *rsp* deletion mutant. Bacterial survival post-phagocytosis was monitored by observing fluorescence at 588 nm, every 24 hours. Human monocyte-derived macrophages were able to eliminate most of the wild type bacteria after 48 hours, which was confirmed by the presence of significantly less and smaller foci of red fluorescence (See Figure 3.18).

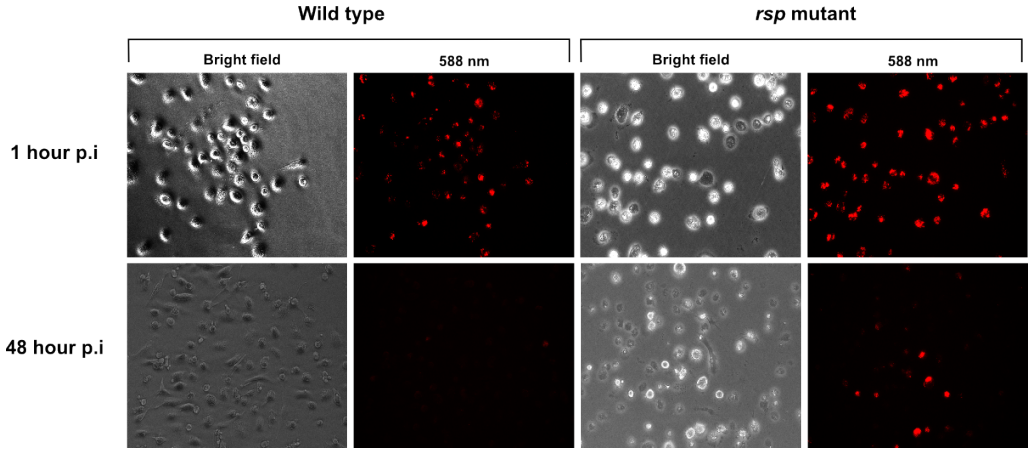

Figure 3.18: *S. aureus rsp* mutants can survive within macrophages for a longer time period. Survival within primary human macrophages over time is shown by the presence of *S. aureus* 6850 producing monomeric red fluorescent protein (mRFP). Macrophages infected with both wild type bacteria and *rsp* deletion mutants, were imaged under bright field and 588 nm for detection of red fluorescence, immediately after infection i.e. 1h p.i and 48h p.i.

Surprisingly in case of the *rsp* mutants, fluorescent foci were relatively more and bigger in size indicating an enhanced potential of the mutants to resist macrophage-mediated killing and prolonged intra-cellular survival (See Figure 3.18).

3.6 Rsp mediates *S. aureus* response against antimicrobial superoxide and neutrophils

To investigate more about the genes regulated by Rsp, the Staphylococcus aureus Transcription Meta-Database (SATMD) [263] was used to search for putative functions. This web-accessible database is a conglomerate of all published transcription data from several *S. aureus* strains, which also includes all supplementary information. Upon individual assessment, it was observed that Rsp regulon consists

of *S. aureus* genes that has been observed in different studies, to increase in abundance upon exposure to reactive oxygen species and host immune defence . These genes included *rsp* has been shown to one of the many genes up-regulated after 30 minutes exposure to 5mM Hydrogen Peroxide (H_2O_2) in *S. aureus* strain MW2 (USA400 genotype)[112], *isd* operon that is important against oxidative stress and intra-neutrophil survival[112], *luk*AB that is upregulated upon exposure to neutrophil granules and hydrogen peroxide in different strains[112,264]. In total, 73 out of 113 genes regulated by Rsp has been associated with neutrophil-mediated stress and oxidative stress (See Figure 3.19).

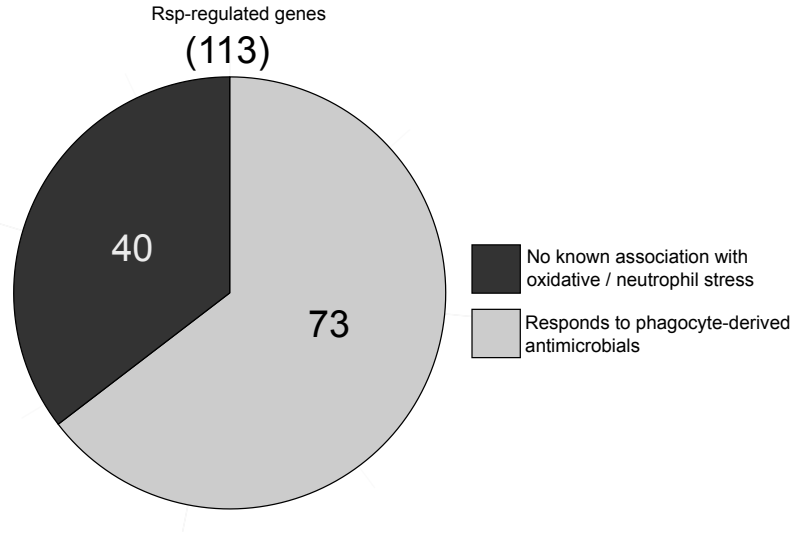

Figure 3.19: A subset of *S. aureus* Rsp regulon is influenced by antimicrobial reactive oxygen species. A Venn diagram showing 73 out of 113 genes regulated by Rsp has been previously shown to respond to phagocyte-derived antimicrobials and reactive oxygen species. The data was mined by using the database *Staphylococcus aureus* transcriptome meta-database (SATMD) and Rsp-regulated genes were searched in the pre-existing record

3.6.1 Up-regulation of *rsp* and a subset of its targets upon exposure to hydrogen peroxide

To further investigate in details, the role of *rsp* upon bacterial exposure to oxidative stress, *S. aureus* were treated with 5mM hydrogen peroxide *in vitro*, which was enough to induce a transcriptional response to minimal loss in bacterial viability[112]. Both exponentially growing (1.5 hours; OD_{540} 0.6) and stationary phase (8 hours; OD_{540} 5.0) bacteria were exposed for 10 minutes to limit them within a single generation of replication, which is approx. 20 minutes for *S. aureus* . The changes in gene expression were analysed by quantitative real time PCR for both 6850 and USA300 LAC* genotypes, and compared to its respective untreated control samples, which were normalized to RQ of 1.

In exponentially growing USA300 LAC*, the relative levels of *rsp* expression; 2.24, 95% CI (1.70 - 2.78), *P*= 0.009, was significantly higher within 10 minutes of exposure to 5mM H_2O_2, which was earlier than previously reported[112]. This effect absent in the *rsp* mutants, however could not be recovered upon complementation (See Figure 3.20A). In wild type bacteria, it was shown for the first time that the expression of *ssr*42 ; 2.14, 95% CI (1.60 - 2.68), *P*= 0.006, was increased upon oxidative stress in an *rsp* -

dependent manner (See Figure 3.20B). To assure that the stimulation with 5mM H_2O_2 was sufficient to induce oxidative stress especially a transcriptional response, the expression of *dps* that encodes a homolog of *Escherichia coli* DNA-binding protein for starved cells (Dps) in *S. aureus* , was examined. Dps expression has been shown to spike when bacteria undergo oxidative stress [112,265], hence served as a positive control indicating that *rsp* mutants also underwent similar oxidative stress as its isogenic wild type and complemented mutants (See Figure 3.20C), while there was no increase in expression of Rsp target genes. Rsp-dependent up-regulation of target genes were evident for *isd*A ; 1.99, 95% CI (1.49 - 2.49), P = 0.02, *luk*AB ; 2.03, 95% CI (1.56 - 2.50), P= 0.0011, *scp*A; 1.42, 95% CI (1.15 - 1.69), P= 0.018, *hlg*A ; 1.48, 95% CI (1.27 - 1.68), P= 0.018, *hlg*CB ; 1.31, 95% CI (1.11 - 1.51), P= 0.042, *luk*S-PVL 1.50, 95% CI (1.33 - 1.66), P< 0.001 (See Figure 3.20B, D, F, G, J, K and L). The transcriptional response of these genes remained unchanged in the absence of *rsp* and were reinstated upon introduction of *rsp* episomally . On the other hand, some of the Rsp-regulated genes such as *hla*, *RNA* III, *chs* had did not show any transcriptional response or Rsp-dependency upon oxidative stress (See Figure 3.20E, H and I).

Interestingly, the expression of certain Rsp-regulated genes significantly declined in the absence of *rsp* , upon oxidative stress. These genes were *luk*AB ; 0.46, 95% CI (0.00 - 0.93), P< 0.001, *scp*A; 0.68, 95% CI (0.41 - 0.95), P= 0.039, *hlg*A ; 0.67, 95% CI (0.47 - 0.88), P< 0.001 and *luk*S-PVL; 0.73, 95% CI (0.57 - 0.90), P= 0.002 (See Figure 3.20F, G, J and L), out of which gene expression was not completely recovered in case of *luk*S-PVL. On the contrary, when bacteria from stationary growth phase were treated with 5mM H_2O_2, the *rsp* -dependent transcriptional response was hardly evident after 10 minutes, indicating differential regulation in the late phase of growth. The relative expressions of *rsp*; 1.23, 95% CI (-8.08 - +10.56), P= 0.17, *hlg*CB; 1.65, 95% CI (1.36 - 1.95), P= 0.17, *luk*S-PVL; 1.60, 95% CI (1.42 - 1.79), P= 0.14, were marginally increased in an *rsp*-dependent manner, although not significant (See Figure 3.21A, K and L). However, there was substantial oxidative stress indicated by the significant up-regulation of *dps* (See Figure 3.21C). Interestingly, the expression of *isd*A increased similarly in case of wild type, mutant and complemented mutants, indicating an rsp-independent effect (See Figure 3.21D).

In exponentially growing 6850, expressions of *rsp* ; 2.07, 95% CI (-3.94 - +8.09) and *ssr*42 ; 1.47, 95% CI (0.96 - 1.99) were also increased upon exposure of wild type bacteria to oxidative stress (See Figure 3.22A and B). This effect was dependent on *rsp* in case of *ssr*42 and was recovered upon complementation. Oxidative stress was evident by the induction of *dps* gene expression (See Figure 3.22C). *rsp* -dependent induction of transcription was evident in case of *isd*A ; 1.71, 95% CI (1.46 - 1.95), P= 0.004, *luk*AB ; 2.21, 95% CI (1.82 - 2.60), P< 0.001, *scp*A; 1.38, 95% CI (1.18 - 1.57), P= 0.03 (See Figure 3.22D, F and G), with no recovery of *isd*A expression in case of *rsp* complementation. Interestingly, the expression of *chs*, *hla* and *hlg*A were increased in an *rsp* -dependent manner, with only *hla* showing significant increase in case of the wild type and induction could not completely recovered upon *rsp* complementation. The expression of *RNA* III and *hlg*CB did not change upon oxidative stress. Hence, indicating regulatory differences between genotypes 6850 and USA300.

Furthermore in 6850 from stationary growth phase, H_2O_2 treatment induced the expression of *rsp* ;

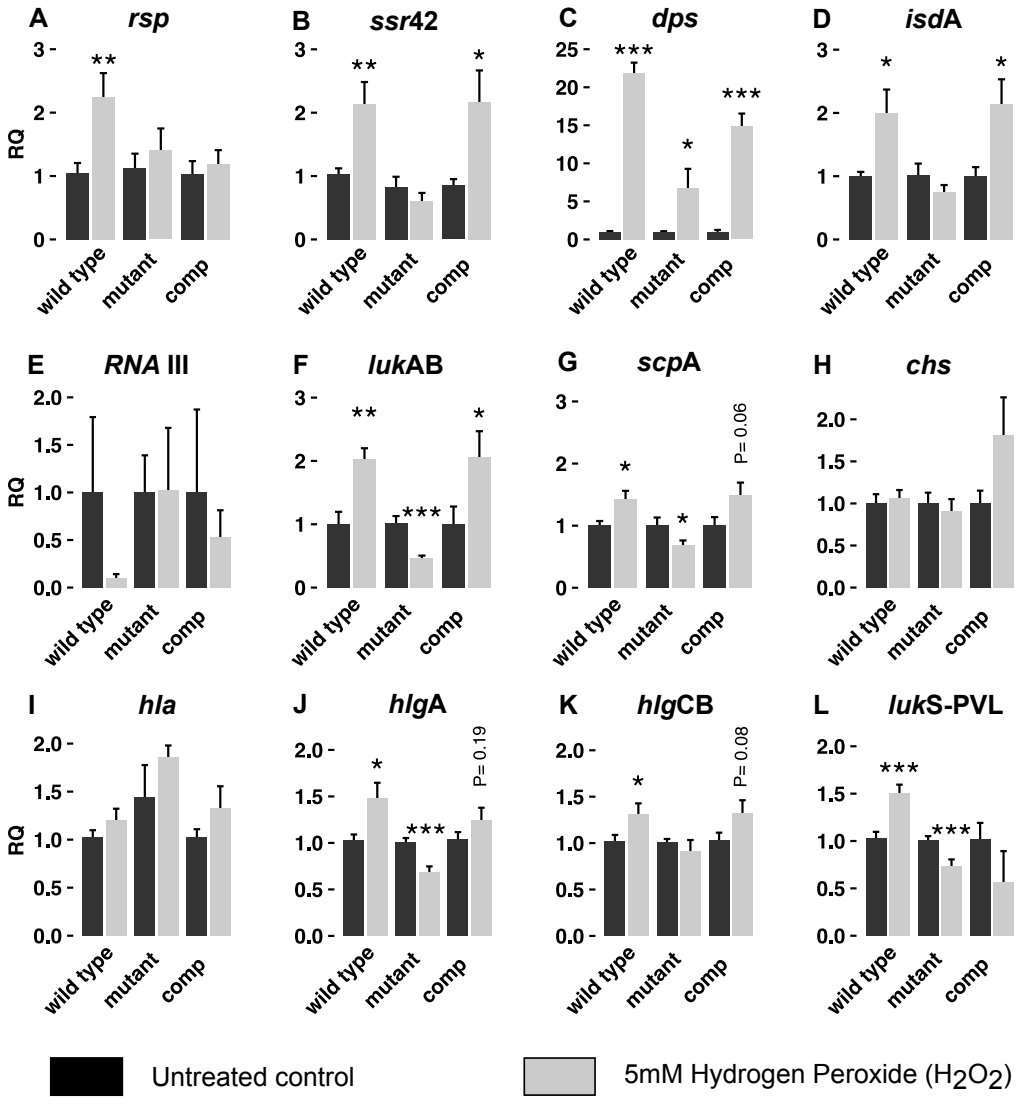

Figure 3.20: Rsp influences *S. aureus* gene expression under peroxide stress in strain USA300 (MRSA) during logarithmic growth phase. Individual gene expression in exponentially growing *Staphylococcus aureus* i.e. OD_{540nm} = 0.6, were assessed by quantitative real time PCR. Vertical axes show the relative quantification (RQ) of mRNA abundance in *rsp* mutants (dark grey) and complemented bacteria (comp, light grey), with reference to the wild type (black). Sample sizes for all experiments were n=6, with exceptions in case of *luk*AB (n=10) and *2128, RNA* III (n=4). Bar plots show mean RQ levels and SEM as error bars. Statistical analysis was done by pair-wise t-test.*; $P < 0.05$, **; $P < 0.01$, ***; $P < 0.001$

1.94, 95% CI (1.59 - 2.28) in the wild type but not in the mutant, which was then recovered upon complementation (See Figure 3.23A). Similar to USA300 LAC* from stationary phase, there was no substantial change in the expression of *ssr*42 , *hla, RNA*III (See Figure 3.23B, E and F), despite the presence of oxidative stress indicated by the up-regulation of *dps* (See Figure 3.23C). Interestingly, the expression of *isd*A ; 1.95, 95% CI (1.43 - 2.48), *P*= 0.01 and *hlg*A ; 3.60, 95% CI (2.36 - 4.85), *P*= 0.01 were induced upon oxidative stress in an *rsp* -dependent manner. In addition to this, only in case of *rsp* mutant the expression of *hlg*CB ; 2.63, 95% CI (2.10 - 3.17) was significantly induced upon H_2O_2 treatment.

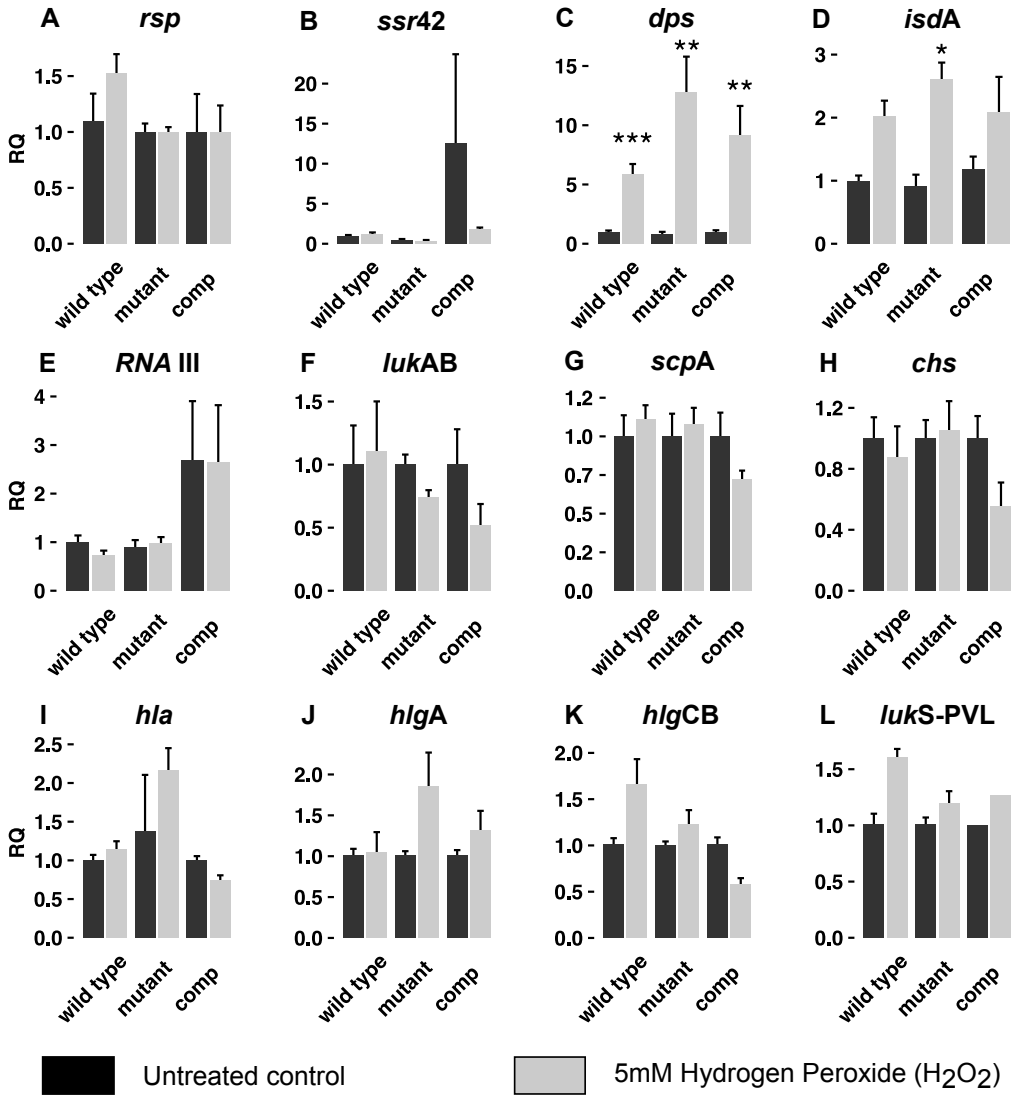

Figure 3.21: Rsp influences *S. aureus* gene expression under peroxide stress in strain USA300 (MRSA) during stationary growth phase. Individual gene expression in exponentially growing *Staphylococcus aureus* i.e. OD_{540nm} = 0.6, were assessed by quantitative real time PCR. Vertical axes show the relative quantification (RQ) of mRNA abundance in *rsp* mutants (dark grey) and complemented bacteria (comp, light grey), with reference to the wild type (black). Sample sizes for all experiments were n=6, with exceptions in case of *luk*AB (n=10) and *2128*, *RNA* III (n=4). Bar plots show mean RQ levels and SEM as error bars. Statistical analysis was done by pair-wise t-test.*; $P<$ 0.05, **; $P<$ 0.01, ***; $P<$ 0.001

3.6.2 Hydrogen peroxide exposure increases *S. aureus* cytotoxicity in an *rsp*- dependent manner

Rsp regulates the expression of major cytotoxins and immune evasion factors (See Section 3.4) and regardless of minor strain differences, Rsp largely mediates *S. aureus* response to oxidative stress (See Section 3.4). Majority of the oxidative stress is imparted by neutrophils, which are pioneers of host immune response at the site of infection. Therefore, in order to investigate whether the *rsp* -dependent transcriptional induction is translated into an observable phenotype and to mimic the situation of neutrophil encounter, *S. aureus* -mediated neutrophil cytotoxicity was analysed after pre-exposure of bacteria to

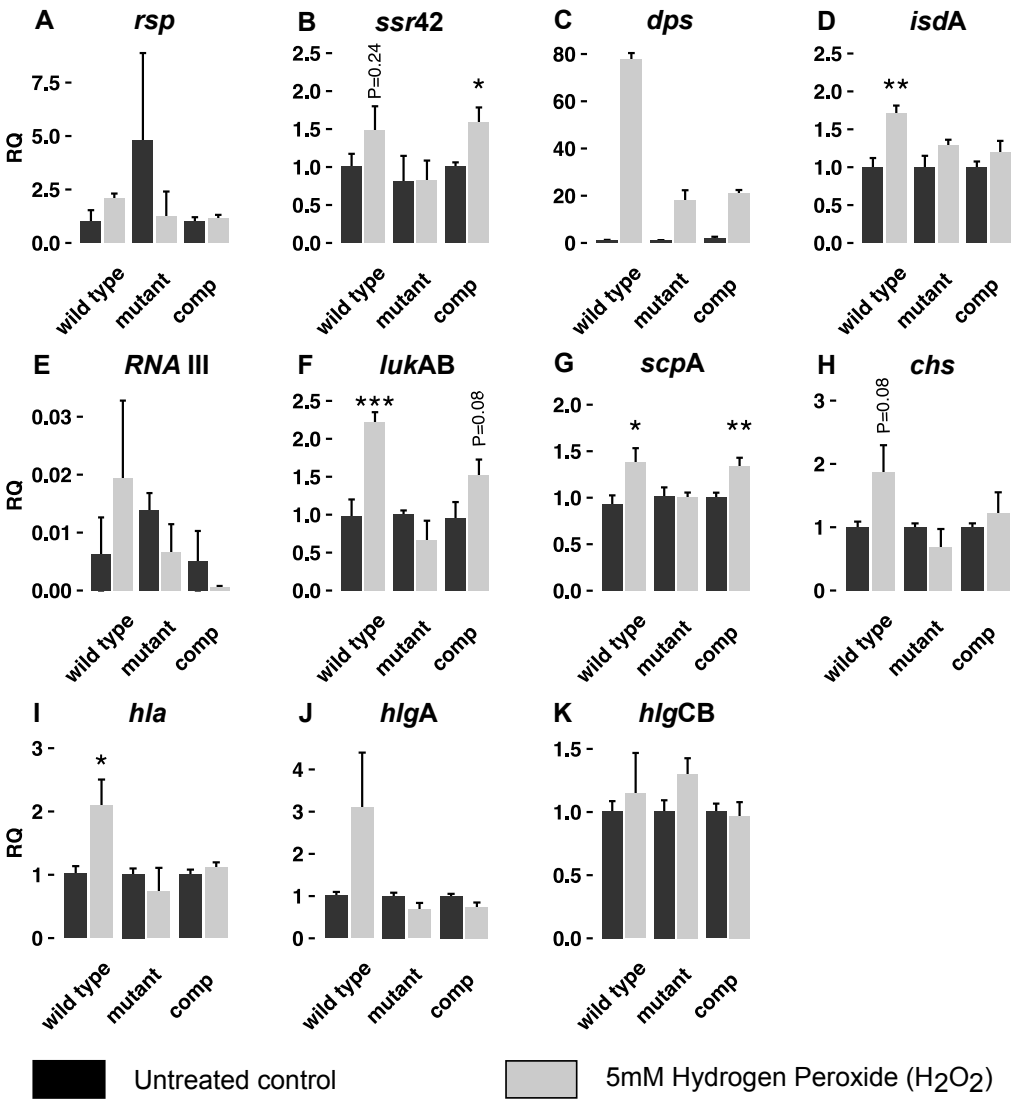

Figure 3.22: Rsp influences *S. aureus* gene expression under peroxide stress in strain 6850 (MSSA) during logarithmic growth phase. Individual gene expression in exponentially growing bacteria, were assessed by quantitative real time PCR. Vertical axes show the relative quantification (RQ) of mRNA abundance in *rsp* mutants (dark grey) and complemented bacteria (comp, light grey), with reference to the wild type (black). Sample sizes for all experiments were n=6, with exceptions in case of *luk*AB (n=10) and *2128, RNA* III (n=4). Bar plots show mean RQ levels and SEM as error bars. Statistical analysis was done by pair-wise t-test *; $P< 0.05$, **; $P< 0.01$, ***; $P< 0.001$

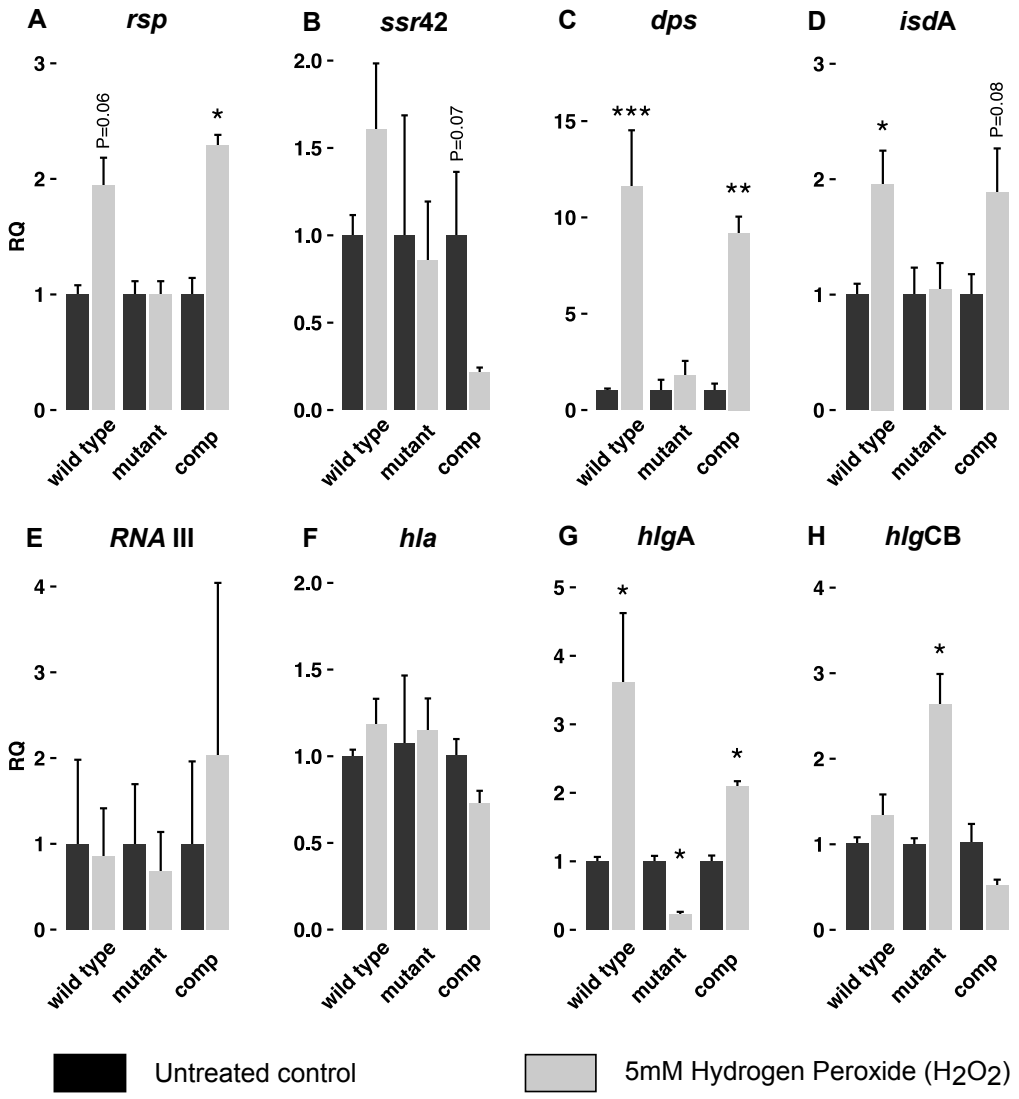

Figure 3.23: Rsp influences *S. aureus* gene expression under peroxide stress in strain 6850 (MSSA) during stationary growth phase. Individual gene expression in exponentially growing *Staphylococcus aureus* i.e. OD_{540nm} = 0.6, were assessed by quantitative real time PCR. Vertical axes show the relative quantification (RQ) of mRNA abundance in *rsp* mutants (dark grey) and complemented bacteria (comp, light grey), with reference to the wild type (black). Sample sizes for all experiments were n=6, with exceptions in case of *luk*AB (n=10) and *2128*, *RNA* III (n=4). Bar plots show mean RQ levels and SEM as error bars. Insets show zoomed plots to illustrate comparisons wherever not visible. Statistical analysis was done by pair-wise t-test.*; $P < 0.05$, **; $P < 0.01$, ***; $P < 0.001$

H_2O_2. Exponentially growing *S. aureus rsp* mutants, wild type and complemented mutants from both genetic backgrounds of 6850 and USA300 LAC*, were exposed to 5mM H_2O_2 and after 8 hours post inoculation (stationary phase), the sterile-filtered supernatants (See Figure 3.24A) were used to intoxicate neutrophils as previously described (See Section 3.5.1). However, H_2O_2 could potentially be toxic for host cells when present in the supernatants of treated samples, hence may provide false positive results. To rule out the presence of H_2O_2 in the spent medium, sterile supernatants were examined using peroxide indicator strips (See Materials and Methods, Section 5.10) that showed no remaining levels of peroxide when tested after 8 hours post inoculation (See Figure 3.24B), after introduction during exponential phase.

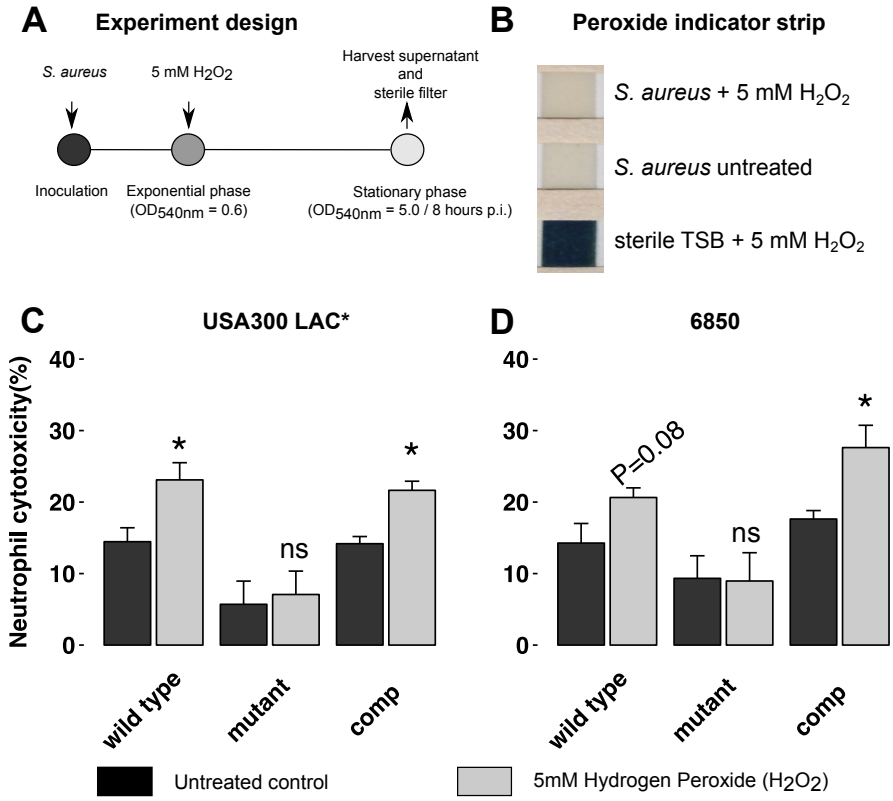

Figure 3.24: Rsp responds to hydrogen peroxide stress and enhances S. aureus exotoxin-mediated neutrophil killing Cytotoxicity in primary human neutrophils (y-axes) was assessed by quantification of released lactate dehydrogenase (LDH), after infection with *S. aureus rsp* mutants in both strains USA300 LAC* and 6850 were compared to isogenic wild types, complemented mutants, 6850 lacking alpha toxin (*hla* mutant) and RN4220 with dysfunctional *agr* quorom sensing system. Neutrophil cytotoxicity was measured after 30 (A), 60 (B), 120 (C) and 240 (D) minutes post infection. Bar plots show mean percentage of neutrophil cytotoxicity and SEM as error bars. Statistical analysis was done by one-way ANOVA and individual comparisons were done by Tukey's HSD test.*; $P < 0.05$

Human PMNs were intoxicated with supernatants from both H_2O_2 -treated and untreated *S.aureus* and examined for cell death. Supernatants from treated wild type bacteria were significantly more toxic to PMNs after 4 hours. This effect on cytotoxicity was independent of genotype and were similar in case of both USA300; Untreated: 14.45%, 95% CI (9.31 - 19.60), Treated: 23.10%, 95% CI (17.95 - 28.24), P = 0.049 and 6850; Untreated: 14.26%, 95% CI (8.44 - 20.08), Treated: 20.64%, 95% CI (14.82 - 26.46), P = 0.08 (See Figure 3.24C and D). Even though *rsp* mutants were treated with H_2O_2, the supernatants did not exhibit substantial increase in neutrophil cytotoxicity, whereas in case of complemented mutants the increase in cytotoxicity was significantly evident. This finding suggests an *rsp* -mediated acceleration of toxin production and consequential neutrophil cell death upon exposure to oxidative stress.

3.7 N-terminal FLAG tag fused Rsp facilitated immunoprecipitation without hindering its function

For further molecular characterisation of the transcriptional regulation of Rsp, its binding to target promoters could be performed. Recent advances in immunoprecipitation technique allows for the pull-

down of a tagged regulatory protein in a DNA-bound state after fixation, in a technique known as Chromatin immunoprecipitation followed by deep sequencing[266]. Prior to this, the protein of interest has to be fused with one of prevalently used tags. In this case, *rsp* mutants were complemented with the pS2217 harboring Rsp fusion protein with triple FLAG (3XFLAG; DYKDHD-G-DYKDHD-I-DYKDDDDK) sequence at the N-terminus, which was constructed by overlap extension PCR (See Figure 3.25).

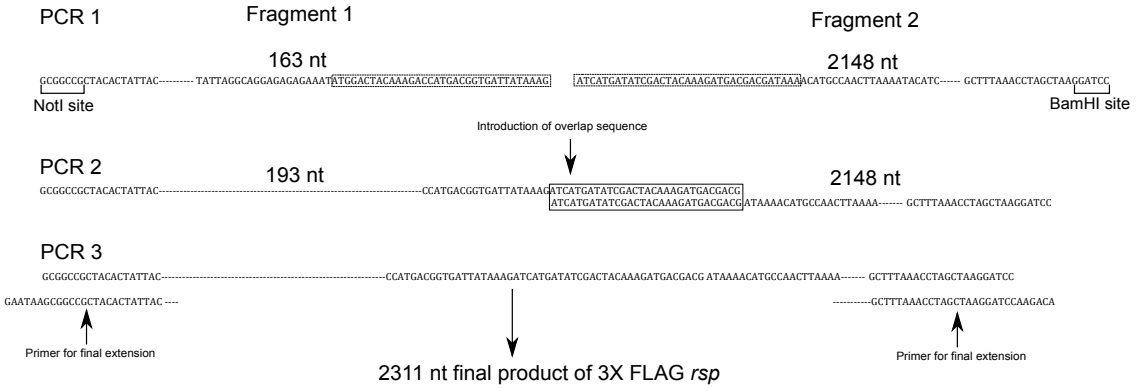

Figure 3.25: Introduction of triple FLAG (3X FLAG) tag at N-terminus of episomally expressed Rsp A triple FLAG tag sequence was fused with *rsp* by overlap extension PCR, where two sequences containing the FLAG tag preceded by a start codon (ATG), NotI restriction enzyme cleavage site at the 5′ end and an overlapping sequence (black rectangle), was fused to another fragment containing the entire protein coding sequence of Rsp followed by a BamHI restriction enzyme cleavage site at the 3′ end. This resulted in a 2311 nt N-terminal fusion of triple FLAG with Rsp$^{\Phi}$

For overlap PCR, two seperate fragments were generated during the PCR 1. Fragment 1 was of 163 nt containing a NotI restriction enzyme cleavage site at the 5′ end, followed by the promoter of *rsp* , then the sequence of the 3X FLAG preceded by an ATG start codon. Fragment 2 was of 2148 nt containing the entire Rsp ORF devoid of only the first start codon, followed by a BamHI restriction enzyme cleavage site at the 3′ end. In the next PCR 2 step, an overlapping sequence from the 5′ end of Fragment 2 was introduced in Fragment 1 resulting in a 193 nt long sequence. Finally, during PCR 3 step both fragments were fused by a combinatorial linear and exponential PCR strategy to obtain a 2311 nt fusion gene that introduced in place of native *rsp* in pS2217 to generate the plasmid pS2217 3XFLAG$^{\Phi}$.

Upon complementation of 6850 *rsp* mutant with pS2217 3XFLAG, the function of *rsp* was investigated in terms of the reappearance of haemolysis on blood agar plates caused by complemented mutants, as previously shown in Section 3.1, Figure 3.1. The diameter of haemolysis obtained in case of *rsp* mutants complemented with pS2217 3XFLAG (6.2 mm, 95% CI (6.09 - 6.30), $P = 0.15$) were similar to that of complementation with pS2217 (6.04 mm, 95% CI (5.93 - 6.15), See Figure 3.26A) expressing untagged Rsp and was similar to wild type haemolysis. Hence, it could rescue the loss of haemolysis in *rsp* mutants (1.72 mm, 95% CI (1.61 - 1.82), $P < 0.001$, See Figure 3.26A).

With successful retainment of function the 3XFLAG Rsp fusion protein, the next step was to investigate whether it can be captured by affinity purification using anti-FLAG antibody. For this purpose, im-

$^{\Phi}$ Overlap extension PCR based construction of Rsp 3XFLAG and pS2217 3XFLAG plasmid complementation, were performed by Mr. Benjamin Orlando Torres Salazar, Matriculation number. 1754107 during Master F1 practical course

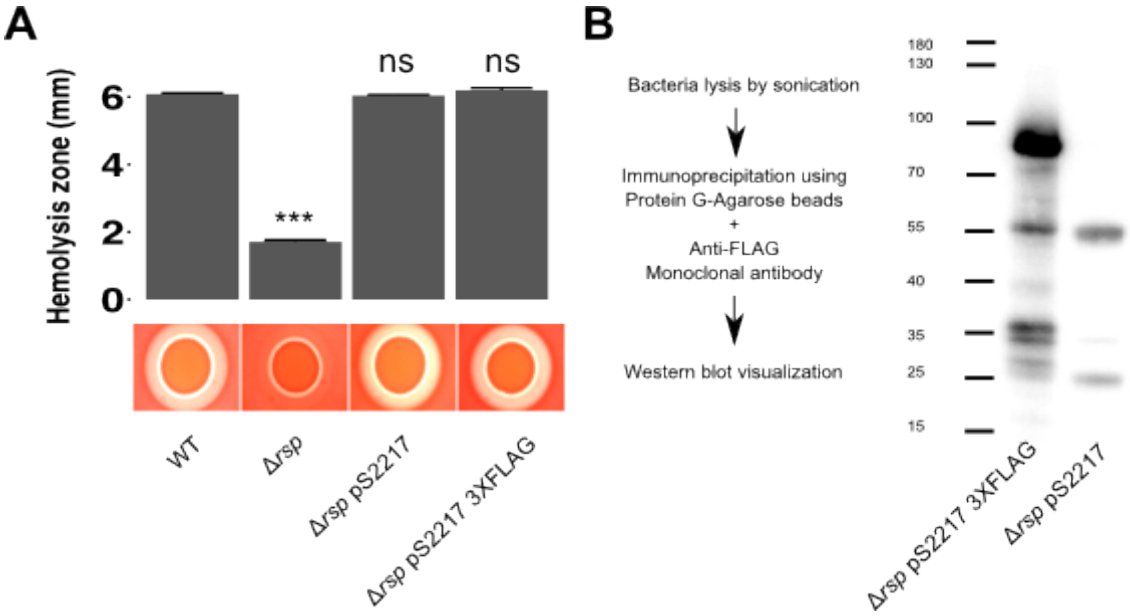

Figure 3.26: N-terminal 3XFLAG Rsp fusion protein retains its function and can be captured by immunoprecipitation (**A**). FLAG *rsp* fusion gene was re-introduced in 6850 *rsp* mutant (Δ *rsp* pS2217 3XFLAG) and haemolysis on blood agar plates was found to be similar to that of wild type (WT) and complemented mutant with untagged Rsp (Δ *rsp* pS2217). Bar plots show mean diameter of haemolysis zone measured with SEM as error bars. Statistical analysis was performed by one-way ANOVA and Tukeyś HSD test for individual comparisons. ***; $P < 0.001$

munoprecipitation was performed using lysates of exponentially growing *S. aureus* 6850 Δ *rsp* pS2217 3XFLAG and 6850 Δ *rsp* pS2217, using Protein G-Agarose beads under native conditions and detected by Western blotting. The results clearly show very efficient pull down of a product detected between 70 - 100 kDa, expected mass of 84.58 kDa (723 a.a)[Υ] for 6850 Δ *rsp* pS2217 3XFLAG (See Figure 3.26B). The 3XFLAG adds 22 a.a to the N-terminus of Rsp, which has a theoretical mass of 81.87 kDa (701 a.a)[Υ]. On the other hand, there was no protein detected by the anti-FLAG antibody in case of 6850 Δ *rsp* pS2217, hence indicating a very specific detection the 3XFLAG Rsp fusion product.

[Υ] All theoretical mass and length calculation of proteins were done using (ExPASy,SIB)

Chapter 4

Discussion

S. aureus is s a facultative intracellular pathogen which is able to kill its host cells upon phagocytosis. However, this process is not understood and many of the involved virulence factors are hitherto unknown. The aim of the present study was to identify bacterial factors required for the enigmatic intracellular pathogenicity of *S. aureus* .

4.1 Transposon insertion site sequencing: an efficient tool for studying bacterial genes involved in virulence

To determine the role of bacterial gene products in bacterial pathogenesis, infection experiments are usually conducted after gene disruption. Insertional mutagenesis is one of the widely used methods for gene disruption, where an unrelated stretch of DNA inserts and disrupts the target gene. Transposons-based approaches are the most prevalent techniques to perform random and unbiased insertional mutagenesis. The ability of transposons to randomly insert into the host genome makes transposon mutagenesis one of the best choices when it comes to unbiased forward genetic strategies. In other bacteria such as *Enterococcus faecalis* and *Listeria monocytogenes* transposon mutants were generated and individually tested to identify novel genes involved in biofilm formation *in vitro*[267,268]. Transposon mutagenesis was also used in *Rhodococcus equi, Francisella tularensis* to identify genes that influence auxotrophy and intracellular virulence[269,270]. However, in these experiments mutants were singly tested for the presence of insertions by either southern blot or sequencing, which made them rather cumbersome.

Eventually, new strategies were developed to expand this technique to a genome-wide scale by signature tagged mutagenesis[271]. With the recent advent of next generation sequencing (NGS) technologies, especially Massively parallel sequencing (MPS), also called deep sequencing, has expanded the horizon for genome-wide studies of genomes, transcriptomes and also transposon insertion sites in various organisms including *Salmonella* Typhimurium, *Staphylococcus aureus* , *Vibrio cholerae, Listeria monocytogenes* and *Streptococcus pneumoniae*[272]. Recent advancements in this technology with regards to

sample multiplexing, increased sequencing capacity of instruments provide with more efficient, highly sensitive, cost and time-effective way of DNA sequencing.

Transposon mutant libraries have been characterised by MPS in a wide variety of strategies such as High-throughput insertion tracking by deep sequencing (HITS)[273], transposon-directed insertion site sequencing (TraDIS)[274], Insertion sequencing (INSeq)[275] and transposon insertion site sequencing (Tn-seq)[276]. Transposon insertion site deep sequencing (Tn-seq) has been employed to other bacteria such as *Salmonella* Typhi to investigate bile-tolerance factors[274], *Haemophilus influenzae* and *Streptococcus pneumoniae* for assessing fitness in lungs[273,276].

In *S. aureus*, transposon insertional mutagenesis using Himar1 derived transposable elements have been used to identify novel virulence factors. Himar1 transposon is a class II family eukaryotic DNA transposons from horn fly, *Haematobia irritans* consisting of a gene encoding transposase enzyme, flanked by inverted terminal repeats (ITRs). The transposon is mobilized in a non-replicative manner by a 'cut and paste' mechanism, which is facilitated by the transposase enzyme that recognizes the ITR and excises the entire transposable element[277], which then jumps onto its target site preferably inserting within the dinucleotide "TA"[278], resulting in a target site duplication[279]. Furthermore, this system has rare chances of multiple insertions per genome, which is due to two major reasons. Firstly, Himar1 transposon mutagenesis relies on a "cut and paste" mechanism, hence the mobile is not replicated but rather dissevered from the plasmid thereby limiting the available fragments for insertions[278]. Secondly, the frequency of transpositions are inherently low[277], even for the hyperactive C9 Himar1 transposase used in this study with frequencies are in the range of 2×10^{-4}.

In a first study using Himar1 within *S. aureus*, mutagenesis was performed by a two-plasmid system, one carrying a reporter gene flanked by the ITRs and another carrying the transposase enzyme, on semi-solid medium. This was followed by picking single colonies and detection of putative mutants by DNA isolation, and amplification with transposon-specific primers. Individually collected mutants were tested for its role in infection by investigated *S. aureus*-mediated nematode killing[280]. In the second study, mutagenesis was performed by a single plasmid system, while bacteria were propagated in liquid medium generating pools of mutants. These mutants were tested for resistance to the anti- microbial peptide, Dermicidin. Resistant mutants were grown on semi-solid medium and tested by transposon-specific PCR to look for insertion sites.[246].

In the present study, genome-wide Himar1-transposon mutagenesis was performed to create *S. aureus* mutant pools (See Section 2.1.1) and Transposon insertion site sequencing (Tn-seq) was used to specifically track the insertion sites (See Section 2.1.3). The advantages of this approach are: 1. High throughput detection of number of mutants and their abundances. 2. Assessment of individual mutant in presence of the entire population and differential roles in specific host niches. This strategy successfully demonstrated a genome-wide coverage with 25,000 transposon insertions sites (TIS) and average insertion interval of 166 bp. These numbers were not restricted as mutant pools created later showed up to 75,000 TIS. However, two independently created mutant pools only showed partial similarity (See

Figure 2.8, R^2=0.49), which reassures the randomness of transposition. In addition to this, the advantages of using Himar1 transposon includes no reported sequence bias, with "TA" dinucleotide as the only prerequisite [278], although it can also insert between other dinucleotides. This was evident by the analysis of base composition downstream of all the insertion sites, where TA was found to be the most abundant with just above 60% but rest consisted of other dinucleotide combinations (See Figure 4.1).

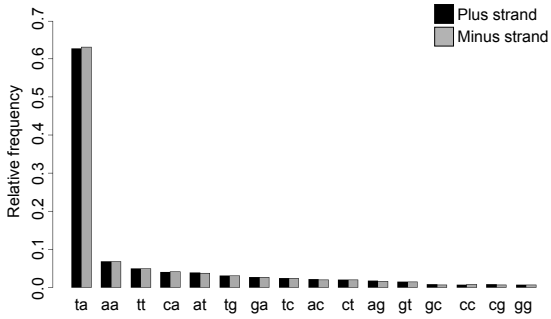

Figure 4.1: Analysis of base composition downstream of TIS to determine preferred dinucleotide for insertion. Barplots showing the relative frequency (y-axis) of different dinucleotides composition (x-axis) that appeared downstream on the ITRs, on both the plus (black) and the minus (grey) strand when analyzed by Tn-seq.

In particular, this study employed Tn-seq screening experiments to investigate bacterial mutants, which were either defective in intracellular cytotoxicity or unable to survive the host cellular environment or important for establishing pneumonia or associated with bacterial systemic dissemination or any combination of these characteristics. All bacterial pools recovered in these experiments, originated from a single source of insertional mutants, hence mutant abundances could be compared between different infection models that comprehensively showed the differential behaviour of mutants in either HeLa cells or mouse organs (See Figure 2.10). Mutant pools recovered from HeLa cells had better correlations with the inoculum (See Figure 2.8, R^2 1), whereas the output libraries from in vivo experiments demonstrated reduced correlation in library complexity (See Figure 2.8, R^2 0.6). This indicates a possible bottleneck effect, which was accounted for during data analysis and statistics (See Section Sections 2.2.2 and 5.9.1.6.

4.2 Uncovering differential roles of *S. aureus* genes during infection

Some of these gene candidates were deemed to be essential, hence a comparison was made with other studies, where similar approaches have been used. This demonstrated both congruence and discordance is terms of gene essentiality and functions (See Table 4.1).

Interestingly, the top candidates identified were regulatory and metabolic genes, instead of toxins. One of the most striking collection of genes that emerged as vital for infection in both HeLa cells and Mouse lungs, were associated with Purine salvage and *de novo* biosynthesis pathway (See Section 2.2.2, Figure 2.8, Tables 2.2 and 2.3). *pbu*X and *gua*A , producing Xanthine permease and bi-functional GMP synthetase respectively, belong to an operon encoding proteins crucial for purine salvage and *de novo* biosynthesis [251]. Both *pbu*X and *gua*A are reportedly expressed under the control of a guanine riboswitch, which was indispensable during murine infection [281]. Although, later studies showed that it

could also be expressed in a riboswitch-independent manner under the control of an alternative promoter[251].

De novo purine biosynthesis is initiated by 5-phosphoribosyl-1-pyrphosphate (PRPP) and available amino acids to make Inosine monophosphate (IMP), which is the immediate precursor of nucleotides[282]. IMP is converted to GMP in two-steps: IMP dehydrogenase catalyzes the conversion of IMP to Xanthine monophosphate (XMP), which is then converted to GMP by GMP sythetase[251,281]. During low availability of precursors, proteins like Xanthine permease aids in salvage of purines, which is converted to IMP or XMP by enyzmes such as hypoxanthine - guanine phosphoribosyltransferase (HGPRT) or Xanthine phosphoribosyltransferase (XPT). Therefore, the disruptions of *pbu*X and *gua*A will lead to improper salvage and biosynthesis of purine bases. Although absence of both genes has been attributed to decreased survival in host cells and cytotoxicity (See Tables 2.2 and 4.1), XMP can still be produced in lower amounts directly from available IMP. But a non-functional GMP synthetase will lead to guanine auxotrophy[251,281].

*gua*A was thought to be essential in some studies (See Table 4.1), however this study found mutants within *gua*A were non-essential while growing in complex medium but were indispensable during infection in human epithelial cells, mouse lungs, kidney, liver and tibia (See Figure 2.10). The reason could be the very low bio-availability of Guanine in host tissue[285].

Furthermore, *pur* operon is involved in the series of reactions that produces IMP from PRPP. *pur*M encodes for phosphoribosylformylglycinamidine cyclo-ligase (PurM) that catalyzes the conversion of N-formylglycinamidine ribonucleotide (FGAM) to aminoimidazole ribonucleotide (AIR)[282]. On the other hand, *pur*R encodes the Purine operon repressor (PurR), which targets the upstream region of *pur*E and regulates the transcription of the entire operon. The activity of PurR is determined by its effector molecule hypoxanthine, which forms a feedback mechanismcho2011purr. Mutants in *pur*M have been observed to be attenuated during infection in skin abscess and nematode killing[280,286] (See Table 4.1). Recently, it has also been shown to be important for persistence in host cells, in the presence of antibiotic Rifampicin[287]. However, the metabolic disadvantage of *pur*M mutants is possibly the reason behind its general inability to survive within human epithelial cells Section 2.2.3 and Table 2.2). Similarly, *pur*R mutants were also defective during skin abscesses[286] and produce decreased levels of secreted proteases[284]. But this study for the first time observes *pur*R to be crucial for intracellular survival in human epithelial cells (See Section 2.2.3 and Table 2.2).

This study shows the novel importance of two genes associated with sugar metabolism; *scr*A and *fba*A, during intracellular virulence. The mutants of these genes were significantly decreased during passage through HeLa cells (See Section 2.2.3 and Table 2.2). *scr*A codes for a phosphotransferase system that is crucial for uptake of sucrose[252], which has been shown required for efficient skin abscess formation and nematode killing[280,286] (See Table 4.1). Although, here whether it is required for invasion or intracellular replication is still not clear. In addition to this, *fba*A codes for the cytoplasmic glycolytic enzyme fructose bisphosphate aldolase, which is excreted by *S. aureus* and has been shown to bind

Table 4.1: Comparison of top genes identified in this study with multiple others involving transposon mutagenesis in *S. aureus* . Genes with no information are left blank.

Gene/Locus ID[a]	**Bae et al. 2004**[b]	**Chaudhuri et al. 2009**[c]	**Fey et al. 2013**[d]	**Valentino et al. 2014**[e]	**Santiago et al. 2015**[f]	**This study**[g]
*csh*A	Nematode killing			Skin abscess/Blood	Domain-essential	Epithelial cells
*def*2		Essential		Skin abscess	Domain-essential at high temperature	Epithelial cells
*fba*A		Essential	Hemolysis	Skin abscess	Non-essential	Epithelial cells
*gua*A	Nematode killing	Essential	Essential	Essential	Essential	Infection only
*hem*L	Nematode killing			Skin abscess	Non-essential	Epithelial cells
*pbu*X	Nematode killing				Non-essential	Epithelial cells
*pur*M	Nematode killing			Skin abscess	Domain-essential	Epithelial cells
*pur*R		Essential	Secreted protease	Skin abscess	Non-essential	Epithelial cells
*ruv*A		Essential	Essential	Skin abscess	High temperature	Epithelial cells
RSAU_0001762	Nematode killing			Skin abscess	Non-essential	Lung infection
*ylm*G	Nematode killing				Non-essential	Lung infection
RSAU_002181	Nematode killing			Skin abscess	Non-essential	Lung infection
*scr*A	Nematode killing			Skin abscess	Non-essential	Epithelial cells
*ure*D	Nematode killing	Non-essential			Non-essential	Lung infection

[a] NCBI Genbank Accession ID CP006706.1.
[b] *bursa aurealis* transposon mutants individually picked, in strain Newman [280].
[c] TMDH approach in strain SH1000 [283].
[d] Extension of *bursa aurealis* method in USA300 JE2, individually picked [284].
[e] Tn-seq approach in strain HG003
[f] Tn-seq approach in strain HG003
[g] Tn-seq approach in strain 6850

to host ECM , which is a vital step preceding invasion (See Section 1.2.1). Therefore, mutants in *fba*A are not be able to invade and kill the host cells efficiently [288], which is confirmed by the low numbers recovered from HeLa cells (See Table 2.2).

Maintenance of proper pH homeostasis within the bacterial cytoplasm and surrounding environment, could be a conspicuous process during infection. Ureases provide bacteria with a way to neutralize hyperacidic environments [289] and has been associated with virulence [290]. The Urease operon codes for two sets of genes producing the Apo-urease enzyme and accessory proteins. *ure*D encodes for one of the accessory proteins; UreD, which forms a complex with the apo-enzyme upon GTP hydrolysis, to assemble the Urease holoenzyme. Besides nematode killing [280], *S. aureus* mutants in *ure*D were found

to be important for survival in mouse lungs (See Section 2.2.4 and Table 2.3). Although, the cell type responsible is still not known, one could envision it to be resident alveolar macrophages, which is predominantly found immune cells in lung[291].

Similarly, this study also revealed for the first that mutants within *ylm*G are required for *S. aureus*-induced lung infection. The gene product YlmG is structurally and functionally conserved within prokaryotes. In Gram-positive bacteria, *ylm*G is located downstream of *fts*Z within the division and cell wall (DCW) gene cluster. Although this gene is non-essential (See Table 4.1), absence of it could hinder proper bacterial proliferation and morphology[292]. Hence could the reason behind mutant's failure in nematode killing[280] and pulmonary infection.

Aureusimines are cyclic dipeptides called produced by non-ribosomal peptide synthetases (NRPS), encoded by two tandemnly located genes: *aus*A and *aus*B[293]. The role of the NRPS products, Tyrvalin and Phevalin, has been disputed during staphylococcal infection[293,294]. However, this study shows for the first time that *aus*A is required for bacterial survival in mouse lungs[295] (See Section 2.2.4 and Table 2.3).

Finally, this study identified the gene *rsp* coding for the Repressor of surface protein (Rsp) and the non-coding RNA *ssr*42 as novel regulators of *S. aureus* intracellular virulence and mouse pnemonia (See Chapter Sections 2.2.3 and 2.2.4).

4.3 Rsp: A master regulator of *S. aureus* virulence

4.3.1 Rsp is an AraC-family transcription regulator

AraC-family transcriptional regulators are broadly distributed within bacteria and are involved in diverse physiological processes ranging from metabolism to virulence[296]. These proteins are named after the regulators: AraC in *E. coli* and XylS in *Pseudomonas putida*, both possessing the prototypical AraC/XylS-type Helix-Turn-Helix (HTH) DNA binding domains and were the first to be biochemically characterized[296].

In *S. aureus* there are five AFTRs, which are highly conserved throughout MSSA and MRSA strains[297]. Three of these have unknown functions and other two known AFTRs are Regulator of biofilm formation (Rbf) and Rsp. Rbf is known to promote biofilm formation by repressing IcaR, thereby activating the *ica* operon for the production of poly-N-acetylglucosamine[298].

Rsp is 701 amino acid protein belonging to AraC-family transcription regulators (AFTR), with theoretical mass of 81.87 kDa. The DNA binding domain spans from 169th till 247th amino acid (See Figure 4.2). In addition to this, it also has a predicted C-terminal glycosyl hydrolase domain of unknown function, spanning from 568th till 696th amino acid. Rsp has been reported to inhibit the production of FnBPA by binding to the promoter of *fnb*A[256]. But in this study, Rsp has been extensively studied for its previously unknown functions in toxin production, host cell death, immune modulation and defined its regulon in *S. aureus*.

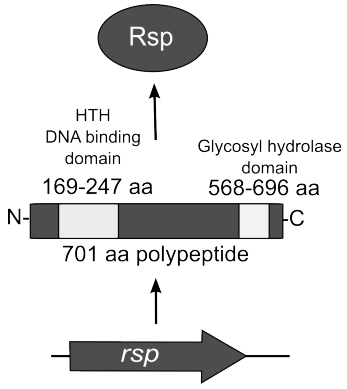

Figure 4.2: Domains of Rsp, an AraC-family DNA binding transcription regulator. *rsp* encodes 701 amino acid (aa) polypeptide that has a N-terminal Helix-Turn-Helix DNA binding domain within 169 - 247 aa. Also, it has a predicted C-terminal glycosyl hydrolase domain within 568 - 696 aa, together forming the Rsp protein

4.3.2 Not the usual suspect: Role of Rsp in *S. aureus* intracellular survival and host cytotoxicity

Mutation in *rsp* altered the dynamics of intracellular *S. aureus*-mediated host cell death in human epithelial cells and neutrophils.

In epithelial cells, the mutants displayed similar non-cytotoxic phenotype as *agr*A and *sae* mutants early (4h) in the infection, when usually the wild type bacteria would kill efficiently. However, unlike the latter mutants there was a gradual rise and eventually *rsp* mutants kill host cells after 24 hours (See Section 3.2.2 and Figure 3.3). *agr*A and *sae* code for two major virulence regulators in *S. aureus* (See Section 1.3.1). Mutation within these genes as anticipated are inefficient in escaping the host phagosomes [229,299] and most of them are degraded by the endo-lysosomal pathway, which translates into low cytotoxicity. In the infection experiments, bacteria were kept strictly intracellular by supplementing the culture medium with gentamicin, which had no extraordinary effect on *rsp* mutants (See Figure 3.4). They had comparable invasion, escape and proliferation rates as the wild type bacteria (See Figure 3.2B, C and D). Hence, these observations suggest *rsp* mutants remained within the host cell cytoplasm. For indication came from striking increase in cytoplasmic granularity of HeLa cells infected with *rsp* mutants, which was unlike any other mutants tested and may be due to the high numbers of bacteria inside. But the trigger for reinstatement of cytotoxicity in case of is still not known.

Activation of quorum sensing via the *agr* operon is key to *S. aureus* replication within host and cell death (See Section 1.3.1). A recent study shows that Rsp positively regulates *agr* genes by interacting with P2 [300]. Hence, *rsp* mutants may lack proper activation of *agr* operon upon internalization by host cells, which is governed by the level of AIPs in the bacterial surroundings (See Section 1.3.1). However, when there are sufficient bacteria within the cells, basal level of AIPs might be enough to trigger the activation of *agr* operon and subsequent production of toxins required for host cell death.

Despite of comparable phagocytosis rates in human neutrophils, *rsp* mutants exhibited sluggish proliferation and reduced intracellular pathogen-mediated host cell death, when compared to wild type bacteria early during infection (See Figure 3.5.2B and C). Although, these experiments should be performed over longer time periods for any foreseeable effects.

Unlike epithelial cells, hMDMs are vigorous killers of pathogens. Occasionally, *S. aureus* can also

survive within post phagocytosis in a MOI-dependent manner[217]. Similarly, at relatively low MOI of 10 the wild type bacteria were efficiently disinfected by hMDMs over the course of 2 days, with only few small foci visible (See Figure 3.5.4). By contrast, the *rsp* mutants could withstand disinfection relatively well and survived in much larger foci, until extended time periods.

These observations exhibit prolonged intracellular survival in case of *rsp* mutants, which could facilitate dissemination.

4.3.3 Virulence switch: Mutation in *rsp* leads to remodelling of gene expression

Gene expression changes in the absence of *rsp* was investigated by RNA-seq in exponentially growing USA300 JE2 strain, which demonstrated both up- and down-regulation of a broad array of genes coding for other regulators, secreted toxins, extracellular enzymes, surface proteins and metabolic enzymes (See Section 3.4.1 and Table 3.1). These effects were further evaluated by quantitative PCRs in USA300 LAC* and 6850 strains during both exponential and stationary growth phase (See Section 3.4.3).

Furthermore, transcriptomics and quantification of exoproteome was conducted for *rsp* mutants in USA300 JE2 strain from stationary growth phase, in collaboration with Nuffield Department of Medicine, University of Oxford[301].

Amongst other known regulators, Rsp is universally required for the expression of *sar*R (See Table 3.1, Section 3.4.3, and Figure 4.3). Since SarA is repressed of SarR, in *rsp* mutants the expression of *sar*A was expected to be up-regulated, which observed only in case of strain 6850 logarithmic growth phase (See Figure 3.11D) but not in stationary growth phase. The expression of *sar*A is usually constant through all growth phases, although mRNAs are differentially transcribed from its promoters P1, P2 and P3[302]. But since, SarA is known to self regulate by binding to its own promoter[163] and only partially regulated by SarR[201], the over expression of *sar*A might not be observed.

Both Rsp and SarR positively regulate *agr*A by binding to P2[201,300] but yet again there were no negative impact on the expression of *agr*A and RNAIII, in the absence of *rsp* (See Section 3.4.3). This could may occur due to the alternative transcription of *agr*A via P1[165], which can be self controlled. In contrast to this observation, Li et al. 2015 showed decrease in mRNA levels of *agr*A, C and D upon mutation in *rsp* . This could be due to two reasons: Firstly, here bacteria were used from early exponential and stationary phases, whereas Li et al. used bacteria mid-exponential phase. Secondly, the strains used by Li et al. were BD02-25 (ST8, USA500) and MW2 (ST1, USA400) from that different time points and strains used in both studies. Therefore, the expression of genes that are exclusively transcribed from P2; *agr*B, C and D, should be further investigated at multiple time points in *rsp* mutants from strain USA300 and 6850.

Interestingly in *agr*A mutants, the expression of *rsp* was decreased in the stationary phase and only in presence of the *agr* operon, *rsp* complementation lead to appearance of hemolysis (See Figure 3.1D and E). Moreover, the transcription of *agr*A was significantly up-regulated in presence of excess Rsp (See Figures 3.12 and 3.13). This suggests that there might a feedback loop existing between *rsp* and *agr* ,

although this needs further investigation.

*luk*AB and *hla* were down-regulated in exponentially growing *rsp* mutants (See Sections 3.4.1 and 3.4.3 and Figure 4.3). The lack of these important cytotoxins was evident from secreted proteome (See Figure 4.4) and might explain the decrease in cytotoxicity in human epithelial cells and human neutrophils (See Figure 3.3 and Section 5.16.2). The effect due to absence of α-toxin was supported by lack of complete haemolysis (See Figure 3.1), decreased lethality in mouse pneumonia (See Figure 3.5) and no change in phagosomal escape[227] (See Figure 3.2C). In addition, α-toxin is known to induce apoptosis in host cells[303], although whether it is the major reason behind the loss in intracellular cytotoxicity still remains unknown (See Section 1.2.2.1).

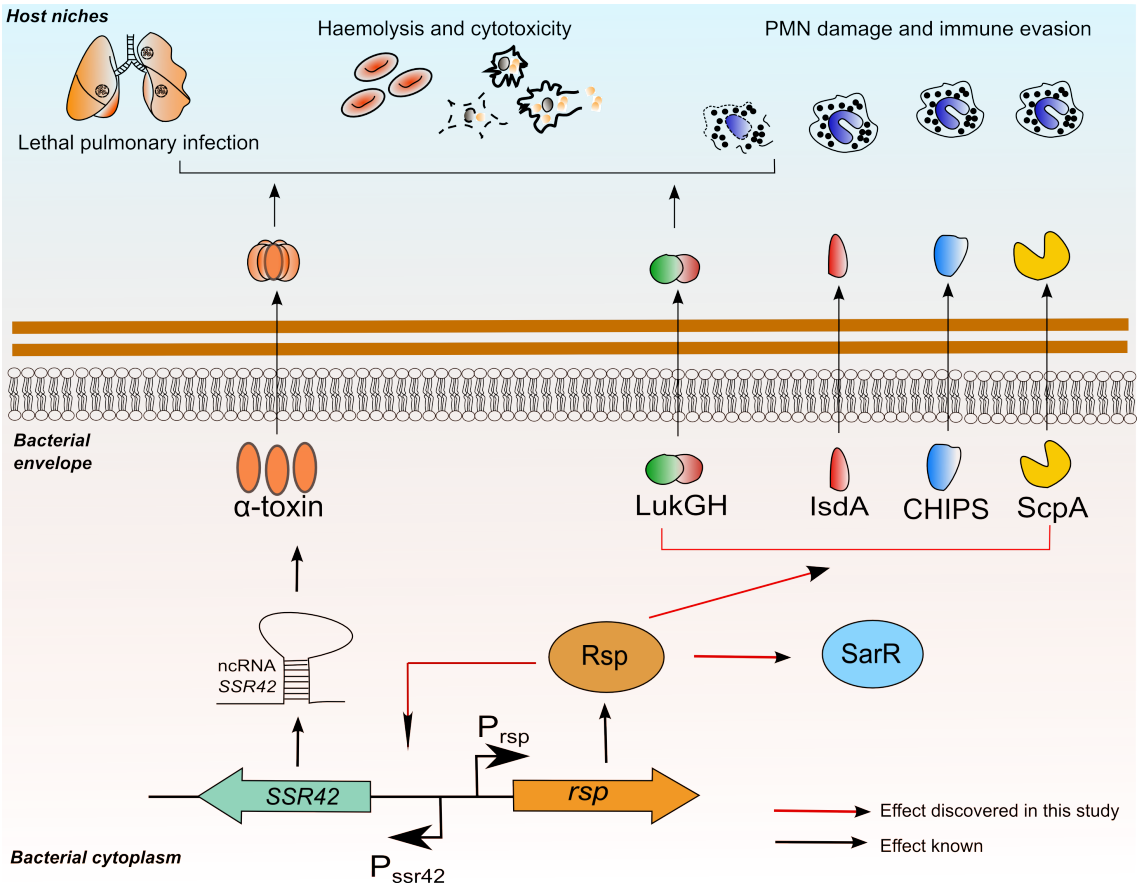

Figure 4.3: A graphical overview of Rsp-mediated activation of virulence gene expression in *S. aureus* This summarizes the findings from this study (red arrows) and others (black arrow) to propose a model representing the a part of Rsp regulon. *rsp* and *ssr*42 are situated in tandemn but in antiparallel orientation, and are transcribed under the control of individual divergent promoters (P_{rsp} and P_{ssr42}). Rsp positively regulates the expression of a non-coding RNA (ncRNA) SSR42, which is known to promote α-toxin production that is vital for *S. aureus*-induced lethal pneumonia, haemolysis and cyotoxicity. In addition to this, Rsp postively regulate th expression of LukGH (LukAB), IsdA, CHIPs and ScpA, which are involved in PMN cytotoxicity and evasion from the host immunne system. Rsp also promotes the transcription of another global virulence regulator SarR.

Furthermore, LukAB is cytotoxic towards human neutrophils both intra-and extra-cellularly[136,137], and monocytes only upon extracellular addition[138] with no evidence of the same in epithelial cells (See Section 1.2.2.1). But LukAB promotes bacterial escape from phagolysomes[299] in human epithelial cells

and may therefore also be important for intracellular cytotoxicity. The role of these toxins can be confirmed by expressing *luk*AB and *hla* episomally in *rsp* mutants, and observing whether cytotoxicity is reinstated.

In addition to these toxins, the expression of genes required for evading the host immune system, were also down-regulated. *chs* and *scp*A code for CHIPS and Staphopain A, which are secreted immune-modulatory proteins (See Section 1.2.3 and Figure 4.3). Both of these genes were down regulated in USA300 LAC* and 6850 strains in both growth phases tested in this study (See Section 3.4.3). Eventually, the lack of these proteins will make *S. aureus rsp* mutants susceptible to phagocytosis and killing by innate immune cells. *isd*A codes for one of the haeme acquisition proteins (See Section 1.2.1.5). It is important for bacterial survival within phagocytes[112], which possibly the reason behind decreased numbers of *rsp* mutants observed within neutrophils (See Figure 3.17). Even though there was no increase in the rate of phagocytosis, the mutants might have disadvantages during infection *in vivo*.

Surprisingly, *luk*AB, *hla* and *chs* were found to up-regulated in USA300 JE2 strain during stationary growth phase in experiments performed by collaborative laboratory. However, the secreted proteins were present in significantly low amounts[301] (See Figure 4.4). This discrepancy between these two studies might arise due to strain and time differences.

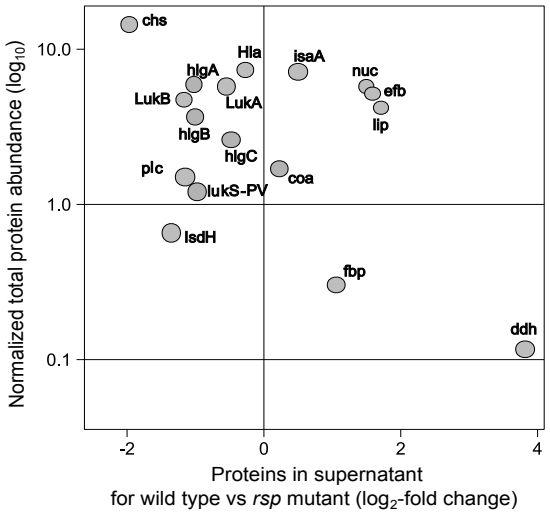

Figure 4.4: Relative abundance of secreted proteins in *S. aureus rsp* mutants Mass spectrophotometry was performed on supernatant from *S. aureus* USA300 wild type and *rsp* mutant from stationary phase of growth in α-MEM medium. The scatter plot shows overall normalized protein abundances in both wild type and mutant (y-axis), which was compared to the relative fold change (x-axis) in those proteins (grey solid circles) in *rsp* mutant.

Some of the most highly up-regulated genes in *rsp* mutants belong to the urease operon, comprising of 7 ORFs; *ure*ABCEFGD. Urease enzyme has been implicated in virulence for a number of bacteria[304] including *S. aureus* , where it was observed to be crucial for bacteraemia in a murine model[257]. It is responsible for the generation of ammonia that can increase the pH of bacterial surroundings, which is congruent with the increase in urease production upon acid shock[305]. Therefore, *rsp* mutants might be more tolerant towards acidic environment like within host phagolysosomes and enhanced survival in human macrophages (See Section 3.5.4), where rapid acidification of endosomes takes place soon after phagocytosis.

In *rsp* mutants, *coa* and *sbi* expression (*coa*) was significantly decreased during exponential growth

phase (See Table 3.1), which on the contrary was up-regulated in stationary phase. This was further supported by increased protein levels in the bacterial secretions[301] (See Figure 4.4). Including SC and Sbi, *rsp* mutants exhibit increased production of FnBPs[256], Efb, ClfB, Nuc[301] in the stationary growth phase (See Table 3.1 and Figure 4.4). All these proteins have been observed to aid in either invasive and systemic infections, interaction to the host ECM, immune evasion and survival in blood[103,105].

In addition, *hlg*A , *hlg*CB and *luk*S-PVL had increased transcription in exponential growth phase but not in stationary phase (See Figures 3.12, 3.14 and 4.5). By contrast in the collaborative study, in USA300 JE2 the expression of *hlg*A and *hlg*CB were significantly increased in the absence of *rsp* , although low amounts of the proteins were detected in the bacterial secretions (See Figure 4.4). These differences might arise due to strain and observed time point, which has to be further investigated.

Strikingly, the absence *rsp* lead to the up-regulation of some of antibiotic resistance genes belonging to the *SCCmec* type IV element in the USA300 genome. *mec*A, codes for the penicillin-binding protein (PBP) 2a, whereas *mec*R1 and *mec*I genes code for methicillin regulatory elements. MecR1 is a transmembrane signal transducing protein that senses the presence of antibiotics and catalyzes the deactivation of the repressor MecI, thereby producing MecA (PBP2a)[306]. Widely distributed amongst MRSA lineages, PBP2a is a transpeptidase enzyme that is anchored to the plasma membrane. Unlike other PBPs, is intractable to β-lactam antibiotics[307].

Another interesting finding came to light that D-Lactate Dehydrogenase enzyme encoded by *ddh*, was over produced when *rsp* was inactivated. NAD^+-linked D-lactate dehydrogenase synthesizes D-lactate, which is incorporated in peptidoglycan chains and links MurNAc to the pentaglycine bridge, instead of D-Alanine[308] (See Section 1.2.1.1). In Gram-positive bacteria including *S. aureus* , this substitution makes the cell wall less susceptible to antibiotic Vancomycin[308]. The up-regulation of these genes creates a new relationship between Rsp and antibiotic resistance, which still remains to be discovered. Even though its elusive, one could envision an advantage for *rsp* mutants in case of exposure to antibiotics during its prolonged survival in both intracellular compartments and blood leading to dissemination within its host.

4.3.4 Rsp and SSR42 partnership: a post-transcriptional link

Inactivation of *rsp* lead to the almost complete abolishment of SSR42 production (See Section 3.4, Figure 3.7, and Table 3.1). The primary transcripts SSR42 is longer; 1232 nt when determined by dRNA-seq (See Section 3.4.2), which is a much more sensitive approach than previously used 5′ RACE PCR method that reported the length to be 891 nt. The genomic proximity *rsp* and *ssr*42 , and the divergent transcription from two individual promoters is similar to that of another major regulatory system; *agr* operon in *S. aureus* (See Figures 3.10 and 4.3 and Section 1.3.1). Similar to RNAIII in *agr* operon, SSR42 might act as the effector controlling transcriptional or post-transcriptional modification for a subset of Rsp-regulated genes.

SSR42 comprises approx. 6% of the total non-ribosomal RNA[301] and is responsible for the tran-

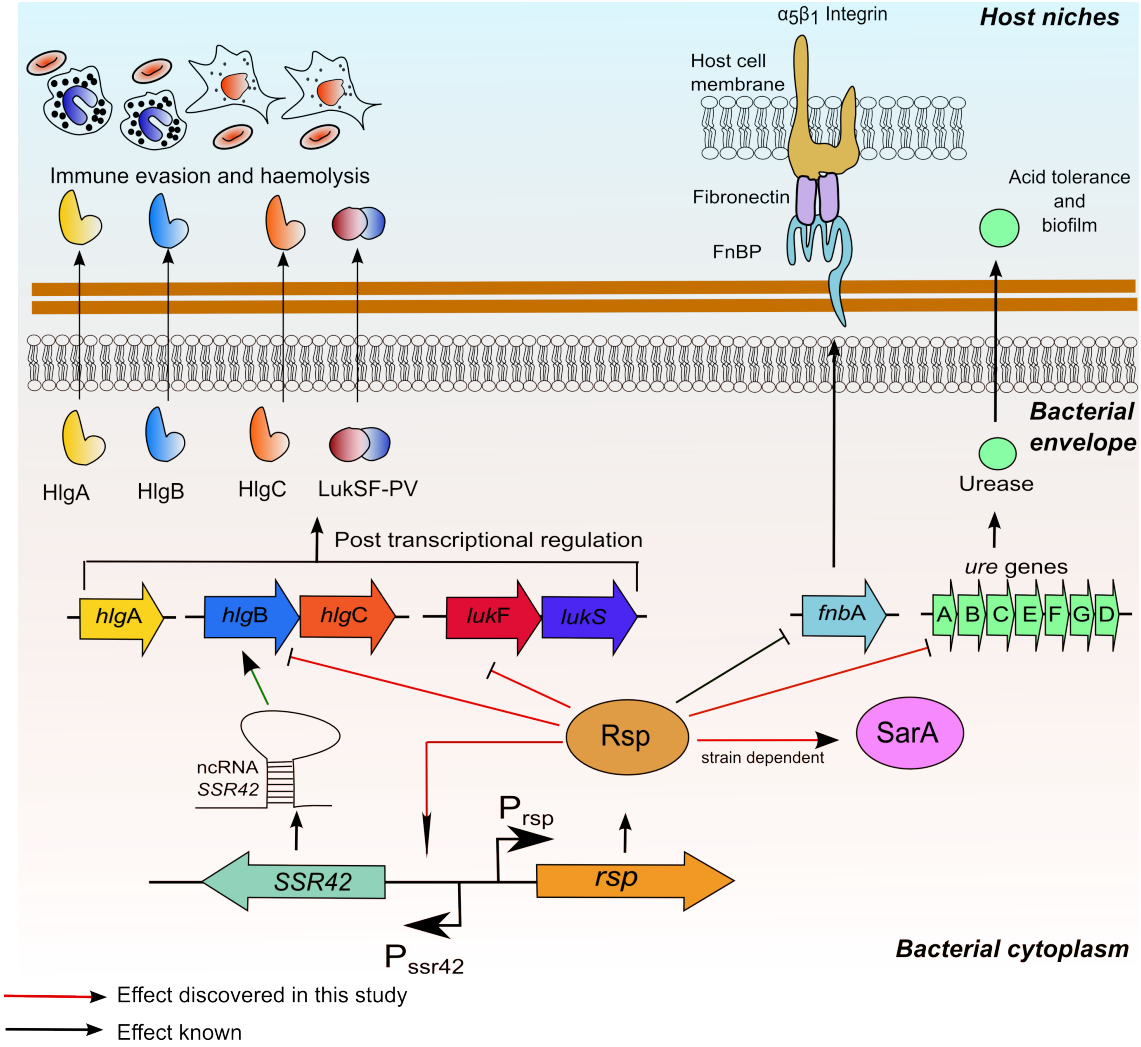

Figure 4.5: A graphical overview of Rsp-mediated repression of virulence gene expression in *S. aureus* This summarizes the findings from this study (red arrows) and others (black arrow) to propose a model representing the a part of Rsp regulon. Rsp represses *hlg*A, *hlg*CB and *luk*SF-PVL and positively regulates SSR42, which promotes the production of *hlg*CB and *luk*S-PV. Eventually, these proteins important for immune evasion and survival in blood were decreased in bacterial secretions. This indicates a post-transcriptional step governing this phenomenon. Rsp impedes the expression of *fnb*A that codes for the MSCRAMM; Fibronectin binding protein (FnBP), which interacts with host $\alpha_5\beta_1$ Integrins via a Fibronectin bridge that mediates bacterial adhesion and subsequent invasion. Rsp also represses the genes encoding Urease enyzme system, which is vital for acid tolerance and another global virulence regulator; SarA, in a strain-dependent manner.

scriptional activation of *hla*[255], which is regulated by Rsp (See Table 3.1). Upon further investigation, it seemed that Rsp positively regulates the production of α-toxin via SSR42, which was indicated by re-appearance of haemolysis upon complementation of *rsp* mutants with pSSR42 plasmid that harbors only *ssr*42 under the control of its native promoter (See Figure 4.6).

Similarly, SSR42 promotes the production of *hlg*CB ,*luk*S-PVL[255], but these including *hlg*A were negatively regulated by Rsp[301] (See Section 4.5). In addition, the expression of TCRS SaeRS was also upregulated during stationary phase in *rsp* mutants[301], which could lead to the observed increased in expression of *chs*, *hlg*CB , *hlg*A ,*hla*, *coa*, *nuc* and *luk*S-PVL[189,190,224]. Hence, the up-regulation of these transcription might be an epistatic effect of *rsp* mutation, which would mean that there may be direct

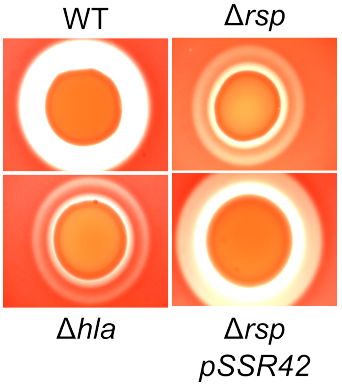

Figure 4.6: Complementation of *rsp* mutants with *ssr*42 rescues β-haemolytic phenotype. Complete haemolysis of strain *S. aureus* 6850 was examined on sheep blood agar by spotting wild type (WT, top left) bacteria along with isogenic *rsp* mutant (Δ*rsp*, top right), α-toxin mutant (Δ*hla*, bottom left) and *rsp* mutant complemented with *ssr*42 with plasmid pSSR42 (Δ*ssr*42, bottom right).

repression of either SaeRS TCRS or of all effectors by Rsp. However, all these proteins except SC and Nuc, were significantly decreased in the exoproteome of *rsp* (See Figure 4.4), which indicates that there could a selective post-transcriptional step involved where SSR42 stabilizes or/and interacts with the 5′-UTRs of mRNAs to promote translation. Similar phenomena have been observed in case of RNAIII in *S. aureus*[176,177].

In summary, Rsp-regulated genes are either targeted against the host immune system; neutrophils and macrophages or facilitate intra-cellular survival. Rsp, both positively and negatively, regulates the expression of several virulence associated genes and for a subset of genes, in a growth phase- and strain-dependent manner. Furthermore, some regulatory effects of Rsp could be epistatic and mediated by other regulatory elements. However, Rsp has been shown to directly bind target sites. Therefore, Rsp can act as virulence switch that upon inactivation turns off toxin production and immune-evasion molecules, but turns on the factors that promote adhesion, invasion and prolonged intracellular survival. This indicates at a conversion of an aggressive bacteria to a much more complaisant but invasive pathogen.

4.4 Enemy encounter: Role of Rsp in *S. aureus* response to phagocytes and phagocyte-derived stimuli

Mammalian immune system is fully equipped for eradication of Gram-positive pathogens[241,309] Circulating neutrophils and monocytes are the primary executors in host innate defence. These cells use a number of different mechanisms to keep up with the invading pathogen, which include migration to site of infection, differentiation of monocytes to macrophages, engulfment and subsequent destruction of pathogens, paracrine signaling using chemokines and cytokines, oxidative burst, Neutrophil Extracellular Traps (NETs), antigen presentation and complement activation[241,309]. It is only natural that a pathogen encounters these immune defences but how it responds determines its success in establishing infection.

S. aureus is one of those pathogens that has an arsenal of virulence factors serving specific purposes in confronting the host immune system, especially against professional phagocytes; neutrophils and

macrophages (See Figure 1.4). There are existing virulence regulatory systems such as SaeRS that has been shown to respond under oxidative stress and neutrophil-derived stimuli [112,192], which also regulates a subset of Rsp target genes. In this study, Rsp also emerged as a major regulator of *S. aureus* genes that are specifically directed against the host immune system (See Sections 3.4 and 3.4.3 and Figure 4.3). These factors participate in various processes during the 'tug of war' between *S. aureus* and phagocytes including toxin-mediated killing of immune cells, interfering in neutrophil communication, acquistion of haeme for withstanding oxidative burst etc (See Figure 4.7). Hence, the absence of *rsp* limits the options for *S. aureus* against neutrophils (See Figures 3.15 to 3.17).

PMNs use Reaction Oxygen Species (ROS) such as H_2O_2, as one of the major anti-microbial strategies. PMNs produce ROS either by degranulation releasing ROS -producing enzymes or by recruitment of NADPH oxidase on to pathogen-containing phagosomes (Amulic 2012). Rsp not only regulates the expression of virulence associated genes under normal circumstances but also promotes their production during oxidative stress. When compared to existing *S. aureus* transcription data [263], approx. 60% of Rsp-regulated genes were reported to be altered upon facing neutrophils and neutrophil-derived stimuli (See Figure 3.19). *rsp* itself along with a subset of its target genes; *ssr*42, *isd*A, *luk*AB, *scp*A, *hlg*CB , *hlg*A ,*luk*S-PVL were up-regulated in exponentially growing bacteria, after administration of non-lethal dosage (5 mM) of H_2O_2 in an *rsp*-dependent manner (See Section 3.6.1). This was supported by enhanced toxicity of bacterial secretions towards neutrophils, in an *rsp*-dependent manner. However, out of two proteins; CHIPS and ScpA that interfere with neutrophil chemotaxis, production of CHIPS was not promoted by Rsp under oxidative stress (See Section 3.6.1). The difference between these two proteins were that CHIPS targets the ligands, whereas ScpA targets the receptors responsible for inter-neutrophil communication. Hence, manipulation of the latter might be beneficial and efficient depending on the urgency and enemy proximity, since receptors can interact with multiple ligand molecules. Furthermore, *chs* up-regulation might not have occurred during the observed time period after treatment with H_2O_2. Interestingly, the expression of *hla* also did not change (See Section 3.6.1), which indicates that α-toxin may not be required against neutrophils. This is in agreement with the observation that *hla* mutants were equally cytotoxic towards PMNs (See Figure 3.16).

Therefore, Rsp is a vital constituent of the bacterial machinery that acts against the threat posed by host immune cells. Upon encountering ROS, it promotes the production of pore-forming toxins to eliminate neutrophils, factors that help in tolerating the conferred oxidative stress and limit the recruitment of more neutrophils (See Figure 4.7)

4.5 Redirection of *S. aureus* infection by mutation in *rsp*

Asymptomatically colonizing *S. aureus* population is responsible invading the same host and development of any causative infection [9]. Previously, there were no reports of niche specific factors that could distinguish carried and invasive isolates, which possess similar genotypes [310]. It is largely believed that the degree of success for bacteria is defined by the host [311], but the conditions that trigger for a pheno-

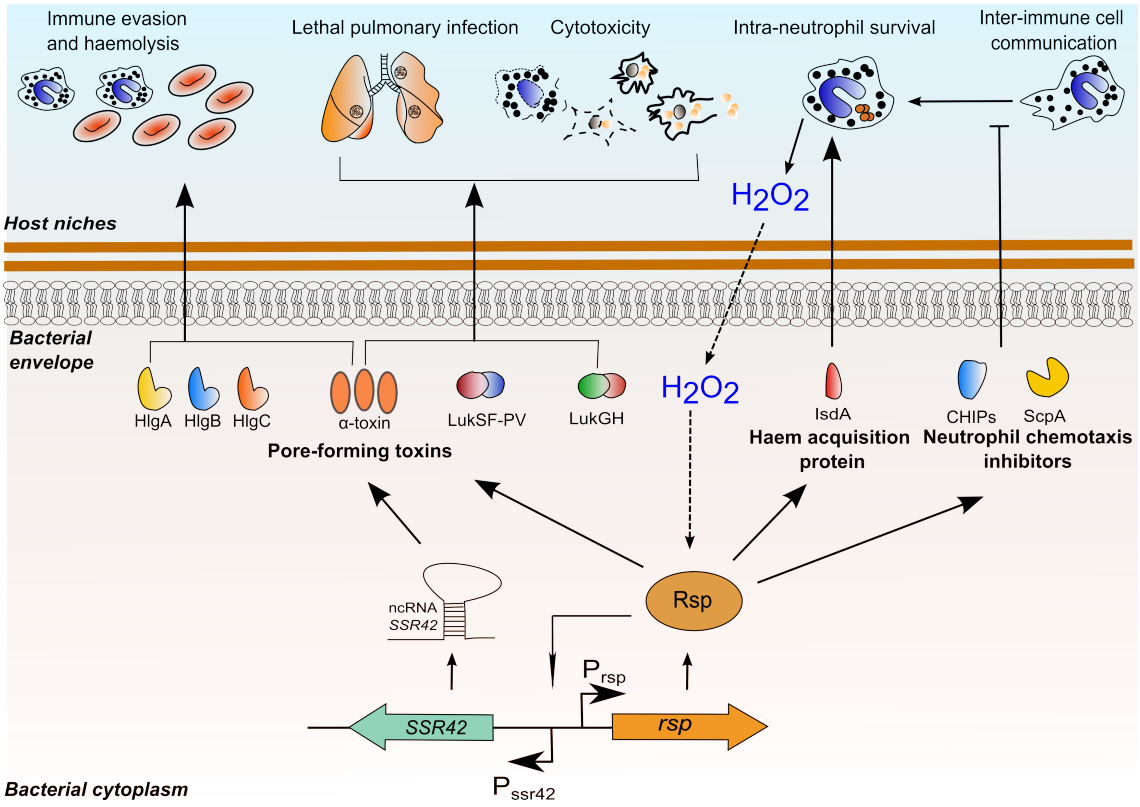

Figure 4.7: Overview of Rsp-mediated gene regulation in *S. aureus* A graphical summary of providing a model for Rsp-regulated processes in bacteria. *rsp* is expressed upon encountering neutrophil derived stimuli such as H_2O_2, which then steps into action by promoting the production of cytolytic pore-forming toxins, Haeme-acquistion proteins for counteracting oxidative stress, Neutrophil chemotaxis inhibitors.

typic switch in bacteria from carriage to invasion within the host are largely unknown.

Recent developments in this area attribute dynamic bacterial evolutionary process in host, as one of the mechanisms, which can facilitate invasive infections[312]. Particularly, the nasal carriage strains have been shown to be more cytotoxic than blood stream isolates[313]. These studies used whole-genome sequencing approaches to study within-host genetic diversity and minute differences in *S. aureus* genes caused by naturally occurring mutations, to propose possible mechanisms by which nasal carriage progresses to invasive disease[314]. But specific factors governing such phenomena were still elusive. Although, this study suggests that *S. aureus* with mutations in *rsp* resemble the non-cytotoxic blood stream isolates previously described[313]. The remodelling of virulence gene expression occuring in *rsp* mutants that resulted in reduced cytotoxicity but increased invasion and intracellular survival factors, make it a possible candidate contributing to such a shift in pathogenicity.

Despite of low toxicity in PMNs, intracellular *rsp* mutants were completely eliminated but rather survived and replicated at a much slower rate (See Figure 3.17B and C), although this was only observed for 4 hours. This phenomenon became more apparent when *rsp* mutants showed prolonged survival; upto 48 hours within hMDMs with elaborate bacterial foci, whereas the wild type bacteria were either eliminated or found in tiny foci (See Figure 3.5.4). This is line with other studies that demonstrate *S. aureus* is capable of surviving in hMDMs for prolonged time periods[217] without inducing cell[315]. Other

gram-positive pathogens such as *Listeria monocytogenes*[316] and *Mycobacterium tubercolosis*[317] have also been shown to disseminate via circulating monocytes. These observations collectively indicate that mutation in *rsp* may direct *S. aureus* towards dissemination from primary focus of infection to other sites.

Further evidence came from a longitudinal study conducted in collaboration with the Nuffield Department of Medicine, University of Oxford, where nasal swabs were collected from several individuals and the bacterial genomes were sequenced. One patient (Designated as P) was admitted to the hospital with blood stream infection, 15 months after joining the study. Bacteria from blood stream were different from its nasal ancestor by a few mutations and one of them was in *rsp*[312] (See Figure 4.8). Another patient (Designated as S) was admitted to the hospital due to blood stream infection, again bacteria in blood differed from the nasal ancestor but this time by one mutation, which was in *rsp*[301] (See Figure 4.8). In both cases, initial symptoms were undetectable until the patients became critical after administration of antibiotics and died later of multiorgan failure. These two isolates belonged to the ST 15 (P) and ST-59 (S) lineages and had similar gene expression profiles and phenotypic characteristics as the laboratory generated *rsp* mutants[301]. These observations indicated that mutations in *rsp* occured naturally within *S. aureus* colonizing healthy individuals. One could envision that this correlates to the extended intracellular survival and delayed toxicity observed in human epithelial cells (See Figure 3.3).

Two different mouse models were used to further assess the observations made in human patients. In both pneumonia and bacteraemia model, *rsp* mutants did not cause acute disease and lethality early in the infection[301] (See Section 3.5A and B) Its cytotoxic wild type counterpart caused fatal and acute pulmonary damage in the first 24 hours, which is attributed to the presence of α-toxin, which is absent in *rsp* mutant. Intriguingly, there was no change in bacterial load in lung after intranasal administration when instilled with sublethal dosage (See Section 3.6A) and exhibited similar magnitude of inflammation and granulocyte infiltration (See Section 3.6B and C). Similarly in a mouse sepsis model, disease severity was remarkably low in mice infected with *rsp* mutants after intravenous administration. Bacterial loads in kidney, liver and spleen were unchanged throughout the course of infection and allowed formation of kidney abscesses[301]. This coincides with the observation made in the mouse Tn-seq screen, where *rsp* mutants were not necessary or even favoured in kidney and liver (See Section 2.10). Previous studies have shown better clearance of *S. aureus* from bloodstream under chemically-induced neutropenia[318] and some clinical cases where neutropenic adults had significantly less bacteraemia, when compared to non-neutropenic patients[319]. Identical neutrophil infiltration and similar bacterial numbers in lung help to speculate phagocyte-mediated dissemination of viable *rsp* mutants, which may cause recurrent infections.

Furthermore, *rsp* mutants induced changes in specific cytokines; decrease in IL-12 and increasse in IL-6, in mouse lungs. *S. aureus* infection stimulates the production of IL-12 and IL-6 in a variety of cell types including osteoblasts[320], PBMCs[321] and lungs[301]. IL-12 is an important pro-inflammatory cytokine prouduced by antigen presenting cells (APCs), wihch promotes the generation and activity of

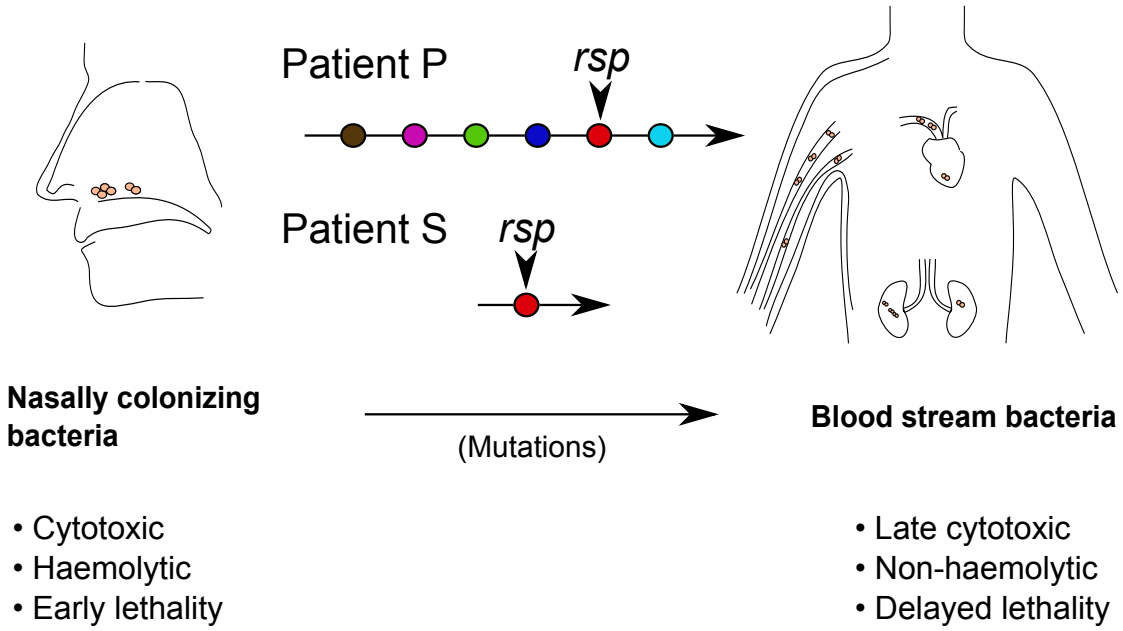

Figure 4.8: Natural mutations in *S. aureus* show the influence of *rsp* on pathogenicity and disease progression in human host. Nasally colonizing *S. aureus* is usually cytotoxic, haemolytic and is capable of causing acute infection with early lethality. During a colonization study, two patients P and S developed fatal blood stream infection from the same bacteria that colonized their nares, with minimum initial symptoms. The blood isolate from Patient P (ST-15) differed from its nasal ancestor by 6 mutations (colored circles) and one of them was in *rsp* (red). In case of Patient S, the blood isolate (ST-59) differed by only 1 mutation, which was in the DNA binding domain of *rsp*. These naturally occurring mutants along with laboratory generated insertional mutant in USA300 LAC* and deletion mutant in 6850, showed similar gene expression, and characteristics of low and late cytotoxicity. They were non-haemolytic, could survive intracellular and induced delayed lethality in human patients. These findings introduce a paradigm shift, and proposes a novel mechanism whereby mutation in a *S. aureus* cytotoxicity and immune-modulatory transcriptional regulator could be responsible for the phenotype switch from an aggressive pathogen to a silent invader.

cytotoxic T-lymphocytes and Natural killer (NK) cells[322]. This process is an integral part of T_H1 immune response against intracellular pathogens[322]. Hence, it could an advantage for *rsp* mutants to mediate the reduction of IL-12 to stay intracellular in APCs like neutrophils and macrophages, which could be correlated to the extended stay within hMDMs (See Figure 3.5.4). Moreover, *S. aureus* infection may stimulate a differential production of IL-6 in lung, depending on stimuli[323]. LTA induces an anti-inflammatory, whereas Peptidoglycan induces pro-inflammatory role of IL-6[323]. However, further investigation is needed to clarify the cell type and role of IL-12 and IL-12 during infection with *rsp* mutants.

In summary, this study produces novel evidence of a transcription regulator; Rsp that regulates cytotoxicity and acute infection, and is conserved in the usually colonizing *S. aureus* strains. However, mutation in *rsp* redirects the pathogenicity where the bacteria become non-cytotoxic, non-haemolytic, could manipulate immune response, can survive intracellular and cause blood stream infection (See Figure 4.8). Therefore, this mutation can occur during carriage in the host and act as a specific factor converting the usually agressive, cytotoxic and colonizing *S. aureus* into an invader and stealthy disseminator.

4.6 Future perspectives

As concluding remarks, one could envision strategies and experiments that would further supplement the findings from this study. *S. aureus* Transposon mutant libraries provide a useful resource for simultaneous assessment of gene functions in various condition (See Sections 2.2.3 and 2.2.4). These can be used in further experiments screening for survival in different cell types, such as human neutrophils, macrophages and under conditions inducing oxidative, nitrosative or antibiotic stress. In addition, library 7 with a higher complexity can be used to screen in experimental animal models of disease such as mouse pneumonia, osteomyelitis and skin abscess, also piglet model of cystic fibrosis.

Rsp shows a delayed cytotoxicity phenomenon unlike any other regulator tested up to 24 hours post infection (See Figure 3.2.2A), which can be prolonged to observe any long term effects. Furthermore, the role of Rsp in intracellular cytotoxicity in other primary cells, such as Human Umbilical Vein Endothelial cells (HUVEC) or respiratory cells like Human Normal Bronchial Epithelial cells (HNBEC) may be investigated. During epithelial cell cytotoxicity assay, remarkable increase in host cell granularity was observed in case of *rsp* mutants (See Figure 3.2.2A). To assess this further, bacteria expressing fluorescent protein may be used in a similar experiment, where the increase in fluorescence should correlate with the granularity. This may indicate that the bacteria were present increased amount until cytotoxicity was induced, although whether this was due to commencement of toxin production as a result of change in bacterial signaling or a host response due to increased bacterial numbers, is still not clear. One possible way to anaylse the former and latter at the same time, would be to perform Dual RNA-seq before and during the time when cytotoxicity was observed.

Global transcription analysis revealed the regulatory effects of Rsp. Currently, there is no information on the genome-wide binding sites of Rsp. But this can be investigated with ChIP-seq experiments performed using a FLAG-tagged protein, which retains its function (See Section 3.7). Furthermore, dRNA-seq experiment may be repeated with multiple strains such as USA300 LAC and 6850, to generate statistically robust transcription initiation site data (See Section 3.4.2). Also, *S. aureus* has a complex regulatory network where crosstalk between several proteins in common. Hence, it is also important to know the interaction partners of Rsp, which can be achieved by immunoprecipitation of Rsp under non-chaotropic conditions, followed by identification by Mass spectrophotometry.

rsp influences haemolysis, which is mediated by SSR42 (See Figure 4.6), but it still begs the question whether Rsp interacts with the promoter of *hla*. Furthermore, *agr* operon also influences *rsp*-mediated haemolysis (See Figure 3.1D) and the expression *rsp* reduces in *agr*A mutants from stationary growth phase (See Figure 3.1D and E), hence in the context of cellular signaling it is important to find out the effects of other regulators on the expression of *rsp* and *ssr*42. A promoter-reporter fusion system; β-galactosidase or fluorescent protein fused to *rsp* promoter may prove useful in investigating the activation of *rsp* under various conditions such as after internalisation by host cells, upon treatment with stress inducer or in the presence of methicillin. These reporter fusion systems can be introduced in mutants

the already existing collection of individual *S. aureus* mutants in other regulators like AgrA, SaeR, SigB or SarR, from the NARSA Transposon mutant library to look for upstream influencing proteins.

Following the indication from macrophage experiments (See Figure 3.5.4), intraPMN survival experiments (See Figure 3.17) can also be prolonged to observe whether *rsp* mutants can also stay within neutrophils. In both cases, bacterial numbers should be deduced either by enumeration of CFUs or by using bacteria expressing fluorescent proteins. Since, *rsp* mutants specifically altered IL-6 and IL-12 levels in mouse lung (See Figure 3.6D-H), it would also be intriguing to measure the same after infection in human macrophages and neutrophils *in vitro* by qPCR and Enzyme-linked immunosorbent assay (ELISA). The reduction of IL-12 production hints towards abolishment of T_H1 immune response and CTL-mediated bacterial clearance. This might facilitate prolonged bacterial survival within phagocytes, which can be assessed by using these APCs, for e.g. Macrophages as target cells and PBMCs as effector cells, and measuring NK cell activity. In addition, it would be interesting to examine the polarisation state; M1 or M2 of the macrophages infected with *rsp* mutants and whether it is different from that of the wild type.

In mouse models of *S. aureus* infection, *rsp* mutants do not lethality upto 3 days post infection (See Figure 3.5), although bacterial load examined at 24 and 48 hours did not change (See Figure 3.6A). Further enumeration can be done to observe long term effects of *rsp* mutants. Since, the infiltration of neutrophils after 24 hours was similar (See Figure 3.6C), it is still not clear whether neutrophils play any role in survival of *rsp* mutants *in vivo*. This can be observed by either by depletion of neutrophils in mice before infection or introduction of infected neutrophils into mice blood stream to monitor infection.

Furthermore in the future, more blood stream isolates from patients can be analyzed for mutation in *rsp* to assess the frequency of in-host evolution in *S. aureus*.

A LysR-type transcription regulator encoded by RSAU_000852 (LTTR 852) was identified in the Tn-seq screens, as another potentially important *S. aureus* virulence regulator (See Sections 2.2.3 and 2.2.4 and Figure 2.10). To investigate further, RNA-seq may be used to deduce its regulatory function and the mutants should be validated in infection models to deduce its precise role in virulence.

Chapter 5

Materials and Methods

5.1 Bacterial culture techniques

5.1.1 Bacterial culture conditions

Escherichia coli were grown in LB broth or agar and *Staphylococcus aureus* were grown in TSB or TSA, supplemented with desired antibiotics when required. Immedietely after transformation *S. aureus* was grown in B2 medium. For generation of pooled mutant libraries, *S. aureus* 6850 was grown in NB or agar. For haemolysis analysis *S. aureus* were grown in Blood agar plates made with Columbia agar base and 5% defibrinated Sheep blood. All strains were grown at 37°C, excluding some cases where the bacteria to be grown at 30°C bearing a temperature sensitive origin of replication.

All bacteria on agar plates were stored at 4-8°C until maximum time of 7 days, otherwise revived again to avoid spontaneous mutations. For bacterial overnight cultures, single colonies were inoculated in sterile glass test tubes containing 5 ml of broth and incubated at 37°C with agitation at 180 rpm. Optical densities (OD) were measured at 600 nm in a spectrophotometer, hereafter denoted as OD_{600nm}, by diluting in a ratio of 1:20 in 1 ml of fresh media. For *in vitro* infection experiments, bacterial overnight cultures were diluted to OD_{600nm} of 0.4 in 10 ml of TSB to prepare the infection sub-culture. This was further incubated for 1 hour at 37°C with agitation at 180 rpm until to reach OD_{600nm} reached 0.6.

For bacterial inoculates used for murine infections, 8-10 *S. aureus* colonies were picked and grown overnight in TSB at 37°C with agitation at 180 rpm. The culture was diluted in a Erlenmeyer flask containing 50 ml TSB to OD_{600nm} of 0.05, which was further incubated at 37°C for 3.5 hours with agitation at 180 rpm. Bacteria were harvested by centrifugation at 3000 xg for 10 minutes at 4°C. Pellets were resuspended in TSB and stored in 2 ml aliquots, and enumerated to determine CFUs per milliliter.

For details on media and manufacturer information, please refer to Appendix A. [§]All bacterial harvest and washing steps were performed by centrifugation at 14,000 rpm in microfuge tubes for 2 minutes, unless and otherwise specified.

5.1.2 Cryo-preservation of *S. aureus*

Bacteria to be cryopreserved were harvested and washed[§] with sterile 1X PBS. The pellets were re-suspended in TSB containing 15% glycerol and stored at -80 °C until use.

5.1.3 Collection of *S. aureus* culture supernatant

S. aureus were grown overnight in TSB for a precise time period and volume i.e. 16 hours in 5 ml and OD_{600nm} were measured and normalized for all cultures (See Section 5.1.1. Bacteria were collected by centrifugation and supernatants were filtered through a 0.22 µm membrane and transfered on ice. These were either used immediately or kept frozen at -20°C for future use.

5.1.4 Bacterial strains & Plasmids

All bacteria used in this study, including organism, species and strain information are listed in Table A.1. All plasmid used and constructed during this study as presented in Table A.2.

5.2 Determination of Staphylococcal growth rate *in vitro*

Bacterial growth over time was determined in a micro-well format aided by automated measurement of OD_{600nm} at fixed intervals, using a multi-mode reader.*S. aureus* was grown overnight in TSB and diluted to OD_{600nm} of 0.1 (See Section 5.1.1) in 400 µl of TSB in each micro-well of 48-well tissue culture plates.

The plate was using the following settings:

- Initial measurement: Orbital shaking, a = 3 mm, λ = 600 nm.
- Wait for Temperature: 37°C
- Kinetic cycle: n = 80, t = 900 seconds, Orbital shaking, a = 3, λ = 600 nm, 37°C.

The absorbance values were automatically documented by the instrument on Microsoft® Excel® software. Data analysis was performed using R statistical package. This experiment was repeated 3 times with 5 technical replicates for each strain. Growth rates were determined from the mean of optical densities at every time point from all experiments and along with a standard deviation.

5.3 Determination of Minimum inhibitory concentration of antibiotics against *S. aureus*

Bacteria were grown overnight and OD_{600nm} was normalized to 0.1 in fresh TSB (See Section 5.1.1). Bacteria were plated on Muller-Hinton agar and Gentamicin Etest® MIC strips were laid on. The plates were incubated at 37°C for 16-18 hours. MIC was determined according to manufacturer's instructions.

5.4 Transformation of *S. aureus*

5.4.1 Preparation of electro-competent *S. aureus*

S. aureus were grown overnight and diluted to OD_{600nm} of 0.1 in 100 ml of fresh TSB (See Section 5.1.1). This sub-culture was incubated at 37°C with intermittent measurement of OD_{600nm} and until it reaches 0.5. Growth was stopped by transferring the culture into 50 ml polypropylene centrifuge tubes and incubating on ice for 15 minutes. Bacteria were harvested by centrifugation at 3000 xg for 10 minutes in a refrigerated centrifuge, followed by washing steps as mentioned below:

- Three consecutive washes with 50, 25 and 10 ml of ice-cold sterile water. Centrifugation was done after each washing step at 3000 xg for 10 minutes.
- Two consecutive washes with 10 and 5 ml of ice-cold 10% glycerol. Centrifugation was done after each washing step at 3500 xg for 15 minutes.

After the final wash, supernatants were removed and pellets were resuspended in 10% glycerol upto a final volume of 1 ml. The mixture was divided into 100 µl aliquots and kept frozen at -80°C. The competent cells used within 6 months of freezing.

5.4.2 Electroporation of *S. aureus* competent cells

Frozen *S. aureus* electro-competent cells were thawed on ice for 5 minutes, followed by incubation at room temperature for 20 minutes. Subsequently, 120 µl of Electroporation buffer and 5 –10 µg of plasmid DNA were added to every aliquot and mixed properly by pipetting. Mixtures were transfered to 2 mm electroporation cuvettes and subjected to electric field using pre-defined settings: Voltage: 1.8 kV, Number of pulses: 1, Time constant: 2.5 milli-seconds. Immediately after electroporation, 1 ml of warm B2 medium was added to mixture, which was incubated at required temperature for 2 hours with agitation at 180 rpm. Bacteria were harvested and resuspended in 200 µl of B2 medium. Aliquots was divided into two parts and plated on to TSA plates with appropriate antibiotics.

5.5 Nucleic acid techniques

5.5.1 Isolation of genomic DNA from *S. aureus* by chloroform extraction

For obtaining larger amounts of genomic DNA from *S. aureus* , a manual chloroform-based isolation method was used. *S. aureus* was grown overnight in TSB and washed[§] with 1X PBS. The pellet was resuspended in 200 µl Tris-Sucrose buffer supplemented with 1mM EDTA, Lysostaphin and RNase A (For

[‡] Concentrations of reagents are mentioned in Appendix A, unless and otherwise specified in the text.

concentrations[‡] see Appendix A). The mixtures were incubated at 37°C for 30 minutes on a thermomixer with shaking at 1200 rpm. After cell wall lysis was achieved, the mixture was diluted with 1.5 volumes of TE buffer and 1 volume of 10% SDS followed by mixing on a vortex. Proteins were digested using Proteinase K to final concentration of 0.5 mg/ml and incubating at 55°C for 30 minutes. This was followed by addition of 0.75 M Sodium perchlorate and 0.5 volume of Chloroform-isoamyl alcohol solution. The solution was thoroughly mixed with constant agitation at room temperature for 30 minutes. The mixture was transfered to Phase Lock Gel tubes and centrifuged for 10 minutes at 14,000 rpm for phase separation. The aqueous phase was mixed with 1 volume of chilled isopropanol and DNA was precipitated by incubating on ice for 30 minutes and centrifugation at 14,000 rpm for 3 minutes. The pellet washed with 70% Ethanol, air-dried and reconstituted with sterile water. Reconstituted DNA was stored at -20°C..

5.5.2 Isolation of genomic DNA from *S. aureus* by commercial kit

For relatively smaller amounts of genomic DNA from *S. aureus* , QIAamp DNA mini kit was used following the manufacturer's instruction for gram-positive bacteria. Briefly, bacteria from overnight culture were harvested, washed and mixed with Bacterial resuspension buffer for genomic DNA (See Appendix A). The mixtures were incubated at 37°C for 30 minutes or until the mixture was clear, indicating cell wall lysis. The lysates were processed as instructed and passed through spin columns. DNA was eluted with sterile water for 5 minutes at room temperature. Reconstituted DNA was stored at -20°C.

5.5.3 Isolation of plasmid DNA from *S. aureus* by commercial kit

For *S. aureus* strains, plasmid DNA was isolated using QIAprep Spin Miniprep Kit according to manufacturer's instructions for gram-positive bacteria, with some modifications. Briefly, *S. aureus* was grown overnight at 37°C. Bacteria were harvested, washed with 1X PBS and mixed with resuspension buffer (P1, QIAGEN). Lysostaphin and RNase A were added and incubated at 37°C for 30 minutes or until the mixture becomes clear. Henceforth, the plasmid DNA were isolated by passing through spin columns and elution with sterile water. Reconstituted DNA was stored at -20°C.

5.5.4 Isolation of plasmid DNA from *E. coli* by commercial kit

For *E. coli* strains, plasmid DNA was isolated using PureLink Miniprep Kit according to manufacturer's instructions, with some modifications. Briefly, *E.coli* was grown overnight at 37°C. From the culture, 1 ml of bacteria were harvested, washed with 1X PBS. Henceforth, DNA were isolated by passing through spin columns and elution with sterile water for 5 minutes. Reconstituted DNA was stored at -20°C.

5.5.5 Isolation of total RNA from *S. aureus*

Total RNA was recovered from *S. aureus* as described elsewhere[324]. Bacteria were grown overnight and diluted to optical density of 0.1 in 100 ml TSB to make a sub-culture. At the desired optical densities, bac-

teria were harvested, flash-frozen in liquid nitrogen and stored at -80°C for future use. When required, the frozen pellets were thawed on ice, followed by addition of 0.5M EDTA. The mixture was resuspended in Buffer A and transfered to Lysis matrix B tubes containing acid-phenol. Lysis was performed on the FastPrep instrument at speed 6.0 for 45 seconds at 4°C followed by separation of phases at 17,900 xg for 10 minutes in a cooling centrifuge. The upper aqueous layer was mixed with TRI reagent and incubated at room temperature for 5 minutes, followed by addition of chloroform and incubation for 3 minutes. The phases were again separated by centrifugation and the aqueous phase was re-incubated with chloroform. The subsequent aqueous phase was mixed with absolute isopropanol and incubated for 15 minutes at room temperature, followed by centrifugation to precipitate RNA. The pellet washed with 70% Ethanol, air-dried, dissolved in DEPC-treated water and stored at -80°C.

5.5.6 Purifying RNA by DNaseI digestion

DNA contamination in RNA samples were removed using TURBO DNA-free^{TM} DNase kit, according to manufacturer's instructions. Briefly, RNA samples were mixed with TURBO DNase buffer and DNaseI enzyme, followed by incubation at 37°C for 30 minutes. The reaction was stopped by addition of a proprietary bead-based DNase inactivation reagent, followed by incubation at ambient temperature for 5 minutes. The mixture was sedimented by centrifugation at 10,000 xg for 2 minutes and the upper aqueous layer was collected and frozen at -20°C, until use in cDNA preparation or other downstream analyses.

5.5.7 Quality control of nucleic acids

Quality and quantity of nucleic acids were assessed by analyzing micro-volumes of reconstituted DNA or RNA on a NanoDrop^{TM} UV-Vis spectrophotometer. Sterile DNase, RNase-free water was used as a standard and 1 µl of sample was applied to the reading lens between the pedestals and measured. Samples were read using presets for DNA or RNA available in the associated software NanoDrop 1000, version 3.8.1.

For more detailed quality control of DNA such as fragment size range and individual quantities, the Agilent high sensitivity DNA kit was used and analysis was done on the 2100 Bioanalyzer instrument. Fragmented DNA was diluted to appropriate ratios and analyzed according to manufacturer's instructions.

5.5.8 Generation of cDNA by reverse transcription

Complementary DNA was generated by reverse transcription of messenger RNA using a commercially available kit - QuantiTect® Reverse Transcription kit, according to manufacturer's recommendations with minor modifications. Briefly, 1 µg total RNA was mixed with a genomic DNA clean-up reagent and incubated at 42°C for 2 minutes. This was followed by the addition of primer mix, reaction buffer, reverse

transcriptase enyzme and incubation at 42°C for 30 minutes. The reaction was terminated by exposing to 95°C. The mixture was diluted 5 times and used for downstream analysis.

5.6 Polymerase Chain Reactions (PCRs)

5.6.1 Non-quantitative PCRs

This includes all PCRs for cloning purposes, overlap extension PCR (See Figure 3.25), PCRs for enriching Transposon ends (See Figure 2.6). These were performed using Taq or Phusion DNA polymerases. Standard protocols according manufacturer's instructions were followed some exceptions such as Arbitrary PCR and amplification of transposon ends.

Arbitrary PCR was performed in two parts, as previously described[246] with erm and arb oligonucleotides (See Appendix B and Table B.1) and minor modifications. Briefly, genomic DNA was isolated from individually picked randoms mutants and used as templates. The first part of PCR was performed by using one of the arbitrary primers (arb1 or arb2; 40 pmol/reaction) and an erm primer (erm-5.3, erm-5.2, erm-3.3, or erm-3.2; 20 pmol/reaction). The cycling conditions were as follows: 95°C for 5 min then 5 cycles of 94°C for 30 seconds, 30°C for 30 seconds, and 72°C for 1 min. This was immediately followed by 30 cycles of 94°C for 30 seconds, 45°C for 30 seconds, and 72°C for 1 min and then final extension at 72°C for 5 minutes. The second part of the PCR was performed with 3 µl of PCR product from part 1 as the template using arb3 (40 pmol/reaction) and an erm primer (erm-5.2, erm-5.1, erm-3.2, or erm-3.1; 20 pmol/reaction). The cycling conditions were as follows: 95°C for 5 min then 30 cycles of 94°C for 30 seconds, 45°C for 15 seconds, 55°C for 15 seconds, 72°C for 1 min and finally 72°C for 5 minutes.

Prior to sequencing, transposon insertion-site containing fragments were enriched, Illumina® specific barcodes and flow cell specific sequences were introduced using PCR 1. For bidirectional amplification of loci at adjacent to the 5′ and 3′ ends of the transposon insertion site, linear amplification for 5 cycles was done by using the oligonucleotide himar-5-PCR and himar-3-PCR (See Appendix B and Table B.1), in two separate PCR reactions. These primers recognize the ITR region of the Himar1 transposon. Thereafter another 5 cycles was done after addition of the MP-TnSeqIndex oligonucleotides to introduce sequence complementary to the adaptor, each carrying a unique 7 nucleotide barcode sequence (See Appendix B and Table B.1). The composition of the PCR reaction is mentioned in Table 5.1.

Table 5.1: Composition of PCR for enrichment of Transposon ends before deep sequencing

Contents	Volume in µl	Concentration
5x HF buffer	10	1X
dNTPs	1	200 µM
Primer (Tn specific)	0.5	100 nM
Template (Adapter ligated fragments)	5	
DMSO	1	2%
Phusion polymerase	0.5	
Ultrapure Water	31.5	
Total volume	49.5	
After 5 cycles		
MP-Index primer	0.5	

Cycling conditions were as follows: 98°C for 30 seconds then 5 cycles of 98°C for 10 seconds, 60°C for 20 seconds and 72°C for 15 seconds. Final extension at 72°C for 5 minutes and then addition of second primer. The reaction products were purified with AMPure XP beads[¶].

For PCR 2, both the 5′ and 3′ reactions were mixed in equimolar ratio and used as template for the next PCR. Th reagents were added directly to the template, which has a bigger volume without addition of any water (See Table 5.1). Similarly, linear amplification was done for 5 cycles using the oligonucleotide TnSeq-HimarPCR-v2-PT (See Appendix B and Table B.1) and addition of primer IS-BC-Reverse, followed by 5 more cycles. Successful incorporation of the required sequences was tested by PCR using IS-Himar-Forward and IS-BC-Reverse (See Appendix B and Table B.1), before sending for deep sequencing.

5.6.2 Quantitative real time PCRs

DNaseI-treated RNA were converted to cDNA (See Sections 5.5.5, 5.5.6 and 5.5.8). Real time PCR was performed on a StepOnePlus™ Real Time PCR system using SYBR® Green PCR master mix (2X) in 96-well format. The reaction composition and cycling settings were chosen as per manufacturer's recommendation. The master mix was diluted to 1X in nuclease-free water and mixed with primers and template in a total volume of 20 µl per well. Reactions were allowed to run for 40 cycles with an initial hold step at 95°C, where each cycle was as follows: 95°C for 15 seconds and 60°C for 1 minute. Primers used are denoted as RT-primers (See Appendix B and Table B.1).

5.7 Mutagenesis in *S. aureus*

5.7.1 Generation of random Transposon mutant pools in *S. aureus*

Pooled mariner transposon mutant libraries were generated as previously described[246]. Briefly, 6850 transformed with plasmid pBTn (See Section 5.4) was revived on TSA Cm 10 plates. An overnight culture was prepared by picking a colony and resuspending in broth with Cm 10 and without Xylose, followed by incubation at 30°C with agitation at 180 rpm. The culture was diluted in ratio 1:100 in fresh broth containing 0.5% Xylose, Cm 10 and Erm 5, followed by overnight incubation at 30°C with agitation at 180 rpm. This was done in 10 replicates simultaneously. The cultures were again diluted in ratio 1:100 in fresh broth containing 0.5% Xylose and Erm 5, followed by overnight incubation at 42°C with agitation at 180 rpm. This step was repeated two more times. All cultures were combined and centrifuged at 3000 xg for 10 minutes. The pellets were mixed with fresh broth so that the OD_{600nm} was 10.0. Stocks were prepared as previously described (See Section 5.1.2). Successful transposition and subsequent loss of plasmid due to temperature elevation was assessed by enumeration of Erm resistant but Cm sensitive bacteria. A trial was made with more than one medium and more than 3 temperatures elevation steps to assess maximum efficiency of transposition (See Section 2.1.1). Colonies were randomly chosen from Erm 5 plates and tested for insertion in the genome by Arbitrary PCR (See Section 5.6.1) followed by

Sanger sequencing$^{\xi}$. Obtained sequences were matched to the *S. aureus* 6850 genome by BLAST tool (See Table 2.1).

5.7.2 Generation of targetted deletion mutants in *S. aureus* by allelic replacement

Targeted gene deletions in *S. aureus*were generated by a markerless allelic replacement strategy, previously described[325]. To summarize briefly, approx. 1 kb regions flanking the target ORFs were amplified by PCR, using oligonucleotides primers sets with SacII restriction sites for concatenation. For e.g. For deleting RSAU_002217(*rsp*) in strain 6850, primers attB1-2217-up-F and 2217-up-R-SacII was used for upstream sequence, and 2217-down-F-SacII and attB2-2217-down-R were used for downstream sequence (See Appendix B and Table B.1). PCR products were individually digested with SacII and ligated with each other to create a fragment flanked by Gateway® cloning compatible *att*B1 and *att*B2 sites. Fragments were inserted into pKOR1 [325] by incubation with BP clonase® enzyme mix according to the manufacturer's instructions. Subsequently, these mixtures were transformed into chemically competent *E. coli* One Shot® TOP10F' and plated. Recombinant plasmids were isolated and confirmed by Sanger sequencing$^{\xi}$. Correct vectors were isolated from *E. coli* (See Section 5.5.4) and were transformed into *S. aureus* RN4220 (See Appendix A and Table A.1 and Section 5.4).

To induced replacement, *S. aureus* with the recombinant pKOR1 were grown in TSB containing 10 µg/ml Chloramphenicol, hereafter referred to as Cm 10, at 30°C. Plasmids were isolated (See Section 5.5.3) and *S. aureus* target strains were transformed (See Section 5.4) and plated on TSA Cm 10, followed by overnight incubation at 30°C. Colonies were inoculated and further grown overnight in TSB Cm 10 at 43°C. Subsequently, cultures were streaked on TSA Cm 10 and incubated overnight at 43°C. At this temperature, the thermo-sensitive origin of replication within pKOR1 did not allow plasmid replication and thus co-integrates within the genome are formed by homologous recombination, guided by the *att* sites. Resulting colonies were grown in TSB without antibiotic at 30°C, which allowed co-integrate resolution. Furthermore, cultures were diluted at a ration of 1:10,000 and plated on TSA containing 100 ng/ml anhydrotetracycline, followed by incubation at 37 or 43°C overnight. This step counter-selected for the presence of plasmid backbones. Resulting colonies were grown overnight in TSB at 37°C and genomic DNA were isolated (See Section 5.5.2). Successful gene deletion were determined by PCR using 'test' oligonucleotides (See Appendix B and Table B.1).

5.7.3 Generation of targetted insertional mutants in *S. aureus* phage transduction

Bacteriophage 80α was used to transduce genetic material from donors to recipients in *S. aureus* USA300$^{\perp}$. Phage lysates of donor strains were prepared by growing bacteria overnight in LB at 37°C, followed by addition of $CaCl_2$ at final concentration of 5 mM. Phages were diluted at a ratio of 1:10 or 1:100 in phage buffer. Phage solution and cultures were mixed at a ratio of 1:4 and incubated at 52°C for 2 minutes and subsequently at ambient temperature for 2-3 hours. These were mixed with warm softagar at 55°C and poured over LB agar, followed by overnight incubation at 37°. Softagar on top should display clear

plaques, which were harvested by scrapping it out with phage buffer into a centrifuge tube. The solution was mixed properly by vortexing and then centrifuged at 6000 rpm for 30 minutes. The solution was filtered through 0.22 µm pore size membrane and stored at 4°C.

Similarly, recipient bacteria were overnight at 37°, followed by the addition of $CaCl_2$. Donor lysates were mixed with the cultures at a ratio of 1:4 and incubated at 52°C for 2 minutes and subsequently at ambient temperature for 15 - 45 minutes. These were mixed with warm softagar at 55°C and poured over LB agar with antibiotic, followed by overnight incubation at 37°.

5.8 Construction of complementation plasmids

Construction of plasmids; pS2217, pSSR42, pS2217 3XFLAG for *in trans* complementation. Required genes with their native promoters were amplified by PCR from *S. aureus* genomic DNA, using oligos having restriction sites matching the plasmid backbone in correct orientation. *rsp* gene was amplified by 2217_intpromoter_F_NotI and 2217_intpromoter_R_BamHI, and *ssr*42 was amplified using SSR42 NotI-F and SSR42 BamHI-R (See Appendix B and Table B.1). Inserts were archived in pCR2.1 TOPO® TA vector and propagated in *E. coli* DH5α (See Appendix A and Table A.1). Plasmids were isolated (See Section 5.5.4) and examined by sequencing using either primer MF88-T7 or MF89M13-20s Appendix B and Table B.1). Inserts were seperated from TA vectors by restriction digestion and ligated to pmRFPmars vector[259] digested with the same set of enzymes, which resulted in the generation of complete plasmids. *E. coli* DH5α were transformed with these plasmids and plated on LB agar supplemented with 100 µg/ml Ampicillin. Plasmids were isolated from *E. coli* (See Section 5.5.4) and sequenced to check for the right insert, orientation or mutations using the oligonucleotides MFpUC19as1 and MF17pC194 (See Appendix B and Table B.1). Subsequently, these plasmid were passaged through *S. aureus* RN4220 (See Section 5.7.2) and finally introduced in desired electro-competent *S. aureus* mutants (See Section 5.7.2) and selected on TSA Cm 10. The resulting strains were grown in TSB at 37°C overnight and stored as glycerol stocks at -80°C.

5.9 High throughput analysis of nucleic acids

5.9.1 Transposon insertion-site deep sequencing (Tn-seq)

Chromosomal DNA was isolated from pooled mariner transposon mutant libraries including inocula and output harvested from various conditions, by the method described in Section 5.5. Fragment DNA libraries were prepared and sequenced using the following steps.

[ξ] All Sanger sequencing were done at Seqlab - Sequence Laboratories GmBH, Göttingen, Germany.
[⊥] Experiments performed by Martina Selle, Institute for Molecular Infection Biology, University of Wuerzburg, Germany.

5.9.1.1 Fragmentation of *S. aureus* genomic DNA

Hydrodynamic shearing of genomic DNA was carried out by application of ultrasonics on a Bioruptor® instrument. 1 ml of DNA dissolved in water were taken in 15 ml polystyrene tubes and sonicated for 10 cycles, with the following specifications. Ultrasonic wave frequency: 20kHz, wave power: H i.e. 320W, time: 1 minute/cycle (30 seconds 'ON' and 30 seconds 'OFF'). Fragmentation was carried out at 4°C to avoid shearing by the heat generated from the sonication probe. This setting consistently resulted in fragments sizes between 100 to 500 nucleotides. The size range was analyzed by agarose gel electrophoresis and on Agilent 2100 Bioanalyzer instrument.

5.9.1.2 End-repair and size selection of DNA fragments

5 µg of fragmented DNA from each sample were repaired using the commercially available NEBNext® End repair module following manufacturer's instructions in a volume of 100 µl. Fragments within the size range of 200-300 nucleotides were selected using a gel-free double-Solid Phase Reversible Immobilization (dSPRI), method G, as previously described[247] using AMPure XP beads[¶] in three steps. Step 1: Immediately after end repair, the samples were mixed with 0.9X volume of beads and incubated at room temperature for 20 minutes. The beads were separated using a magnetic rack and the residual solution was transfered to a fresh microfuge tube. Step 2: The DNA solution was subsequently mixed with 0.11X volume of beads and incubated at room temperature for 7 minutes. The beads were again separated and the residual solution was disposed. Step 3: The beads were washed twice with 70% Ethanol for 30 seconds without removing tubes from the magnetic rack. The beads were air-dried for 2-3 minutes and eluted in 42 µl of sterile nuclease-free water. If required, the size range was confirmed by agarose gel electrophoresis.

5.9.1.3 dA-tailing of blunt end DNA fragments

After the correct size of DNA fragments were obtained, NEBNext® dA-Tailing module was used to add non-templated deoxy-Adenosine monophosphate (dAMP) molecules to the 3′ ends, according to manufacturer's instructions. The DNA fragments were purified using AMPure XP beads[¶] and eluted into 30 µl of sterile nuclease-free water.

5.9.1.4 Generation and ligation of adapters to DNA fragments

For generation of multiplexing dsDNA adapters compatible with Illumina® sequencing platform, two separate oligonucleotides were used. MultiPlex-Y-Adapt_f with a 5′ phosphorylation and MultiPlex-Y-Adapt_r with a 3′ terminal phosphorothioate linkage, were mixed in equimolar concentrations in 1X Oligo-annealing buffer. The reaction mixture was heated to 94°C for 5 minutes followed by gradual

[¶] AMPure XP SPRI beads were routinely used for purifying DNA from reactions following manufacturer's instructions, but double SPRI method was only used in case of size selection, as mentioned in Section 5.9.1.2

cooling to room temperature and finally incubated on ice. Adaptors were ligated to dA-tailed fragments overnight at 16°C using T4 DNA ligase in the presence of 1X T4 ligase buffer and 50% Polyethylene glycol (PEG), added to the previous reaction from Section 5.9.1.3. Upon completion, DNA fragments were purified with AMPure XP beads and eluted in 25 µl of sterile nuclease-free water.

5.9.1.5 Massively parallel sequencing on Illumina® platform

Before sequencing transposon ends were enriched by aforementioned PCR steps (See Section 5.6.1), purified with AMPure XP beads[¶] and checked for quality (See Section 5.5.7). The resulting DNA fragment libraries were sequenced on the Illumina® Hi-Seq 2500 platform obtaining 10-30 million single reads per sample with indices, using the transposon-specific oligonucleotide primer Himar1-Seq[€].

5.9.1.6 Tn-seq data analysis

Sequencing files were obtained and was processed and analyzed[ϱ], as previously described[301,326]. In brief, Illumina® adapter sequences were removed using cutadapt version 1.2.1[327]. The sequence reads were checked for the nucleotide pattern 'CAACCTGT' originating from the transposon ITR. Only reads containing this specific sequence with an allowance of one mismatch or gap and with minimum length of 16 nucleotides were used for further analyses. Further, the reads were mapped to the *Staphylococcus aureus* 6850 genome (GenBank accession CP006706) using Bowtie 2 algorithm version 2.1.0[328]. To identify transposon insertion sites (TIS), the aligned start positions of mapped reads were extracted and each position on the genome, covered by at least one alignment start, was annotated as TIS. The genomic position was adjusted strand-specifically to account for the 1 nucleotide shift of the reads mapping on the positive or negative strand.

Statistical analysis of enriched or depleted reads from each TIS, was performed using DESeq2 version 1.6.2[261]. The HeLa infection experiment was modelled as a time course including a technical replicate with the input libraries as time t_0. For the mouse lung infection experiment, the 3 output libraries were compared to the input libraries. Genes with very low mean normalized read depth (mnrd) <4 were excluded in the HeLa experiment and those with mnrd 8 were excluded from the animal experiments. The *P*-values were corrected for multiple testing and the TIS with adjusted *P*-value ≤0.05 were considered as significantly increased or decreased.

5.9.2 RNA deep sequencing

RNA were isolated as previously described (See Section 5.5.5), followed by removal of DNA using DNase I enzyme (See Section 5.5.6). Quantity and quality of RNA was determined by spectrophotometric method using Nanodrop and 1.8% agarose gel containing formamide. mRNA enrichment was performed by Ribodepletion Kits followed by library Preparation for Illumina®. Depletion of processed transcripts, were performed by using Terminal 5'-phosphate-dependent exonuclease (TEX) as previously described (Sharma 2010). Briefly, RNA samples were poly(A)-tailed using poly(A) polymerase.

5'-triphosphates were removed by treatment with tobacco acid pyrophosphatase (TAP). RNA adapters were ligated to the 5'-phosphate ends and first-strand cDNA were generated using an oligo(dT)-primer and M-MLV reverse transcriptase. High fidelity DNA polymerase cDNA was amplified by PCR[Π]. cDNA were sequenced on Illumina® HiSeq platform[ϵ], yielding 100 bp paired end reads. Adapters removed and trimmed to 70 bp using Trimmomatic (Bolger 2014) and only reads exceeding a mean base quality 5 within all sliding windows of 5bp were mapped to the *S. aureus* USA300 FPR3757 genome (NCBI accession NC_007793.1), using Bowtie2 (25). Only paired and concordant alignments were considered further, yielding at least 12 million uniquely mapped read pairs per replicate. A total of 2693 coding and non-coding transcripts were identified for further analysis. Differential transcript abundance analysis was performed using the DESeq2 package v.1.5.9 (12) in R[ʊ].

5.10 Hydrogen Peroxide stimulation assay

For logarithmic phase cultures, *S. aureus* were grown overnight and diluted to OD_{600nm} of 0.1 in fresh TSB (See Section 5.1.1). This sub-culture was incubated at 37°C with intermittent measurement of OD_{600nm} and until it reaches 0.6. For stationary phase cultures, the overnight cultures were washed with PBS and resuspended in fresh TSB. At Bacteria cultures were transferred to microfuge tubes and either left untreated or treated with Hydrogen Peroxide (H_2O_2) at a final concentration of 5 mM, followed by incubation at 37°C for 10 minutes with agitation at 180 rpm. At time point, bacteria were quickly harvested by centrifugation for 30 seconds and pellets were flash frozen in liquid nitrogen. The tubes were then transferred to -80°C for long-term storage or immediately used for RNA extraction (See Section 5.5.5). For cytotoxicity assays, exponentially growing bacteria treated and untreated were incubated until 8 hours post inoculation treatment. The supernatants were collected as previously described (See Section 5.1.3). The presence of H_2O_2 in the spent medium was examined by using QUANTOFIX® Peroxide 100 test strips according to manufacturer's instructions.

5.11 Cell culture techniques

5.11.1 Cell culture conditions

HeLa 229 cells were propagated in Roswell Park Memorial Institute (RPMI)-1640[329] full medium and diluted 10 times to the next passage when they were 80-90% confluent i.e. every 2-3 days, which was limited to 10. Mouse Fibroblasts; L929 were cultivated in Dulbecco's Modified Eagle's full medium (DMEM)

[Π] Enzymatic processing and library preparation was done at Vertis Biotechnology AG, Germany.
[ϵ] Sequenced on Illumina® HiSeq platform was performed by the group of Prof. Dr. Richard Reinhardt at the Max Planck Genome Center, Cologne, Germany.
[ϱ] Tn-seq data processing, filtering, mapping and partial statistical analysis including DESeq2, was done by Christian Remmele and Dr. Dr. Marcus Dittrich, Chair of Bioinformatics, University of Würzburg, Germany.
[ʊ] RNA-seq and dRNA-seq data processing, application of DESeq2 and statistical analyses were performed by Dr. Konrad Förstner, Institute for Molecular Infection Biology, University of Wuerzburg, Germany.

for 7 days until fully confluent and for only 2 passages after which they were cyro-preserved. hMDMs were differentiated for 7 days, in RPMI 1640 full medium supplemented with Macrophage-colony stimulating factor (M-CSF). hPMNs were kept resuspended in 1X Hank's Balanced Salt Solution (HBSS) and for infection experiments in Neutrophil infection medium (NIM). Adherent cells were propagated in cell culture flasks. To passage or seed for an infection experiment, the cells were enzymatically detached and transfered to new flasks or cell culture micro-well plates of varied sizes.

5.11.2 Detachment of adherent cells

Enzymatic digestion procedure was applied to remove adherent cells from cell culture treated surfaces. The cells were washed twice with 1X DPBS before adding commercially available TrypLE express standard solution and incubated at 37°C for 5 minutes.

5.11.3 Cryopreservation of cells

All propagable cells were grown up to confluency and detached by enzymatic digestion. The cells were washed once with 1X DPBS and centrifuged at 1500 rpm for 10 minutes at room temperature. The pellet was carefully resuspended in 1 ml of cell-freezing medium (Appendix A, see Table C.1) and transfered to -80°C.

5.11.4 Inactivation of sera

Sera from both human and bovine, were inactivated by exposure to 56°C for 30 minutes, followed by gradual cooling to room temperature. Aliquots were frozen at -20°C for future use.

5.11.5 Cell types

All mammalian cell types used in this study are listed below in Table A.3.

5.12 Analysis of *S. aureus* -mediated haemolysis

5.12.1 Haemolytic activity assay

Red blood cell (RBC) disruption caused by secreted bacterial haemolysins, leads to the release of haemoglobin. Haemolysis activity is defined by the quantity of released Haemoglobin over a given period of time and was performed as previously described[149] with minor modifications. Briefly, *S. aureus* was grown overnight, as described in Section 5.1.1 and bacterial culture filtrates were collected using the method described in Section

Before doing the actual experiment, the 50% lethal dosage (LD_{50}) was determined by intoxicating blood solution with increases doses of culture filtrates and haemoglobin release was compared to total

For details on media and manufacturer information, please refer to Appendix A

or maximum lysis with water. The absorbance values were plotted as function of intoxication ratios and fitted into a linear model of simple regression to calculate co-linearity using Pearson's correlation co-efficient (R). LD_{50} was considered as the dilution ratio where absorbance was half-maximum.

5.12.2 Haemolysis zone measurement

Complete haemolysis was also quantified by measuring the diameter of clear yellow zone around *S. aureus* colony. Bacteria were grown overnight as described previously in Section 5.1.1 and the optical densities of all samples in question were normalized. The bacterial culture was then dilution 100 times, before carefully and aseptically spotting a 10 µl droplet, with the help of a micrpipette on sheep blood agar. The droplet was avoid to dry completely before inverting the plates and incubating a 37°C overnight. Every sample was spotted in duplicates with defined distance from each other.

Images of every bacterial spot were acquired using a Zoom Stereo Microscope with 5X objective and Leica LAS EZ software. For precise measurements, a bacterial spot was imaged with a short piece of paper ruler, placed under in the same field of view. Image processing and diameter measurement was done using ImageJ software. A straight line was drawn on the paper ruler and the actual length was set manually by "Set Scale" function, as the reference scale. Consequently, a new line could be drawn between two points and measure by the "Measure" function. Using this method, the diameter of bacterial colony (d_{colony}) were measured by drawing lines from edge to edge and measuring the length. Similarly, the diameter of full haemolysis zone with the colony (d_{full}) was measured. Finally the exclusion diameter, hereafter analyse to as zone of haemolysis (Δd) was calculated by subtracting both the measurements.

Calculation of haemolysis zone diameter:

$$\Delta d = d_{\text{full}} - d_{\text{colony}} \qquad \text{.... (mm)}$$

The values were plotted to compare haemolysis zone diameters and statistical significance was determined by one-way ANOVA and Tukey's HSD test for individual comparisons.

5.13 *In vitro* infection of mammalian epithelial cells with *S. aureus*

5.13.1 Lysostaphin-Gentamicin protection assay

HeLa cells were cultivated as previously described in Section 5.11. Cells were detached (See Section 5.11.2) and seeded in 12-well cell culture plates at a density of 1 x 10^5 per well with RPMI full medium. The next day, the cells were washed with 1X DPBS and culture medium was exchanged with RPMI infection medium, at least 4 hours pre-infection. Bacteria were grown and infection subcultures were prepared following the described method in Section 5.1.1. Bacteria were harvested and enumerated using a Thoma counting chamber, before infecting HeLa cells at an MOI of 10. Infection was synchronized by centrifuging at 1,000 rpm for 10 minutes at room temperature and further incubated at 37°C for 60 minutes in

a humidified incubator with 5% CO_2. Extra-cellular bacteria were removed by treatment with a mixture of Lysostaphin (20 µg/ml) and Gentamicin (100 µg/ml) for 30 minutes. For checking invasion rates of *S. aureus* , HeLa cells were lysed immediately after treatment or the medium was exchanged with RPMI infection medium containing only Gentamicin (100 µg/ml), for intra-cellular replication or cell death assays.

Internalized bacteria were recovered by hyposomotic lysis; HeLa cells were washed once with 1 ml 1X DPBS and once with sterile water for a very short time, before incubation with 500 µl sterile water for 20 minutes. The cell lysate was homogenized by vigorous pipetting and transfered to a microfuge tube containing 500 µl RPMI infection medium. The mixture was serially diluted and plated on TSA.

5.13.2 Intracellular cytotoxicity screen in HeLa cells using *S. aureus* transposon mutant library

HeLa cells were cultivated as previously described in (See Section 5.11) and prepared for infection in 6-well cell culture plates at a density of 1.5 x 10^6 as previously described (See Sections 5.11.2 and 5.13.1).

Mutant library was revived from stock (See Section 5.7.1) in warm NB and incubated at 37°C for 30 minutes to achieve metabolically active state. Bacteria were harvested, enumerated and used for infection at MOI of 1, as previously described (See Section 5.13.1). This formed the input library and was plated onto TSA Erm 5 in 150 mm petri dishes. Subsequently, the medium was exchanged with RPMI infection medium containing only Gentamicin (100 µg/ml). After 8 hours, internalized bacteria were recovered by hyposomotic lysis, as previously described (See Section 5.13.1). Entire lysates were divided into equal parts plated onto TSA Erm 5 in 150 mm petri dishes, which formed the output library 1. All input and outputs were harvested by scrapping off the agar with NB medium and stored as previously described (See Section 5.1.2). The entire process was repeated 2 more using the previous output as input (See Figure 2.7G).

5.13.3 Phagosomal escape assay

Phagosomal escape was investigated as described previously with some modifications[153,228] ⊛. Briefly, HeLa cells expressing YFP-CWT fusion[153] were cultivated in dark 24-well plates (ibidi µ-clear) with RPMI1640 infection medium. *S. aureus* were grown overnight and infection subcultures were prepared as previously described (See Section 5.1.1). Bacteria were harvested by centrifugation, labelled with 50 µg/ml Tetramethylrhodamine (TRITC) for 30 minutes at 37°C and washed several times with 1X PBS. Host cells were infected with labelled bacteria using the method described in Section 5.13.1, at an MOI of 10. At 3 hours post infection, the cells were washed with PBS^{2+} and subsequently fixed with 4% para-formaldehyde. The samples were examined on an automated Operetta® Fluorescence Microscope.

Phagosomal escape rates were quantified by investigating co-localization of YFP and TRITC signals with the embedded Harmony® high-content imaging and analysis software. The mean escape scores

were plotted as relative percentage to the signal obtained from the wild type bacteria, as reference. Statistical analysis was performed by one-way ANOVA and Tukey's HSD tests for individual comparisons.

5.14 Detection and quantification of cytotoxicity in mammalian cells

Cytotoxicity in various mammalian cells was quantified by multiple methods, which depended on the type of experiment and host cell type. Individual methods are mentioned as follows:

5.14.1 Measurement of cell death assisted by flow cytometry

HeLa cells were infected with *S. aureus* as aforementioned in Section 5.13.1, with an MOI of 10. At each time point, the culture medium from each well was transfered to a microfuge tube and the HeLa cells were detached from the surface by a method described earlier in Section 5.11.2. The same medium transfered to tubes was used to stop the detachment reaction, to also collect the pre-detached and dead cells. Cells were harvested by centrifugation at 800 xg for 10 minutes and gently resuspended in 100 µl FACS labeling solution containing 1 µg/ml Propidium Iodide. Staining was performed at room temperature for 10 minutes in dark, followed by diluting the PI stain with an additional 400 µl FACS labeling solution. The cells were kept on ice and fluorescence was measured using the Accuri C6 flow cytometer, at 530 nm (FL-1 filter).

5.14.2 Analysis of host cell granularity assisted by flow cytometry

During the analysis of cell death by flow cytometry, a gate is set encompassing viable host cell population in the FSC vs SSC plot. The cells within this gate were analysed for uptake of PI, although as the infected cell starts dying its size and granularity, adjudged by SSC profile may change. Hence, two gates; one bigger and one smaller were applied to the analysis and any difference between these two gates in terms of increased SSC can be calculated by subtracting them from each other. Hence, the formula used to decipher the difference in cellular granularity is as follows:

$$\Delta R = R1 - R2 \qquad \ldots. (\%)$$

where, ΔR is the percentage increased granularity.

R1 is the percentage of entire cell population from the infected sample in the bigger gate.

R2 is the percentage of viable cell population from the uninfected sample in the smaller gate.

Therefore, ΔR was determine and plotted against each time point for infection groups. Statistical analysis was performed using two-way ANOVA and Tukey's HSD test for individual comparisons.

[*] Experiments performed by Sebastian Blättner, Chair of Microbiology, University of Würzburg, Germany.

5.14.3 Measurement of released cytoplasmic Lactate Dehydrogenase (LDH)

Roche Cytotoxicity detection kit^{PLUS} was used for quantifying released LDH upon cell death of mammalian cells. The reaction mixture was prepared according to manufacturer's instructions by adding the catalyst (blue cap) to the dye solution (red cap). The mixture for desired number of reactions i.e. wells required, were calculated accordingly. The reaction mixture was kept on ice and protected from light until used. After the catalyst has been added to the dye solution, the mixture should not kept for longer periods of time i.e. more than 1 hour. Hence, fresh reaction mixtures should be prepared just before each time point.

For each reaction, 100 µl of sample supernatant was mixed with equal volume of LDH reaction mixture and incubated for 10 minutes at room temperature in dark. For positive control, PMNs were lysed using 5 µl Lysis solution (white cap) for 15 minutes at room temperature with intermittent mixing and only PMNs were used as negative control. The reactions were stopped by adding 50 µl of Stop solution (green cap) to samples. The optical densities were measured in a multimode reader at 490 nm.

Calculation of cytotoxicity using LDH assay:

$$\textit{Percentage cytotoxicity(\%)} = \frac{exp.value - neg.control}{pos.control - neg.control} \times 100$$

5.15 Isolation of Mammalian Leukocytes

5.15.1 Isolation of Polymorphonuclear neutrophils (PMNs)

Leukocytes were separated by density gradient centrifugation using a polysaccharide of precise density, as previously described with minor modifications[330]. Briefly, blood was collected from healthy human individuals in 10 mL S-monovette® lithium heparin tubes and carefully layered on 15 mL Ficoll-Paque PLUS (Density:1.077 g/L) in 50 ml polypropylene centrifuge tubes at room temperature. The layers were separated by centrifugation at 1000 rpm for 30 minutes at 20°C in a swinging-bucket rotor without brakes.

Usually the granulocytes and erythrocytes end up at bottom of the tube and peripheral blood mononuclear cells (PBMCs) remains at the interface of plasma and Ficoll. The PBMCs were transfered to a new tube by sterile plastic disposable pasteur pipette and proceeded to Macrophage differentiation method (See Section 2.4.2). The rest of plasma and ficoll was aspirated out and the pellet was gently mixed with 1% Polyvinyl alcohol (PVA) solution at three times the volume of blood, followed by incubation at room temperature for 45 minutes. PVA is a synthetic polymer that binds and sediments RBCs and hence they settle down at the bottom and the supernatant containing the granulocytes was transfered carefully to another 50 ml centrifuge tube. The PMNs were collected by centrifugation at 1000 rpm for 5 minutes at 20°C and residual erythrocytes were removed by osmotic lysis using water for 30 seconds and reconstitution with 5X PBS. The PMNs were harvested by centrifugation at 1000 rpm for 5 minutes and resuspended in 1X HBSS, until used in an experiment within 8 hours of isolation. PMNs were confirmed

by using anti-CD11b and anti-CD66b antibodies.

5.15.2 Isolation of PBMCs

PMBCs from density gradient centrifugation (See Section 5.15.1) were washed twice by adding 1X PBS up to 40 ml followed by centrifugation at 1300 rpm for 10 minutes. The residual erythrocytes, if any, were removed by osmotic lysis with sterile water for 30 seconds and reconstituting with 5X PBS. The PBMCs were harvested by centrifugation at 1300 rpm for 10 minutes and resuspended in RPMI full medium.

5.15.3 Differentiation of human monocyte-derived macrophages (hMDMs)

Primary human monocyte-derived macrophages were cultivated from PBMCs by enhancing monocyte attachment by Phytohemagglutinin (PHA) and differentiation to macrophages using human recombinant macrophage-colony stimulating factor (M-CSF). The overall procedure requires 8 days, from isolation till fully differentiated macrophages to work with.

Resuspended PBMCs (See Section 5.15.2) in RPMI full medium were supplemented with PHA and enumerated using a Neubauer cell counting chamber. These cells were then transfered to 24-well tissue culture plates with $1x10^6$ cells per well and incubated for 24 hours at 37°C, in a humidified incubator with 5% CO_2. This was considered to be day 1. On day 2, the monocytes were attached to well surface leaving out the lymphocytes in suspension. The spent medium was removed by aspiration and the monocytes were gently washed twice with 1X DPBS, followed by the addition of 500 µl fresh RPMI full medium supplemented with 100 ng/ml M-CSF. The monocytes were incubated for following days at 37°C in the incubator. This step was repeated on day 5, but without washing and 50 ng/ml M-CSF. Finally on day 8, fully differentiated macrophages were obtained, which were examined microscopically for morphology and viability.

5.16 *In vitro* infection of mammalian immune cells with *S. aureus* or *S. aureus* secretions

5.16.1 Intra-neutrophil survival of *S. aureus*

Intracellular survival potential of *S. aureus* in primary human neutrophils was tested as previously described[235]. PMNs were centrifuged (See Section 5.15.1) and resuspended in NIM at 1 x 10^6/mL. The cells were further divided into 500 µl aliquots in sterile 1.5 mL microfuge tubes, to achieve a final cell density of 5 x 10^5/ aliquot. Bacterial infection cultures were prepared (See Section 5.1.1) harvested by centrifugation at 14000 rpm for 2 minutes and resuspended in opsonisation buffer and tumbled on a revolving wheel at 37°C for 20 minutes. After opsonisation, the bacteria were washed twice with 1X PBS and resuspension in NIM. Bacterial numbers were determined using a Thoma counting chamber and the PMNs were infected at an MOI of 10. The infection mixtures were tumbled for 10 minutes at 37°C.

After 10 minutes, the PMNs were collected by centrifugation at 500 xg for 5 minutes at room temperature and the medium was removed by aspiration. This step removes extracellular bacteria and serves as time zero i.e. t_0, which crucial for checking phagocytosis efficiency.

PMN containing ingested bacteria were resuspended in the original volume of NIM, except for t_0. Bacteria were recovered by osmotic lysis of the PMNs by adding alkaline water and incubation for 5 minutes at room temperature. The PMN lysates were vortexed and serially diluted in 1X PBS and were plated drop-wise (25 µl/ drop) on TSA plates in duplicates and incubated overnight at 37°C for CFU enumeration.
Similarly, aliquots were obtained at subsequent time points to quantify bacterial killing within PMN over time and Neutrophil killing by *Staphylococcus aureus*.

5.16.2 Neutrophil cytotoxicity induced by intracellular *S. aureus*

Intracellular *S. aureus* -induced PMN cytotoxicity was quantified by measuring release LDH (See Section 5.14.3). PMNs were infected with *S. aureus* as mentioned before (See Section 5.16.1), with 2 additional aliquots without bacteria for control samples. At each time point, the PMNs were collected by centrifugation and the supernatant from all samples were removed carefully from top and transfered into a 96-well plate (this was done in duplicates). For positive control, PMNs were lysed using the lysis reagent provided with the assay kit. In addition, to this an uninfected sample was used for control for spontaneous cell death and background correction. To all the samples, the LDH reagent mix was added and the reaction was incubated in dark at room temperature for 10 minutes. The LDH reaction was stopped and read immediately in the multimode reader. The time-points included in this assay were 10, 60, 120 and 240 minutes post-infection.

5.16.3 Intoxication of Neutrophils *S. aureus* culture filtrates

PMNs were isolated and prepared as previously described (See Sections 5.15.2 and 5.16.1). Cells were intoxicated 1% (v/v) with *S. aureus* filtrates from untreated or H_2O_2-treated cultures and tumbled on a revolving wheel at 37°C for desired time points. Control samples were treated with sterile fresh medium. Cytotoxicity was measured as previously described (See Section 5.14.3).

5.16.4 Intracellular survival of *S. aureus* in hMDMs

hMDMs were differentiated as previously described (See Section 5.16.1). Monocytes comprises of approx. 10% of PBMC population hence the final cell density considered was $1x10^5$ cells/ well after seeding and differentiation. Infection cultures of *S. aureus* 6850 pmRFPmars and 6850 Δ*rsp* pmRFPmars were prepared (See Section 5.1.1) and added to the wells at MOI of 10. Infection was synchronized by centrifuging at 1,000 rpm for 10 minutes at room temperature and further incubated at 37°C for 30 minutes in a humidified incubator with 5% CO_2, to allow phagocytosis by macrophages. Extra-cellular bacteria were removed by treatment with a mixture of Lysostaphin (20 µg/ml) and Gentamicin (100 µg/ml) for 30

minutes. The cells were incubated further in the presence of Gentamicin for upto 72 hours. After every 24 hours microscopic images at 200x magnification were obtained using both bright field and 588 nm channels.

5.17 Animal experimentation with murine infection models

5.17.1 Ethics statement

Animal studies were either approved by the local government of Franconia, Germany (approval nos. 2531.01-06/12 and 2532-2- 155) and performed in strict accordance with the guidelines for animal care and experimentation of German Animal Protection Law or were approved under the Animal Scientific Procedures Act 1986 (Project license 30/2825). Experiments were only conducted by individuals licensed under FELASA, Category B, European Union.

5.17.2 General practice and infection doses

Female BALB/c mice aged 6 week were kept in individually ventilated cages on a normal diet in groups of not more than in each cage. At 8 weeks, groups of 10 mice were infected intra-nasally$^{\perp}$ with a bacterial suspension, prepared as described previously (See Section 5.1.1). The lethal and sub-lethal doses of *S. aureus* strains USA300 and 6850 were determined by titration with different bacterial CFU numbers. Mice were monitored for weight loss, illness and survival every 24 hours post infection.

5.17.3 Lung infection screen using *S. aureus* 6850 transposon mutant library in acute pneumonia model

The sub-lethal doses for *S. aureus* 6850 were 0.3 x 10^8 CFUs in a (20 µl inoculum. The mutant library was administered intra-nasally$^{\perp}$ with similar doses and 24 hours post infection, the mice were euthanized by CO_2 inhalation. For harvesting output library, lungs were surgically removed, homogenized with 1X PBS in GentleMACS, M-tubes. Entire lung lysates from each animal and the administered input, were plated on TSA and incubated for 24 hours at 37°C. The bacteria were scraped off the agar plates and cryo-preserved until further use in downstream applications.

5.17.4 Determination of bacterial load after administration of *S. aureus* in acute pneumonia model

Sub-lethal doses of the bacterial strain to be tested were administered intra-nasally$^{\perp}$ and after 24 hours post infection, mice were euthanized by CO_2 inhalation. The lungs were aseptically removed and homogenized with 1X PBS in GentleMACS, M-tubes. For enumeration of CFUs, lung lysates were serially diluted in 1X PBS and several dilutions were plated on TSA. The plates were incubated for 24 hours at

37°C and the organ loads were compared within mice groups. and analyzed by one-way ANOVA, followed by Tukey's post-hoc pairwise analysis.

5.17.5 Host survival after intra-nasal infection of *S. aureus* in acute pneumonia model

Lethal doses for strains USA300 and 6850 were 2 x 10^8 CFUs and 0.7 x 10^8 CFUs in a 20 µl inoculum. Mice were administered with lethal doses and monitored for 24, 48 and 72 hours post infection[⊥]. At each time point deceased mice were removed from the cages and transferred for proper disposal. During the entire 3 days, the number of survivors from each infection group was noted and at the end of the experiment remaining mice were euthanized by CO_2 inhalation to end the experiment.

5.17.6 Histopathological evaluation of tissue

Tissue section to be analyzed were fixed in 1% Paraformaldehyde for at least 24 hours or longer, embedded in paraffin, cut into 5 µm thick section using a microtome and mounted on glass slides[⏀]. For Haematoxylin and Eosin (H&E) staining, samples were de-paraffinised and rehydrated in distilled water. The slides were stained with Hämalaun nach Mayer working solution for 10 minutes, washed with distilled water and stained with Eosin solution for 10 minutes. Subsequently, samples were rinsed with distilled water, treated with 96% Ethanol and dehydrated with Xyline. Sections were preserved with VectaMount^{TM} with a cover slip on top. The slides were visualized and imaged using an inverted microscope under bright field and 200x magnification.

For immunohistochemical analysis; Neutrophil Ly6G staining[⏀], de-paraffinised sections were washed with 1X DPBS, treated with Blocking buffer for 30 minutes and incubated overnight with primary antibody; Rat anti-mouse Ly6G (1A8 clone) at a dilution of 1:200 in 1%BSA PBS at 4°C. Next day, slides were washed with 1X DPBS and incubated with secondary antibody; Anti-rat Alexa Fluor 488 at dilution of 1:500 in 1%BSA PBS for 2 hours. The slides were again washed with 1X DPBS, allowed to dry before addition of VECTASHIELD mounting medium and preserved with cover slip. The slides were stored at 4°C and imaged with a fluorescence microscope at 200x magnification.

5.18 Statistical methods

All data were checked for for normality distribution by Shapiro-wilk and a combination of tests in the 'norm' package in R.

[⊥] Experiments performed in collaboration with Dr. Babett Österreich and Martina Selle, Institute for Molecular Infection Biology, University of Wuerzburg, Germany.
[⏀] Histopathological evaluation was conducted in collaboration with Melanie Schott and Prof. Dr. Alma Zernecke, Institute for Experimental Biomedicine, University of Wuerzburg, Germany.

Regression analysis were done by fitting the data into a linear model of single or multiple regression in R. Used for Tn-seq statistics and correlations, for dose dependencies in haemolysis experiments, bacterial growth over time. For intracellular replication assay using fluorescent bacteria, the mean fluorescence values obtained were fitted in to a linear model for multiple regression analysis.The slopes obtained for both wild type and *rsp* mutants were compared using analysis of co-variance (ANCOVA).

Survival rates were analyzed by Kaplan-Meier estimate and statistical evaluation was done using Mantel-Cox Log-rank test. For mean escape scores, cell death analysis, qRT-PCRs Statistical analysis was performed by one-way ANOVA and Tukey's HSD tests for individual comparisons. For bacterial survival in PMNs, peroxide treated qRT-PCRs and PMN cell death pairwise T-tests were performed.

Appendix A

List of bacterial strains, plasmids and cell lines

Table A.1: Details of bacterial strains used in this study

Strain	Description	Source or Reference
Escherichia coli		
DH5α	Non-pathogenic laboratory strain of *E. coli*, vastly used for cloning. Reference genome: strain K-12 substrain MG1655, NCBI Accession: NC_000913, *fhu*A2 *lac*ΔU169 *pho*A *gln*V44 ϕ80$'$ *lacZ*ΔM15 *gyr*A96 *rec*A1 *rel*A1 *end*A1 thi-1 *hsd*R17.	Life technologies,[331],[332]
TOP10F$'$	Non-pathogenic laboratory strain of *E. coli*, vastly used for cloning. Reference genome: strain K-12 substrain MG1655, NCBI Accession: NC_000913, F$'$[*lac*I^{q} Tn10(*tet*^{R})] *mcr*A δ(*mrr-hsd*RMS-*mcr*BC) φ80*lacZ*δM15 δ*lac*X74 *deo*R *nup*G *rec*A1 *ara*D139 δ(*ara-leu*)7697 *gal*U *gal*K *rps*L(Str^{R}) *end*A1 λ^{-}.	Invitrogen^{TM},[333],[334]
Staphylococcus aureus		
RN4220	Non-hemolytic derivative of NCTC 8325-4, *sau1*$^{-}$, *hsdR*$^{-}$ developed for cloning and laboratory studies. Reference Genome: NCTC 8325, NCBI Accession: NC_007795	[335]
RN4220 pS2217	RN4220 with *rsp* complementation *in trans* by pS2217.	This study
RN6911	Derivative of NCTC 8325-4 with deleted *agr* operon.	[175]
RN6911 pS2217	RN6911 with *rsp* complementation plasmid pS2217.	This study
LAC	USA300 CA-MRSA, SCC*mec* type IV, *spa* type 1, ST8, CC8. Genome: USA300 FPR3757, NCBI Accession: NC_007793. An epidemic community-acquired strain isolated from outbreaks of soft tissue infections, severe septicemia, necrotising pneumonia, and necrotising fasciitis.	[336]
JE2	Plasmid-cured derivative of USA300 LAC.	NARSA,[284]

NE1304	JE2 transposon insertion mutant within *rsp*, locus ID: SAUSA300_2326.	NARSA, [284]
NE1532	JE2 transposon insertion mutant within *agr*A, locus ID: SAUSA300_1992.	[284]
LAC* (AH1263)	Erythromycin-sensitive derivative of USA300 LAC, cured of plasmid pUSA03	[337]
LAC* *rsp*::*erm*B	Phage-transduced LAC* recipient of NE1304	This study
LAC* *rsp*::*erm*B pS2217	LAC* *rsp*::*erm*B complemented *in trans* for *rsp* with plasmid pS2217.	This study
6850	MSSA but β-lactam resistant, *spa* type t185, ST50, no CC (Singleton). Isolated from a patient with a skin abscess, progressed to bacteraemia, osteomyelitis, septic arthritis, and multiple systemic abscesses.	[338], [245]
6850 pBTn	6850 with plasmid pBTn [246] for generation of random transposon mutagenesis.	This study
6850 Δ*rsp*	6850 with targeted deletion of gene locus RSAU_002217 (*rsp*).	This study
6850 Δ*rsp* pS2217	6850 Δ*rsp* complemented *in trans* for RSAU_002217 (*rsp*) with plasmid pS2217.	This study
6850 Δ*hla*	6850 with targeted deletion of *hla* gene coding for alpha-toxin.	This study
6850 Δ*rsp* pSSR42	6850 Δ*rsp* expressing the non-coding regulatory RNA; SSR42 *in trans* driven by its native promoter from the plasmid pSSR42.	This study
6850 pmRFPmars	6850 constitutively expressing an enhanced monomeric red fluorescent protein (mRFPmars) [339] *in trans* driven by staphylococcal *sar*A promoter 1 (*sar*AP1) from plasmid pmRFPmars.	[259]
6850 Δ*rsp* pmRFPmars	6850 Δ*rsp* constitutively expressing mRFPmars from plasmid pmRFPmars	This study

Table A.2: Details of plasmids used in this study

Plasmid	Description	Source or Reference
pCR2.1 TOPO® TA	Ligase-independent cloning vector	Life technologies
pBTn	Single plasmid system with transposase and transposon for induction of insertional mutagenesis in *S. aureus* [246]. The backbone carries the transposable element that contains a erythromycin resistance gene (*erm*B) flanked by Inverted Terminal Repeats derived from Himar1 transposon [278] and the C9 transposase enyzme [277].	Kindly provided by Prof. Dr. Michael Otto, NIH, USA
pKOR1	Plasmid used for targeted gene deletion by allelic replacement in *S. aureus* [325].	Kindly provided by Prof. Dr. Olaf Schneewind, University of Chicago, USA.

pmRFPmars	Plasmid expressing enhanced monomeric red fluorescent protein (mRFPmars) [339] driven by staphylococcal *sar*AP1 promoter.	[259]
pS2217	Plasmid expressing *rsp in trans* driven by its native promoter cloned into the backbone of pmRFPmars [259]	This study.
pSSR42	Plasmid expressing *ssr*42 *in trans* driven by its native promoter cloned into the backbone of pmRFPmars [259]	This study.
pS2217 3XFLAG	Plasmid expressing *rsp* fused with 3XFLAG at its N-terminus *in trans* driven by its native promoter cloned into the backbone of pmRFPmars [259]	Benjamin O.T. Salazar, Master F1 Practical

Table A.3: Details of cell lines & Primary cells used in this study

Cell line	Description	Source or Reference
HeLa 229	Adherent tumor epithelial cells derived from human cervix adenocarcinoma containing human papilloma virus (HPV-18).	ATCC
Human PMNs	Polymorphonuclear neutrophils (PMNs), freshly isolated by density gradient separation of heparinized human venous blood	Healthy human individuals.
Human MDMs	Monocyte-derived macrophages (MDMs) differentiated from primary monocytes derived from freshly isolated peripheral blood mononuclear cells separated from heparinized human venous blood.	Healthy human individuals
Defibrinated Sheep blood	Sheep blood deprived of coagulation factors for haemolysis assays and addition in sheep blood agar	Fiebig Nährstofftechnik, Germany

Appendix B

List of oligonucleotides

Table B.1: List of oligonucleotides used in this study, with detailed information. Syntheses of all oligonucleotides were done by Sigma-Aldrich Chemie GmbH, Germany

ID[ϰ]	Name	GC%	Tm	Length	Sequence	Modifications	Scale[*]	Grade[o]
7	MFpUC19as1	52.38	59	21	GTTGTGTGGAATTGTGAGCGG		0.01	DST
17	MF17pC194	55	59	20	GCATGTAACTGGGCAGTGTC		0.01	DST
88	MF88-T7	40	51.6	20	TAATACGACTCACTATAGGG		0.01	DST
89	MF89M13-20s	56.25	58.2	16	GTAAAACGACGGCCAG		0.01	DST
370	Himar1-Seq	54.8	75.8	31	ACAGGTTGGCTGATAAGTCCCCGGTCTCTAG		0.025	HPLC
380	erm-5.1	33.2	56.1	24	GCTTCTAAGTCTTATTTCCATAAC		0.025	DST
381	erm-5.2	37.5	58.8	24	AGATAATGCACTATCAACACACTC		0.025	DST
382	erm-5.3	34.7	59.5	23	TCTACATTACGCATTTGGAATAC		0.025	DST
383	erm-3.1	40.9	52.1	22	TAGGTATACTACTGACAGCTTC		0.025	DST
384	erm-3.2	33.2	55.7	21	ATTCTATGAGTCGCTTTTGTA		0.025	DST
385	erm-3.3	30.4	52.8	23	TACTTATGAGCAAGTATTGTCTA		0.025	DST
386	arb1	40	77.5	35	GGCCACGCGTCGACTAGTCANNNNNNNNNNGATAT		0.025	DST
387	arb2	42.8	80.5	35	GGCCACGCGTCGACTAGTCANNNNNNNNNNGATCA		0.025	DST
388	arb3	65	70.9	20	GGCCACGCGTCGACTAGTCA		0.025	DST
456	himar-3-PCR	53.8	70.5	26	CAGCTTCCAAGGAGCTAAAGAGGTCC	5'[Btn]	0.05	HPLC
457	himar-5-PCR	42.3	65	26	CCATAACTTTAGGGTTAACCATACGC	5'[Btn]	0.05	HPLC
458	TnSeq-HimarPCR-cor-PT	51	85.4	47	AATGATACGGCGACCACCGAGATCTACGGACTTATCAGCCAACCTGT	5'[Btn], 3'[*]	0.05	HPLC
431	Himar-TnSeq-Read1	50	75.3	32	ACCGAGATCTACGGACTTATCAGCCAACCTGT		0.05	HPLC
432	MultiPlex-Y-Adapt-f	55	64.5	20	GATCGGAAGAGCACACGTCT	5'[Phos]	0.05	HPLC
433	MultiPlex-Y-Adapt-r	51.5	77.3	33	ACACTCTTTCCCTACACGACGCTCTTCCGATCT	3'[*]	0.05	HPLC
434	MP-TnSeq_Index1	51.5	91.4	64	CAAGCAGAAGACGGCATACGAGATCGTGATGTGACTGGAGTTCAGACGTGTGCTCTTCCGATCT		0.05	PAGE
435	MP-TnSeq_Index2	51.5	90.6	64	CAAGCAGAAGACGGCATACGAGATACATCGGTGACTGGAGTTCAGACGTGTGCTCTTCCGATCT		0.05	PAGE
436	MP-TnSeq_Index3	51.5	90.2	64	CAAGCAGAAGACGGCATACGAGATGCCTAAGTGACTGGAGTTCAGACGTGTGCTCTTCCGATCT		0.05	PAGE
437	MP-TnSeq_Index4	51.5	90.9	64	CAAGCAGAAGACGGCATACGAGATTGGTCAGTGACTGGAGTTCAGACGTGTGCTCTTCCGATCT		0.05	PAGE
438	TnSeq-HimarPCR_cor	51	85.3	47	AATGATACGGCGACCACCGAGATCTACGGACTTATCAGCCAACCTGT	5'[Btn]	0.05	HPLC
439	MP-TnSeq_Index5	51,5	91	64	CAAGCAGAAGACGGCATACGAGATCACTGTGTGACTGGAGTTCAGACGTGTGCTCTTCCGATCT		0.05	PAGE
440	MP-TnSeq_Index6	51,5	91	64	CAAGCAGAAGACGGCATACGAGATATTGGCGTGACTGGAGTTCAGACGTGTGCTCTTCCGATCT		0.05	PAGE
443	IS-Himar-forward	52	72.8	25	AATGATACGGCGACCACCGAGATCT		0.025	DST
444	IS-BC-Reverse	50	69.2	24	CAAGCAGAAGACGGCATACGAGAT		0.025	DST
462	MP-TnSeq_Index7	51.5	91	64	CAAGCAGAAGACGGCATACGAGATGATCTGGTGACTGGAGTTCAGACGTGTGCTCTTCCGATCT		0.05	PAGE

463	MP-TnSeq_Index8	50	90.2	64	CAAGCAGAAGACGGCATACGAGATTCAAGTGTGACTGGAGTTCAGACGTGTGCTCTTCCGATCT		0.05	PAGE
464	MP-TnSeq_Index9	51.5	91	64	CAAGCAGAAGACGGCATACGAGATCTGATCGTGACTGGAGTTCAGACGTGTGCTCTTCCGATCT		0.05	PAGE
465	MP-TnSeq_Index10	50	88.3	64	CAAGCAGAAGACGGCATACGAGATAAGCTAGTGACTGGAGTTCAGACGTGTGCTCTTCCGATCT		0.05	PAGE
468	Himar-TnSeq-Read1-v2	56.2	77.7	32	ACCGAGATCTACGAGACCGGGGACTTATCAGC		0.05	HPLC
469	TnSeq-HimarPCR-v2-PT	55.3	85.8	47	AATGATACGGCGACCACCGAGATCTACGAGACCGGGGACTTATCAGC	5'[Btn], 3'[*]	0.05	HPLC
476	MP-TnSeq_Index11	53.1	91.3	64	CAAGCAGAAGACGGCATACGAGATGTAGCCGTGACTGGAGTTCAGACGTGTGCTCTTCCGATCT		0.05	PAGE
477	MP-TnSeq_Index12	50	89.4	64	CAAGCAGAAGACGGCATACGAGATTACAAGGTGACTGGAGTTCAGACGTGTGCTCTTCCGATCT		0.05	PAGE
478	MP-TnSeq_Index13	50	90.2	64	CAAGCAGAAGACGGCATACGAGATTTGACTGTGACTGGAGTTCAGACGTGTGCTCTTCCGATCT		0.05	PAGE
479	MP-TnSeq_Index14	51.5	90.9	64	CAAGCAGAAGACGGCATACGAGATGGAACTGTGACTGGAGTTCAGACGTGTGCTCTTCCGATCT		0.05	PAGE
480	MP-TnSeq_Index15	50	90.7	64	CAAGCAGAAGACGGCATACGAGATTGACATGTGACTGGAGTTCAGACGTGTGCTCTTCCGATCT		0.05	PAGE
481	Mp-TnSeq_Index16	54.6	92.7	64	CAAGCAGAAGACGGCATACGAGATGGACGGGTGACTGGAGTTCAGACGTGTGCTCTTCCGATCT		0.05	PAGE
482	Mp-TnSeq_Index17	51.5	89.8	64	CAAGCAGAAGACGGCATACGAGATCTCTACGTGACTGGAGTTCAGACGTGTGCTCTTCCGATCT		0.05	PAGE
483	MP-TnSeq_Index18	54.6	93.1	64	CAAGCAGAAGACGGCATACGAGATGCGGACGTGACTGGAGTTCAGACGTGTGCTCTTCCGATCT		0.05	PAGE
484	MP-TnSeq_Index19	50	90.6	64	CAAGCAGAAGACGGCATACGAGATTTTCACGTGACTGGAGTTCAGACGTGTGCTCTTCCGATCT		0.05	PAGE
485	MP-TnSeq_Index20	54.6	93.1	64	CAAGCAGAAGACGGCATACGAGATGGCCACGTGACTGGAGTTCAGACGTGTGCTCTTCCGATCT		0.05	PAGE
497	attB1-2127-up-F	42.3	84.2	52	GGGGACAAGTTTGTACAAAAAAGCAGGCTTTGTTGTTGCACTATCTTGGTGA		0.025	DST
498	2127-up-R-SacII	40.9	79.5	44	TCGATCCCGCGGATTTCTCTCTCCTGCCTAATATATATTGAAAT		0.025	DST
499	2127-down-F-SacII	41.8	77	43	GATCGACCGCGGTAAATACTAACAGTCCTCTTGTGTTTAGTTT		0.025	DST
500	attB2-2127-down-R	42.5	83.8	54	GGGGACCACTTTGTACAAGAAAGCTGGGTACGTTTTTCTCAATGCTTTCATCTT		0.025	DST
517	attB1-hla-up-F	38.7	83.3	54	GGGGACAAGTTTGTACAAAAAAGCAGGCTTCCGCATCATTTGTTGTTAATAATG		0.025	DST
518	hla-up-R-SacII	29.7	75.0	47	GATCGACCGCGGTAATGTAAATTATTTGTTCATGTACAAATAAATAT		0.025	DST
519	hla-down-F-SacII	39	79.5	41	GATCGACCGCGGTTTCATCATCCTTCTATTTTTTAAAACGA		0.025	DST
520	attB2-hla-down-R	41	81.0	56	GGGGACCACTTTGTACAAGAAAGCTGGGTTAATCGTTCTAAATCTAGCATCTTCTA		0.025	DST
525	2127-intpromoter-F-NotI	41	78.5	39	GACAATGCGGCCGCCACTATTACCTTTTCAAAAATATTC		0.025	DST
526	2127-intpromoter-R-BamHI	33.2	71.5	42	GATGTCGGATCCTTAGCTAGGTTTAAAGCAAATATATTTAAC		0.025	DST
531	2127_test_F	33.2	55.2	21	ATATCTTGTTGCTGCTAATTC		0.025	DST
532	2127_test_R	40	58	20	AACCGGAAATAGATTGACAC		0.025	DST
539	RT-gyrB-F	45	59.2	20	CGACTTTGATCTAGCGAAAG		0.025	DST
540	RT-gyrB-R	40	58.5	20	ATAGCCTGCTTCAATTAACG		0.025	DST
541	RT-sarA-F	30.4	58.7	23	AATGATTGCTTTGAGTTGTTATC		0.025	DST
542	RT-sarA-R	42.8	58.3	21	CGCTGATGTATGTCAATACAG		0.025	DST
543	RT-agrA-F	47.3	59.1	19	TATGAGGTGCTTGAGCAAG		0.025	DST
544	RT-agrA-R	45	59	20	GTTACCAACTGGATCATGCT		0.025	DST
545	RT-sigB-F	40	59	20	CTTTGAACGGAAGTTTGAAG		0.025	DST
546	RT-sigB-R	40	59.9	20	GGCCCAATTTCTTTAATACG		0.025	DST
547	RT-saeS-F	42.1	59.7	19	TTGCAACCATATGAGCAAC		0.025	DST
548	RT-saeS-R	38	58.1	21	AATATCAATGCGACTACCAAC		0.025	DST
549	RT-sarR-F	42.1	59.3	19	GTCAACGCAACATTTCAAG		0.025	DST
550	RT-sarR-R	42.8	58.4	21	TCTGAGCACTTAGCAATCTCT		0.025	DST
553	hla_test_F	26	54.6	23	ATATGTTTATTCATGATGTTGAC		0.025	DST
554	hla_test_R	42.1	55.5	19	AGAATTGGGAGTAGGAATG		0.025	DST
569	RT-2127-F	38	58.3	21	TTCACTCGTTTCCAAGATTAC		0.025	DST
570	RT-2127-R	42.1	58.2	19	GACTTCGATCTTTCGGATT		0.025	DST
614	SSR42 BamHI-R	33.2	67	30	GGATCCAATATTTGCAACACTCTATTATCA		0.025	DST
613	SSR42 NotI-F	45.7	73.4	35	GCGGCCGCTCATGGATAGTATACCTATTATAGTTG		0.025	DST

608	SSR42 BamHI Reverse	38.2	72	34	TATGTTGGATCCTAATTACCATTTTAGCTGTGGG		0.025	DST
607	SSR42 NotI Forward	38.4	77.2	39	AAATATGCGGCCGCAATACGTAACGCTTGTTATATTTTC		0.025	DST
606	RT-RNAIII-R	40	58.7	20	TCGACACAGTGAACAAATTC		0.025	DST
605	RT-RNAIII-F	50	59.4	20	ACATAGCACTGAGTCCAAGG		0.025	DST
604	RT-lukG-reverse	40.9	58.7	22	GATTAAACCCTTCAGACACAGT		0.025	DST
603	RT-lukG-forward	39.1	59.8	23	CATGACCATACGAGACAATTAAC		0.025	DST
602	PCR3-BamHI-reverse	41.3	67.5	0	TGTCTTGGATCCTTAGCTAGGTTTAAAGC		0.025	DST
601	PCR3-NotI_forward	50	68	24	GAATAAGCGGCCGCACACTATTAC		0.025	DST
600	PCR2-FLAG-overlap-reverse	40	80.8	50	CGTCGTCATCTTTGTAGTCGATATCATGATCTTTATAATCACCGTCATGG		0.025	DST
599	PCR1-BamHI-reverse	43.4	60.2	23	GGATCCTTAGCTAGGTTTAAAGC		0.025	DST
598	PCR1-FLAG-2127- forward	33.2	79.7	57	ATCATGATATCGACTACAAAGATGACGACGATAAAACATGCCAACTTAAAATACATC		0.025	DST
597	PCR1-FLAG-reverse	38.1	79	57	CTTTATAATCACCGTCATGGTCTTTGTAGTCCATATTTCTCTCTCCTGCCTAATA		0.05	PAGE
596	PCR1-NotI-forward	61.1	64.2	18	GCGGCCGCACACTATTAC		0.05	PAGE
595	RT-hla-R	35	58	20	CAATTTGTTGAAGTCCAATG		0.025	DST
594	RT-hla-F	40.9	58.5	22	GATCCTAACAAAGCAAGTTCTC		0.025	DST
593	RT-2128-R	42.8	60.1	21	CCTTAGCAGAATGGATATTCG		0.025	DST
592	RT-2128-F	40.9	60.4	22	GTAACTCACAAGCAATTCAAGC		0.025	DST
591	RT-CHIPS-R	34.7	58.9	23	ATCAGTACACACCATCATTCAG		0.025	DST
590	RT-CHIPS-F	40.9	59	22	ATCAGTACACACCATCATTCAG		0.025	DST
579	RT-lukH-F	33.2	58.1	21	CAATTCGACTTTATCGATGAT		0.025	DST
580	RT-lukH-R	37.5	58.3	24	CTTGAAAATCTACATGGTACTCAC		0.025	DST
581	RT-scpA-F	42.8	59.4	21	TTAATGTCGAGGACAAGAGTG		0.025	DST
582	RT-scpA-R	47.6	58.6	21	GGTTCACCAAGTGTATACGAG		0.025	DST
583	RT-SSR42-F	32	60.2	25	TATCTTGTTGCTGCTAATTCTATTG		0.025	DST
584	RT-SSR42-R	32	59.4	25	CACCTAACATCAAAGAATATTCATC		0.025	DST
585	RT_2126_F	33.2	58.9	21	AATGCTTTTGATCATATGTGG		0.025	DST
586	RT_2126_R	36.2	60.1	22	TCTAATAAAGTTTGGGTGTCGA		0.025	DST
634	RT-dps-F	38	58.4	21	AATCAACAAGTAGCAAACTGG		0.025	DST
635	RT-dps-R	40.9	58.5	22	TTAATGTACCTACAGGGTTTCC		0.025	DST
636	RT-isdA- F	40.9	59.4	22	GCTACGAACGCAACTAATAATC		0.025	DST
652	RT-isdA-R-cor	38	57.7	21	GTATTCTTTCCAGAATGATGC		0.025	DST
779	RT-lukS-PV-F	40	58.9	20	GTGGCCTTTCCAATACAATA		0.025	DST
780	RT-lukS-PV-R	50	59	18	TCCTGTTGATGGACCACT		0.025	DST
781	RT-hlgA-F	36.2	58.3	22	CCTTTAGCCAATCCATTTATAG		0.025	DST
782	RT-hlgA-R	42.1	59.8	19	TGATGATTTCTGCACCTTG		0.025	DST
783	RT-hlgC-F	40.9	58.9	22	ATCTACAAACGTGAGTCAGACA		0.025	DST
784	RT-hlgC-R	47.3	60.4	19	TGATCCATTACCACCGAGT		0.025	DST

$^{\propto}$ These numbers were used for archiving and internal identification purposes, by the working group.
* Synthesis scale in µmoles.
^{o} Purification grade used after synthesis and process codes are abbreviated: DST- Desalted, HPLC- High Performance Liquid Chromatography, PAGE- Polyacrylamide gel electrophoresis separation.

Appendix C

List of reagents and media

Table C.1: Detailed list of reagents and media with their manufacturer information.

Particulars	Description/Composition	Manufacturer
Bacterial culture media and supplements		
Luria-Bertani Broth	Tryptone (10 g/l*)	Oxoid, UK
	Sodium Chloride (10 g/l)	VWR, Germany
	Bacto^{TM} Yeast extract (5 g/l)	BD, USA
50% Glucose solution	D-(+)-Glucose (500g/l) in distilled water	Sigma, USA
Tryptic Soy Broth	Tryptic Soy Broth without Dextrose (27.5 g/l)	Sigma, USA
	50% Glucose solution (0.25% v/v†)	Sigma, USA
Tryptic Soy Agar	Tryptic Soy Broth with Dextrose (30 g/l)	Sigma, USA
	European agar (15 g/l)	BD, France
Mueller Hinton Agar	Mueller Hinton Broth (23 g/l)	Sigma, USA
	European agar (15 g/l)	BD, France
B2 medium	Casein hydrolysate (10 g/l)	BD, USA
	Bacto^{TM} Yeast extract (25 g/l)	BD, USA
	Sodium Chloride (NaCl)(25 g/l)	VWR, Germany
	Dipotassium Hydrogen Phosphate (K_2HPO_4)(1 g/l)	Merck, Germany
	D-(+)-Glucose (5 g/l)	Sigma, USA
Columbia Blood Agar	BBL^{TM} Columbia Agar base	BD, USA
	Defibrinated Sheep blood (5% v/v)	Fiebig Nährstofftechnik, Germany
Nutrient Broth	Nutrient Broth powder (13 g/l) in distilled water	Oxoid, UK
Nutrient Agar	Nutrient Broth powder (13 g/l)	Oxoid, UK
	European agar (15 g/l)	BD, France
S.O.C medium		Invitrogen^{TM}, USA
Antibiotics		
Erythromycin stock solution	Erythromycin powder (10 mg/ml)	VWR, Germany

Note: Compositions are only mentioned for items that had been prepared by mixing individual components, not for Pre-mixed or ready-to-use items. *Solutes are mentioned in g/L and †solvents as % v/v, as final concentrations, with some mentioned in molarity (M)

	99% Ethanol	Sigma, USA
Chloramphenicol stock solution	Chloramphenicol powder (10 mg/ml)	Carl-Roth, Germany
	99% Ethanol	Sigma, USA
Ampicillin stock solution	Ampicillin powder (100 mg/ml) in water	Carl-Roth, Germany
Gentamicin MIC strips	Etest® MIC strips	BioMérieux, France
Tissue culture media and supplements		
RPMI full medium	RPMI 1640, Glutamax™	GIBCO®, USA
	Fetal Bovine Serum‡ (10% v/v)	GE Healthcare, UK
	Penicillin-Streptomycin (1000 U/ml & 1000 µg/ml)	GIBCO®, USA
	Sodium Pyruvate (1mM†)	GIBCO®, USA
RPMI infection medium	RPMI 1640, Glutamax™	GIBCO®, USA
	Fetal Bovine Serum‡ (10% v/v)	GE Healthcare, UK
	Sodium Pyruvate (1 mM)	GIBCO®, USA
DMEM full medium	DMEM	Sigma, USA
	Fetal Bovine Serum‡ (10% v/v)	GE Healthcare, UK
	Penicillin-Streptomycin (1000 U/ml & 1000 µg/ml)	GIBCO®, USA
Neutrophil infection medium (NIM)	1X HBSS	GIBCO®, USA
	HEPES (20 mM)	GIBCO®, USA
	Human Serum Albumin (1% v/v)	Sigma, USA
	Calcium Chloride ($CaCl_2$) (1.26 mM)	VWR, Germany
	Magnesium Chloride($MgCl_2$) (0.5 mM)	VWR, Germany
Cell-freezing medium	Fetal Bovine Serum‡(70% v/v)	GE Healthcare, UK
	RPMI full-medium (20% v/v)	
	Dimethylsulfoxide (DMSO) (10% v/v)	Carl-Roth, Germany
Opsonisation medium	Neutrophil infection medium (NIM)	
	Pooled Human Serum‡(10% v/v)	
Buffers & Solutions		
Dulbecco's Phosphate Buffer Saline (DPBS), 1X	Cell culture grade, sterile and individually bottled	GIBCO®, USA
Ficoll	Ficoll® Paque Plus, Endotoxin free, sterile	GE, UK
PVA solution	Polyvinyl alcohol (1%)	Sigma, USA
	NaCl (0.8%)	VWR, Germany
Phosphate Buffer Saline (PBS), Dulbecco's	Ready-made powder dissolved in distilled water to make 1 X (9.55 g/L) or 5X (47.75 g/L) and sterilized by autoclave.	Applichem, USA
Hank's Balanced Salt Solution (HBSS), 1X	Hank's Balanced Salt Solution (HBSS), 10X	GIBCO®, USA
	1:10 in sterile water to make 1X.	
M Sodium Hydroxide (NaOH)	Sodium Hydroxide (NaOH) pellets	VWR, Germany
	Dissolved in water at 40 grams/l and sterilized by autoclave	
Tris-HCL, pH 7.5 (for DNA)	Trizma® base (Tris)	Sigma, USA
	32% Hydrochloric acid (HCl)	Carl-Roth, Germany
	Dissolved in sterile water to make 1M solution and pH was adjusted using HCl.	
Tris-HCL, pH 8.0 (for DNA)	Trizma® base (Tris)	Sigma, USA

Note: BD stands for Becton Dickinson, abbreviated to reduce space usage. GIBCO®, Invitrogen™ are labels under the Life Technologies brand of the Thermo Fischer Scientific corporation

	32% Hydrochloric acid (HCl)	Carl-Roth, Germany
	Dissolved in sterile water to make 1M solution and pH was adjusted using HCl.	
Sucrose solution (25%)	Sucrose	Sigma, USA
	0.25 g/ml dissolved in sterile water and sterilized by autoclave.	
Tris-Sucrose buffer	Tris-HCl, pH 7.5 (10mM)	
	Sucrose solution (25%)	
Ethylenediaminetetraacetic acid (EDTA), pH 8.0 (for DNA)	Ethylenediaminetetraacetic acid (EDTA) Disodium Salt Dihydrate	Applichem, Germany
	Mixed with water to make 0.5 M solution and pH was adjusted with 1 M Sodium hydroxide to dissolve. The solution was sterilized by autoclave.	
Tris-EDTA (TE) buffer	Tris-HCl, pH 7.5 (10 mM)	
	EDTA (1 mM)	
Sodium Dodecyl Sulphate (SDS) (10%)	Sodium Dodecyl Sulphate (SDS) pellets dissolved at 0.1 g/ml in water and sterilized by autoclave	Applichem, Germany
Bacterial resuspension buffer for genomic DNA	Lysostaphin (200 µg/ml)	AMBI, USA
	Tris-HCl, pH 8.0 (20 mM)	
	EDTA (2 mM)	
	Triton X-100 (1.2% v/v)	Sigma, USA
Electroporation buffer	Sucrose (0.5M)	Carl Roth, Germany
	Glycerol (10%)	Carl Roth, Germany
Oligo-annealing buffer	100 mM Tris-HCl, pH 7.5	
	10 mM EDTA	
	500 mM NaCl	VWR, Germany
Hemalum solution	Mayer's hematoxylin solution	Carl Roth, Germany
Eosin Y solution	Eosin Y (0.5%) dissolved in water	Carl Roth, Germany
Inducers, inhibitors & fine chemicals		
Xylose solution (10%)	D-(+)-Xylose powder	Sigma, USA
	Reconstituted in water at 0.1 g/ml and used at 0.5% (v/v)	
Phytohemagglutinin solution (PHA)	Phytohemagglutinin-M(PHA) powder	Sigma, USA
	Reconstituted in water and used at 250 ng/ml.	
Enzymes, antibodies & recombinant proteins		
SYBR Green PCR enzyme mix	Master mix with AmpliTaq® Gold DNA polymerase for real time PCR	Thermo Scientific, USA
Taq DNA polymerase	DNA-directed DNA polymerase (EC 2.7.7.7) used at a concentration recommended by manufacturer	Genaxxon Bioscience, Germany
Phusion DNA polymerase	Phusion High-Fidelity DNA-directed DNA polymerase (EC 2.7.7.7) used at a concentration 1 unit per reactions	Invitrogen™, USA
Human macrophage-colony stimulating factor (M-CSF)	Recombinant protein expressed in *E. coli.* Used for stimulation of monocytes leading to differentiation, at a concentration of 100 ng/ml.	eBioscience, USA

Ambicin® L (Lysostaphin)	Metallo-endopeptidase (EC 3.4.24.75) derived from *Staphylococcus simulans* and recombinantly expressed in *E. coli*. Lyophilized powder reconstituted in sterile water and used at a concentration of 200 µg/ml.	AMBI, USA
Ribonuclease A (RNase A)	Bovine pancreatic ribonuclease (EC 3.1.27.5) for degradation of RNA. Reconstituted in sterile water and used at a concentration of 200 µg/ml.	Carl-Roth, Germany
Proteinase K	A non-specific peptidase (EC 3.4.21.64) from *Tritirachium album*, with strong proteolytic activity for degrading proteins. Reconstituted in sterile water and used at a concentration of 500 µg/ml.	Carl-Roth, Germany
Deoxyribonuclease I (DNase I)	Hyperactive DNase I (EC 3.1.21.1) for degradation of DNA. Supplied by the manufacturer in a kit (See Commercial kit section in Appendix D). Used at a concentration of 2 Kunitz units per reaction.	Ambion, USA
Mouse anti-human CD66b PE	Human monoclonal antibody (clone ID: G10F5) against surface antigen CD66b, raised in mice and conjugated with PE for flow cytometry. Stored in aqueous buffered solution containing BSA and ≤ 0.09% sodium azide.	BD, USA
Rat anti-human & mouse CD11b FITC	Human monoclonal antibody (clone ID: M1/70.15.11.5) gainst surface antigen CD11b, raised in rats and conjugated with FITC for flow cytometry. Stored in aqueous buffered solution containing BSA and ≤ 0.05% sodium azide.	Miltenyi Biotec, Germany

Appendix D

List of laboratory appliances, kits & consumables

Table D.1: Detailed list of laboratory instruments, kits and consumables used, with their manufacturer information.

Particulars	Specifications	Manufacturers
Instruments & Appliances		
Electroporation system	MicroPulser^{TM} portable electroporation apparatus, Voltage range: 0.2 - 3.0 kV	Bio-Rad, USA
Chemiluminescence imager	INTAS Cooled CCD Sensor with ChemoStar imaging software	INTAS Science Imaging Instruments GmbH, Germany
Gel imager	Biostep Dark hood DH-40/50 with Argus X1 gel documentation software v7.6	Biostep GmbH, Germany
Multimode microplate reader	TECAN Infinite M200 with i-control 1.10 reader software	TECAN, Switzerland
UV-Vis Micro spectrophotometer	NanoDrop 1000 with ND-1000 software v3.7	Thermo Scientific, USA
UV-Vis spectrophotometer	Ultraspec 2100 Pro	Amersham Biosciences(GE), UK
Ultrasonic cell disruptor, Probe type	Branson Sonifier® 250 Analog ultrasonic cell disruptor with microtip	Branson Ultrasonics, USA
Sonication device, Bath type	Bioruptur® Plus, Auto-revolving, uniform wave, bath type	Diagenode, Belgium
Bioanalyzer	2100 Bioanalyzer Instrument for on-chip electrophoresis, with 2100 Expert Software	Agilent, USA
Microcentrifuge (non-refrigerated)	Hettich MIKRO 200 centrifuge with fixed angle rotor, max. 18,000 xg	Hettich Lab tech., USA
Microcentrifuge (refrigerated)	Hitachi himac CT15RE centrifuge with fixed angle rotor, max. 21,500 xg	Hitachi-Koki, Japan
Bench centrifuge(refrigerated)	Heraeus^{TM} Megafuge^{TM} 1.0. Medium bench centrifuge with swinging bucket rotor, max. 6,240 xg	Thermo Scientific, USA
PCR Thermocycler	PEQLAB peqSTAR 96x universal gradient thermal cycler	VWR International, Germany

Flow cytometer	BD Accuri C6 flow cytometer and software v2.3 with standard optical filters	BD, USA
Real time quantitative PCR	StepOnePlus™ Real-Time PCR system operated by StepOne™ software v2.3	Thermo Scientific, USA
BSL-2 sterile hood	Herasafe™ KS (NSF) Class II, Type A2 Biological Safety cabinets	Thermo Scientific, USA
Electrophoresis power supplies	Peqlab EV202 for PAGE & CONSORT microcomputer for Agarose gels	Peqlab, Germany and Consort, Belgium
Laboratory refrigerators	Refrigerators with freezers (4°C and -20°C)	Liebherr, Germany
Ultra low temperature freezers	New Brunswick™ Innova® upright freezer U535	Eppendorf, Germany
Disposables		
Electroporation cuvettes	Sterile and disposable, Gap: 2 mm, Volume capacity: 400 µl	VWR, Germany
Centrifuge tubes	Falcon® Centrifuge Tubes (50ml, 15ml), Polypropylene, Sterile	Corning, USA
Microcentrifuge tubes	Micro tube (1.5 ml, 2 ml) with attached EASY CAP, Polypropylene	Sarstedt, Germany
Microcentrifuge tubes(RNase-free)	Sterile RNase-free Microfuge tubes (1.5 ml, 2 ml), Polypropylene	Thermo Scientific, USA
Disposable Pipettes	Sterile cell culture grade (1 ml, 5 ml, 10 ml and 25 ml), Polystyrene	Sarstedt, Germany
Cell culture T-flasks	Corning® sterile cell culture grade (T-25, T-75 and T-150), Polystyrene	Corning, USA
Phase lock tubes	Phase Lock Gel tubes, 2 ml, Sterile and disposable	5Prime, Germany
Blood collection tubes	S-monovette® with Lithium-Heparin beads, 10 ml, sterile	Sarstedt, Germany
Glasswares		
Glass bottles	Duran® graudated glass bottles (1000ml, 500ml, 250 ml, 100 ml)	DURAN Group GmbH
Erlenmeyer flasks	Duran® graudated glass flasks (1000ml, 500ml, 250 ml, 100 ml)	DURAN Group GmbH
Test tubes	5 ml capacity with metal caps	A. Hartenstein GmbH
Commercial kits		
PureLink® Quick Plasmid Miniprep kit	Kit for plasmid DNA extraction by centrifugation, used according to manufacturer's instructions	Invitrogen™, USA
QIAprep Spin Miniprep kit	Kit for plasmid DNA extraction by centrifugation, used according to manufacturer's instructions	QIAGEN, Germany
QIAGEN Plasmid Mini kit	Kit for plasmid DNA extraction by anion-exchange on gravity flow columns, used according to manufacturer's instructions	QIAGEN, Germany
TURBO DNA-*free*™ kit	DNA digestion kit consisting of DNase buffer, DNase I enzyme and DNase Inactivation reagent, used in RNA extractions according to manufacturer's instructions	Ambion, USA
TOPO® TA Cloning® kit	Kit for TOPO TA cloning, used according to manufacturer's instructions	Invitrogen™, USA

QuantiTect® Reverse Transcription Kit	Kit for conversion of RNA to cDNA, used according to manufacturer's instructions	QIAGEN, Germany
NEBNext® End repair module	Kit for end polishing staggered DNA fragments, used according to manufacturer's instructions	NEB, USA
NEBNext® dA-tailing module	Kit for incorporating non-templated dAMP on the 3′ end of a blunt DNA fragment, used according to manufacturer's instructions	NEB, USA
Agilent High Sensitivity DNA Kit	Kit for the separation, sizing and quantification of low concentrated dsDNA samples from 50-7000 bp, used according to manufacturer's instructions	Agilent, USA
Cytotoxicity detection kit^{PLUS} (LDH)	Kit for measurement of lactate dehydrogenase (LDH) activity released from the cytosol of damaged cells into the supernatant, used according to manufacturer's instructions	Roche, Switzerland
Gateway® BP® clonase kit	Kit for *in vitro* recombination of PCR products or DNA segments from clones (containing *att*B sites) and a Donor vector (containing *att*P sites) to generate Entry clones	Invitrogen^{TM}, USA
Agencourt® AMPure® XP beads	SPRI magnetic beads for purification of PCR products	Beckman Coulter GmbH, Germany

Appendix E

List of publications and presentations

Research articles

- Natural mutations in a *Staphylococcus aureus* virulence regulator attenuate cytotoxicity but permit bacteremia and abscess formation
  Sudip Das, Claudia Lindemann, B.C. Young, J. Muller, B. Österreich, N. Ternette, A.C. Winklera, K. Paprotkaa, R. Reinhardt, K.U. Förstner, E. Allen, A. Flaxman, Y. Yamaguchi, C. S. Rollier, P. Van Diemen, S. Blättner, C. W. Remmele, M. Selle, M. Dittrich, T. Müller, J. Vogel, K. Ohlsen, D. Crook, R. Massey, Daniel J. Wilson, Thomas Rudel, David H. Wyllie and Martin J. Fraunholz. *Proceedings of the National Academy of Sciences (PNAS)* 2016, *doi: 10.1073/pnas.1520255113*.

- *Staphylococcus aureus* exploits a non-ribosomal cyclic dipeptide to modulate survival within epithelial cells and phagocytes.
  Sebastian Blättner, **Sudip Das**, Kerstin Paprotka, Ursula Eilers, Markus Krischke, Dorothee Kretschmer, Christian W. Remmele, Marcus Dittrich, Tobias Mueller, Christina Schülein-Völk, Tobias Hertlein, Martin Müller, Richard Reinhardt, Knut Ohlsen, Thomas Rudel and Martin J. Fraunholz. *PLoS Pathogens* 2016, *doi: 10.1371/journal.ppat.1005857*.

Posters[†]

- A novel virulence regulator modulating cytotoxicity and immune evasion in *Staphylococcus aureus*.
  Sudip Das, Babett Österreich, Christian Remmele, Kerstin Paprotka, Sebastian Blättner, Konrad Förstner, Marcus Dittrich, Richard Reinhardt, Jörg Vogel, Knut Ohlsen, Thomas Rudel, Martin Fraunholz. EMBO | EMBL Symposium: New Approaches and Concepts in Microbiology **(2015)**

- A non-ribosomal peptide synthase is important for intracellular survival of *Staphylococcus aureus*.
  Sebastian Blättner, **Sudip Das**, Ursula Eilers, Markus Krischke, Christina Schühlein-Völk,Martin Eilers, Martin Müller, Thomas Rudel, Martin Fraunholz. EMBO | EMBL Symposium: New Approaches and Concepts in Microbiology **(2015)**

- *Simkania* infection interfaces with host ER, mitochondria and trafficking pathway to form the *Simkania*-contaning vacoule.
  Jo-Ana Herweg, Vera-Kozjak-Pavlovic, Christina Miller, Suvagata Roy Chowdhury, **Sudip Das**, Adrian Mehlitz and Thomas Rudel*. SPP1580 National Meeting, Bonn, Germany **(2015)**.

- Transposon insertion site deep sequencing identifies a novel virulence regulator in *Staphylococcus aureus*.
  Sudip Das, Babett Österreich, Kerstin Paprotka, Ann-Cathrin Winkler, Konrad Förstner, Bruno Huettel, Richard Reinhardt, Jörg Vogel, Knut Ohlsen,Thomas Rudel and Martin Fraunholz*. 3rd Mol Micro Meeting, IMIB, University of Wuerzburg, Germany **(2014)**

- Identification of *Staphylococcus aureus* virulence factors mediating phagosomal escape in cystic fibrosis cells.
  Ashley Norris, **Sudip Das**, Martin Fraunholz*. Eureka!, 9th International GSLS Symposium, Rudolf-Virchow-Center, University of Wuerzburg, Germany **(2014)**

- Himar-transposon mutant library for genome-wide identification of virulence factors in *Staphylococcus aureus* by means of deep sequencing.
  Sudip Das, Martin Fraunholz, Christian Remmele, Bruno Huettel, Richard Reinhardt and Thomas Rudel*. 2nd International conference on Pathophysiology of Staphylococci in the post-genomic era by German Research Association, Kloster Banz, Germany **(2012)**.

- Investigating the role of Reactive Oxygen Species (ROS) produced by phagocytic NADPH oxidase against *Salmonella Typhimurium*
  Sudip Das, Pascal Songhet, Wolf-Dietrich Hardt and Mrutyunjay Suar*. International Conference on Cell Signaling and Diseases, KIIT University, India **(2010)**.

Oral presentations

- From colonizer to invader: Redirection of *Staphylococcus aureus* infection by mutation in a transcriptional regulator. Biocenter Science Award, University of Wuerzburg, Germany (**2016**).

- Assessing staphylococcal intracellular virulence by genome-wide strategies. PhD meeting, DFG Transregional Collaborative Research Centre 34, Wuerzburg, Germany **(2015)**

- Identification and evaluation of staphylococcal factors supporting host cell death. 1st Annual meeting on the Pathophysiology of Staphylococci in the post-genomic era (SFB TRR34), Muenster, Germany **(2011)**.

†Full name is shown in **bold**, wherever contributed and underline denotes presenting author, *corresponding author

Appendix F

Curriculum Vitae

Sudip Das

B.Sc.(Hons), M.Sc.

Personal details

E-mail	sudip.das@uni-wuerzburg.de
Date of Birth	04.06.1987
Nationality	Indian

Research experience

- **Doctoral Researcher (2011 - Present)**
  Chair of Microbiology, Biocenter, Julius-Maxmilians University of Wuerzburg, Germany
  Advisor: Prof. Dr. Thomas Rudel.

  Major tasks: Development of screening strategies using bacterial mutant libraries for the investigation of staphylococcal factors, associated with intracellular virulence and cytotoxicity in mice and human cells. Global analysis of pathogen behavior in host by Transposon-insertion site deep sequencing (Tn-seq).

- **Research Trainee (2010)**
  Institute of Microbiology, Eidgenoessische Technische Hochschule (ETH), 8093 Zuerich, Switzerland.
  Advisor: Prof. Dr. Wolf-Dietrich Hardt.

  Major tasks: Validation of mutants identified from transposon-mediated differential hybridisation (TMDH) experiments, with *Salmonella* Typhimurium. Examination of attenuated bacterial mutants aimed at developing a safe oral vaccine carrier in an immune-compromised murine model of enterocolitis.

Education

- **Doctor of Philosophy (2011 – Present)** in Molecular infection biology. University of Wuerzburg, Germany.

- **Master of Science (2008 – 2010)**, Major: Biotechnology, School of Biotechnology, KIIT University, Orissa, India.
- **Bachelor of Science (Honours) (2005 – 2008)**, Major: Biotechnology and Chemistry, Utkal University, Bhubaneswar, India.
- **Higher Secondary School (2003-2005)**, Major: Science, Stewart School, Bhubaneswar, India.
- **Primary & High school (up to 2003)**, Indian Certificate of Secondary Education, Julien Day School, Kolkata, India

---

Awards and Scholarships

- Biocenter Science Award from Biocenter, University of Wuerzburg, Germany **(2016)**.
- Career Development Fellowship for short-term postdoctoral research from the Graduate School of Life Sciences, University of Wuerzburg, Germany **(2016)**.
- Paper of the Month - June 2016, German Society for Hygiene and Microbiology, Germany **(2016)**.
- Deutscher Akademischer Austauschdienst (DAAD)-Stipendien- und Betreuungsprogramme (STIBET) fellowship for completion of doctoral thesis, Germany **(2016)**.
- Research fellowship from the Swiss Academy of Sciences, Commission for Research Partnerships with Developing Countries-KFPE for Master's thesis, Switzerland **(2010)**.
- A+ grade and Honors with Bachelors degree in Biotechnology, India **(2008)**.

Skills & Expertise

- Standard microbiological practices with BSL-1 & -2 bacteria.
- Generation of transposon mutant libraries of bacteria and genome-wide screens *in vitro* and *in vivo*.
- Next generation sequencing technologies - Tn-Seq, RNA-seq, illumina platform-based library preparation protocols.
- Cell-based assays including infection protocols, flow cytometry and fluorescence microscopy.
- Handling animal experiments with murine models- Mouse enteric infection and pneumonia model.
- Human and murine *ex vivo* cell culture and infections – Whole blood, monocytes and granulocytes.
- Statistical analysis with R, programming with C, Data structure, RDBMS (MySQL Server), PERL.
- Documentation with LaTeX package.

Certifications

- Animal experiments under FELASA, Category B, EU, University of Wuerzburg, Germany.
- German language from Language center, University of Wuerzburg, Germany
- Industry certified GxP by Aeterna Zentaris GmbH, University of Wuerzburg, Germany.
- Rules of good scientific practice from the University of Wuerzburg, Germany.
- Desktop publishing with LaTeX documentation package from the University of Wuerzburg, Germany
- R statistical program from the University of Wuerzburg, Germany.

Teaching experience

- Supervision of Master F1 research practical of Mr. Benjamin Orlando Torres Salazar, University of Wuerzburg, Germany **(2014)**.
- Co-supervision of Bachelor research thesis of Ms. Linda Raupach, University of Wuerzburg, Germany **(2014)**.
- Teaching Assistant for Advance Microbiology practical course for 5th Semester, Bachelor of Science, University of Wuerzburg, Germany **(2012-2015)**.
- Teaching Assistant for Basic Microbiology practical course for 1st Semester, Bachelor of Science, University of Wuerzburg, Germany **(2011-2014)**.

Languages

- English - Bilingual proficiency.
- Hindi - Bilingual proficiency.
- Bangla - Bilingual proficiency.
- German – Elementary proficiency.

Date:

Place: Würzburg Signature

Appendix G

Transposon insertion-site deep sequencing data tables

Table G.1: Detailed table of gene-wise analysis of *S. aureus* 6850 tranposon mutant library from HeLa cell non-cytotoxicity screening, performed using DESeq2.

Locus	Trend	*P*	adj.*P*	Gene	R1I	R1O1	R1O2	R1O3	R2I	R2O1	R2O2	R2O3
RSAU_003007	Increase	0.0000	0.0000	ssr42	3310	5057	24061	262004	915	5665	14927	84727
RSAU_000335	Decrease	0.0000	0.0002	guaA	9842	2424	122	97	16160	749	131	487
RSAU_002217	Increase	0.0000	0.0003	rsp	84894	331588	687597	3169492	40687	322288	284554	699681
RSAU_000220	Decrease	0.0000	0.0003	NA	149	16	6	0	61	166	23	7
RSAU_000333	Decrease	0.0000	0.0003	pbuX	152	22	1	0	211	95	90	13
RSAU_000958	Decrease	0.0000	0.0003	purM	40	5	1	0	28	4	0	0
RSAU_001920	Decrease	0.0003	0.0008	NA	42	3	1	0	55	13	0	2
RSAU_002160	Decrease	0.0003	0.0008	NA	18	0	0	0	26	16	0	0
RSAU_000433	Decrease	0.0005	0.0012	purR	67	49	16	0	46	0	3	0
RSAU_001914	Decrease	0.0009	0.0018	NA	18	34	2	0	11	0	0	0
RSAU_001097	Decrease	0.0016	0.0029	def2	24	33	0	2	27	19	0	0
RSAU_000132	Decrease	0.0022	0.0035	NA	100	29	1	0	47	54	14	20
RSAU_000181	Decrease	0.0024	0.0035	NA	42	2	5	0	52	9	15	0
RSAU_002215	Decrease	0.0025	0.0035	scrA	32	37	1	0	14	50	34	2
RSAU_001963	Decrease	0.0026	0.0035	fbaA	29	32	1	0	12	26	0	2
RSAU_000266	Increase	0.0029	0.0036	geh	0	1	7	9	1	0	14	9
RSAU_001503	Increase	0.0038	0.0044	ruvA	10	6	21	104	5	3	6	54
RSAU_002327	Decrease	0.0042	0.0046	NA	21	6	0	0	5	20	6	0
RSAU_001526	Increase	0.0047	0.0049	hemL	0	1	1	2	0	0	3	42
RSAU_000901	Decrease	0.0064	0.0064	ltaA	961	775	546	281	809	736	174	123
RSAU_000062	Increase	0.0069	0.0065	NA	0	1	2	7	0	3	13	7
RSAU_000531	Decrease	0.0080	0.0070	thiD1	6	1	0	0	7	33	7	0
RSAU_002292	Increase	0.0080	0.0070	NA	0	0	0	22	1	0	1	11
RSAU_002389	Decrease	0.0085	0.0070	clpL	18	13	0	0	48	3	3	4
RSAU_001996	Decrease	0.0092	0.0073	fmtB	181	69	20	7	91	113	139	49
RSAU_002369	Decrease	0.0099	0.0074	srtA	13	16	1	0	3	0	0	0
RSAU_002083	Increase	0.0101	0.0074	rplB	0	0	6	22	1	0	0	7
RSAU_000942	Increase	0.0108	0.0077	NA	17	102	90	574	7	53	44	9
RSAU_001895	Decrease	0.0133	0.0090	21	6	0	0	7	13	3	2	
RSAU_001696	Decrease	0.0136	0.0090	ecsA	135	39	0	2	40	143	66	60
RSAU_001068	Decrease	0.0153	0.0098	NA	17	7	5	0	7	1	0	0
RSAU_002179	Decrease	0.0164	0.1021	gltS	35	62	20	0	22	37	20	4
RSAU_001747	Increase	0.0171	0.1033	NA	0	0	3	0	2	1	42	9
RSAU_001393	Increase	0.0193	0.1130	accC1	0	0	3	4	2	1	23	7
RSAU_000072	Decrease	0.0204	0.1163	sbnC	26	1	4	0	6	1	0	0
RSAU_001052	Decrease	0.0246	0.1360	NA	52	114	19	7	24	19	20	4
RSAU_001501	Increase	0.0294	0.1584	queA	0	0	2	4	12	1	25	60
RSAU_001540	Increase	0.0315	0.1613	lysP	0	2	2	4	2	1	16	18
RSAU_002463	Decrease	0.0316	0.1613	NA	9	6	0	0	0	37	8	2
RSAU_002449	Decrease	0.0359	0.1757	NA	27	0	2	0	21	0	3	2
RSAU_001335	Decrease	0.0370	0.1757	NA	27	8	0	2	2	6	0	0
RSAU_002539	Increase	0.0376	0.1757	cna	1	1	9	7	3	0	22	9
RSAU_000065	Increase	0.0379	0.1757	spa	0	2	9	4	1	1	16	0
RSAU_002341	Increase	0.0433	0.1959	fnbA	3	1	14	22	7	1	32	16
RSAU_001094	Increase	0.0462	0.2027	priA	0	0	2	2	3	4	30	4
RSAU_000106	Increase	0.0468	0.2027	capD	1	1	2	4	4	4	14	47
RSAU_002264	Decrease	0.0495	0.2099	bioB	15	17	1	0	8	9	34	0

Table G.2: Detailed table of by-site analysis of *S. aureus* 6850 tranposon mutant library from HeLa cell non-cytotoxicity screening, performed using DESeq2.

Position	base mean	log2FC	*P*	adj. *P*	strand	gene	Locus
17600	1.98	-2.91	0.0043	0.0418	+		RSAU_000013
27102	0.76	-0.83	0.4324	0.6507	+	yycH	RSAU_000022
27487	11.55	-1.61	0.0069	0.0528	+	yycH	RSAU_000022
31612	0.93	-2.05	0.0377	0.1511	+	sasH	RSAU_000025
32205	16.31	-0.07	0.9112	0.9712	+	sasH	RSAU_000025
32832	0.95	0.08	0.937	0.9838	+	sasH	RSAU_000025
33893	0.23	0.47	0.6603	0.8407	+		RSAU_000028
33894	0.88	-0.26	0.7739	0.9017	+		RSAU_000028
37126	5.32	-0.6	0.2156	0.4184	+	putative transposase	RSAU_000032
37364	1.76	-1.92	0.0287	0.1255	+	putative transposase	RSAU_000032
37838.0	6.82	-1.58	0.0077	0.0559	+	putative transposase	RSAU_000034
38529.0	0.24	-0.42	0.6897	0.8485	+	putative transposase	RSAU_000035
39369.0	2.2	-3.04	0.0028	0.0303	-	dus	RSAU_000036
46330.0	0.38	0.0	0.9997	0.9997	+		RSAU_000043
52368.0	1.12	-0.73	0.3981	0.6158	+	plc	RSAU_000049
64625.0	0.27	-1.47	0.1672	0.3477	-		RSAU_000061
65123.0	3.58	-0.89	0.0582	0.1974	-		RSAU_000061
73809.0	2.8	-3.25	0.0013	0.0171	-	sirC	RSAU_000067
79411.0	7.2	-4.08	0.0	9.0E-4	+	sbnC	RSAU_000072
81165.0	164.38	0.19	0.6649	0.8442	+	sbnC	RSAU_000073
85247.0	0.31	-0.97	0.3602	0.5792	+		RSAU_000076
86522.0	3.1	-3.2	0.0015	0.0196	+		RSAU_000077
91109.0	3.46	-1.76	0.0596	0.201	+		RSAU_000082
93697.0	0.47	-0.79	0.4599	0.6675	+	capH2	RSAU_000085
94424.0	3.18	-1.2	0.1151	0.2945	+	capH2	RSAU_000085
106208.0	0.74	-2.1	0.0459	0.1711	-		RSAU_000097
109446.0	6.16	0.05	0.9492	0.9838	+	cpdB	RSAU_000099
110032.0	2.11	-2.32	0.0090	0.062	+	cpdB	RSAU_000099
112823.0	1.0	-0.33	0.6579	0.8407	+	adhE	RSAU_000102
118097.0	0.45	-0.17	0.8733	0.9538	+	capD	RSAU_000106
118997.0	0.82	0.46	0.5061	0.7134	+	capD	RSAU_000106
119055.0	0.47	-0.79	0.4599	0.6675	+	capD	RSAU_000106
119260.0	0.34	-0.34	0.7181	0.8672	+	capD	RSAU_000106
128205.0	5.05	-3.81	1.0E-4	0.0030	+	capL	RSAU_000114
133831.0	0.98	-0.1	0.8993	0.9689	+	aldA1	RSAU_000121
134575.0	8.26	-1.01	0.1045	0.2785	+	aldA1	RSAU_000121
139928.0	0.47	-0.79	0.4599	0.6675	+		RSAU_000127
143463.0	0.35	-1.66	0.1197	0.2945	+		RSAU_000129
149611.0	15.96	-1.94	4.0E-4	0.0068	+		RSAU_000130
152321.0	47.95	-1.64	0.0013	0.0172	-		RSAU_000132
154295.0	37.74	-0.98	0.1616	0.3477	-	argJ	RSAU_000134
159078.0	0.24	-0.42	0.6897	0.8485	-		RSAU_000138
159767.0	6.67	-1.57	0.0079	0.0566	-		RSAU_000138
160237.0	1.99	-1.87	0.0178	0.0945	-		RSAU_000138
160475.0	5.14	-0.56	0.2497	0.457	-		RSAU_000138
160526.0	2.54	-2.01	0.0204	0.1036	-		RSAU_000138
164639.0	2.23	-2.95	0.0039	0.0392	-	glcA	RSAU_000140
165013.0	1.42	0.01	0.983	0.9907	-	glcA	RSAU_000140
165014.0	380.21	0.02	0.9527	0.9838	-	glcA	RSAU_000140
165015.0	1.68	0.4	0.5519	0.7623	-	glcA	RSAU_000140
172283.0	2.09	-1.51	0.1389	0.3286	+	hsdR	RSAU_000147
183849.0	0.27	-1.47	0.1672	0.3477	-		RSAU_000154
188492.0	1.63	-1.58	0.087	0.2529	+		RSAU_000158
191384.0	0.38	-1.42	0.1554	0.3477	+		RSAU_000161
197103.0	1.01	-1.21	0.1901	0.3831	-		RSAU_000167
206378.0	16.51	-0.41	0.512	0.7193	-		RSAU_000174
206379.0	11.74	-0.86	0.1367	0.3265	-		RSAU_000174
209575.0	0.99	0.26	0.8064	0.9159	-	fadA	RSAU_000176
210527.0	0.53	0.66	0.5342	0.7427	-	fadA	RSAU_000176
211350.0	1.04	-0.43	0.6895	0.8485	-	fadB	RSAU_000177
215508.0	0.96	1.23	0.2325	0.4377	-	fadE	RSAU_000179
218017.0	25.05	-2.37	4.0E-4	0.0068	+		RSAU_000181
222818.0	2.09	0.62	0.4503	0.6675	-		RSAU_000185
222819.0	0.29	1.1	0.2986	0.5152	-		RSAU_000185
231826.0	0.59	-0.54	0.5697	0.774	+	gatC2	RSAU_000192
236267.0	0.67	-1.97	0.0627	0.2048	+		RSAU_000196
236314.0	0.55	-1.92	0.07	0.2176	+		RSAU_000196
237582.0	4.0	-2.78	3.0E-4	0.0057	+		RSAU_000197
244221.0	1.34	-1.74	0.0962	0.2616	+		RSAU_000202
246259.0	3.36	-3.39	7.0E-4	0.0111	+		RSAU_000203
246394.0	1.03	-1.97	0.0358	0.1445	+		RSAU_000203
247549.0	1.43	0.19	0.7979	0.9159	-		RSAU_000204
250851.0	1.63	-1.07	0.1625	0.3477	+	lytS	RSAU_000207
258828.0	1.02	1.43	0.0861	0.2518	-	rbsK	RSAU_000215
258926.0	111.35	-0.05	0.7522	0.8921	-	rbsK	RSAU_000215
258927.0	67.52	0.01	0.9473	0.9838	-	rbsK	RSAU_000215
258928.0	2.94	-0.02	0.9621	0.9854	-	rbsK	RSAU_000215
263873.0	0.41	-0.97	0.3571	0.5792	-		RSAU_000220
263874.0	68.05	-2.55	0.0	1.0E-4	-		RSAU_000220
265654.0	1.11	-0.34	0.7064	0.8581	+	lytM	RSAU_000222
268854.0	4.4	-3.68	2.0E-4	0.0049	-		RSAU_000225

273461.0	0.46	-0.57	0.5459	0.756	+	esaA	RSAU_000229
275073.0	1.08	-0.43	0.5758	0.7789	+	esaA	RSAU_000229
278780.0	1.02	-1.33	0.1484	0.3465	+	essC	RSAU_000233
281530.0	0.82	-0.31	0.7728	0.9015	+	essC	RSAU_000233
282101.0	2.41	-0.59	0.5213	0.7285	+	essC	RSAU_000233
294446.0	0.42	-1.79	0.0912	0.2559	-		RSAU_000251
295562.0	0.44	0.31	0.7721	0.9015	-	brnQ	RSAU_000252
295901.0	0.47	-1.77	0.0961	0.2616	-	brnQ	RSAU_000252
297515.0	0.2	-0.78	0.465	0.6675	+		RSAU_000253
302760.0	4.63	-0.56	0.1259	0.305	+		RSAU_000257
307908.0	0.27	-1.47	0.1672	0.3477	+		RSAU_000262
307960.0	0.68	0.16	0.8789	0.9538	+		RSAU_000262
313014.0	0.26	0.05	0.9597	0.9838	+	geh	RSAU_000266
316080.0	0.2	-0.78	0.465	0.6675	-		RSAU_000268
319558.0	0.43	-0.79	0.4027	0.6201	+		RSAU_000272
319677.0	2.16	-2.89	0.0046	0.0428	+		RSAU_000272
325334.0	0.94	-2.24	0.0322	0.1358	-		RSAU_000278
329985.0	0.42	-1.79	0.0912	0.2559	-	glpT	RSAU_000282
333288.0	0.23	-0.16	0.8808	0.9538	+		RSAU_000285
369648.0	0.27	-0.52	0.6268	0.8237	-	ahpF	RSAU_000323
369938.0	2.37	-0.19	0.7008	0.8546	-	ahpF	RSAU_000323
372158.0	0.3	0.26	0.8096	0.9159	+		RSAU_000325
379470.0	0.58	-0.52	0.5679	0.774	+	pbuX	RSAU_000333
379471.0	109.62	-2.14	1.0E-4	0.0023	+	pbuX	RSAU_000333
379472.0	0.73	-0.37	0.6843	0.8485	+	pbuX	RSAU_000333
381527.0	4.77	-3.43	3.0E-4	0.0057	+	guaA	RSAU_000335
381548.0	5.72	-1.63	0.0348	0.1433	+	guaA	RSAU_000335
381572.0	0.7	-2.13	0.0431	0.1648	+	guaA	RSAU_000335
381579.0	0.27	-0.52	0.6268	0.8237	+	guaA	RSAU_000335
382063.0	1.38	-2.06	0.0192	0.1008	+	guaA	RSAU_000335
382064.0	251.65	-2.18	0.0	0.0011	+	guaA	RSAU_000335
382065.0	0.5	-1.9	0.072	0.2176	+	guaA	RSAU_000335
382084.0	1.4	-2.65	0.0101	0.0683	+	guaA	RSAU_000335
382692.0	22.28	-3.35	0.0	3.0E-4	+	guaA	RSAU_000335
382693.0	6372.68	-2.34	0.0	0.0	+	guaA	RSAU_000335
382694.0	58.06	-3.65	0.0	0.0	+	guaA	RSAU_000335
386984.0	2.9	-2.72	0.0025	0.0286	-		RSAU_000340
392010.0	6.14	-1.6	0.0064	0.0502	-		RSAU_000347
392484.0	1.76	-1.92	0.0287	0.1255	-		RSAU_000349
392722.0	5.14	-0.56	0.2497	0.457	-		RSAU_000349
415957.0	2.99	-0.86	0.2006	0.3997	+		RSAU_000371
417511.0	0.61	-0.34	0.715	0.8665	+		RSAU_000373
431831.0	1.05	-2.43	0.0196	0.1012	+		RSAU_000390
433015.0	1.23	-2.56	0.0135	0.0799	+		RSAU_000391
433026.0	21.06	-1.14	0.0051	0.0442	+		RSAU_000391
433164.0	10.44	-0.57	0.3835	0.5993	+		RSAU_000391
435928.0	0.83	-0.25	0.8173	0.918	+	cysM	RSAU_000393
445107.0	0.27	-1.47	0.1672	0.3477	-	gltC	RSAU_000404
464136.0	25.68	-0.19	0.6723	0.8478	+		RSAU_000416
471665.0	2.7	-0.95	0.2083	0.4104	+		RSAU_000424
477203.0	0.64	-0.11	0.8844	0.9557	+	ksgA	RSAU_000430
479732.0	5.9	-1.95	0.0043	0.0418	+	purR	RSAU_000433
479863.0	29.53	-2.43	1.0E-4	0.0017	+	purR	RSAU_000433
479864.0	0.31	-0.97	0.3602	0.5792	+	purR	RSAU_000433
487303.0	0.34	0.29	0.7632	0.8976	+	mfd	RSAU_000442
488484.0	1.15	-0.55	0.4669	0.6685	+	mfd	RSAU_000442
488672.0	1.02	-0.04	0.9562	0.9838	+	mfd	RSAU_000442
488673.0	184.23	-0.27	0.537	0.7456	+	mfd	RSAU_000442
488674.0	0.7	0.32	0.7301	0.8778	+	mfd	RSAU_000442
489417.0	0.68	-1.83	0.0623	0.2048	+	mfd	RSAU_000442
495336.0	1.21	0.96	0.2033	0.4028	+	hpt	RSAU_000449
498902.0	0.31	-0.97	0.3602	0.5792	+	hslO	RSAU_000451
508846.0	25.44	-0.18	0.7002	0.8546	+		RSAU_000467
509183.0	0.29	1.1	0.2986	0.5152	+		RSAU_000467
519523.0	0.58	-2.0	0.0582	0.1974	+	clpC	RSAU_000476
533868.0	0.23	-0.16	0.8808	0.9538	+		RSAU_000493
551286.0	1.8	-1.94	0.015	0.0855	+	araB	RSAU_000504
564062.0	0.69	0.56	0.4749	0.678	+	sdrD	RSAU_000515
564625.0	0.32	-0.12	0.9136	0.9712	+	sdrD	RSAU_000515
565436.0	0.85	-2.28	0.0292	0.1258	+	sdrD	RSAU_000515
570831.0	0.3	0.48	0.6526	0.8407	+	sdrE	RSAU_000517
579162.0	1.23	-1.52	0.1014	0.2715	+		RSAU_000526
586351.0	6.55	-1.78	0.0023	0.0267	-	thiD1	RSAU_000531
588803.0	0.55	0.21	0.8419	0.9385	+		RSAU_000535
592289.0	0.26	0.05	0.9597	0.9838	-		RSAU_000539
599327.0	2.03	-2.96	0.0036	0.0381	-		RSAU_000546
602052.0	3.73	-0.93	0.1907	0.3836	+		RSAU_000548
605325.0	1.79	-0.22	0.7635	0.8976	+		RSAU_000552
612088.0	0.89	-1.48	0.1119	0.2916	+		RSAU_000561
612092.0	0.27	0.94	0.3764	0.5918	+		RSAU_000561
621938.0	0.55	0.22	0.7536	0.8928	+		RSAU_000571
621939.0	215.91	-0.06	0.7189	0.8673	+		RSAU_000571
621940.0	1.61	0.14	0.8116	0.9159	+		RSAU_000571
622026.0	2.97	-2.52	0.0085	0.059	+		RSAU_000571
622226.0	0.27	-1.47	0.1672	0.3477	+		RSAU_000571
623143.0	0.38	0.58	0.583	0.7818	+		RSAU_000572
628050.0	3.84	-1.83	0.0397	0.1566	+	mnhA1	RSAU_000578

629095.0	1.16	-1.13	0.2785	0.4917	+	mnhA1	RSAU_000578
635066.0	0.95	-2.34	0.0249	0.1151	+		RSAU_000585
635970.0	63.92	-0.32	0.2248	0.4316	-	rsaC	RSAU_000586
635971.0	0.31	-0.93	0.3387	0.5643	-	rsaC	RSAU_000586
658762.0	0.7	-2.13	0.0431	0.1648	+		RSAU_000609
658849.0	5.21	-1.13	0.0261	0.1194	+		RSAU_000609
660491.0	0.59	-0.54	0.5697	0.774	+		RSAU_000611
665956.0	0.97	-2.36	0.0235	0.1112	+		RSAU_000616
669868.0	2.09	-2.89	0.0046	0.0428	+		RSAU_000621
669996.0	2.57	-1.97	0.0235	0.1112	+		RSAU_000621
670047.0	5.14	-0.56	0.2497	0.457	+		RSAU_000621
670285.0	3.14	-1.96	0.013	0.0787	+		RSAU_000621
670755.0	7.04	-1.6	0.0074	0.0549	+		RSAU_000621
671444.0	0.24	-0.42	0.6897	0.8485	+		RSAU_000621
694194.0	1.85	-1.58	0.0869	0.2529	+		RSAU_000642
699387.0	0.68	0.16	0.8789	0.9538	+		RSAU_000647
700736.0	2.97	0.02	0.9823	0.9907	+		RSAU_000648
702481.0	0.96	0.14	0.863	0.9538	+		RSAU_000650
702743.0	15.54	-0.45	0.4559	0.6675	+		RSAU_000650
704313.0	2.98	-0.37	0.6749	0.8485	+		RSAU_000653
708533.0	2.04	-2.71	0.0047	0.0434	-	uppP	RSAU_000659
709492.0	12.9	0.05	0.9284	0.982	+		RSAU_000660
712604.0	2.21	-1.17	0.0697	0.2176	-	mgrA	RSAU_000662
723843.0	0.88	-1.56	0.1371	0.3265	+	fruB	RSAU_000674
724172.0	0.27	-1.47	0.1672	0.3477	+	fruB	RSAU_000674
724189.0	0.65	-2.08	0.048	0.1732	+	fruB	RSAU_000674
724193.0	0.27	-1.47	0.1672	0.3477	+	fruB	RSAU_000674
738831.0	1.97	-2.95	0.0039	0.0392	+	pabB	RSAU_000689
745476.0	0.54	-0.59	0.5828	0.7818	+		RSAU_000694
751039.0	0.63	0.48	0.618	0.8173	+		RSAU_000697
753400.0	0.81	-1.57	0.0936	0.2616	+		RSAU_000699
754746.0	0.73	-0.37	0.6843	0.8485	-		RSAU_000700
755741.0	2.01	-2.86	0.0050	0.0442	+		RSAU_000701
755869.0	2.57	-1.97	0.0235	0.1112	+		RSAU_000701
755920.0	5.34	-0.57	0.2584	0.4666	+		RSAU_000701
756158.0	3.06	-1.94	0.0143	0.0821	+		RSAU_000701
756628.0	7.24	-1.62	0.0065	0.0507	+		RSAU_000701
757317.0	0.24	-0.42	0.6897	0.8485	+		RSAU_000701
763671.0	0.53	0.09	0.9301	0.982	+	nrdE	RSAU_000706
767624.0	0.58	-0.52	0.5679	0.774	+		RSAU_000710
773930.0	0.87	-2.12	0.0439	0.1652	+	glxK	RSAU_000717
774023.0	1.59	-1.12	0.2784	0.4917	+	glxK	RSAU_000717
778095.0	2.01	-2.78	0.0035	0.0378	-		RSAU_000721
778205.0	0.37	-0.5	0.6393	0.8334	-		RSAU_000721
783157.0	0.27	-1.47	0.1672	0.3477	+	comFA	RSAU_000725
792508.0	0.72	-1.73	0.0654	0.2123	+	uvrB	RSAU_000733
793666.0	3.28	-3.37	8.0E-4	0.0116	+	uvrA	RSAU_000734
794056.0	3.28	-1.77	0.045	0.1683	+	uvrA	RSAU_000734
794666.0	0.27	-1.47	0.1672	0.3477	+	uvrA	RSAU_000734
808707.0	3.15	0.05	0.9439	0.9838	-		RSAU_000746
808708.0	429.29	-0.22	0.7063	0.8581	-		RSAU_000746
820120.0	0.2	-0.06	0.9554	0.9838	+	est	RSAU_000757
825481.0	1.88	-0.14	0.8638	0.9538	-		RSAU_000761
833985.0	0.31	-0.97	0.3602	0.5792	+	emp	RSAU_000767
848926.0	0.68	-1.95	0.0462	0.1717	+		RSAU_000787
854796.0	0.23	-0.16	0.8808	0.9538	+	sufD	RSAU_000793
862365.0	2.53	-0.28	0.6971	0.8541	+		RSAU_000800
863721.0	0.47	-1.77	0.0961	0.2616	+		RSAU_000801
867543.0	0.42	-1.79	0.0912	0.2559	+		RSAU_000806
868043.0	3.43	-2.28	0.0036	0.0381	+	gD	RSAU_000807
875953.0	0.7	-1.39	0.1889	0.3821	-		RSAU_000815
881048.0	0.87	-2.12	0.0439	0.1652	+		RSAU_000820
918922.0	0.85	-1.95	0.0482	0.1736	+	clpB	RSAU_000851
921653.0	0.65	-0.53	0.5022	0.7113	-		RSAU_000852
921654.0	55.29	-0.55	0.0011	0.0154	-		RSAU_000852
921655.0	10687.17	-0.77	0.0	0.0	-		RSAU_000852
921656.0	43.77	-0.43	0.062	0.2048	-		RSAU_000852
921722.0	0.48	-0.87	0.3015	0.5178	-		RSAU_000852
936927.0	1.56	-2.68	0.0092	0.0627	+	oppA2	RSAU_000865
940241.0	0.86	0.51	0.4438	0.6628	+	oppB2	RSAU_000868
941617.0	0.3	0.26	0.8096	0.9159	+		RSAU_000870
947346.0	3.12	-1.23	0.1838	0.3738	+		RSAU_000876
966349.0	5.35	-0.59	0.2192	0.4235	+		RSAU_000896
966587.0	1.76	-1.92	0.0287	0.1255	+		RSAU_000896
967061.0	6.14	-1.6	0.0064	0.0502	+		RSAU_000898
967765.0	0.56	-1.01	0.2258	0.4327	+		RSAU_000900
968101.0	0.47	-1.77	0.0961	0.2616	-	ltaA	RSAU_000901
968212.0	0.73	-2.15	0.0401	0.1571	-	ltaA	RSAU_000901
968241.0	97.5	-0.61	0.1011	0.2715	-	ltaA	RSAU_000901
968242.0	0.58	-0.89	0.2352	0.4407	-	ltaA	RSAU_000901
968303.0	2.9	-2.09	0.0297	0.1273	-	ltaA	RSAU_000901
968305.0	12.2	-1.07	0.0017	0.0207	-	ltaA	RSAU_000901
968340.0	2.13	-1.26	0.0197	0.1012	-	ltaA	RSAU_000901
968341.0	532.11	-1.6	0.0	0.0	-	ltaA	RSAU_000901
968342.0	3.81	-0.85	0.0506	0.1796	-	ltaA	RSAU_000901
968470.0	3.3	-1.66	0.0206	0.1036	-	ltaA	RSAU_000901
968484.0	1.47	-1.13	0.066	0.2129	-	ltaA	RSAU_000901

968502.0	0.47	-1.77	0.0961	0.2616	-	ltaA	RSAU_000901
968571.0	0.27	-1.47	0.1672	0.3477	-	ltaA	RSAU_000901
968588.0	3.31	-1.69	0.0325	0.1359	-	ltaA	RSAU_000901
968626.0	1.48	-0.04	0.9543	0.9838	-	ltaA	RSAU_000901
968672.0	5.17	-0.67	0.3516	0.5792	-	ltaA	RSAU_000901
968711.0	5.67	-3.27	3.0E-4	0.0057	-	ltaA	RSAU_000901
968717.0	1.57	-0.94	0.2358	0.4407	-	ltaA	RSAU_000901
968912.0	0.98	-0.39	0.6938	0.8515	-	ltaA	RSAU_000901
968930.0	4.77	-0.06	0.9215	0.9759	-	ltaA	RSAU_000901
968940.0	0.86	-1.16	0.2143	0.418	-	ltaA	RSAU_000901
968947.0	9.14	-0.65	0.1427	0.3353	-	ltaA	RSAU_000901
969043.0	29.12	-0.93	0.0066	0.0514	-	ugtP	RSAU_000902
969044.0	0.28	0.04	0.9679	0.9865	-	ugtP	RSAU_000902
969128.0	0.27	-1.47	0.1672	0.3477	-	ugtP	RSAU_000902
969195.0	1.95	-1.26	0.0783	0.2319	-	ugtP	RSAU_000902
969412.0	0.54	-0.6	0.519	0.7263	-	ugtP	RSAU_000902
969522.0	28.96	-0.58	0.1179	0.2945	-	ugtP	RSAU_000902
969582.0	0.63	-0.95	0.3651	0.5808	-	ugtP	RSAU_000902
969636.0	2.5	-0.46	0.4158	0.6376	-	ugtP	RSAU_000902
969706.0	0.32	-0.02	0.983	0.9907	-	ugtP	RSAU_000902
970029.0	3.23	-0.19	0.7669	0.8976	-	ugtP	RSAU_000902
970060.0	11.49	-2.85	1.0E-4	0.0026	-	ugtP	RSAU_000902
970081.0	0.47	-0.5	0.5972	0.7988	-	ugtP	RSAU_000902
970668.0	0.5	-0.46	0.575	0.7789	+	murE	RSAU_000903
970670.0	1.12	1.27	0.1734	0.3576	+	murE	RSAU_000903
970687.0	2.53	-0.2	0.7335	0.8788	+	murE	RSAU_000903
973433.0	6.32	-3.04	5.0E-4	0.0087	+	prfC	RSAU_000905
984800.0	5.21	-0.56	0.2582	0.4666	+		RSAU_000917
985038.0	1.76	-1.92	0.0287	0.1255	+		RSAU_000917
985512.0	6.14	-1.6	0.0064	0.0502	+		RSAU_000919
1011361.0	0.42	0.95	0.3639	0.5808	-		RSAU_000942
1011362.0	75.88	0.54	0.1206	0.2954	-		RSAU_000942
1011363.0	0.62	0.63	0.4314	0.6502	-		RSAU_000942
1013989.0	1.63	-2.71	0.0083	0.0578	+	fmtA	RSAU_000944
1014066.0	4.29	-0.5	0.1851	0.3752	+	fmtA	RSAU_000944
1016905.0	0.74	-1.01	0.1672	0.3477	-	qoxB	RSAU_000947
1028973.0	15.9	-3.77	0.0	0.0	+	purM	RSAU_000958
1029478.0	1.33	-2.57	0.0129	0.0787	+	purM	RSAU_000958
1030332.0	158.25	-0.56	0.074	0.2222	+	purH	RSAU_000960
1030333.0	1.31	-0.79	0.3936	0.6097	+	purH	RSAU_000960
1049784.0	3.83	-0.29	0.5613	0.7712	+		RSAU_000977
1050262.0	2.46	-0.63	0.2604	0.4686	+		RSAU_000977
1054670.0	1.42	0.1	0.8685	0.9538	+	pdhD	RSAU_000981
1058301.0	24.55	-0.76	0.1057	0.2802	+	potB	RSAU_000985
1088349.0	0.45	-0.04	0.9728	0.9873	+	isdC	RSAU_001015
1122480.0	0.23	-0.16	0.8808	0.9538	-		RSAU_001048
1128265.0	40.62	-1.38	3.0E-4	0.0057	-		RSAU_001052
1133324.0	1.02	-2.34	0.0251	0.1156	+		RSAU_001058
1145260.0	6.79	-2.09	0.0016	0.0204	+		RSAU_001068
1147069.0	6.97	-0.89	0.2295	0.4367	+	ylmG	RSAU_001071
1149322.0	0.64	0.52	0.5049	0.7134	+	lileS	RSAU_001074
1150296.0	0.63	-0.95	0.3651	0.5808	+	lileS	RSAU_001074
1153570.0	1.39	-1.03	0.2789	0.4917	-		RSAU_001076
1158958.0	1.44	0.83	0.4219	0.6441	+	pyrB	RSAU_001083
1172061.0	0.64	-0.37	0.693	0.8515	+	priA	RSAU_001094
1176597.0	18.52	-2.38	2.0E-4	0.0039	+	def2	RSAU_001097
1178449.0	0.34	1.63	0.1269	0.305	+	sun	RSAU_001099
1180291.0	4.26	-1.58	0.0152	0.0861	+	rlmN	RSAU_001100
1192892.0	0.78	0.01	0.9925	0.9953	+	fabD	RSAU_001112
1203877.0	1.64	1.06	0.2962	0.5152	+	trmD	RSAU_001122
1205504.0	0.2	-0.78	0.465	0.6675	-		RSAU_001124
1207545.0	1.71	-1.82	0.0385	0.1532	-		RSAU_001124
1228587.0	1.03	-2.39	0.0216	0.1049	+		RSAU_001144
1228588.0	2.04	-2.74	0.0042	0.0418	+		RSAU_001144
1228595.0	11.33	-1.32	0.0073	0.0544	+		RSAU_001144
1229140.0	0.27	-1.47	0.1672	0.3477	+		RSAU_001144
1229404.0	0.98	-0.43	0.687	0.8485	+		RSAU_001144
1229450.0	36.29	0.03	0.9693	0.987	+		RSAU_001144
1229451.0	0.24	-0.42	0.6897	0.8485	+		RSAU_001144
1244820.0	0.38	0.58	0.583	0.7818	+	pnpA	RSAU_001157
1247609.0	0.7	0.04	0.9478	0.9838	+		RSAU_001158
1258190.0	1.45	-1.47	0.0659	0.2129	+	ci	RSAU_001167
1266892.0	0.56	1.91	0.071	0.2176	+	miaB	RSAU_001175
1268730.0	0.8	-0.52	0.5712	0.7747	+	thiW	RSAU_001177
1270994.0	0.2	-0.06	0.9554	0.9838	+	mutS	RSAU_001178
1293752.0	0.26	0.05	0.9597	0.9838	+		RSAU_001199
1298369.0	0.28	-0.97	0.3608	0.5792	+	cls1	RSAU_001205
1299070.0	2.05	-1.01	0.2268	0.4337	+	cls1	RSAU_001205
1302428.0	0.65	-2.08	0.048	0.1732	+		RSAU_001208
1305469.0	0.27	0.94	0.3764	0.5918	+	thrC	RSAU_001211
1316615.0	0.88	-2.28	0.0289	0.1255	+		RSAU_001222
1324966.0	1.14	0.3	0.7791	0.9038	-	mscL	RSAU_001230
1326206.0	0.27	-1.47	0.1672	0.3477	+	opuD	RSAU_001231
1326705.0	0.46	0.31	0.7406	0.8827	+	opuD	RSAU_001231
1348181.0	1.15	-2.51	0.0155	0.0867	-	tyrA	RSAU_001246
1351570.0	5.93	-0.1	0.8092	0.9159	+	trpE	RSAU_001248
1360051.0	0.23	-0.16	0.8808	0.9538	+	femB	RSAU_001256

1363390.0	0.62	-0.61	0.5627	0.7712	-	oppD3	RSAU_001260
1366554.0	0.3	0.26	0.8096	0.9159	+	pepF	RSAU_001264
1369278.0	0.3	-0.35	0.7417	0.8827	-	pstB	RSAU_001266
1369510.0	0.87	-2.12	0.0439	0.1652	-	pstB	RSAU_001266
1371401.0	0.44	-0.42	0.6662	0.8442	-	pstC	RSAU_001268
1375557.0	56.58	-0.58	0.1508	0.3477	+		RSAU_001271
1382959.0	1.72	0.46	0.4033	0.6201	+	alr	RSAU_001278
1383183.0	0.27	-1.47	0.1672	0.3477	+	alr	RSAU_001278
1384585.0	0.39	-0.35	0.7181	0.8672	+	lysA	RSAU_001279
1387147.0	3.75	-3.13	2.0E-4	0.0049	+		RSAU_001284
1415224.0	0.84	-1.29	0.2133	0.4172	+		RSAU_001311
1419360.0	0.26	0.05	0.9597	0.9838	-		RSAU_001312
1422523.0	0.42	-0.25	0.812	0.9159	-		RSAU_001312
1422524.0	85.7	-1.26	8.0E-4	0.0116	-		RSAU_001312
1424364.0	8.3	-1.46	0.0542	0.191	-		RSAU_001312
1435690.0	0.45	-0.04	0.9728	0.9873	-		RSAU_001316
1436781.0	1.3	-2.6	0.0118	0.0756	-		RSAU_001317
1455593.0	8.54	-2.07	8.0E-4	0.0122	-		RSAU_001335
1456659.0	0.27	-1.47	0.1672	0.3477	-	aroA	RSAU_001336
1462884.0	0.35	-1.66	0.1197	0.2945	-		RSAU_001342
1470522.0	0.77	-0.35	0.6997	0.8546	+	ansA	RSAU_001349
1470923.0	2.75	-2.12	0.0141	0.0821	+	ansA	RSAU_001349
1491235.0	1.8	-2.87	0.0050	0.0442	-		RSAU_001369
1499615.0	0.27	-1.47	0.1672	0.3477	-		RSAU_001376
1508049.0	0.96	1.65	0.117	0.2945	-		RSAU_001384
1509754.0	0.5	-1.24	0.2439	0.4528	-	lpdA	RSAU_001385
1526169.0	1.88	1.26	0.1602	0.3477	-	gcvT	RSAU_001403
1529518.0	0.38	-0.48	0.6512	0.8407	-	comGB	RSAU_001408
1536141.0	0.3	0.26	0.8096	0.9159	-	pbp3	RSAU_001417
1546269.0	1.1	-2.25	0.0205	0.1036	-	dG	RSAU_001427
1546589.0	6.41	-0.34	0.2578	0.4666	-	dG	RSAU_001427
1554439.0	0.28	0.04	0.9679	0.9865	-	phoH	RSAU_001436
1567370.0	3.74	-2.87	0.0013	0.0172	-	hemN	RSAU_001448
1567371.0	2.1	-2.99	0.0033	0.0355	-	hemN	RSAU_001448
1567706.0	4.51	0.18	0.7995	0.9159	-	hemN	RSAU_001448
1567763.0	9.39	-1.75	0.0048	0.0442	-	hemN	RSAU_001448
1567793.0	10.75	-2.23	0.0	4.0E-4	-	hemN	RSAU_001448
1571278.0	0.27	-1.47	0.1672	0.3477	-	holA	RSAU_001451
1572002.0	0.27	-1.47	0.1672	0.3477	-	comEC	RSAU_001452
1572701.0	0.3	-0.35	0.7417	0.8827	-	comEC	RSAU_001452
1583613.0	1.0	-2.4	0.0209	0.1043	-		RSAU_001465
1587707.0	0.2	-0.06	0.9554	0.9838	-	accC2	RSAU_001468
1593905.0	0.65	0.77	0.3217	0.5437	-		RSAU_001476
1600217.0	0.27	-1.47	0.1672	0.3477	-		RSAU_001481
1600769.0	0.7	-0.69	0.4518	0.6675	-		RSAU_001481
1609947.0	4.17	-3.63	3.0E-4	0.0057	-	aspS	RSAU_001491
1617963.0	12.07	-0.68	0.0716	0.2176	-	recJ	RSAU_001497
1618619.0	2.33	-2.93	0.0020	0.0243	-	recJ	RSAU_001497
1618912.0	0.42	-1.79	0.0912	0.2559	-	recJ	RSAU_001497
1625210.0	0.54	1.13	0.2784	0.4917	-	queA	RSAU_001501
1626495.0	0.42	0.38	0.6326	0.8294	-	ruvA	RSAU_001503
1626510.0	13.4	1.07	0.0013	0.0172	-	ruvA	RSAU_001503
1626521.0	1.26	0.15	0.8077	0.9159	-	ruvA	RSAU_001503
1626526.0	2.81	-0.12	0.8225	0.9198	-	ruvA	RSAU_001503
1627570.0	0.57	-0.67	0.4706	0.6729	-	obgE	RSAU_001505
1653092.0	3.23	-1.75	0.0884	0.2559	-	hemX	RSAU_001530
1663075.0	0.29	1.1	0.2986	0.5152	-	lysP	RSAU_001540
1663188.0	0.41	0.18	0.8688	0.9538	-	lysP	RSAU_001540
1674357.0	0.8	-2.22	0.0339	0.1401	-	polA	RSAU_001548
1678198.0	1.49	-0.22	0.7347	0.8793	-	phoR	RSAU_001550
1680917.0	0.43	-0.69	0.4618	0.6675	-	citC	RSAU_001552
1686128.0	1.14	-1.26	0.2276	0.4338	-	pfkA	RSAU_001556
1689791.0	1.44	2.49	0.0165	0.0915	-		RSAU_001559
1689861.0	1.01	0.39	0.5699	0.774	-		RSAU_001559
1689891.0	1.13	0.91	0.2317	0.4373	-		RSAU_001559
1699151.0	1.41	-2.6	0.0115	0.0749	+		RSAU_001565
1705050.0	0.55	-1.92	0.07	0.2176	-		RSAU_001571
1723193.0	12.36	-1.11	0.0107	0.0707	+		RSAU_001586
1726199.0	4.25	0.23	0.7785	0.9038	-	sasI	RSAU_001587
1732527.0	1.85	-2.11	0.0169	0.0923	+	acuC	RSAU_001591
1743195.0	1.12	-0.44	0.4264	0.6472	-		RSAU_001599
1744185.0	0.23	0.47	0.6603	0.8407	-		RSAU_001600
1747381.0	1.34	-2.46	0.0179	0.0945	-		RSAU_001604
1750127.0	0.38	0.58	0.583	0.7818	-	dat	RSAU_001607
1756344.0	0.72	0.98	0.3425	0.5689	+		RSAU_001612
1759647.0	1.19	0.33	0.6571	0.8407	-		RSAU_001613
1777521.0	0.27	-1.47	0.1672	0.3477	-		RSAU_001626
1795897.0	4.03	-2.66	3.0E-4	0.0065	-		RSAU_001646
1813182.0	0.34	0.29	0.7632	0.8976	-	hsdM	RSAU_001665
1824418.0	0.2	-0.78	0.465	0.6675	-	lukE	RSAU_001675
1824419.0	0.48	0.28	0.7319	0.8788	-	lukE	RSAU_001675
1835877.0	0.3	-0.35	0.7417	0.8827	-	hemG	RSAU_001691
1838935.0	0.5	-1.9	0.072	0.2176	-	ecsB	RSAU_001695
1840124.0	0.35	-1.66	0.1197	0.2945	-	ecsA	RSAU_001696
1840660.0	74.48	-1.22	0.0332	0.1382	-	ecsA	RSAU_001696
1840661.0	0.23	-0.16	0.8808	0.9538	-	ecsA	RSAU_001696
1869613.0	26.45	-0.19	0.6721	0.8478	-		RSAU_001745

1876745.0	0.27	-1.47	0.1672	0.3477	+	gsaB	RSAU_001751
1885203.0	0.27	0.94	0.3764	0.5918	-		RSAU_001758
1887781.0	0.27	-1.47	0.1672	0.3477	-	mgt	RSAU_001761
1889276.0	22.47	-1.2	0.0116	0.0749	-		RSAU_001762
1889867.0	4.62	0.48	0.5291	0.7376	+		RSAU_001764
1905136.0	0.62	-0.49	0.6137	0.8146	+		RSAU_001781
1907410.0	6.07	-1.21	0.2033	0.4028	-		RSAU_001783
1908104.0	2.23	-3.05	0.0027	0.0297	-	TrmA family R methyltransferase	RSAU_001784
1908435.0	0.27	-0.52	0.6268	0.8237	-	TrmA family R methyltransferase	RSAU_001784
1935170.0	1.27	-1.33	0.1407	0.3323	-		RSAU_001804
1944160.0	0.26	0.05	0.9597	0.9838	+		RSAU_001812
1944395.0	0.24	-0.42	0.6897	0.8485	-		RSAU_001813
1945084.0	6.97	-1.59	0.0075	0.0551	-		RSAU_001813
1945554.0	3.06	-1.94	0.0143	0.0821	-		RSAU_001813
1945792.0	5.47	-0.58	0.2319	0.4373	-		RSAU_001813
1945843.0	2.57	-1.97	0.0235	0.1112	-		RSAU_001813
1945971.0	2.01	-2.86	0.0050	0.0442	-		RSAU_001813
1958402.0	1.95	-0.39	0.6663	0.8442	-	pmtB	RSAU_001827
1964367.0	0.27	-1.47	0.1672	0.3477	-		RSAU_001833
1967617.0	1.03	-2.39	0.0216	0.1049	-	lukG	RSAU_001837
1970608.0	3.0	-3.32	0.0010	0.0139	+	dapE	RSAU_001839
1985392.0	19.33	-0.68	0.4667	0.6685	-		RSAU_001854
1985393.0	0.31	-0.97	0.3602	0.5792	-		RSAU_001854
1988106.0	0.53	-0.07	0.9368	0.9838	+	int	RSAU_001859
1990112.0	0.27	0.94	0.3764	0.5918	-	groEL	RSAU_001860
1991341.0	0.3	0.26	0.8096	0.9159	+		RSAU_001862
1991439.0	0.27	-1.47	0.1672	0.3477	+		RSAU_001862
1991610.0	0.27	-1.47	0.1672	0.3477	+		RSAU_001862
1991614.0	0.47	-1.77	0.0961	0.2616	+		RSAU_001862
1993486.0	0.64	-1.25	0.2312	0.4373	+		RSAU_001864
2001149.0	0.23	-0.16	0.8808	0.9538	-	scrB	RSAU_001874
2003603.0	0.33	0.5	0.6412	0.8334	-	amt	RSAU_001876
2005814.0	1.8	0.71	0.4251	0.6466	-		RSAU_001878
2011379.0	0.55	-1.92	0.07	0.2176	-	gcp	RSAU_001882
2012365.0	0.3	0.26	0.8096	0.9159	-	gcp	RSAU_001882
2015345.0	2.91	-1.23	0.1773	0.3622	+	ilvD	RSAU_001886
2017379.0	0.68	0.16	0.8789	0.9538	+	ilvB	RSAU_001887
2021812.0	0.72	-1.16	0.2718	0.4843	+	leuB	RSAU_001891
2022633.0	0.3	0.26	0.8096	0.9159	+	leuC	RSAU_001892
2023235.0	0.35	0.11	0.9181	0.9733	+	leuC	RSAU_001892
2026230.0	1.74	-2.36	0.0116	0.0749	+	putative transposase	RSAU_001895
2026565.0	4.04	-1.66	0.0178	0.0945	+	putative transposase	RSAU_001895
2026567.0	3.15	-2.25	0.0075	0.0551	+	putative transposase	RSAU_001895
2029265.0	26.45	-0.13	0.7692	0.8993	-		RSAU_001898
2029622.0	0.29	1.1	0.2986	0.5152	-		RSAU_001898
2042049.0	2.19	-0.22	0.7329	0.8788	-		RSAU_001912
2043146.0	1.71	-0.26	0.6348	0.8312	-		RSAU_001913
2044110.0	11.84	-2.59	4.0E-4	0.0069	-		RSAU_001914
2046387.0	0.2	-0.78	0.465	0.6675	-	kdpB	RSAU_001916
2051283.0	3.19	-1.19	0.1353	0.3245	+	kdpD	RSAU_001918
2053740.0	0.2	-0.78	0.465	0.6675	-		RSAU_001920
2053981.0	0.35	-1.66	0.1197	0.2945	-		RSAU_001920
2054331.0	23.65	-3.93	0.0	0.0	-		RSAU_001920
2070953.0	10.95	-0.11	0.7596	0.8976	-	murAA	RSAU_001938
2081546.0	1.11	-0.01	0.9904	0.9942	-	glyA	RSAU_001951
2081556.0	17.15	0.28	0.3344	0.5615	-	glyA	RSAU_001951
2081559.0	1.75	1.76	0.0242	0.1137	-	glyA	RSAU_001951
2081567.0	1.74	0.8	0.1805	0.3679	-	glyA	RSAU_001951
2081571.0	4.92	1.06	0.038	0.1517	-	glyA	RSAU_001951
2081610.0	0.6	1.16	0.2081	0.4104	-	glyA	RSAU_001951
2081628.0	0.93	-0.59	0.506	0.7134	-	glyA	RSAU_001951
2081630.0	0.31	-0.97	0.3602	0.5792	-	glyA	RSAU_001951
2081631.0	4.23	0.08	0.848	0.9444	-	glyA	RSAU_001951
2081637.0	1.25	0.01	0.9806	0.9907	-	glyA	RSAU_001951
2081638.0	5.04	0.08	0.8564	0.9528	-	glyA	RSAU_001951
2081682.0	1.18	-0.64	0.2688	0.4804	-	glyA	RSAU_001951
2093115.0	0.27	-1.47	0.1672	0.3477	-	fbaA	RSAU_001963
2093116.0	15.29	-2.01	5.0E-4	0.0077	-	fbaA	RSAU_001963
2093117.0	0.47	-1.77	0.0961	0.2616	-	fbaA	RSAU_001963
2094484.0	0.27	-1.47	0.1672	0.3477	+		RSAU_001964
2096876.0	21.35	-0.62	0.1016	0.2715	-	rpoE	RSAU_001966
2097182.0	13.7	0.17	0.7748	0.9018	-	rpoE	RSAU_001966
2097262.0	0.2	-0.78	0.465	0.6675	-	rpoE	RSAU_001966
2100171.0	33.69	0.05	0.9312	0.9823	-		RSAU_001969
2111705.0	1.14	0.79	0.4448	0.6628	-	ma1	RSAU_001980
2112488.0	0.5	-1.9	0.072	0.2176	-	ma1	RSAU_001980
2113393.0	2.77	-1.04	0.1895	0.3826	-		RSAU_001981
2118585.0	0.57	-1.51	0.114	0.2945	+		RSAU_001986
2118920.0	2.53	-0.99	0.2912	0.5092	+		RSAU_001986
2118922.0	3.12	-2.3	0.0081	0.0571	+		RSAU_001986
2132391.0	0.68	-1.83	0.0623	0.2048	-	fmtB	RSAU_001996
2132392.0	88.9	-1.78	1.0E-4	0.0035	-	fmtB	RSAU_001996
2132393.0	0.43	-0.79	0.4027	0.6201	-	fmtB	RSAU_001996
2139221.0	2.63	0.78	0.4565	0.6675	-	fmtB	RSAU_001996
2146436.0	25.49	-0.19	0.6836	0.8485	-		RSAU_002008
2148925.0	0.98	0.77	0.4597	0.6675	-		RSAU_002009
2149153.0	0.32	-0.12	0.9136	0.9712	-		RSAU_002009

2152234.0	1.89	-1.61	0.0405	0.1581	-		RSAU_002011
2155109.0	9.01	-0.45	0.3852	0.6002	-		RSAU_002013
2160373.0	1.14	-0.34	0.5469	0.7564	-	htsC	RSAU_002019
2166341.0	0.96	-0.97	0.3539	0.5792	-		RSAU_002024
2215752.0	1.78	2.13	0.0135	0.0799	-	rplB	RSAU_002083
2218993.0	7.55	0.31	0.6076	0.8097	+		RSAU_002088
2218995.0	5.25	0.57	0.3365	0.5642	+		RSAU_002088
2219163.0	0.67	0.54	0.5552	0.7659	+		RSAU_002088
2221514.0	0.23	-0.16	0.8808	0.9538	-	topB	RSAU_002090
2221738.0	0.62	-2.03	0.054	0.191	-	topB	RSAU_002090
2231335.0	0.84	-0.54	0.4307	0.6501	-	femX	RSAU_002097
2231696.0	1.85	-0.3	0.5431	0.753	-	femX	RSAU_002097
2237326.0	0.46	0.52	0.5815	0.7818	-	moaA	RSAU_002102
2250743.0	1.33	-2.57	0.0129	0.0787	-		RSAU_002119
2254911.0	2.58	0.15	0.8852	0.9557	+	ureC	RSAU_002123
2256998.0	11.02	-1.28	0.0243	0.1138	+	ureD	RSAU_002127
2266499.0	11.08	-0.28	0.6018	0.803	+		RSAU_002135
2269681.0	6.34	-1.62	0.0055	0.0478	-		RSAU_002139
2270155.0	1.76	-1.92	0.0287	0.1255	-		RSAU_002141
2270393.0	5.21	-0.58	0.2307	0.4373	-		RSAU_002141
2273519.0	0.26	0.05	0.9597	0.9838	-		RSAU_002144
2280131.0	2.41	-2.58	0.0058	0.0494	-		RSAU_002148
2283833.0	1.33	-2.57	0.0129	0.0787	+		RSAU_002152
2291977.0	2.86	-3.18	0.0017	0.0204	+		RSAU_002160
2291978.0	8.08	-2.92	9.0E-4	0.0128	+		RSAU_002160
2293298.0	0.47	-1.77	0.0961	0.2616	-		RSAU_002162
2297000.0	0.26	0.05	0.9597	0.9838	-		RSAU_002165
2307310.0	1.23	-2.56	0.0135	0.0799	-	galM	RSAU_002173
2308636.0	0.79	-1.03	0.2719	0.4843	-		RSAU_002175
2311991.0	4.74	0.02	0.9588	0.9838	+		RSAU_002178
2312713.0	29.59	-1.67	4.0E-4	0.0069	+	gltS	RSAU_002179
2315600.0	37.1	-1.18	0.0315	0.1338	-		RSAU_002181
2317106.0	3.87	-2.31	0.0091	0.0623	-		RSAU_002184
2317656.0	11.14	-1.14	0.0431	0.1648	-		RSAU_002184
2323285.0	0.34	1.63	0.1269	0.305	-	tcaB	RSAU_002189
2323287.0	0.64	0.3	0.6975	0.8541	-	tcaB	RSAU_002189
2323292.0	0.47	-0.53	0.519	0.7263	-	tcaB	RSAU_002189
2323331.0	0.27	-1.47	0.1672	0.3477	-	tcaB	RSAU_002189
2323370.0	0.52	0.47	0.6562	0.8407	-	tcaB	RSAU_002189
2323436.0	1.34	-0.15	0.8297	0.927	-	tcaB	RSAU_002189
2323454.0	0.66	-0.58	0.4538	0.6675	-	tcaB	RSAU_002189
2323477.0	0.68	0.82	0.3047	0.5217	-	tcaB	RSAU_002189
2323582.0	0.23	0.47	0.6603	0.8407	-	tcaB	RSAU_002189
2324479.0	0.7	-2.13	0.0431	0.1648	-	tcaA	RSAU_002190
2324945.0	0.42	-1.79	0.0912	0.2559	-	tcaA	RSAU_002190
2345256.0	0.27	-1.47	0.1672	0.3477	-		RSAU_002210
2350033.0	0.35	-1.66	0.1197	0.2945	-	scrA	RSAU_002215
2350307.0	20.79	-2.23	5.0E-4	0.0078	-	scrA	RSAU_002215
2352161.0	1.37	-2.59	0.0123	0.077		SSR42	
2352229.0	88.55	-0.3	0.5064	0.7134		SSR42	
2352274.0	2.91	-0.13	0.8138	0.9159		SSR42	
2352778.0	0.65	0.71	0.3202	0.5437		SSR42	
2352952.0	1.36	1.64	0.0466	0.1723		SSR42	
2353020.0	1.37	1.09	0.1757	0.3602		SSR42	
2353021.0	0.46	1.84	0.0824	0.2414		SSR42	
2353022.0	0.66	1.3	0.2117	0.4148		SSR42	
2353023.0	217.62	1.92	0.0	0.0		SSR42	
2353024.0	31105.06	1.6	0.0	0.0		SSR42	
2353025.0	134.44	1.6	0.0	0.0		SSR42	
2353319.0	0.35	-1.66	0.1197	0.2945	+	rsp	RSAU_002217
2353323.0	29.65	1.16	0.0	0.0	+	rsp	RSAU_002217
2353324.0	5748.97	0.85	0.0	0.0	+	rsp	RSAU_002217
2353325.0	33.73	0.99	0.0	0.0010	+	rsp	RSAU_002217
2353331.0	0.69	-1.56	0.1012	0.2715	+	rsp	RSAU_002217
2353358.0	1.33	-0.64	0.4415	0.6616	+	rsp	RSAU_002217
2353367.0	0.58	-0.26	0.7893	0.9126	+	rsp	RSAU_002217
2353378.0	23.97	-0.58	0.1768	0.3619	+	rsp	RSAU_002217
2353387.0	0.73	0.79	0.299	0.5152	+	rsp	RSAU_002217
2353388.0	2.48	-2.13	0.0062	0.0502	+	rsp	RSAU_002217
2353394.0	2.85	0.11	0.8734	0.9538	+	rsp	RSAU_002217
2353424.0	0.23	0.47	0.6603	0.8407	+	rsp	RSAU_002217
2353428.0	1.61	1.86	0.0173	0.0936	+	rsp	RSAU_002217
2353431.0	2289.19	1.1	0.0	1.0E-4	+	rsp	RSAU_002217
2353432.0	237623.39	0.9	0.0	0.0	+	rsp	RSAU_002217
2353433.0	779.44	1.1	0.0	0.0	+	rsp	RSAU_002217
2353435.0	500.69	1.11	0.0	0.0	+	rsp	RSAU_002217
2353436.0	83470.82	0.97	0.0	0.0	+	rsp	RSAU_002217
2353437.0	284.14	1.28	0.0	0.0	+	rsp	RSAU_002217
2353439.0	1.75	0.81	0.2535	0.4616	+	rsp	RSAU_002217
2353440.0	77.54	0.03	0.9571	0.9838	+	rsp	RSAU_002217
2353442.0	2.72	-0.75	0.1943	0.3887	+	rsp	RSAU_002217
2353445.0	1.0	-0.1	0.9138	0.9712	+	rsp	RSAU_002217
2353450.0	1.64	0.12	0.8843	0.9557	+	rsp	RSAU_002217
2353454.0	0.28	-0.97	0.3608	0.5792	+	rsp	RSAU_002217
2353466.0	1.12	0.39	0.6152	0.8156	+	rsp	RSAU_002217
2353469.0	1.53	1.07	0.2271	0.4337	+	rsp	RSAU_002217
2353470.0	1.58	-1.22	0.0421	0.1637	+	rsp	RSAU_002217

2353475.0	1.24	0.34	0.7289	0.8774	+	rsp	RSAU_002217
2353493.0	0.37	0.07	0.9464	0.9838	+	rsp	RSAU_002217
2353510.0	0.67	-0.31	0.7024	0.8551	+	rsp	RSAU_002217
2353527.0	0.59	-0.32	0.7612	0.8976	+	rsp	RSAU_002217
2353573.0	0.79	-0.04	0.9653	0.9862	+	rsp	RSAU_002217
2353582.0	2.44	1.83	0.0045	0.0427	+	rsp	RSAU_002217
2353586.0	0.37	0.4	0.6761	0.8485	+	rsp	RSAU_002217
2353590.0	0.89	-0.02	0.9833	0.9907	+	rsp	RSAU_002217
2353595.0	1.9	-0.24	0.7771	0.9035	+	rsp	RSAU_002217
2353657.0	0.35	-1.66	0.1197	0.2945	+	rsp	RSAU_002217
2353667.0	16.75	-0.73	0.0647	0.2105	+	rsp	RSAU_002217
2353672.0	1.15	-0.8	0.2526	0.4607	+	rsp	RSAU_002217
2353680.0	1.68	1.48	0.0212	0.1048	+	rsp	RSAU_002217
2353681.0	428.84	0.85	0.0	1.0E-4	+	rsp	RSAU_002217
2353685.0	9.13	-0.61	0.4404	0.6609	+	rsp	RSAU_002217
2353686.0	0.24	-0.42	0.6897	0.8485	+	rsp	RSAU_002217
2353697.0	0.56	-0.13	0.8898	0.9597	+	rsp	RSAU_002217
2353767.0	12.8	-0.56	0.2986	0.5152	+	rsp	RSAU_002217
2353769.0	0.35	-1.66	0.1197	0.2945	+	rsp	RSAU_002217
2353808.0	1.18	-2.48	0.0165	0.0915	+	rsp	RSAU_002217
2353946.0	1.82	-0.78	0.2736	0.4861	+	rsp	RSAU_002217
2353976.0	1.2	-2.54	0.0142	0.0821	+	rsp	RSAU_002217
2353985.0	1.0	-2.4	0.0209	0.1043	+	rsp	RSAU_002217
2354116.0	0.27	-1.47	0.1672	0.3477	+	rsp	RSAU_002217
2354134.0	0.35	-1.66	0.1197	0.2945	+	rsp	RSAU_002217
2354156.0	3.91	-1.1	0.0477	0.1732	+	rsp	RSAU_002217
2354171.0	0.8	-1.51	0.1054	0.2802	+	rsp	RSAU_002217
2354173.0	5.72	-1.28	0.0687	0.2176	+	rsp	RSAU_002217
2354215.0	0.42	-1.79	0.0912	0.2559	+	rsp	RSAU_002217
2354245.0	0.35	-1.66	0.1197	0.2945	+	rsp	RSAU_002217
2354362.0	4.63	-0.12	0.8224	0.9198	+	rsp	RSAU_002217
2354398.0	0.43	-1.22	0.2482	0.457	+	rsp	RSAU_002217
2354417.0	0.5	-1.9	0.072	0.2176	+	rsp	RSAU_002217
2354452.0	2.27	-1.04	0.2149	0.418	+	rsp	RSAU_002217
2354484.0	4.42	-1.61	0.0061	0.0502	+	rsp	RSAU_002217
2354486.0	1.46	-1.5	0.0584	0.1974	+	rsp	RSAU_002217
2354531.0	0.27	-1.47	0.1672	0.3477	+	rsp	RSAU_002217
2354560.0	0.73	-1.2	0.2037	0.4029	+	rsp	RSAU_002217
2354601.0	0.58	-2.0	0.0582	0.1974	+	rsp	RSAU_002217
2354603.0	2.54	-0.71	0.3178	0.5406	+	rsp	RSAU_002217
2354729.0	0.58	-1.05	0.2641	0.4728	+	rsp	RSAU_002217
2354778.0	1.91	-1.7	0.0698	0.2176	+	rsp	RSAU_002217
2354804.0	2.9	-1.42	0.0443	0.1661	+	rsp	RSAU_002217
2354823.0	5.78	0.95	0.0011	0.0156	+	rsp	RSAU_002217
2354824.0	1295.54	0.79	0.0	1.0E-4	+	rsp	RSAU_002217
2354825.0	6.59	0.73	0.0389	0.154	+	rsp	RSAU_002217
2354828.0	1.02	-0.63	0.44	0.6609	+	rsp	RSAU_002217
2354839.0	1.8	0.78	0.1429	0.3353	+	rsp	RSAU_002217
2354856.0	2.32	-2.11	0.0216	0.1049	+	rsp	RSAU_002217
2354858.0	0.99	-0.71	0.4429	0.6628	+	rsp	RSAU_002217
2354895.0	34.53	1.54	0.0	0.0	+	rsp	RSAU_002217
2354896.0	28308.14	0.94	0.0	0.0	+	rsp	RSAU_002217
2354897.0	15667.76	0.99	0.0	0.0	+	rsp	RSAU_002217
2354898.0	163.11	1.15	0.0	6.0E-4	+	rsp	RSAU_002217
2354950.0	4.58	-1.64	0.0218	0.1052	+	rsp	RSAU_002217
2354953.0	4.85	-1.09	0.0361	0.1453	+	rsp	RSAU_002217
2354970.0	0.88	-2.28	0.0289	0.1255	+	rsp	RSAU_002217
2354991.0	1.12	-2.49	0.0166	0.0915	+	rsp	RSAU_002217
2355019.0	1.93	-2.73	0.0044	0.0418	+	rsp	RSAU_002217
2355023.0	22.12	-0.53	0.2302	0.4372	+	rsp	RSAU_002217
2355068.0	0.98	-0.77	0.331	0.5577	+	rsp	RSAU_002217
2355072.0	0.65	-2.08	0.048	0.1732	+	rsp	RSAU_002217
2355076.0	0.42	-1.79	0.0912	0.2559	+	rsp	RSAU_002217
2355109.0	0.52	0.47	0.6562	0.8407	+	rsp	RSAU_002217
2355136.0	3.17	0.42	0.4838	0.6899	+	rsp	RSAU_002217
2355137.0	560.18	0.45	0.2186	0.4235	+	rsp	RSAU_002217
2355138.0	7.86	0.25	0.6408	0.8334	+	rsp	RSAU_002217
2355178.0	0.35	-1.66	0.1197	0.2945	+	rsp	RSAU_002217
2355267.0	0.78	-1.95	0.0475	0.1732	+	rsp	RSAU_002217
2355271.0	1.14	0.26	0.7011	0.8546	+	rsp	RSAU_002217
2355272.0	0.27	-1.47	0.1672	0.3477	+	rsp	RSAU_002217
2355295.0	1.37	-0.41	0.6674	0.8443	+	rsp	RSAU_002217
2355385.0	1.01	2.38	0.0222	0.1066	+	rsp	RSAU_002217
2355386.0	572.31	1.15	0.0	8.0E-4	+	rsp	RSAU_002217
2355387.0	99339.93	1.09	0.0	0.0	+	rsp	RSAU_002217
2355388.0	552.38	1.47	0.0	0.0	+	rsp	RSAU_002217
2355389.0	1.05	-0.25	0.7641	0.8976	+	rsp	RSAU_002217
2355683.0	0.46	-0.84	0.4195	0.6423	+		RSAU_002218
2357619.0	7.2	-1.61	0.0072	0.0544	-		RSAU_002221
2358089.0	3.14	-1.96	0.013	0.0787	-		RSAU_002221
2358327.0	5.14	-0.56	0.2497	0.457	-		RSAU_002221
2358378.0	2.54	-2.01	0.0204	0.1036	-		RSAU_002221
2358506.0	2.01	-2.86	0.0050	0.0442	-		RSAU_002221
2369603.0	4.95	-1.26	0.0792	0.234	-	rH	RSAU_002234
2375646.0	1.34	-0.72	0.2848	0.4996	-		RSAU_002236
2375656.0	2.06	-2.95	0.0039	0.0392	-	nirD	RSAU_002237
2375658.0	0.6	-1.34	0.1648	0.3477	-	nirD	RSAU_002237

2377350.0	0.56	0.25	0.8132	0.9159	-	nirB	RSAU_002238
2380914.0	0.83	-0.12	0.905	0.9712	-		RSAU_002241
2390601.0	0.25	0.32	0.7657	0.8976	-		RSAU_002253
2401642.0	1.18	0.21	0.7365	0.8804	-	bioF	RSAU_002263
2402743.0	12.62	-1.16	0.1068	0.2818	-	bioB	RSAU_002264
2403110.0	0.27	-0.52	0.6268	0.8237	-	bioA	RSAU_002265
2404557.0	1.7	-0.33	0.5818	0.7818	-	bioD	RSAU_002266
2404558.0	2.54	-0.33	0.679	0.8485	-	bioD	RSAU_002266
2412817.0	0.35	-0.34	0.7468	0.8868	+		RSAU_002274
2414732.0	1.82	0.67	0.3646	0.5808	+		RSAU_002276
2415583.0	0.67	-1.97	0.0627	0.2048	-		RSAU_002277
2418407.0	0.68	2.09	0.0472	0.1732	+		RSAU_002279
2420049.0	3.21	-0.78	0.4556	0.6675	-		RSAU_002280
2421201.0	0.35	-1.66	0.1197	0.2945	-		RSAU_002280
2426890.0	7.02	-0.31	0.6551	0.8407	-		RSAU_002284
2428038.0	0.23	-0.16	0.8808	0.9538	-	opuCD	RSAU_002285
2435408.0	0.34	1.63	0.1269	0.305	+	pnbA	RSAU_002291
2439697.0	0.62	-0.47	0.6571	0.8407	-	pepA2	RSAU_002295
2448461.0	0.97	-1.28	0.2149	0.418	-	opp1C	RSAU_002303
2458746.0	0.55	-1.92	0.07	0.2176	-		RSAU_002312
2469805.0	0.96	-0.97	0.3539	0.5792	-		RSAU_002326
2470806.0	1.66	-2.31	0.0141	0.0821	+		RSAU_002327
2471141.0	3.9	-1.56	0.0485	0.1738	+		RSAU_002327
2471143.0	3.53	-2.04	0.0078	0.0565	+		RSAU_002327
2475184.0	3.39	-0.62	0.3439	0.5704	-		RSAU_002332
2483137.0	0.76	-0.85	0.2232	0.4301	-	galU	RSAU_002339
2500548.0	1.86	0.64	0.3549	0.5792	-		RSAU_002349
2502627.0	3.74	-3.47	5.0E-4	0.0081	+		RSAU_002351
2502762.0	1.03	-1.97	0.0358	0.1445	+		RSAU_002351
2504348.0	6.21	-1.6	0.0063	0.0502	-		RSAU_002354
2504822.0	1.76	-1.92	0.0287	0.1255	-		RSAU_002356
2505060.0	5.14	-0.56	0.2497	0.457	-		RSAU_002356
2514520.0	0.25	0.32	0.7657	0.8976	+	ldhD	RSAU_002365
2518450.0	6.16	-2.32	0.0056	0.0478	-	srtA	RSAU_002369
2524525.0	0.78	-1.14	0.2368	0.4419	+		RSAU_002375
2527353.0	5.69	-0.66	0.3867	0.6003	-	glcB	RSAU_002379
2534718.0	0.27	-1.47	0.1672	0.3477	-	mvaA	RSAU_002385
2537662.0	34.37	-0.46	0.2089	0.4108	-		RSAU_002387
2537663.0	0.31	-0.93	0.3387	0.5643	-		RSAU_002387
2537803.0	126.11	-0.12	0.6365	0.8314	-		RSAU_002387
2537804.0	0.6	-0.89	0.3413	0.5678	-		RSAU_002387
2539962.0	16.49	-3.15	4.0E-4	0.0068	+	clpL	RSAU_002389
2539963.0	0.67	-1.97	0.0627	0.2048	+	clpL	RSAU_002389
2543042.0	0.47	-1.77	0.0961	0.2616	-	feoB1	RSAU_002391
2543449.0	1.92	-2.22	0.0177	0.0945	-	feoB1	RSAU_002391
2555486.0	1.91	-2.26	0.0067	0.0518	-		RSAU_002401
2557896.0	0.33	0.5	0.6412	0.8334	-	crtM	RSAU_002403
2558696.0	0.6	0.14	0.8591	0.9538	-		RSAU_002404
2558697.0	129.86	-0.96	0.0029	0.0318	-		RSAU_002404
2558698.0	0.82	-1.2	0.1924	0.3862	-		RSAU_002404
2559117.0	2.64	-2.1	0.0213	0.1048	-		RSAU_002404
2561557.0	0.27	-1.47	0.1672	0.3477	-		RSAU_002406
2561558.0	1.27	-1.76	0.0498	0.1773	-		RSAU_002406
2567559.0	1.09	-0.72	0.4205	0.643	-		RSAU_002411
2567916.0	0.31	-0.97	0.3602	0.5792	-		RSAU_002411
2568494.0	0.93	-1.02	0.321	0.5437	-		RSAU_002411
2576944.0	0.27	-1.47	0.1672	0.3477	-	feoB	RSAU_002424
2577147.0	5.29	0.33	0.6892	0.8485	-	feoB	RSAU_002424
2591848.0	0.31	-0.97	0.3602	0.5792	-	panB	RSAU_002440
2598175.0	6.76	-1.27	0.1261	0.305	-		RSAU_002445
2600881.0	3.92	-2.13	0.0135	0.0799	-	mqo2	RSAU_002448
2602861.0	10.62	-4.55	0.0	1.0E-4	-		RSAU_002449
2603417.0	0.55	-1.92	0.07	0.2176	-		RSAU_002449
2605759.0	0.24	-0.42	0.6897	0.8485	-	cdh	RSAU_002452
2611881.0	0.27	-1.47	0.1672	0.3477	-	cudT	RSAU_002456
2616610.0	1.15	-2.51	0.0155	0.0867	-		RSAU_002459
2618807.0	0.58	-2.0	0.0582	0.1974	-	cysJ	RSAU_002461
2621173.0	7.77	-1.34	0.056	0.1962	-		RSAU_002463
2622532.0	0.82	-0.09	0.9087	0.9712	-		RSAU_002465
2623442.0	1.9	-1.36	0.1477	0.3457	-		RSAU_002465
2625663.0	0.23	-0.16	0.8808	0.9538	-		RSAU_002467
2625802.0	0.67	-1.97	0.0627	0.2048	-		RSAU_002467
2629929.0	0.85	-0.9	0.38	0.5956	-	estA	RSAU_002472
2633759.0	0.42	-0.25	0.812	0.9159	-	arcR	RSAU_002474
2637057.0	4.49	-1.37	0.0891	0.2559	-	arcB2	RSAU_002477
2643636.0	0.53	0.09	0.9301	0.982	+		RSAU_002483
2649620.0	2.83	-1.94	0.0129	0.0787	-		RSAU_002486
2651822.0	0.36	-0.48	0.6104	0.8113	+		RSAU_002487
2660419.0	4.0	-0.35	0.6494	0.8407	-	secA2	RSAU_002492
2665905.0	2.74	-1.07	0.1149	0.2945	-	asp1	RSAU_002495
2666659.0	0.3	0.26	0.8096	0.9159	-	secY2	RSAU_002496
2668046.0	6.41	-1.95	0.0197	0.1012	-	sraP	RSAU_002497
2669336.0	2.29	-3.06	0.0026	0.0296	-	sraP	RSAU_002497
2670672.0	0.49	-0.25	0.7872	0.9113	-	sraP	RSAU_002497
2682680.0	1.01	1.62	0.0761	0.2269	-	capC2	RSAU_002507
2686911.0	0.47	-1.77	0.0961	0.2616	+	icaA	RSAU_002511
2689040.0	0.33	-0.19	0.8621	0.9538	+	icaC	RSAU_002513

2689120.0	0.43	0.03	0.9733	0.9873	+	icaC	RSAU_002513
2690509.0	0.31	-0.97	0.3602	0.5792	-	lip	RSAU_002514
2695145.0	0.68	-1.83	0.0623	0.2048	-	hisA	RSAU_002519
2698015.0	0.8	-0.55	0.5596	0.7699	-	hisD	RSAU_002523
2701355.0	0.77	-1.45	0.1181	0.2945	-		RSAU_002526
2704134.0	0.52	0.48	0.5563	0.7664	-		RSAU_002529
2710121.0	0.47	-1.77	0.0961	0.2616	+	pcp	RSAU_002535
2712809.0	0.41	0.4	0.675	0.8485	-	c	RSAU_002539
2719231.0	2.96	-0.4	0.2995	0.5153	+		RSAU_002542
2719232.0	436.3	-0.2	0.2738	0.4861	+		RSAU_002542
2719233.0	1.0	-0.68	0.3147	0.5361	+		RSAU_002542
2720367.0	1.14	0.79	0.4448	0.6628	+	nixA	RSAU_002543
2731704.0	1.5	-2.72	0.0081	0.0571	-	rsmG	RSAU_002558
2732120.0	0.31	-0.97	0.3602	0.5792	-	trmFo	RSAU_002559
2732641.0	0.32	-0.12	0.9136	0.9712	-	trmFo	RSAU_002559

Table G.3: Detailed table of by-site analysis from Mouse lung screen screening performed using DESeq2.

Position	**baseMean**	**log2FC**	***P***	**adj. *P***	**strand**	**gene**	**locus_tag**
376.0	0.71	-0.48	0.5476	0.9042	+	dA	RSAU_000001
10584.0	2.62	-1.35	0.1256	0.5985	+	hutH	RSAU_000008
10847.0	0.38	-0.16	0.8442	0.9889	+	hutH	RSAU_000008
11092.0	0.36	-0.19	0.8176	0.9889	+	hutH	RSAU_000008
12088.0	2.2	1.11	0.2139	0.5985			
17600.0	6.11	0.05	0.9496	0.9889	+		RSAU_000013
23712.0	2.78	-0.92	0.2972	0.6789			
25469.0	0.62	-0.45	0.5761	0.9244	+	vicK	RSAU_000021
26724.0	0.2	0.02	0.9822	0.9889	+	vicK	RSAU_000021
27101.0	7.46	1.07	0.2289	0.5985	+	yycH	RSAU_000022
27102.0	11.33	1.44	0.1073	0.5985	+	yycH	RSAU_000022
27486.0	0.7	1.72	0.053	0.5815	+	yycH	RSAU_000022
27487.0	58.76	0.95	0.0574	0.5815	+	yycH	RSAU_000022
28205.0	0.41	-0.22	0.7855	0.9889	+	yycH	RSAU_000022
29952.0	0.2	0.02	0.9822	0.9889	+	yycJ	RSAU_000024
30823.0	0.31	0.98	0.2331	0.5985	+	sasH	RSAU_000025
31612.0	3.42	-0.61	0.4298	0.8225	+	sasH	RSAU_000025
32205.0	6.91	-0.9	0.3068	0.6932	+	sasH	RSAU_000025
32832.0	0.49	-0.1	0.9006	0.9889	+	sasH	RSAU_000025
33894.0	0.37	-1.09	0.1867	0.5985	+		RSAU_000028
36603.0	0.36	-0.19	0.8176	0.9889			
36944.0	1.36	0.11	0.902	0.9889			
37107.0	0.2	0.02	0.9822	0.9889	+	putative transposase	RSAU_000032
37126.0	10.25	0.98	0.0926	0.5985	+	putative transposase	RSAU_000032
37364.0	1.91	-0.43	0.6145	0.9442	+	putative transposase	RSAU_000032
37838.0	7.78	-2.23	0.0107	0.2403	+	putative transposase	RSAU_000034
37860.0	0.6	-0.49	0.545	0.9042	+	putative transposase	RSAU_000034
37971.0	1.88	-0.11	0.8996	0.9889			
38462.0	0.36	-0.19	0.8176	0.9889	+	putative transposase	RSAU_000035
38528.0	0.22	0.04	0.9554	0.9889	+	putative transposase	RSAU_000035
38529.0	0.32	0.98	0.2303	0.5985	+	putative transposase	RSAU_000035
38536.0	0.2	0.02	0.9822	0.9889	+	putative transposase	RSAU_000035
39369.0	7.73	-0.06	0.9412	0.9889	-	dus	RSAU_000036
43415.0	1.27	0.13	0.883	0.9889			
43881.0	1.09	-0.68	0.388	0.79	+		RSAU_000041
47665.0	1.09	-0.68	0.388	0.79	+	putative helicase	RSAU_000044
52368.0	3.24	0.73	0.3673	0.7714	+	plc	RSAU_000049
56126.0	1.36	-2.15	0.0159	0.3165			
63118.0	0.43	1.17	0.1679	0.5985	+		RSAU_000060
64625.0	0.37	-1.09	0.1867	0.5985	-		RSAU_000061
65123.0	8.46	1.44	0.0596	0.5843	-		RSAU_000061
66641.0	0.26	0.96	0.2392	0.5985	-		RSAU_000062
70221.0	1.46	1.47	0.0985	0.5985			
70316.0	1.54	1.79	0.043	0.5604			
72421.0	0.57	-1.32	0.1225	0.5985	-	sarS	RSAU_000066
72423.0	0.72	-0.72	0.3868	0.79	-	sarS	RSAU_000066
73251.0	0.31	0.98	0.2331	0.5985	-	sirC	RSAU_000067
73808.0	0.46	1.17	0.1668	0.5985	-	sirC	RSAU_000067
73809.0	12.04	-0.4	0.6116	0.9442	-	sirC	RSAU_000067
74343.0	0.56	1.53	0.0824	0.5985	-	sirB	RSAU_000068
79411.0	10.87	-2.85	9.0E-4	0.0545	+	sbnC	RSAU_000072
81164.0	0.32	0.32	0.6918	0.9852	+	sbnC	RSAU_000073
81165.0	37.15	-0.29	0.6327	0.9483	+	sbnC	RSAU_000073
83937.0	2.22	-0.12	0.8887	0.9889	+		RSAU_000075
84938.0	1.2	1.56	0.0737	0.5985	+		RSAU_000075
86522.0	6.39	-2.96	6.0E-4	0.0446	+		RSAU_000077
91109.0	6.2	0.32	0.7191	0.9889	+		RSAU_000082
91177.0	0.43	-0.1	0.9048	0.9889	+		RSAU_000082
94424.0	3.72	0.38	0.6581	0.9656	+	capH2	RSAU_000085
97641.0	1.33	-0.7	0.4229	0.8147	+	sasD	RSAU_000088
97643.0	0.41	-1.31	0.1267	0.5985	+	sasD	RSAU_000088
101411.0	1.29	-0.76	0.3884	0.79	+	deoC1	RSAU_000092

101813.0	0.41	0.46	0.6005	0.9402	+	deoC1	RSAU_000092
105228.0	0.69	-0.52	0.5174	0.9024	-	phnC	RSAU_000096
106206.0	1.82	-0.77	0.3846	0.7877	-		RSAU_000097
106208.0	1.27	-0.8	0.3672	0.7714	-		RSAU_000097
109172.0	1.57	-0.69	0.3713	0.7746	+	cpdB	RSAU_000099
109446.0	5.84	-0.82	0.3213	0.7152	+	cpdB	RSAU_000099
109866.0	0.31	0.98	0.2331	0.5985	+	cpdB	RSAU_000099
110032.0	2.27	-2.58	0.0036	0.1465	+	cpdB	RSAU_000099
112823.0	1.33	-1.29	0.1472	0.5985	+	adhE	RSAU_000102
114043.0	3.98	-1.39	0.0973	0.5985	+	adhE	RSAU_000102
119055.0	1.14	-0.55	0.54	0.9042	+	capD	RSAU_000106
119093.0	0.53	-1.15	0.1672	0.5985	+	capD	RSAU_000106
122859.0	1.1	-0.41	0.5969	0.9402	+	capG	RSAU_000109
123971.0	0.33	-1.08	0.1895	0.5985	+	capH1	RSAU_000110
126681.0	0.26	0.96	0.2392	0.5985	+	capK	RSAU_000113
128205.0	11.22	-0.65	0.4619	0.8493	+	capL	RSAU_000114
128206.0	0.41	-0.22	0.7855	0.9889	+	capL	RSAU_000114
128324.0	0.38	-0.16	0.8442	0.9889	+	capL	RSAU_000114
129390.0	0.38	1.17	0.1692	0.5985	+	capN	RSAU_000116
133831.0	0.54	0.16	0.8538	0.9889	+	aldA1	RSAU_000121
134575.0	9.06	-2.46	0.0039	0.1465	+	aldA1	RSAU_000121
135555.0	0.31	0.98	0.2331	0.5985			
135556.0	24.72	0.8	0.2789	0.6499			
137572.0	0.32	0.32	0.6918	0.9852	+		RSAU_000124
139928.0	0.69	-0.52	0.5174	0.9024	+		RSAU_000127
142122.0	0.32	0.32	0.6918	0.9852			
142441.0	0.39	-0.39	0.6404	0.9553	+		RSAU_000129
142525.0	1.97	-0.49	0.563	0.9148	+		RSAU_000129
142620.0	2.37	1.75	0.0466	0.5706	+		RSAU_000129
143463.0	0.46	-1.31	0.1257	0.5985	+		RSAU_000129
145620.0	0.22	0.04	0.9554	0.9889	+		RSAU_000130
146143.0	0.41	-0.22	0.7855	0.9889	+		RSAU_000130
149611.0	21.3	-2.7	3.0E-4	0.024	+		RSAU_000130
152320.0	0.95	-0.86	0.3237	0.7152	-		RSAU_000132
152321.0	90.37	-0.91	0.1111	0.5985	-		RSAU_000132
154295.0	53.97	-1.59	0.037	0.5052	-	argJ	RSAU_000134
154296.0	0.46	0.66	0.4528	0.8474	-	argJ	RSAU_000134
154646.0	0.38	-0.16	0.8442	0.9889	-	argJ	RSAU_000134
155106.0	0.47	-0.13	0.8717	0.9889	-	argC1	RSAU_000135
155853.0	2.39	0.84	0.3304	0.7244	-	argC1	RSAU_000135
159071.0	0.37	-0.43	0.6051	0.9402	-		RSAU_000138
159078.0	0.32	0.98	0.2303	0.5985	-		RSAU_000138
159145.0	0.36	-0.19	0.8176	0.9889	-		RSAU_000138
159610.0	0.41	-0.22	0.7855	0.9889	-		RSAU_000138
159635.0	2.12	-0.2	0.8091	0.9889	-		RSAU_000138
159745.0	0.6	-0.49	0.545	0.9042	-		RSAU_000138
159767.0	7.37	-1.7	0.0563	0.5815	-		RSAU_000138
160237.0	2.39	-0.84	0.3442	0.7425	-		RSAU_000138
160475.0	10.16	1.02	0.0829	0.5985	-		RSAU_000138
160494.0	0.43	0.05	0.9531	0.9889	-		RSAU_000138
160526.0	2.01	-2.56	0.0040	0.1465	-		RSAU_000138
161847.0	8.15	0.27	0.6894	0.9852	-	ipdC	RSAU_000139
164639.0	14.16	0.94	0.2536	0.6197	-	glcA	RSAU_000140
165013.0	2.0	-1.05	0.2404	0.5989	-	glcA	RSAU_000140
165014.0	211.6	-1.09	0.0842	0.5985	-	glcA	RSAU_000140
165015.0	1.67	1.18	0.1722	0.5985	-	glcA	RSAU_000140
167746.0	0.6	-0.49	0.545	0.9042	+		RSAU_000144
172283.0	1.43	-0.59	0.4562	0.8489	+	hsdR	RSAU_000147
183375.0	0.43	-0.1	0.9048	0.9889	+	ggt	RSAU_000153
183849.0	0.37	-1.09	0.1867	0.5985	-		RSAU_000154
184768.0	0.22	0.04	0.9554	0.9889	-	azoR	RSAU_000155
184830.0	0.36	-0.19	0.8176	0.9889	-	azoR	RSAU_000155
184993.0	0.53	0.02	0.9779	0.9889	-	azoR	RSAU_000155
187108.0	1.18	-1.08	0.2188	0.5985	+		RSAU_000157
188492.0	4.06	0.46	0.5346	0.9042	+		RSAU_000158
188546.0	1.4	-0.41	0.639	0.9553	+		RSAU_000158
191021.0	1.4	-0.01	0.9892	0.9933			
191384.0	0.65	-0.11	0.9007	0.9889	+		RSAU_000161
191944.0	0.38	1.17	0.1692	0.5985	+		RSAU_000161
192193.0	3.46	-1.65	0.0639	0.5985			
192194.0	792.22	-3.0	0.0	0.0083			
192195.0	4.28	-2.27	0.0106	0.2403			
197103.0	1.87	1.18	0.183	0.5985	-		RSAU_000167
201143.0	1.56	-0.73	0.3481	0.7474	+	pflB	RSAU_000170
203737.0	0.38	-0.16	0.8442	0.9889	+	pflA	RSAU_000171
204796.0	2.96	-0.29	0.7455	0.9889	+		RSAU_000172
205823.0	0.2	0.02	0.9822	0.9889	+		RSAU_000172
206378.0	13.43	-1.07	0.1486	0.5985	-		RSAU_000174
206379.0	10.88	-1.08	0.1107	0.5985	-		RSAU_000174
210132.0	0.26	0.96	0.2392	0.5985	-	fadA	RSAU_000176
212310.0	0.53	-1.15	0.1672	0.5985	-	fadB	RSAU_000177
217883.0	1.15	0.19	0.8308	0.9889			
218016.0	0.44	1.33	0.1252	0.5985	+		RSAU_000181
218017.0	56.85	-0.72	0.2151	0.5985	+		RSAU_000181
218018.0	0.6	-0.08	0.9254	0.9889	+		RSAU_000181
221167.0	5.21	0.14	0.8757	0.9889	-		RSAU_000183
222818.0	1.0	-0.08	0.9222	0.9889	-		RSAU_000185

231038.0	0.38	-0.16	0.8442	0.9889			
231826.0	0.66	-1.31	0.1224	0.5985	+	gatC2	RSAU_000192
234705.0	0.33	-1.08	0.1895	0.5985			
235137.0	0.53	-1.15	0.1672	0.5985	+		RSAU_000195
236267.0	0.95	-1.41	0.0992	0.5985	+		RSAU_000196
236314.0	0.75	-1.5	0.0839	0.5985	+		RSAU_000196
236785.0	1.06	1.55	0.0759	0.5985	+		RSAU_000196
237582.0	9.76	0.17	0.8402	0.9889	+		RSAU_000197
244221.0	1.61	-1.76	0.0445	0.5626	+		RSAU_000202
246259.0	9.02	-0.42	0.6249	0.9445	+		RSAU_000203
246394.0	6.96	0.86	0.2599	0.6303	+		RSAU_000203
247549.0	2.09	1.03	0.1973	0.5985	-		RSAU_000204
247728.0	5.3	-0.44	0.6196	0.9445	-		RSAU_000204
248134.0	0.26	0.96	0.2392	0.5985	+		RSAU_000205
248135.0	0.37	-0.43	0.6051	0.9402	+		RSAU_000205
250042.0	0.53	-1.15	0.1672	0.5985	+	lytS	RSAU_000207
250571.0	0.69	-0.28	0.7505	0.9889	+	lytS	RSAU_000207
250851.0	7.98	0.72	0.4107	0.8073	+	lytS	RSAU_000207
253170.0	0.52	0.1	0.902	0.9889	+	lrgB	RSAU_000210
254752.0	1.13	0.58	0.467	0.8527	+		RSAU_000212
256187.0	1.74	-1.33	0.1357	0.5985	+	bglA	RSAU_000213
258926.0	117.03	-0.89	0.1905	0.5985	-	rbsK	RSAU_000215
258927.0	68.85	-1.02	0.1454	0.5985	-	rbsK	RSAU_000215
258928.0	2.33	-0.29	0.7338	0.9889	-	rbsK	RSAU_000215
258935.0	0.26	0.96	0.2392	0.5985	-	rbsK	RSAU_000215
261076.0	0.22	0.04	0.9554	0.9889	-		RSAU_000218
263873.0	0.74	-0.29	0.741	0.9889	-		RSAU_000220
263874.0	138.78	-0.38	0.503	0.8913	-		RSAU_000220
263875.0	0.99	0.99	0.2662	0.6354	-		RSAU_000220
263993.0	3.11	-1.1	0.179	0.5985			
265654.0	0.82	-1.32	0.1186	0.5985	+	lytM	RSAU_000222
265729.0	0.43	-0.1	0.9048	0.9889	+	lytM	RSAU_000222
268854.0	8.84	-0.37	0.6809	0.981	-		RSAU_000225
273461.0	0.66	0.38	0.668	0.9723	+	esaA	RSAU_000229
275073.0	0.98	-0.63	0.4213	0.8128	+	esaA	RSAU_000229
278780.0	1.2	-0.65	0.4573	0.8493	+	essC	RSAU_000233
279385.0	1.01	-0.92	0.2992	0.6823	+	essC	RSAU_000233
280537.0	1.08	0.09	0.9045	0.9889	+	essC	RSAU_000233
281530.0	1.84	-0.48	0.5875	0.9341	+	essC	RSAU_000233
282101.0	1.85	-0.6	0.494	0.879	+	essC	RSAU_000233
284587.0	0.43	-0.1	0.9048	0.9889	+		RSAU_000238
286765.0	0.62	0.17	0.8289	0.9889	+		RSAU_000240
290228.0	0.62	1.34	0.119	0.5985			
291264.0	0.89	0.25	0.7702	0.9889	+		RSAU_000246
291772.0	2.96	1.66	0.0583	0.5815	+		RSAU_000247
293065.0	0.38	1.17	0.1692	0.5985			
293067.0	0.26	0.96	0.2392	0.5985			
294446.0	3.98	0.83	0.2892	0.6667	-		RSAU_000251
295901.0	1.72	0.11	0.8925	0.9889	-	brnQ	RSAU_000252
299243.0	0.58	-1.56	0.0751	0.5985	+		RSAU_000254
302760.0	4.9	-2.72	8.0E-4	0.0512	+		RSAU_000257
305553.0	0.26	0.96	0.2392	0.5985	-		RSAU_000260
307908.0	0.37	-1.09	0.1867	0.5985	+		RSAU_000262
307960.0	0.46	0.66	0.4528	0.8474	+		RSAU_000262
310730.0	0.27	0.1	0.8977	0.9889	-		RSAU_000265
316080.0	0.22	0.04	0.9554	0.9889	-		RSAU_000268
317968.0	0.81	-0.27	0.7257	0.9889	+		RSAU_000269
318684.0	0.36	-0.19	0.8176	0.9889	+		RSAU_000271
319558.0	0.49	-0.51	0.5578	0.9121	+		RSAU_000272
319677.0	16.87	0.73	0.4056	0.8012	+		RSAU_000272
321985.0	0.53	-1.15	0.1672	0.5985	+		RSAU_000274
324543.0	0.72	-0.54	0.5336	0.9042	-		RSAU_000277
325334.0	1.32	-1.62	0.0631	0.5985	-		RSAU_000278
329985.0	1.14	0.07	0.94	0.9889	-	glpT	RSAU_000282
338839.0	1.99	-0.53	0.5361	0.9042	+	fepC	RSAU_000290
339379.0	0.42	-0.19	0.8115	0.9889	+	fepC	RSAU_000290
342743.0	0.33	-1.08	0.1895	0.5985	+		RSAU_000296
351225.0	0.6	-0.49	0.545	0.9042	-	metE2	RSAU_000302
359577.0	0.26	0.96	0.2392	0.5985			
360852.0	0.33	-1.08	0.1895	0.5985	-		RSAU_000313
362961.0	0.96	0.6	0.491	0.8774			
367311.0	1.25	0.12	0.8955	0.9889	-		RSAU_000321
369120.0	1.11	0.03	0.9675	0.9889	-		RSAU_000322
369648.0	0.92	0.77	0.3893	0.7907	-	ahpF	RSAU_000323
369938.0	2.3	-2.0	0.0232	0.3993	-	ahpF	RSAU_000323
370733.0	1.22	-0.16	0.8536	0.9889	-	ahpF	RSAU_000323
371669.0	0.2	0.02	0.9822	0.9889			
372663.0	0.27	0.1	0.8977	0.9889	+		RSAU_000325
372780.0	0.69	-0.52	0.5174	0.9024			
378242.0	0.43	0.05	0.9531	0.9889	+	xpt	RSAU_000332
379426.0	1.59	-0.55	0.5184	0.9024	+	pbuX	RSAU_000333
379470.0	1.36	0.72	0.4193	0.8128	+	pbuX	RSAU_000333
379471.0	268.3	-0.16	0.8355	0.9889	+	pbuX	RSAU_000333
379472.0	1.71	0.08	0.9243	0.9889	+	pbuX	RSAU_000333
381419.0	0.31	0.98	0.2331	0.5985	+	guaA	RSAU_000335
381527.0	10.04	-3.09	0.0	0.0064	+	guaA	RSAU_000335
381548.0	9.81	-3.16	0.0	0.0038	+	guaA	RSAU_000335

381572.0	1.76	-1.93	0.0266	0.4269	+	guaA	RSAU_000335
382063.0	2.21	-1.88	0.0338	0.4817	+	guaA	RSAU_000335
382064.0	415.85	-4.27	0.0	0.0	+	guaA	RSAU_000335
382065.0	1.6	-2.35	0.0083	0.207	+	guaA	RSAU_000335
382084.0	3.77	-3.18	2.0E-4	0.024	+	guaA	RSAU_000335
382305.0	0.53	-1.15	0.1672	0.5985	+	guaA	RSAU_000335
382692.0	43.97	-2.93	2.0E-4	0.024	+	guaA	RSAU_000335
382693.0	10212.53	-4.2	0.0	0.0	+	guaA	RSAU_000335
382694.0	105.51	-3.24	1.0E-4	0.0167	+	guaA	RSAU_000335
382708.0	0.38	-0.16	0.8442	0.9889	+	guaA	RSAU_000335
383693.0	0.32	0.32	0.6918	0.9852	+		RSAU_000336
385985.0	29.28	1.04	0.0308	0.4602			
385986.0	0.61	0.2	0.8159	0.9889			
386982.0	0.43	0.05	0.9531	0.9889	-		RSAU_000340
386984.0	9.59	0.46	0.5487	0.9048	-		RSAU_000340
386985.0	0.2	0.02	0.9822	0.9889	-		RSAU_000340
389380.0	2.38	-1.96	0.0261	0.4234			
389752.0	1.78	0.34	0.6988	0.9889	-		RSAU_000344
390074.0	0.46	1.17	0.1668	0.5985	-		RSAU_000344
391306.0	0.2	0.02	0.9822	0.9889	-		RSAU_000345
391383.0	0.36	-0.19	0.8176	0.9889	-		RSAU_000345
391876.0	1.74	-0.2	0.8159	0.9889	-		RSAU_000346
392010.0	6.95	-1.68	0.059	0.5815	-		RSAU_000347
392484.0	1.91	-0.43	0.6145	0.9442	-		RSAU_000349
392722.0	10.16	1.02	0.0829	0.5985	-		RSAU_000349
392741.0	0.2	0.02	0.9822	0.9889	-		RSAU_000349
392904.0	1.16	0.24	0.7845	0.9889			
397743.0	0.67	-0.61	0.4825	0.8707	+		RSAU_000354
410232.0	4.42	0.7	0.4212	0.8128	+		RSAU_000365
415957.0	2.41	0.78	0.3828	0.786	+		RSAU_000371
416051.0	2.59	0.56	0.4927	0.8775	+		RSAU_000371
417022.0	0.53	-1.15	0.1672	0.5985	+		RSAU_000372
418679.0	1.15	-1.9	0.0324	0.4762	+		RSAU_000374
427764.0	0.36	-0.19	0.8176	0.9889	+		RSAU_000386
430478.0	0.79	0.32	0.6801	0.981	-		RSAU_000388
430522.0	1.54	0.98	0.2684	0.6369	-		RSAU_000388
431831.0	4.53	-0.67	0.4272	0.8206	+		RSAU_000390
432898.0	0.33	-1.08	0.1895	0.5985	+		RSAU_000391
433015.0	2.47	-0.24	0.7771	0.9889	+		RSAU_000391
433025.0	0.31	0.98	0.2331	0.5985	+		RSAU_000391
433026.0	49.68	0.66	0.1605	0.5985	+		RSAU_000391
433027.0	0.39	1.17	0.1684	0.5985	+		RSAU_000391
433152.0	2.25	0.0	0.995	0.9974	+		RSAU_000391
433163.0	0.85	0.26	0.7406	0.9889	+		RSAU_000391
433164.0	40.23	0.91	0.1683	0.5985	+		RSAU_000391
435338.0	0.26	0.96	0.2392	0.5985	+	cysM	RSAU_000393
435904.0	0.26	0.96	0.2392	0.5985	+	cysM	RSAU_000393
437279.0	0.22	0.04	0.9554	0.9889	+	metN	RSAU_000394
439205.0	0.89	-0.89	0.3086	0.6954	+		RSAU_000396
439497.0	4.72	0.43	0.6261	0.9445			
440977.0	3.4	0.44	0.6203	0.9445	-		RSAU_000399
443102.0	0.67	-0.36	0.6483	0.9604	-		RSAU_000403
443459.0	0.36	-0.19	0.8176	0.9889	-		RSAU_000403
445105.0	0.36	-0.19	0.8176	0.9889	-	gltC	RSAU_000404
445107.0	0.37	-1.09	0.1867	0.5985	-	gltC	RSAU_000404
452122.0	385.21	-1.06	0.1814	0.5985			
464135.0	0.41	-0.22	0.7855	0.9889	+		RSAU_000416
464136.0	18.98	-1.01	0.2555	0.6227	+		RSAU_000416
464345.0	0.67	0.43	0.6214	0.9445	+		RSAU_000416
464379.0	0.36	-0.19	0.8176	0.9889	+		RSAU_000416
465193.0	0.32	0.98	0.2303	0.5985	+		RSAU_000416
465339.0	0.38	1.17	0.1692	0.5985	+		RSAU_000416
465745.0	0.38	1.17	0.1692	0.5985	+		RSAU_000417
466332.0	0.38	-0.16	0.8442	0.9889			
468656.0	5.72	1.4	0.1007	0.5985	+	yaaQ	RSAU_000420
471665.0	1.78	-0.55	0.537	0.9042	+		RSAU_000424
473020.0	0.44	0.49	0.5479	0.9042	+		RSAU_000426
477203.0	0.55	-0.7	0.4273	0.8206	+	ksgA	RSAU_000430
479732.0	8.16	-2.56	0.0021	0.097	+	purR	RSAU_000433
479823.0	0.33	-1.08	0.1895	0.5985	+	purR	RSAU_000433
479863.0	48.66	-1.13	0.1934	0.5985	+	purR	RSAU_000433
479864.0	0.41	-0.22	0.7855	0.9889	+	purR	RSAU_000433
482277.0	0.39	1.17	0.1684	0.5985	+	glmU	RSAU_000438
487303.0	0.2	0.02	0.9822	0.9889	+	mfd	RSAU_000442
487354.0	1.39	-1.44	0.092	0.5985	+	mfd	RSAU_000442
488484.0	1.07	-0.74	0.4038	0.8012	+	mfd	RSAU_000442
488672.0	1.11	0.0	0.9995	0.9995	+	mfd	RSAU_000442
488673.0	100.58	-0.38	0.4816	0.8707	+	mfd	RSAU_000442
488674.0	0.7	0.19	0.8104	0.9889	+	mfd	RSAU_000442
489417.0	0.75	-1.5	0.0839	0.5985	+	mfd	RSAU_000442
489955.0	0.68	0.66	0.4164	0.8128	+	mfd	RSAU_000443
490186.0	0.53	-1.15	0.1672	0.5985	+	mfd	RSAU_000443
495336.0	0.2	0.02	0.9822	0.9889	+	hpt	RSAU_000449
498113.0	12.76	-0.18	0.8222	0.9889			
498630.0	0.26	0.96	0.2392	0.5985	+	hslO	RSAU_000451
498902.0	0.77	-1.33	0.1183	0.5985	+	hslO	RSAU_000451
501039.0	0.62	0.17	0.8289	0.9889	+	folP	RSAU_000453

502000.0	0.2	0.02	0.9822	0.9889	+	folK	RSAU_000455
504631.0	0.96	-0.01	0.9931	0.9968	+		RSAU_000457
506017.0	0.43	1.17	0.1679	0.5985	+		RSAU_000466
507003.0	0.62	-0.45	0.5761	0.9244	+		RSAU_000466
508845.0	0.41	-0.22	0.7855	0.9889	+		RSAU_000467
508846.0	18.29	-1.01	0.255	0.6224	+		RSAU_000467
509055.0	0.67	0.43	0.6214	0.9445	+		RSAU_000467
509809.0	0.39	1.17	0.1684	0.5985	+		RSAU_000467
509902.0	0.32	0.98	0.2303	0.5985	+		RSAU_000467
510048.0	0.38	1.17	0.1692	0.5985	+		RSAU_000467
510613.0	0.41	-0.22	0.7855	0.9889			
519523.0	1.83	-0.08	0.9263	0.9889	+	clpC	RSAU_000476
520418.0	0.77	-0.32	0.7153	0.9889			
525391.0	4.6	-2.25	0.0060	0.1823			
530192.0	0.41	0.06	0.9415	0.9889	+	secE	RSAU_000487
533625.0	0.2	0.02	0.9822	0.9889			
535928.0	0.36	-0.19	0.8176	0.9889	+	rpoB	RSAU_000494
546815.0	0.68	1.26	0.14	0.5985	+	tuf	RSAU_000500
550001.0	0.42	-0.19	0.8115	0.9889			
551248.0	0.96	-0.19	0.8308	0.9889	+	araB	RSAU_000504
551249.0	0.64	-0.87	0.3279	0.7212	+	araB	RSAU_000504
551286.0	6.88	0.35	0.6664	0.9723	+	araB	RSAU_000504
551287.0	0.36	-0.19	0.8176	0.9889	+	araB	RSAU_000504
552213.0	0.31	0.98	0.2331	0.5985	+	araB	RSAU_000504
552272.0	0.53	-1.15	0.1672	0.5985	+	araB	RSAU_000504
556307.0	0.65	0.36	0.6578	0.9656			
556605.0	0.82	-1.32	0.1186	0.5985	-		RSAU_000508
558486.0	1.22	-1.04	0.2316	0.5985	+		RSAU_000511
562648.0	0.5	1.28	0.1358	0.5985	+	sdrC	RSAU_000513
563836.0	0.22	0.04	0.9554	0.9889	+	sdrD	RSAU_000515
564625.0	0.41	-0.22	0.7855	0.9889	+	sdrD	RSAU_000515
565436.0	1.56	-0.48	0.5848	0.9313	+	sdrD	RSAU_000515
566950.0	0.51	1.35	0.1191	0.5985	+	sdrD	RSAU_000515
570146.0	0.26	0.96	0.2392	0.5985	+	sdrE	RSAU_000517
570828.0	0.67	-0.61	0.4825	0.8707	+	sdrE	RSAU_000517
578023.0	7.19	-1.45	0.0949	0.5985	+	hps	RSAU_000524
578150.0	0.31	0.98	0.2331	0.5985	+	hps	RSAU_000524
579162.0	2.63	-0.41	0.6211	0.9445	+		RSAU_000526
579372.0	0.26	0.96	0.2392	0.5985	+		RSAU_000526
581487.0	0.22	0.04	0.9554	0.9889			
585714.0	1.55	-0.55	0.483	0.8709			
586351.0	13.71	0.78	0.2613	0.6329	-	thiD1	RSAU_000531
586352.0	0.36	-0.19	0.8176	0.9889	-	thiD1	RSAU_000531
593214.0	0.38	-0.16	0.8442	0.9889	+	pta	RSAU_000540
599327.0	10.95	0.32	0.7151	0.9889	-		RSAU_000546
602052.0	13.16	0.5	0.4215	0.8128	+		RSAU_000548
605038.0	0.36	-0.19	0.8176	0.9889	+		RSAU_000552
605325.0	1.91	-1.08	0.2269	0.5985	+		RSAU_000552
605954.0	1.15	-0.25	0.7674	0.9889	+		RSAU_000553
606089.0	0.58	-0.22	0.7924	0.9889	+		RSAU_000553
609141.0	0.53	-1.15	0.1672	0.5985	+		RSAU_000557
610348.0	0.77	-1.33	0.1183	0.5985	+		RSAU_000559
610583.0	0.63	-0.68	0.4155	0.8128			
612088.0	1.74	-1.01	0.2396	0.5985	+		RSAU_000561
613318.0	1.05	0.23	0.7988	0.9889	+	adhA	RSAU_000562
614150.0	0.32	0.32	0.6918	0.9852			
616319.0	24.03	-0.58	0.5085	0.8989			
617101.0	1.17	1.17	0.1848	0.5985	+		RSAU_000565
621938.0	0.53	0.75	0.3988	0.8008	+		RSAU_000571
621939.0	180.53	-0.3	0.5211	0.903	+		RSAU_000571
621940.0	1.52	-0.16	0.8587	0.9889	+		RSAU_000571
622026.0	10.44	-0.59	0.4972	0.8839	+		RSAU_000571
622226.0	1.56	0.43	0.628	0.9445	+		RSAU_000571
622526.0	1.03	-1.58	0.0691	0.5985			
627559.0	0.38	1.17	0.1692	0.5985	+	mnhA1	RSAU_000578
628050.0	6.18	1.01	0.1606	0.5985	+	mnhA1	RSAU_000578
629095.0	2.49	-0.93	0.2955	0.6778	+	mnhA1	RSAU_000578
630521.0	0.62	-0.45	0.5761	0.9244	+	mnhD1	RSAU_000581
634670.0	0.48	0.07	0.9354	0.9889	+		RSAU_000585
634984.0	0.2	0.02	0.9822	0.9889	+		RSAU_000585
635066.0	2.69	-0.43	0.6174	0.9445	+		RSAU_000585
635969.0	0.38	-0.16	0.8442	0.9889	-	rsaC	RSAU_000586
635970.0	68.55	-0.71	0.2498	0.6134	-	rsaC	RSAU_000586
635971.0	0.57	-0.13	0.8857	0.9889	-	rsaC	RSAU_000586
640894.0	0.71	0.39	0.6541	0.9656	+	tagA	RSAU_000592
640896.0	0.77	-1.33	0.1183	0.5985	+	tagA	RSAU_000592
642622.0	18.75	0.77	0.2934	0.6739			
642623.0	1996.71	-0.09	0.8746	0.9889			
642624.0	11.28	0.09	0.897	0.9889			
642844.0	0.38	-0.16	0.8442	0.9889	+	tagG	RSAU_000594
651465.0	5.86	0.18	0.7992	0.9889			
653760.0	0.47	-0.13	0.8717	0.9889	+		RSAU_000606
654870.0	0.6	0.2	0.798	0.9889	+		RSAU_000608
658762.0	2.74	0.24	0.7816	0.9889	+		RSAU_000609
658849.0	3.86	-0.99	0.1875	0.5985	+		RSAU_000609
659036.0	0.36	-0.19	0.8176	0.9889	+		RSAU_000609
659256.0	0.36	-0.19	0.8176	0.9889	+		RSAU_000609

659499.0	0.71	-0.48	0.5476	0.9042	+		RSAU_000609
660491.0	1.28	0.08	0.9323	0.9889	+		RSAU_000611
660540.0	0.22	0.04	0.9554	0.9889	+		RSAU_000611
660564.0	1.65	-2.05	0.0209	0.3773	+		RSAU_000611
665956.0	1.29	-1.85	0.0364	0.5052	+		RSAU_000616
666477.0	0.62	-1.49	0.088	0.5985			
669868.0	6.99	-0.45	0.6062	0.9402	+		RSAU_000621
669996.0	1.92	-2.54	0.0042	0.147	+		RSAU_000621
670028.0	0.43	0.05	0.9531	0.9889	+		RSAU_000621
670047.0	10.3	1.04	0.0786	0.5985	+		RSAU_000621
670285.0	3.01	-1.14	0.1961	0.5985	+		RSAU_000621
670755.0	7.8	-1.72	0.0542	0.5815	+		RSAU_000621
670777.0	0.6	-0.49	0.545	0.9042	+		RSAU_000621
670827.0	0.36	0.36	0.6599	0.9656	+		RSAU_000621
670887.0	2.98	-0.26	0.7559	0.9889	+		RSAU_000621
670912.0	0.41	-0.22	0.7855	0.9889	+		RSAU_000621
671377.0	0.36	-0.19	0.8176	0.9889	+		RSAU_000621
671444.0	0.32	0.98	0.2303	0.5985	+		RSAU_000621
671451.0	0.29	-0.27	0.7469	0.9889	+		RSAU_000621
675412.0	0.2	0.02	0.9822	0.9889	+	fhuB	RSAU_000624
675568.0	0.32	0.98	0.2303	0.5985	+	fhuB	RSAU_000624
676407.0	0.6	-0.49	0.545	0.9042	+	fhuG	RSAU_000625
677409.0	0.38	-0.16	0.8442	0.9889	+	dhaK	RSAU_000626
679195.0	0.39	1.17	0.1684	0.5985			
684805.0	1.78	-0.01	0.9953	0.9974	+		RSAU_000634
691937.0	0.93	-0.22	0.8058	0.9889			
692045.0	1.02	0.72	0.3677	0.7714			
694194.0	1.34	-0.08	0.9269	0.9889	+		RSAU_000642
694943.0	0.93	0.17	0.8511	0.9889	+		RSAU_000643
696619.0	1.63	-1.57	0.0695	0.5985	+		RSAU_000643
699146.0	0.22	0.04	0.9554	0.9889			
699159.0	32.56	1.09	0.1312	0.5985			
699160.0	0.42	-0.19	0.8115	0.9889			
699275.0	8.13	-1.97	0.0114	0.2499			
700736.0	2.74	-0.1	0.9112	0.9889	+		RSAU_000648
700737.0	0.77	1.55	0.0771	0.5985	+		RSAU_000648
702481.0	0.85	-0.23	0.7669	0.9889	+		RSAU_000650
702742.0	0.32	0.98	0.2303	0.5985	+		RSAU_000650
702743.0	24.59	0.68	0.3666	0.7714	+		RSAU_000650
703594.0	0.38	-0.16	0.8442	0.9889	-		RSAU_000651
704313.0	3.17	-1.32	0.1286	0.5985	+		RSAU_000653
708179.0	1.29	-0.66	0.3999	0.8008	-	uppP	RSAU_000659
708533.0	3.02	-0.97	0.2666	0.6354	-	uppP	RSAU_000659
708767.0	0.26	0.96	0.2392	0.5985			
709492.0	3.23	-1.42	0.0653	0.5985	+		RSAU_000660
712604.0	2.4	-0.86	0.3313	0.7244	-	mgrA	RSAU_000662
715612.0	0.76	-0.39	0.6177	0.9445	+		RSAU_000666
717851.0	0.26	0.96	0.2392	0.5985	+		RSAU_000667
720516.0	2.99	-0.78	0.3056	0.6927	+	norA	RSAU_000670
720564.0	1.63	-0.9	0.314	0.7026	+	norA	RSAU_000670
722921.0	0.48	-0.5	0.5479	0.9042			
723843.0	2.68	-0.44	0.5949	0.9402	+	fruB	RSAU_000674
723902.0	0.37	-0.43	0.6051	0.9402	+	fruB	RSAU_000674
724172.0	0.37	-1.09	0.1867	0.5985	+	fruB	RSAU_000674
724189.0	0.8	-1.66	0.0586	0.5815	+	fruB	RSAU_000674
724193.0	0.51	-0.49	0.5791	0.9253	+	fruB	RSAU_000674
724360.0	0.39	-0.39	0.6404	0.9553	+	fruB	RSAU_000674
726759.0	1.52	-0.82	0.3602	0.7631			
728708.0	0.26	0.96	0.2392	0.5985	+		RSAU_000677
731103.0	2.28	0.02	0.9771	0.9889	+		RSAU_000679
734382.0	1.4	0.0	0.9992	0.9995			
738079.0	0.37	-1.09	0.1867	0.5985			
738831.0	2.54	-2.07	0.0195	0.365	+	pabB	RSAU_000689
741922.0	0.36	-0.19	0.8176	0.9889	+	atzF2	RSAU_000692
743976.0	0.26	0.96	0.2392	0.5985	+	ltaS	RSAU_000693
745476.0	1.21	-0.37	0.6757	0.9797	+		RSAU_000694
747003.0	0.31	0.98	0.2331	0.5985	+		RSAU_000694
748450.0	0.26	0.96	0.2392	0.5985	+	recQ1	RSAU_000695
752022.0	0.88	-0.04	0.9594	0.9889	+	hisC2	RSAU_000698
753400.0	1.34	-0.25	0.7817	0.9889	+		RSAU_000699
754746.0	0.37	-1.09	0.1867	0.5985	-		RSAU_000700
755495.0	0.2	0.02	0.9822	0.9889			
755741.0	6.92	-0.3	0.731	0.9889	+		RSAU_000701
755867.0	1.06	-0.81	0.3228	0.7152	+		RSAU_000701
755869.0	1.92	-2.54	0.0042	0.147	+		RSAU_000701
755901.0	0.43	0.05	0.9531	0.9889	+		RSAU_000701
755920.0	10.16	1.02	0.0829	0.5985	+		RSAU_000701
756158.0	2.92	-1.11	0.2074	0.5985	+		RSAU_000701
756628.0	8.08	-1.73	0.0518	0.5815	+		RSAU_000701
756650.0	0.6	-0.49	0.545	0.9042	+		RSAU_000701
756700.0	0.36	0.36	0.6599	0.9656	+		RSAU_000701
756760.0	3.26	-0.15	0.8598	0.9889	+		RSAU_000701
756785.0	0.41	-0.22	0.7855	0.9889	+		RSAU_000701
757250.0	0.36	-0.19	0.8176	0.9889	+		RSAU_000701
757316.0	0.77	0.9	0.3061	0.693	+		RSAU_000701
757317.0	0.32	0.98	0.2303	0.5985	+		RSAU_000701
757324.0	0.2	0.02	0.9822	0.9889	+		RSAU_000701

759395.0	9.38	1.25	0.1359	0.5985	-	queF	RSAU_000703
760429.0	0.59	0.19	0.8284	0.9889	-		RSAU_000704
761336.0	0.77	-0.43	0.6277	0.9445			
763670.0	0.38	-0.16	0.8442	0.9889	+	nrdE	RSAU_000706
763671.0	1.48	0.46	0.5955	0.9402	+	nrdE	RSAU_000706
765187.0	0.41	-0.22	0.7855	0.9889			
767624.0	0.75	-0.88	0.3234	0.7152	+		RSAU_000710
773930.0	5.4	0.5	0.5733	0.923	+	glxK	RSAU_000717
774023.0	0.94	-0.9	0.3025	0.6889	+	glxK	RSAU_000717
774519.0	0.2	0.02	0.9822	0.9889	+	glxK	RSAU_000717
774626.0	0.61	0.2	0.8159	0.9889			
775373.0	0.47	-0.13	0.8717	0.9889	-	pepT	RSAU_000718
777423.0	0.26	0.96	0.2392	0.5985			
777424.0	0.5	1.28	0.1358	0.5985			
778095.0	8.27	0.11	0.8971	0.9889	-		RSAU_000721
780272.0	0.26	0.96	0.2392	0.5985	-		RSAU_000723
781599.0	0.31	0.98	0.2331	0.5985	+		RSAU_000724
782254.0	0.73	1.38	0.1095	0.5985	+	comFA	RSAU_000725
783157.0	0.86	-1.71	0.0534	0.5815	+	comFA	RSAU_000725
789755.0	0.69	0.1	0.9093	0.9889	+		RSAU_000730
790389.0	0.89	1.05	0.2315	0.5985	+		RSAU_000731
792508.0	0.63	-1.55	0.0762	0.5985	+	uvrB	RSAU_000733
793666.0	5.42	-1.74	0.0387	0.5099	+	uvrA	RSAU_000734
794056.0	4.26	0.36	0.6668	0.9723	+	uvrA	RSAU_000734
794666.0	0.37	-1.09	0.1867	0.5985	+	uvrA	RSAU_000734
796099.0	0.36	-0.19	0.8176	0.9889	+	uvrA	RSAU_000734
796107.0	0.22	0.04	0.9554	0.9889	+	uvrA	RSAU_000734
796398.0	0.7	-1.03	0.2484	0.6118			
797954.0	0.38	-0.16	0.8442	0.9889	+	hprK	RSAU_000735
808707.0	7.34	0.55	0.5339	0.9042	-		RSAU_000746
808708.0	744.72	1.01	0.2294	0.5985	-		RSAU_000746
808709.0	7.72	1.58	0.0745	0.5985	-		RSAU_000746
811298.0	0.75	0.02	0.9767	0.9889			
821251.0	0.36	-0.19	0.8176	0.9889	+	vacB	RSAU_000758
821560.0	0.54	0.16	0.8538	0.9889	+	vacB	RSAU_000758
822122.0	0.38	1.17	0.1692	0.5985	+	vacB	RSAU_000758
824157.0	0.2	0.02	0.9822	0.9889			
824282.0	1.08	0.76	0.3921	0.7926			
824283.0	3.33	0.95	0.2187	0.5985			
825481.0	2.33	-0.57	0.5208	0.903	-		RSAU_000761
825482.0	1.43	-0.19	0.8331	0.9889	-		RSAU_000761
825483.0	0.76	-0.39	0.6177	0.9445	-		RSAU_000761
829375.0	0.26	0.96	0.2392	0.5985	+	clfA	RSAU_000765
832069.0	0.33	-1.08	0.1895	0.5985	+		RSAU_000766
837300.0	8.7	0.83	0.2768	0.6475			
837301.0	0.46	1.17	0.1668	0.5985			
841409.0	2.33	0.83	0.2882	0.6651	-		RSAU_000776
848926.0	0.83	-1.12	0.2075	0.5985	+		RSAU_000787
853093.0	0.65	-0.64	0.4606	0.8493	-		RSAU_000791
862365.0	3.38	-0.94	0.2823	0.6556	+		RSAU_000800
863721.0	0.66	-1.31	0.1224	0.5985	+		RSAU_000801
864173.0	3.78	2.44	0.0062	0.1863	+		RSAU_000802
864215.0	3.7	1.28	0.1501	0.5985	+		RSAU_000802
864421.0	0.31	0.98	0.2331	0.5985	+		RSAU_000802
864759.0	0.41	-0.22	0.7855	0.9889	+		RSAU_000802
866626.0	5.08	0.38	0.6463	0.9604	+		RSAU_000804
866879.0	0.72	-0.54	0.5336	0.9042	+		RSAU_000804
867318.0	0.71	-0.38	0.6726	0.9775			
867543.0	2.06	0.8	0.3562	0.7589	+		RSAU_000806
868043.0	9.29	0.48	0.561	0.9148	+	gD	RSAU_000807
876545.0	0.2	0.02	0.9822	0.9889			
876849.0	0.38	-0.16	0.8442	0.9889	+		RSAU_000817
879035.0	1.3	-1.54	0.0741	0.5985	+	ampA	RSAU_000819
879708.0	1.34	0.49	0.5804	0.9259	+	ampA	RSAU_000819
881004.0	1.26	-0.29	0.7117	0.9889	+		RSAU_000820
881048.0	1.65	-0.52	0.546	0.9042	+		RSAU_000820
881106.0	5.85	1.23	0.1487	0.5985	+		RSAU_000820
881233.0	0.91	0.74	0.401	0.8008	+		RSAU_000820
881495.0	0.38	1.17	0.1692	0.5985	+		RSAU_000820
881929.0	1.33	1.95	0.0289	0.4415	+		RSAU_000820
883833.0	1.61	0.88	0.3082	0.6954			
890986.0	0.91	0.73	0.3678	0.7714			
898421.0	1.27	-0.7	0.3745	0.7781	-	argH	RSAU_000837
898444.0	0.39	1.17	0.1684	0.5985	-	argH	RSAU_000837
902130.0	2.82	-0.72	0.3992	0.8008			
903551.0	0.64	0.62	0.4462	0.8384	+	spsA	RSAU_000841
907715.0	1.05	-0.5	0.5148	0.9024	+	rexB	RSAU_000843
916794.0	0.53	1.28	0.1367	0.5985			
917474.0	0.97	0.35	0.6562	0.9656	+		RSAU_000850
918922.0	2.44	0.04	0.9648	0.9889	+	clpB	RSAU_000851
921636.0	0.55	0.22	0.798	0.9889	-		RSAU_000852
921653.0	0.82	-1.11	0.214	0.5985	-		RSAU_000852
921654.0	120.75	0.35	0.5596	0.914	-		RSAU_000852
921655.0	14163.99	-0.22	0.6128	0.9442	-		RSAU_000852
921656.0	79.4	0.5	0.4097	0.8062	-		RSAU_000852
921722.0	0.8	-0.83	0.3523	0.754	-		RSAU_000852
921726.0	1.27	0.31	0.7193	0.9889	-		RSAU_000852

921743.0	0.52	0.1	0.902	0.9889	-		RSAU_000852
925285.0	0.71	-0.77	0.3804	0.785	+		RSAU_000855
928386.0	0.36	-0.19	0.8176	0.9889	+	fabF	RSAU_000859
929713.0	0.26	0.96	0.2392	0.5985			
936927.0	4.93	0.17	0.8411	0.9889	+	oppA2	RSAU_000865
940241.0	0.22	0.04	0.9554	0.9889	+	oppB2	RSAU_000868
940487.0	0.38	1.17	0.1692	0.5985			
940562.0	0.39	1.17	0.1684	0.5985	+		RSAU_000869
940563.0	0.37	-0.43	0.6051	0.9402	+		RSAU_000869
945452.0	1.08	0.08	0.9293	0.9889	+		RSAU_000875
946708.0	0.84	1.13	0.2041	0.5985	+		RSAU_000876
947346.0	10.98	-0.3	0.6317	0.9476	+		RSAU_000876
948933.0	0.26	0.96	0.2392	0.5985	+		RSAU_000879
948934.0	0.37	-0.43	0.6051	0.9402	+		RSAU_000879
957519.0	0.58	-0.74	0.4002	0.8008			
959565.0	0.86	1.75	0.0489	0.5815	-		RSAU_000890
964947.0	0.42	-0.19	0.8115	0.9889			
966167.0	1.08	0.37	0.678	0.98			
966330.0	0.2	0.02	0.9822	0.9889	+		RSAU_000896
966349.0	10.16	1.02	0.0829	0.5985	+		RSAU_000896
966587.0	1.91	-0.43	0.6145	0.9442	+		RSAU_000896
967061.0	6.95	-1.68	0.059	0.5815	+		RSAU_000898
967195.0	1.99	-0.29	0.7283	0.9889	+		RSAU_000899
967688.0	0.36	-0.19	0.8176	0.9889	+		RSAU_000900
967765.0	0.49	-0.51	0.5578	0.9121	+		RSAU_000900
967852.0	1.08	0.16	0.8578	0.9889	-	ltaA	RSAU_000901
967856.0	0.92	0.82	0.3545	0.757	-	ltaA	RSAU_000901
968101.0	0.66	-1.31	0.1224	0.5985	-	ltaA	RSAU_000901
968156.0	0.43	-0.1	0.9048	0.9889	-	ltaA	RSAU_000901
968172.0	0.82	-1.32	0.1186	0.5985	-	ltaA	RSAU_000901
968212.0	0.88	-1.69	0.0543	0.5815	-	ltaA	RSAU_000901
968240.0	1.01	0.84	0.3426	0.7423	-	ltaA	RSAU_000901
968241.0	190.98	1.13	0.0011	0.0672	-	ltaA	RSAU_000901
968242.0	1.42	0.41	0.6282	0.9445	-	ltaA	RSAU_000901
968301.0	0.31	0.98	0.2331	0.5985	-	ltaA	RSAU_000901
968302.0	5.3	2.0	0.0245	0.4141	-	ltaA	RSAU_000901
968303.0	12.66	0.78	0.3542	0.757	-	ltaA	RSAU_000901
968304.0	0.31	0.98	0.2331	0.5985	-	ltaA	RSAU_000901
968305.0	56.93	1.89	3.0E-4	0.027	-	ltaA	RSAU_000901
968340.0	11.19	0.38	0.6278	0.9445	-	ltaA	RSAU_000901
968341.0	1289.31	-0.32	0.5008	0.8886	-	ltaA	RSAU_000901
968342.0	9.7	-0.42	0.6061	0.9402	-	ltaA	RSAU_000901
968355.0	0.42	-0.19	0.8115	0.9889	-	ltaA	RSAU_000901
968361.0	3.39	-0.71	0.349	0.7484	-	ltaA	RSAU_000901
968470.0	4.23	-2.14	0.011	0.2447	-	ltaA	RSAU_000901
968484.0	2.0	-1.39	0.0979	0.5985	-	ltaA	RSAU_000901
968502.0	10.11	1.81	0.0369	0.5052	-	ltaA	RSAU_000901
968571.0	0.37	-1.09	0.1867	0.5985	-	ltaA	RSAU_000901
968588.0	4.08	-1.37	0.1249	0.5985	-	ltaA	RSAU_000901
968626.0	4.76	1.77	0.0192	0.3634	-	ltaA	RSAU_000901
968672.0	8.35	0.95	0.2044	0.5985	-	ltaA	RSAU_000901
968711.0	15.5	-0.1	0.9088	0.9889	-	ltaA	RSAU_000901
968712.0	0.26	0.96	0.2392	0.5985	-	ltaA	RSAU_000901
968717.0	1.87	-2.56	0.0038	0.1465	-	ltaA	RSAU_000901
968721.0	1.77	0.45	0.555	0.9111	-	ltaA	RSAU_000901
968912.0	10.05	2.11	0.0049	0.1553	-	ltaA	RSAU_000901
968930.0	13.25	1.9	0.0084	0.207	-	ltaA	RSAU_000901
968935.0	4.43	0.76	0.3111	0.6985	-	ltaA	RSAU_000901
968940.0	7.22	3.24	0.0	0.0064	-	ltaA	RSAU_000901
968947.0	21.95	0.69	0.3625	0.7672	-	ltaA	RSAU_000901
969041.0	0.2	0.02	0.9822	0.9889	-	ltaA	RSAU_000901
969042.0	0.77	0.56	0.5217	0.903	-	ugtP	RSAU_000902
969043.0	88.61	1.62	0.0045	0.1486	-	ugtP	RSAU_000902
969044.0	0.84	1.85	0.0381	0.5062	-	ugtP	RSAU_000902
969112.0	1.3	1.25	0.159	0.5985	-	ugtP	RSAU_000902
969128.0	0.37	-1.09	0.1867	0.5985	-	ugtP	RSAU_000902
969195.0	5.68	0.52	0.4779	0.8648	-	ugtP	RSAU_000902
969412.0	1.16	0.03	0.9747	0.9889	-	ugtP	RSAU_000902
969493.0	0.41	-0.22	0.7855	0.9889	-	ugtP	RSAU_000902
969521.0	0.86	0.63	0.4762	0.8627	-	ugtP	RSAU_000902
969522.0	75.67	0.72	0.2969	0.6789	-	ugtP	RSAU_000902
969523.0	0.27	0.1	0.8977	0.9889	-	ugtP	RSAU_000902
969601.0	0.29	-0.27	0.7469	0.9889	-	ugtP	RSAU_000902
969636.0	3.82	-1.23	0.1071	0.5985	-	ugtP	RSAU_000902
969706.0	0.44	0.49	0.5479	0.9042	-	ugtP	RSAU_000902
969984.0	2.3	-0.49	0.5787	0.9253	-	ugtP	RSAU_000902
970029.0	5.12	0.24	0.7627	0.9889	-	ugtP	RSAU_000902
970060.0	22.94	-0.22	0.709	0.9889	-	ugtP	RSAU_000902
970081.0	0.58	-0.74	0.4002	0.8008	-	ugtP	RSAU_000902
970235.0	26.59	0.62	0.411	0.8073			
970236.0	2049.8	0.66	0.1327	0.5985			
970237.0	5.67	1.12	0.1522	0.5985			
970241.0	2.1	-1.0	0.2491	0.6127			
970255.0	20.5	0.54	0.4884	0.8755			
970256.0	1808.84	-0.16	0.7725	0.9889			
970257.0	6.95	0.24	0.7129	0.9889			
970264.0	32.99	-0.35	0.6812	0.981			

970265.0	4132.69	-0.89	0.1783	0.5985			
970266.0	33.35	-0.91	0.269	0.6369			
970288.0	21.41	-3.16	0.0	0.0048			
970298.0	315.02	0.91	0.154	0.5985			
970299.0	32027.05	0.28	0.4763	0.8627			
970300.0	100.1	0.48	0.3924	0.7926			
970333.0	0.36	-0.15	0.8534	0.9889			
970350.0	0.61	-0.46	0.5717	0.9216			
970353.0	3.29	0.04	0.9605	0.9889			
970358.0	4.38	-2.31	0.0076	0.2032			
970363.0	0.51	1.17	0.1666	0.5985			
970365.0	2.32	-2.39	0.0073	0.2032			
970370.0	17.67	0.48	0.4867	0.8749			
970371.0	1539.68	-0.05	0.8998	0.9889			
970372.0	7.54	0.16	0.8139	0.9889			
970373.0	10.1	0.42	0.5544	0.9111			
970374.0	1.05	-0.5	0.5148	0.9024			
970380.0	2.77	0.79	0.3652	0.7714			
970387.0	0.47	-0.47	0.5929	0.9382			
970391.0	0.32	0.98	0.2303	0.5985			
970392.0	4.77	-2.8	0.0011	0.0672			
970394.0	0.53	-1.15	0.1672	0.5985			
970395.0	0.61	0.2	0.8159	0.9889			
970398.0	1571.14	1.29	0.1369	0.5985			
970399.0	27.75	0.68	0.3368	0.7329			
970405.0	15.4	-2.64	6.0E-4	0.0473			
970407.0	1.92	0.54	0.5412	0.9042			
970408.0	4.33	0.94	0.281	0.6533			
970410.0	3.36	0.48	0.543	0.9042			
970411.0	0.87	1.05	0.234	0.5985			
970418.0	1.01	0.77	0.3842	0.7877			
970421.0	1.62	-1.14	0.1998	0.5985			
970425.0	0.31	0.98	0.2331	0.5985			
970426.0	24.26	-0.9	0.1854	0.5985			
970427.0	0.79	-0.21	0.807	0.9889			
970428.0	1425.54	1.42	0.0088	0.2085			
970429.0	249530.12	0.36	0.4401	0.8319			
970430.0	2288.49	0.67	0.2651	0.6354			
970431.0	43468.4	0.05	0.9104	0.9889			
970432.0	483.76	0.28	0.5212	0.903			
970433.0	0.99	0.96	0.2799	0.6514			
970438.0	236.09	0.9	0.1297	0.5985			
970439.0	35086.35	-0.14	0.7605	0.9889			
970440.0	254.53	0.16	0.8111	0.9889			
970451.0	0.39	0.44	0.6147	0.9442			
970452.0	0.9	-0.16	0.8499	0.9889			
970455.0	6.69	1.34	0.0806	0.5985			
970458.0	0.27	0.1	0.8977	0.9889			
970460.0	26.9	-2.23	0.0038	0.1465			
970461.0	0.37	-1.09	0.1867	0.5985			
970465.0	0.27	0.1	0.8977	0.9889			
970483.0	377.01	0.7	0.2688	0.6369			
970484.0	42640.75	-0.08	0.8278	0.9889			
970485.0	220.59	-0.12	0.865	0.9889			
970488.0	0.79	0.23	0.793	0.9889			
970491.0	2.39	-0.16	0.849	0.9889			
970492.0	4.44	0.03	0.9682	0.9889			
970493.0	2686.22	1.15	0.055	0.5815			
970494.0	299016.33	0.14	0.7435	0.9889			
970495.0	2160.05	0.03	0.9625	0.9889			
970496.0	13.45	-2.94	1.0E-4	0.0109			
970499.0	32.78	-2.98	1.0E-4	0.0114			
970501.0	1.61	-0.93	0.2973	0.6789			
970504.0	1.38	-0.17	0.8382	0.9889			
970506.0	4.14	-1.66	0.0474	0.5767			
970508.0	2.89	0.16	0.8521	0.9889			
970511.0	5.49	-1.6	0.0642	0.5985			
970512.0	10.27	-0.23	0.7846	0.9889			
970513.0	1.72	-0.87	0.327	0.7208			
970514.0	668.15	0.58	0.3133	0.7018			
970515.0	143054.31	-0.6	0.2283	0.5985			
970516.0	1650.83	-0.46	0.5287	0.9042			
970517.0	1.18	-0.07	0.9408	0.9889			
970518.0	20.22	-2.09	0.0017	0.0879			
970519.0	17.33	-2.13	0.0080	0.2044			
970522.0	1.06	-0.58	0.5068	0.8968			
970525.0	3.68	-0.96	0.2512	0.6155			
970536.0	0.53	-1.15	0.1672	0.5985			
970539.0	194.84	-2.8	1.0E-4	0.0133			
970540.0	1.63	-1.57	0.0695	0.5985			
970541.0	174.23	-0.16	0.7929	0.9889			
970542.0	169732.98	-0.66	0.2336	0.5985			
970543.0	62952.08	0.4	0.338	0.7339			
970544.0	886.21	1.04	0.0458	0.5692			
970545.0	0.46	1.17	0.1668	0.5985			
970547.0	32.73	-2.43	0.0021	0.097			
970548.0	0.85	-0.71	0.4167	0.8128			

970549.0	133.94	-2.27	0.0024	0.1022			
970550.0	0.66	-1.31	0.1224	0.5985			
970551.0	0.47	-0.47	0.5929	0.9382			
970552.0	2.0	-1.05	0.2404	0.5989			
970556.0	0.53	-1.15	0.1672	0.5985			
970579.0	0.38	-0.16	0.8442	0.9889			
970589.0	2.1	-1.47	0.0845	0.5985			
970590.0	272.75	-3.03	0.0	0.0048			
970591.0	0.77	-0.99	0.2652	0.6354			
970592.0	3.66	-1.9	0.0216	0.3786			
970595.0	57.26	-2.58	7.0E-4	0.0473			
970596.0	4.31	-1.59	0.0619	0.5978			
970597.0	0.56	0.06	0.9447	0.9889			
970601.0	17.86	-2.12	0.0074	0.2032			
970602.0	3.38	-1.17	0.1879	0.5985			
970603.0	24.36	-0.41	0.6456	0.96			
970604.0	0.43	-0.1	0.9048	0.9889			
970607.0	1.59	-1.61	0.064	0.5985			
970608.0	0.36	-0.19	0.8176	0.9889			
970621.0	1.91	-0.63	0.4044	0.8012			
970645.0	0.53	-1.15	0.1672	0.5985	+	murE	RSAU_000903
970646.0	0.47	-0.13	0.8717	0.9889	+	murE	RSAU_000903
970668.0	0.37	-1.09	0.1867	0.5985	+	murE	RSAU_000903
970685.0	0.43	-0.1	0.9048	0.9889	+	murE	RSAU_000903
970687.0	2.3	0.11	0.9041	0.9889	+	murE	RSAU_000903
970761.0	2.1	-0.43	0.5549	0.9111	+	murE	RSAU_000903
973432.0	0.39	1.17	0.1684	0.5985	+	prfC	RSAU_000905
973433.0	15.86	-0.47	0.583	0.9292	+	prfC	RSAU_000905
973926.0	1.28	0.81	0.3129	0.7017			
977208.0	0.26	0.96	0.2392	0.5985	+		RSAU_000907
980206.0	0.6	-0.49	0.545	0.9042	+		RSAU_000909
984618.0	1.08	0.37	0.678	0.98			
984781.0	0.2	0.02	0.9822	0.9889	+		RSAU_000917
984800.0	10.35	1.05	0.0744	0.5985	+		RSAU_000917
985038.0	1.91	-0.43	0.6145	0.9442	+		RSAU_000917
985512.0	6.95	-1.68	0.059	0.5815	+		RSAU_000919
985646.0	1.74	-0.2	0.8159	0.9889	+		RSAU_000920
986139.0	0.36	-0.19	0.8176	0.9889	+		RSAU_000921
986216.0	0.2	0.02	0.9822	0.9889	+		RSAU_000921
986576.0	0.31	0.98	0.2331	0.5985			
987998.0	0.41	-0.22	0.7855	0.9889	+		RSAU_000923
989653.0	1.0	-0.33	0.6732	0.9776	+		RSAU_000924
1000363.0	2.66	-2.4	0.0071	0.2032			
1004649.0	0.49	-0.51	0.5578	0.9121			
1007535.0	1.04	0.77	0.3383	0.7339	-	atl	RSAU_000940
1011362.0	19.43	-0.64	0.4618	0.8493	-		RSAU_000942
1011363.0	0.26	0.96	0.2392	0.5985	-		RSAU_000942
1013565.0	6.09	0.52	0.4627	0.8493	+	fmtA	RSAU_000944
1013989.0	23.9	1.15	0.1853	0.5985	+	fmtA	RSAU_000944
1014066.0	43.89	1.25	0.1474	0.5985	+	fmtA	RSAU_000944
1014221.0	13.56	0.62	0.3799	0.785	+	fmtA	RSAU_000944
1014842.0	0.33	-1.08	0.1895	0.5985			
1014995.0	0.65	0.16	0.8432	0.9889			
1016905.0	1.75	-0.04	0.9641	0.9889	-	qoxB	RSAU_000947
1023133.0	0.31	0.98	0.2331	0.5985	+	purK	RSAU_000952
1024579.0	1.27	1.22	0.1636	0.5985	+	purQ	RSAU_000955
1027756.0	0.2	0.02	0.9822	0.9889	+	purF	RSAU_000957
1028973.0	37.72	-1.41	0.0019	0.0929	+	purM	RSAU_000958
1029478.0	5.99	0.12	0.8888	0.9889	+	purM	RSAU_000958
1030331.0	0.7	1.72	0.053	0.5815	+	purH	RSAU_000960
1030332.0	172.13	-0.63	0.0997	0.5985	+	purH	RSAU_000960
1030333.0	1.57	0.08	0.9242	0.9889	+	purH	RSAU_000960
1031919.0	5.49	1.86	0.0258	0.4234	+	purD	RSAU_000961
1036704.0	0.83	0.66	0.406	0.8012			
1042703.0	1.51	0.54	0.5446	0.9042			
1044955.0	0.33	-1.08	0.1895	0.5985	+	cydB	RSAU_000972
1049784.0	20.16	0.9	0.2849	0.6584	+		RSAU_000977
1050104.0	21.4	0.26	0.687	0.9852	+		RSAU_000977
1050262.0	14.1	1.15	0.1948	0.5985	+		RSAU_000977
1050309.0	47.73	1.14	0.1737	0.5985	+		RSAU_000977
1050310.0	0.92	0.75	0.3569	0.7595	+		RSAU_000977
1054490.0	0.26	0.96	0.2392	0.5985	+	pdhD	RSAU_000981
1054670.0	0.72	-0.54	0.5336	0.9042	+	pdhD	RSAU_000981
1054881.0	0.38	-0.16	0.8442	0.9889	+	pdhD	RSAU_000981
1056660.0	0.2	0.02	0.9822	0.9889	+	potA	RSAU_000984
1056758.0	3.22	1.98	0.0241	0.4105	+	potA	RSAU_000984
1058300.0	0.38	1.17	0.1692	0.5985	+	potB	RSAU_000985
1058301.0	57.5	0.15	0.7322	0.9889	+	potB	RSAU_000985
1058365.0	2.33	-0.27	0.7572	0.9889	+	potB	RSAU_000985
1059123.0	1.6	0.39	0.6475	0.9604	+	potC	RSAU_000986
1059190.0	0.62	-0.16	0.8434	0.9889	+	potC	RSAU_000986
1067390.0	0.53	0.02	0.9779	0.9889	+	typA	RSAU_000994
1067723.0	0.26	0.96	0.2392	0.5985			
1075012.0	0.41	-0.22	0.7855	0.9889	-	ctaA	RSAU_001000
1079267.0	0.57	0.24	0.785	0.9889	-		RSAU_001005
1080325.0	1.26	2.25	0.0115	0.2499			
1081152.0	0.92	-1.72	0.05	0.5815	+		RSAU_001008

1084832.0	0.85	-0.61	0.4405	0.8319	-	isdB	RSAU_001013
1086870.0	2.09	0.55	0.5184	0.9024	-	isdA	RSAU_001014
1087046.0	2.61	0.68	0.4255	0.8188	-	isdA	RSAU_001014
1087436.0	1.32	0.5	0.5168	0.9024	-	isdA	RSAU_001014
1088347.0	0.7	-1.03	0.2484	0.6118	+	isdC	RSAU_001015
1088502.0	0.5	0.19	0.8249	0.9889	+	isdD	RSAU_001016
1089629.0	1.84	-0.75	0.3317	0.7244	+	isdE	RSAU_001017
1092236.0	0.53	-1.15	0.1672	0.5985	+	isdG	RSAU_001020
1100267.0	0.32	0.32	0.6918	0.9852	+		RSAU_001027
1110192.0	0.51	-0.49	0.5791	0.9253			
1110194.0	0.31	-0.23	0.7798	0.9889			
1116334.0	0.27	0.1	0.8977	0.9889			
1122417.0	0.41	-0.22	0.7855	0.9889			
1124755.0	0.98	-0.49	0.5667	0.9185	+	arcC1	RSAU_001050
1126504.0	0.53	-1.15	0.1672	0.5985	+		RSAU_001051
1127540.0	1.11	0.38	0.6192	0.9445			
1127554.0	0.38	1.17	0.1692	0.5985			
1128264.0	0.39	0.44	0.6147	0.9442	-		RSAU_001052
1128265.0	79.29	0.21	0.6402	0.9553	-		RSAU_001052
1128266.0	0.44	1.33	0.1252	0.5985	-		RSAU_001052
1129001.0	0.36	-0.19	0.8176	0.9889	-		RSAU_001052
1130109.0	3.24	0.29	0.7456	0.9889			
1133324.0	1.41	-1.73	0.049	0.5815	+		RSAU_001058
1138319.0	1.81	-0.91	0.2831	0.656			
1139236.0	0.53	0.02	0.9779	0.9889	+	mraY	RSAU_001063
1142937.0	0.98	-0.63	0.4213	0.8128	+	ftsA	RSAU_001066
1145260.0	10.43	-1.14	0.2018	0.5985	+		RSAU_001068
1147069.0	8.19	-2.21	0.0050	0.1553	+	ylmG	RSAU_001071
1148801.0	0.2	0.02	0.9822	0.9889	+		RSAU_001073
1149322.0	0.33	-1.08	0.1895	0.5985	+	lileS	RSAU_001074
1150296.0	0.53	-1.15	0.1672	0.5985	+	lileS	RSAU_001074
1152267.0	0.69	0.1	0.9093	0.9889	+		RSAU_001075
1153120.0	0.36	-0.19	0.8176	0.9889	-		RSAU_001076
1155770.0	0.39	1.17	0.1684	0.5985	+	lspA	RSAU_001080
1159438.0	3.53	-0.74	0.4058	0.8012	+	pyrC	RSAU_001084
1159439.0	5.1	-1.24	0.1594	0.5985	+	pyrC	RSAU_001084
1164298.0	0.26	0.96	0.2392	0.5985	+	pyrAB	RSAU_001086
1164377.0	0.77	-1.33	0.1183	0.5985	+	pyrAB	RSAU_001086
1166348.0	0.75	-1.03	0.2467	0.6106			
1167623.0	2.31	1.4	0.0953	0.5985			
1169340.0	0.89	-0.4	0.6542	0.9656	-		RSAU_001090
1172061.0	0.83	-0.32	0.7119	0.9889	+	priA	RSAU_001094
1176597.0	52.23	0.13	0.8081	0.9889	+	def2	RSAU_001097
1176598.0	1.03	0.14	0.8794	0.9889	+	def2	RSAU_001097
1180291.0	2.02	-0.49	0.572	0.9216	+	rlmN	RSAU_001100
1184954.0	0.32	0.98	0.2303	0.5985	+	thiN	RSAU_001105
1185991.0	0.31	0.98	0.2331	0.5985	-	rpmB	RSAU_001106
1192892.0	0.56	0.59	0.4672	0.8527	+	fabD	RSAU_001112
1194204.0	0.47	-0.13	0.8717	0.9889			
1194205.0	41.41	-2.86	2.0E-4	0.024			
1197612.0	0.43	-0.1	0.9048	0.9889	+	smc	RSAU_001116
1204992.0	3.9	0.31	0.685	0.9842			
1205187.0	1.24	0.15	0.8607	0.9889	-		RSAU_001124
1207221.0	0.22	0.04	0.9554	0.9889	-		RSAU_001124
1207545.0	7.24	0.51	0.563	0.9148	-		RSAU_001124
1207546.0	0.41	-0.22	0.7855	0.9889	-		RSAU_001124
1209324.0	0.47	-0.13	0.8717	0.9889	+	rnhB	RSAU_001126
1214136.0	1.05	0.05	0.9468	0.9889	+	dprA	RSAU_001131
1221888.0	3.26	-0.02	0.9798	0.9889	+	codY	RSAU_001137
1225250.0	0.2	0.02	0.9822	0.9889	+	pyrH	RSAU_001140
1228383.0	0.26	0.96	0.2392	0.5985	+		RSAU_001144
1228587.0	4.49	0.53	0.5505	0.9069	+		RSAU_001144
1228588.0	7.51	0.5	0.5159	0.9024	+		RSAU_001144
1228595.0	30.28	-0.9	0.2267	0.5985	+		RSAU_001144
1228596.0	0.81	-0.19	0.8277	0.9889	+		RSAU_001144
1229140.0	0.37	-1.09	0.1867	0.5985	+		RSAU_001144
1229449.0	0.2	0.02	0.9822	0.9889	+		RSAU_001144
1229450.0	15.15	-1.17	0.1559	0.5985	+		RSAU_001144
1229543.0	0.82	-1.32	0.1186	0.5985	+		RSAU_001144
1243981.0	0.63	-1.55	0.0762	0.5985			
1246373.0	4.44	-1.33	0.1187	0.5985			
1247609.0	1.76	1.56	0.0721	0.5985	+		RSAU_001158
1248256.0	0.6	-0.49	0.545	0.9042			
1249394.0	0.98	-0.63	0.4213	0.8128	+	ftsK	RSAU_001159
1250481.0	0.41	-0.22	0.7855	0.9889	+	ftsK	RSAU_001159
1250842.0	1.04	-1.11	0.212	0.5985	+		RSAU_001160
1251198.0	0.2	0.02	0.9822	0.9889	+		RSAU_001160
1256910.0	0.48	-0.5	0.5479	0.9042			
1257413.0	1.33	0.03	0.9728	0.9889			
1258190.0	3.94	-0.01	0.9889	0.9933	+	ci	RSAU_001167
1268730.0	0.46	-1.31	0.1257	0.5985	+	thiW	RSAU_001177
1272056.0	0.29	-0.27	0.7469	0.9889	+	mutL	RSAU_001179
1272614.0	2.76	-1.38	0.119	0.5985	+	mutL	RSAU_001179
1274791.0	0.53	-1.15	0.1672	0.5985			
1274866.0	0.26	0.96	0.2392	0.5985	+		RSAU_001181
1274867.0	0.37	-0.43	0.6051	0.9402	+		RSAU_001181
1278258.0	10.77	1.16	0.1637	0.5985			

1284862.0	0.6	-0.49	0.545	0.9042	+		RSAU_001190
1289760.0	0.45	-0.5	0.5715	0.9216			
1296878.0	0.41	-0.22	0.7855	0.9889	-		RSAU_001203
1298369.0	0.79	0.64	0.4684	0.8542	+	cls1	RSAU_001205
1299070.0	2.02	-1.93	0.0288	0.4415	+	cls1	RSAU_001205
1302428.0	1.04	-0.78	0.3801	0.785	+		RSAU_001208
1303153.0	0.47	-0.13	0.8717	0.9889	-		RSAU_001209
1305036.0	0.29	-0.27	0.7469	0.9889	+	dhoM	RSAU_001210
1307134.0	0.48	0.07	0.9354	0.9889	+	thrB	RSAU_001212
1307852.0	1.1	-0.41	0.5969	0.9402	+		RSAU_001213
1308414.0	22.78	-0.04	0.9367	0.9889			
1308450.0	1.54	-0.74	0.4036	0.8012			
1312817.0	16.85	-0.32	0.6489	0.9605			
1312818.0	0.31	-0.23	0.7798	0.9889			
1315717.0	0.39	1.17	0.1684	0.5985			
1316615.0	1.05	-1.73	0.0493	0.5815	+		RSAU_001222
1319399.0	0.36	-0.19	0.8176	0.9889			
1323764.0	0.37	-0.43	0.6051	0.9402	+		RSAU_001228
1324966.0	0.6	0.74	0.4026	0.8012	-	mscL	RSAU_001230
1326206.0	0.37	-1.09	0.1867	0.5985	+	opuD	RSAU_001231
1326705.0	0.46	1.17	0.1668	0.5985	+	opuD	RSAU_001231
1329690.0	0.49	1.17	0.167	0.5985	+	citB	RSAU_001232
1337056.0	0.88	-1.69	0.0543	0.5815			
1339685.0	2.7	-0.01	0.9871	0.9928	+	glcT	RSAU_001239
1347644.0	0.33	-1.08	0.1895	0.5985	+		RSAU_001245
1347974.0	0.58	1.53	0.0821	0.5985			
1348181.0	2.52	-2.43	0.0042	0.147	-	tyrA	RSAU_001246
1351569.0	0.48	0.07	0.9354	0.9889	+	trpE	RSAU_001248
1351570.0	16.22	1.3	0.0133	0.2799	+	trpE	RSAU_001248
1360051.0	0.44	0.49	0.5479	0.9042	+	femB	RSAU_001256
1360836.0	0.33	-1.08	0.1895	0.5985	+		RSAU_001257
1363390.0	2.1	2.52	0.0044	0.1486	-	oppD3	RSAU_001260
1364994.0	0.81	1.37	0.1122	0.5985	-	oppB3	RSAU_001262
1368238.0	0.53	0.02	0.9779	0.9889	-	phoU	RSAU_001265
1369179.0	0.27	0.1	0.8977	0.9889	-	pstB	RSAU_001266
1369278.0	1.04	0.97	0.2713	0.6407	-	pstB	RSAU_001266
1369510.0	2.32	-0.65	0.4659	0.8527	-	pstB	RSAU_001266
1375486.0	7.68	0.76	0.3501	0.7501	+		RSAU_001271
1375556.0	0.65	0.36	0.6578	0.9656	+		RSAU_001271
1375557.0	366.11	0.77	0.3454	0.7425	+		RSAU_001271
1378585.0	2.06	1.44	0.1063	0.5985	+	asd	RSAU_001273
1382959.0	1.47	-0.1	0.9009	0.9889	+	alr	RSAU_001278
1383183.0	0.37	-1.09	0.1867	0.5985	+	alr	RSAU_001278
1383452.0	4.23	-0.09	0.9114	0.9889	+	alr	RSAU_001278
1384176.0	3.71	0.38	0.6537	0.9656	+	lysA	RSAU_001279
1384585.0	0.37	-1.09	0.1867	0.5985	+	lysA	RSAU_001279
1387147.0	5.46	-1.21	0.173	0.5985	+		RSAU_001284
1387453.0	2.46	-0.12	0.8904	0.9889	+	xpaC	RSAU_001285
1389445.0	0.62	0.17	0.8289	0.9889	-	braB	RSAU_001287
1391604.0	0.26	0.96	0.2392	0.5985	-		RSAU_001288
1392474.0	4.05	0.93	0.2846	0.6584	-		RSAU_001288
1392999.0	0.38	-0.16	0.8442	0.9889	-		RSAU_001289
1394308.0	0.43	-0.1	0.9048	0.9889	-		RSAU_001291
1397835.0	0.33	-1.08	0.1895	0.5985	-	odhA	RSAU_001293
1402142.0	0.64	0.62	0.4462	0.8384			
1409285.0	0.36	-0.19	0.8176	0.9889	-		RSAU_001304
1411598.0	4.9	1.07	0.177	0.5985			
1411599.0	0.53	-1.15	0.1672	0.5985			
1413312.0	0.26	0.96	0.2392	0.5985	-		RSAU_001308
1415224.0	1.97	-1.99	0.0249	0.4178	+		RSAU_001311
1422523.0	0.77	-0.32	0.7153	0.9889	-		RSAU_001312
1422524.0	100.12	-0.8	0.0261	0.4234	-		RSAU_001312
1422525.0	0.46	1.17	0.1668	0.5985	-		RSAU_001312
1424363.0	0.65	-0.64	0.4606	0.8493	-		RSAU_001312
1424364.0	20.17	-0.02	0.969	0.9889	-		RSAU_001312
1424963.0	0.31	0.98	0.2331	0.5985	-		RSAU_001312
1426233.0	0.41	-0.22	0.7855	0.9889	-		RSAU_001312
1428935.0	0.36	-0.19	0.8176	0.9889	-		RSAU_001312
1435690.0	3.03	0.8	0.3702	0.7738	-		RSAU_001316
1436780.0	1.72	0.06	0.9365	0.9889	-		RSAU_001317
1436781.0	2.8	-1.34	0.1237	0.5985	-		RSAU_001317
1441953.0	1.9	-0.72	0.4042	0.8012	+	pbp2	RSAU_001322
1446446.0	1.19	-1.27	0.1536	0.5985			
1451498.0	0.26	0.96	0.2392	0.5985	-	bshA	RSAU_001330
1451518.0	0.53	1.28	0.1367	0.5985	-	bshA	RSAU_001330
1451761.0	0.38	1.17	0.1692	0.5985	-	bshA	RSAU_001330
1454473.0	0.26	0.96	0.2392	0.5985	-		RSAU_001333
1455593.0	14.05	-1.38	0.0863	0.5985	-		RSAU_001335
1456659.0	0.37	-1.09	0.1867	0.5985	-	aroA	RSAU_001336
1461597.0	0.36	-0.19	0.8176	0.9889	-	gerCC	RSAU_001340
1461641.0	0.53	-1.15	0.1672	0.5985	-	gerCC	RSAU_001340
1462884.0	4.62	0.51	0.5621	0.9148	-		RSAU_001342
1467339.0	0.37	-0.43	0.6051	0.9402	-		RSAU_001346
1467340.0	0.26	0.96	0.2392	0.5985	-		RSAU_001346
1470522.0	0.71	-0.48	0.5476	0.9042	+	ansA	RSAU_001349
1470923.0	6.94	-0.45	0.5645	0.9165	+	ansA	RSAU_001349
1491235.0	4.23	-1.55	0.0441	0.5626	-		RSAU_001369

1491935.0	1.39	1.04	0.2421	0.6016	+	proC	RSAU_001370
1491989.0	0.96	-1.2	0.1765	0.5985	+	proC	RSAU_001370
1493861.0	4.37	-0.73	0.3886	0.79			
1499615.0	0.37	-1.09	0.1867	0.5985	-		RSAU_001376
1509801.0	5.33	1.47	0.0934	0.5985			
1510153.0	1.32	-1.99	0.0254	0.422	-	recN	RSAU_001386
1512137.0	1.01	0.99	0.2656	0.6354			
1512138.0	150.23	1.79	0.0	7.0E-4			
1512139.0	1.73	1.6	0.0671	0.5985			
1514031.0	1.49	-2.03	0.0222	0.3858	-	xseA	RSAU_001390
1515243.0	0.26	0.96	0.2392	0.5985	-	nusB	RSAU_001391
1517139.0	0.43	-0.1	0.9048	0.9889	-	accB1	RSAU_001394
1528700.0	0.38	-0.16	0.8442	0.9889	-	comGC	RSAU_001407
1529906.0	0.47	-0.13	0.8717	0.9889	-	comGA	RSAU_001409
1536141.0	0.65	0.97	0.2745	0.6438	-	pbp3	RSAU_001417
1546269.0	1.53	-1.03	0.2473	0.6113	-	dG	RSAU_001427
1546406.0	0.26	0.96	0.2392	0.5985	-	dG	RSAU_001427
1546589.0	21.83	0.91	0.2344	0.5985	-	dG	RSAU_001427
1546617.0	0.26	0.96	0.2392	0.5985	-	dG	RSAU_001427
1552135.0	0.32	0.98	0.2303	0.5985	-	recO	RSAU_001431
1555363.0	0.58	0.84	0.3444	0.7425			
1556022.0	0.42	-0.19	0.8115	0.9889	-		RSAU_001437
1558419.0	0.22	0.04	0.9554	0.9889	-	rpsU	RSAU_001440
1558510.0	0.43	-0.1	0.9048	0.9889			
1558511.0	9.87	0.12	0.8649	0.9889			
1558514.0	46.73	0.63	0.3917	0.7926			
1558516.0	1.14	-0.8	0.3705	0.7738			
1566624.0	0.48	0.1	0.9093	0.9889			
1566625.0	57.01	-0.91	0.1211	0.5985			
1566626.0	362.42	-1.56	0.0077	0.2032			
1567370.0	6.37	-0.96	0.2639	0.6351	-	hemN	RSAU_001448
1567371.0	3.41	-2.7	0.0014	0.0772	-	hemN	RSAU_001448
1567706.0	1.38	0.78	0.3672	0.7714	-	hemN	RSAU_001448
1567707.0	1.88	0.59	0.4921	0.8774	-	hemN	RSAU_001448
1567763.0	15.17	0.67	0.2312	0.5985	-	hemN	RSAU_001448
1567791.0	0.33	-1.08	0.1895	0.5985	-	hemN	RSAU_001448
1567793.0	29.06	-0.17	0.7672	0.9889	-	hemN	RSAU_001448
1567794.0	0.8	0.3	0.6977	0.9889	-	hemN	RSAU_001448
1569156.0	1.6	0.89	0.3055	0.6927	-	lepA	RSAU_001449
1571278.0	0.37	-1.09	0.1867	0.5985	-	holA	RSAU_001451
1572002.0	0.75	-0.88	0.3234	0.7152	-	comEC	RSAU_001452
1573000.0	0.53	0.24	0.766	0.9889	-	comEC	RSAU_001452
1573882.0	0.87	-1.19	0.1801	0.5985	-	comEC	RSAU_001452
1575673.0	1.8	0.34	0.6973	0.9889	-		RSAU_001455
1581232.0	1.88	-0.18	0.8319	0.9889			
1581263.0	0.53	-1.15	0.1672	0.5985			
1583613.0	1.26	-1.89	0.033	0.4796	-		RSAU_001465
1583719.0	0.39	1.17	0.1684	0.5985	-		RSAU_001465
1598428.0	0.8	0.64	0.4742	0.8606			
1598912.0	0.31	0.98	0.2331	0.5985	-		RSAU_001481
1599872.0	0.29	-0.27	0.7469	0.9889	-		RSAU_001481
1600217.0	0.56	-0.43	0.6266	0.9445	-		RSAU_001481
1600416.0	0.72	-0.23	0.7684	0.9889	-		RSAU_001481
1600769.0	0.64	-0.87	0.3279	0.7212	-		RSAU_001481
1600801.0	0.26	0.96	0.2392	0.5985	-		RSAU_001481
1601583.0	3.36	0.61	0.4871	0.8749	-		RSAU_001482
1602018.0	0.22	0.04	0.9554	0.9889			
1603598.0	0.26	0.96	0.2392	0.5985	-		RSAU_001484
1609947.0	12.32	-0.43	0.604	0.9402	-	aspS	RSAU_001491
1609948.0	0.53	-1.15	0.1672	0.5985	-	aspS	RSAU_001491
1610388.0	0.36	-0.19	0.8176	0.9889	-	aspS	RSAU_001491
1614135.0	0.6	-0.49	0.545	0.9042	-	lytH	RSAU_001493
1617115.0	0.6	1.27	0.1383	0.5985			
1617963.0	34.58	1.36	0.0439	0.5626	-	recJ	RSAU_001497
1617964.0	0.52	0.1	0.902	0.9889	-	recJ	RSAU_001497
1618333.0	1.54	0.11	0.9003	0.9889	-	recJ	RSAU_001497
1618619.0	12.02	0.54	0.5334	0.9042	-	recJ	RSAU_001497
1618620.0	0.26	0.96	0.2392	0.5985	-	recJ	RSAU_001497
1618912.0	4.74	1.12	0.2016	0.5985	-	recJ	RSAU_001497
1618913.0	0.38	1.17	0.1692	0.5985	-	recJ	RSAU_001497
1619549.0	4.07	-0.58	0.5104	0.9014	-	recJ	RSAU_001497
1619693.0	0.72	0.4	0.6224	0.9445	-	recJ	RSAU_001497
1624351.0	1.84	0.97	0.2723	0.6409	-	tgt	RSAU_001500
1624986.0	0.42	-0.19	0.8115	0.9889	-	queA	RSAU_001501
1625128.0	0.66	0.13	0.8713	0.9889	-	queA	RSAU_001501
1625159.0	6.45	-0.75	0.3951	0.7964	-	queA	RSAU_001501
1626510.0	3.26	-1.01	0.2558	0.6228	-	ruvA	RSAU_001503
1626521.0	0.54	-1.45	0.0941	0.5985	-	ruvA	RSAU_001503
1626526.0	1.81	-2.36	0.0081	0.2044	-	ruvA	RSAU_001503
1627570.0	0.46	-1.31	0.1257	0.5985	-	obgE	RSAU_001505
1627596.0	1.87	-1.03	0.2311	0.5985	-	obgE	RSAU_001505
1629478.0	0.52	0.1	0.902	0.9889	-	rpmA	RSAU_001506
1630224.0	0.42	-0.19	0.8115	0.9889	-	rplU	RSAU_001508
1633777.0	1.48	0.34	0.6976	0.9889			
1640859.0	2.2	1.75	0.0463	0.5706	-		RSAU_001519
1644293.0	0.53	-1.15	0.1672	0.5985	-	valS	RSAU_001523
1646488.0	0.36	-0.19	0.8176	0.9889			

1647996.0	0.67	-1.63	0.0641	0.5985	-		RSAU_001525
1653092.0	4.33	-0.45	0.5271	0.9042	-	hemX	RSAU_001530
1658140.0	3.15	0.6	0.4184	0.8128	-	tig	RSAU_001534
1658701.0	0.41	-0.22	0.7855	0.9889	-	tig	RSAU_001534
1658766.0	0.79	-1.84	0.0381	0.5062			
1658812.0	0.32	0.32	0.6918	0.9852			
1669218.0	0.8	0.64	0.4742	0.8606			
1672985.0	0.38	-0.16	0.8442	0.9889	-	polA	RSAU_001548
1674357.0	1.83	-2.01	0.0204	0.3773	-	polA	RSAU_001548
1678198.0	2.0	-0.11	0.8979	0.9889	-	phoR	RSAU_001550
1682741.0	0.32	0.98	0.2303	0.5985	+	aapA	RSAU_001554
1685007.0	0.38	-0.16	0.8442	0.9889	-	pykA	RSAU_001555
1696807.0	0.32	0.98	0.2303	0.5985			
1699151.0	2.01	-0.84	0.3346	0.73	+		RSAU_001565
1699638.0	0.39	1.17	0.1684	0.5985			
1705050.0	1.96	-2.33	0.0088	0.2085	-		RSAU_001571
1713090.0	0.22	0.04	0.9554	0.9889			
1714574.0	0.38	-0.16	0.8442	0.9889	+	serA	RSAU_001580
1716099.0	0.36	-0.19	0.8176	0.9889	-		RSAU_001581
1718550.0	3.85	0.67	0.4283	0.8209	-	ptaA	RSAU_001582
1721806.0	0.26	0.96	0.2392	0.5985	-	tyrS	RSAU_001585
1722597.0	4.91	0.26	0.7397	0.9889			
1723192.0	0.38	1.17	0.1692	0.5985	+		RSAU_001586
1723193.0	21.45	0.2	0.7752	0.9889	+		RSAU_001586
1726198.0	0.53	-1.15	0.1672	0.5985	-	sasI	RSAU_001587
1726199.0	2.33	-1.35	0.1229	0.5985	-	sasI	RSAU_001587
1726223.0	0.53	-1.15	0.1672	0.5985	-	sasI	RSAU_001587
1728463.0	1.28	-0.12	0.889	0.9889			
1731179.0	0.81	1.37	0.1122	0.5985	+	acuA	RSAU_001590
1732112.0	0.42	-0.19	0.8115	0.9889	+	acuC	RSAU_001591
1732149.0	1.1	-1.4	0.1	0.5985	+	acuC	RSAU_001591
1732154.0	0.31	0.98	0.2331	0.5985	+	acuC	RSAU_001591
1732527.0	5.74	0.17	0.8271	0.9889	+	acuC	RSAU_001591
1736140.0	1.23	-0.69	0.4363	0.8297	-	YtxH-like protein	RSAU_001594
1740375.0	0.41	-0.22	0.7855	0.9889	-		RSAU_001598
1743195.0	0.91	-0.62	0.484	0.8717	-		RSAU_001599
1744983.0	0.26	0.96	0.2392	0.5985	-		RSAU_001601
1747381.0	4.54	-0.47	0.598	0.9402	-		RSAU_001604
1749803.0	12.49	0.88	0.2687	0.6369			
1750127.0	0.36	-0.19	0.8176	0.9889	-	dat	RSAU_001607
1751505.0	0.76	-0.39	0.6177	0.9445	-		RSAU_001608
1756272.0	0.5	1.28	0.1358	0.5985	+		RSAU_001612
1756368.0	0.41	-0.22	0.7855	0.9889	+		RSAU_001612
1756866.0	0.51	1.17	0.1666	0.5985	+		RSAU_001612
1757306.0	0.84	1.13	0.2041	0.5985			
1759536.0	1.05	0.05	0.9468	0.9889	-		RSAU_001613
1759647.0	0.82	-1.32	0.1186	0.5985	-		RSAU_001613
1769930.0	1.41	-0.13	0.8779	0.9889	+		RSAU_001618
1776817.0	1.48	-0.04	0.9578	0.9889			
1777521.0	3.88	0.56	0.5253	0.9042	-		RSAU_001626
1779146.0	0.26	0.96	0.2392	0.5985			
1781330.0	4.14	-0.09	0.9033	0.9889			
1788905.0	0.5	0.52	0.5218	0.903	+	crcB2	RSAU_001640
1794239.0	0.26	0.96	0.2392	0.5985	+	pckA	RSAU_001644
1795448.0	0.52	0.1	0.902	0.9889	-		RSAU_001645
1795897.0	9.11	-0.32	0.7111	0.9889	-		RSAU_001646
1796723.0	0.2	0.02	0.9822	0.9889	-	menC	RSAU_001648
1799852.0	1.1	-1.84	0.0379	0.5062			
1804130.0	2.23	-0.49	0.558	0.9121	-		
1806361.0	0.96	1.06	0.2261	0.5985	-		RSAU_001659
1807648.0	1.8	-1.03	0.234	0.5985			
1809465.0	0.29	-0.27	0.7469	0.9889	+	hysA	RSAU_001662
1811211.0	0.81	-1.42	0.0972	0.5985	-		RSAU_001663
1813240.0	0.33	-1.08	0.1895	0.5985	-	hsdM	RSAU_001665
1813303.0	4.51	0.65	0.3727	0.7767	-	hsdM	RSAU_001665
1814601.0	0.79	-0.3	0.7071	0.9889			
1818036.0	7.51	0.62	0.467	0.8527			
1819383.0	0.9	-0.04	0.9593	0.9889			
1822585.0	3.33	-1.5	0.0754	0.5985			
1823309.0	0.41	-0.22	0.7855	0.9889	-	lukD	RSAU_001674
1824418.0	1.27	0.74	0.4063	0.8012	-	lukE	RSAU_001675
1824419.0	0.33	-1.08	0.1895	0.5985	-	lukE	RSAU_001675
1830266.0	0.29	-0.27	0.7469	0.9889	-		RSAU_001679
1831361.0	0.42	-0.19	0.8115	0.9889			
1833577.0	0.37	-1.09	0.1867	0.5985			
1834508.0	0.82	-1.32	0.1186	0.5985			
1835877.0	0.53	-0.73	0.4074	0.8026	-	hemG	RSAU_001691
1838935.0	1.7	0.28	0.7454	0.9889	-	ecsB	RSAU_001695
1840070.0	1.07	-0.27	0.7589	0.9889	-	ecsA	RSAU_001696
1840124.0	0.46	-1.31	0.1257	0.5985	-	ecsA	RSAU_001696
1840659.0	0.46	0.66	0.4528	0.8474	-	ecsA	RSAU_001696
1840660.0	99.88	-0.58	0.4329	0.8257	-	ecsA	RSAU_001696
1840661.0	0.58	0.84	0.3444	0.7425	-	ecsA	RSAU_001696
1840819.0	0.33	-1.08	0.1895	0.5985			
1851852.0	0.61	0.37	0.6764	0.98	-		RSAU_001705
1853641.0	0.53	-1.15	0.1672	0.5985	-		RSAU_001708
1868411.0	0.38	1.17	0.1692	0.5985	-		RSAU_001745

1868557.0	0.32	0.98	0.2303	0.5985	-		RSAU_001745
1869404.0	0.67	0.43	0.6214	0.9445	-		RSAU_001745
1869613.0	20.04	-1.09	0.2164	0.5985	-		RSAU_001745
1869614.0	0.41	-0.22	0.7855	0.9889	-		RSAU_001745
1870650.0	0.32	0.98	0.2303	0.5985	-		RSAU_001745
1872213.0	0.26	0.96	0.2392	0.5985	-		RSAU_001747
1875884.0	1.18	-1.76	0.0457	0.5692	+	gsaB	RSAU_001751
1876661.0	1.02	-1.41	0.0987	0.5985	+	gsaB	RSAU_001751
1876745.0	0.37	-1.09	0.1867	0.5985	+	gsaB	RSAU_001751
1878605.0	0.92	-1.72	0.051	0.5815			
1878633.0	4.11	1.36	0.1052	0.5985	-		RSAU_001753
1882602.0	1.74	0.91	0.2906	0.6692			
1886120.0	0.57	-1.32	0.1225	0.5985	-		RSAU_001758
1887679.0	0.53	-1.15	0.1672	0.5985	-	mgt	RSAU_001761
1887781.0	0.37	-1.09	0.1867	0.5985	-	mgt	RSAU_001761
1889276.0	23.21	-3.32	0.0	0.0017	-		RSAU_001762
1889867.0	1.63	-0.83	0.3371	0.7329	+		RSAU_001764
1890796.0	2.66	-0.57	0.5185	0.9024	+		RSAU_001764
1892097.0	1.97	0.23	0.7831	0.9889	-	pepS	RSAU_001766
1899709.0	0.56	0.33	0.7066	0.9889			
1901186.0	5.71	0.93	0.296	0.6782			
1905136.0	3.66	0.56	0.5222	0.903	+		RSAU_001781
1906068.0	0.91	-0.02	0.9804	0.9889	-	dinB	RSAU_001782
1906069.0	3.47	-0.77	0.3829	0.786	-	dinB	RSAU_001782
1907393.0	2.89	-0.23	0.7955	0.9889	-		RSAU_001783
1907410.0	0.93	0.04	0.9681	0.9889	-		RSAU_001783
1907438.0	0.29	-0.27	0.7469	0.9889	-		RSAU_001783
1908104.0	3.01	-1.42	0.1103	0.5985	-	TrmA family R methyltransferase	RSAU_001784
1908435.0	0.66	0.38	0.668	0.9723	-	TrmA family R methyltransferase	RSAU_001784
1922868.0	0.91	0.66	0.4546	0.8474	-	purB	RSAU_001795
1925875.0	1.11	0.14	0.8532	0.9889	+	sspA	RSAU_001796
1935110.0	0.32	0.98	0.2303	0.5985	-		RSAU_001804
1935170.0	5.31	1.16	0.1677	0.5985	-		RSAU_001804
1935254.0	3.5	0.79	0.3554	0.7581			
1935984.0	1.22	0.0	0.9995	0.9995	+		RSAU_001805
1943464.0	0.91	-0.7	0.43	0.8225	+	blaZ	RSAU_001811
1944160.0	0.43	-0.1	0.9048	0.9889	+		RSAU_001812
1944388.0	0.2	0.02	0.9822	0.9889	-		RSAU_001813
1944395.0	0.32	0.98	0.2303	0.5985	-		RSAU_001813
1944396.0	0.33	-1.08	0.1895	0.5985	-		RSAU_001813
1944462.0	0.36	-0.19	0.8176	0.9889	-		RSAU_001813
1944927.0	0.41	-0.22	0.7855	0.9889	-		RSAU_001813
1944952.0	3.12	-0.2	0.8109	0.9889	-		RSAU_001813
1945012.0	0.36	0.36	0.6599	0.9656	-		RSAU_001813
1945062.0	0.6	-0.49	0.545	0.9042	-		RSAU_001813
1945084.0	7.71	-1.71	0.0546	0.5815	-		RSAU_001813
1945554.0	2.92	-1.11	0.2074	0.5985	-		RSAU_001813
1945792.0	10.71	1.06	0.0744	0.5985	-		RSAU_001813
1945793.0	0.31	0.98	0.2331	0.5985	-		RSAU_001813
1945811.0	0.43	0.05	0.9531	0.9889	-		RSAU_001813
1945843.0	2.29	-2.29	0.0078	0.2032	-		RSAU_001813
1945971.0	6.66	-0.38	0.6591	0.9656	-		RSAU_001813
1951390.0	2.85	-0.75	0.4005	0.8008			
1951543.0	0.81	-0.27	0.7257	0.9889	+		RSAU_001818
1951739.0	0.43	0.05	0.9531	0.9889			
1954065.0	0.41	-0.22	0.7855	0.9889	-		RSAU_001821
1954086.0	0.57	-0.13	0.8857	0.9889	-		RSAU_001821
1956135.0	0.74	-0.27	0.7596	0.9889	+		RSAU_001824
1958402.0	0.77	-0.32	0.7153	0.9889	-	pmtB	RSAU_001827
1958474.0	2.64	1.47	0.0987	0.5985	-	pmtB	RSAU_001827
1958475.0	0.26	0.96	0.2392	0.5985	-	pmtB	RSAU_001827
1962436.0	0.47	-0.13	0.8717	0.9889	+		RSAU_001831
1964017.0	0.26	0.96	0.2392	0.5985	-		RSAU_001833
1964367.0	0.37	-1.09	0.1867	0.5985	-		RSAU_001833
1966107.0	0.38	-0.16	0.8442	0.9889	+	hlb	RSAU_001834
1966471.0	1.84	0.1	0.9062	0.9889	+	hlb	RSAU_001834
1967617.0	1.47	-2.31	0.0097	0.2224	-	lukG	RSAU_001837
1970608.0	6.96	-1.95	0.0067	0.196	+	dapE	RSAU_001839
1972764.0	0.45	-0.5	0.5715	0.9216			
1973964.0	0.38	1.17	0.1692	0.5985			
1974834.0	0.54	-1.45	0.0941	0.5985			
1978163.0	1.35	-1.68	0.057	0.5815			
1982318.0	0.38	-0.16	0.8442	0.9889	-		RSAU_001851
1983461.0	1.06	-1.47	0.0873	0.5985	-		RSAU_001853
1985392.0	5.02	-0.97	0.2746	0.6438	-		RSAU_001854
1988106.0	0.78	0.51	0.5627	0.9148	+	int	RSAU_001859
1989311.0	0.26	0.96	0.2392	0.5985	-	groEL	RSAU_001860
1990112.0	0.36	-0.19	0.8176	0.9889	-	groEL	RSAU_001860
1991200.0	0.2	0.02	0.9822	0.9889			
1991435.0	1.82	0.82	0.3298	0.7244	+		RSAU_001862
1991439.0	0.87	-0.5	0.5702	0.9216	+		RSAU_001862
1991610.0	1.1	-1.84	0.0379	0.5062	+		RSAU_001862
1991614.0	3.75	0.06	0.944	0.9889	+		RSAU_001862
1993486.0	0.55	-0.62	0.455	0.8474	+		RSAU_001864
1994620.0	1.25	-1.13	0.2	0.5985	+		RSAU_001865
2003077.0	0.22	0.04	0.9554	0.9889	-	amt	RSAU_001876
2005282.0	4.17	0.79	0.3437	0.7425	-		RSAU_001878

2005537.0	0.39	1.17	0.1684	0.5985	-		RSAU_001878
2007438.0	1.18	0.86	0.3311	0.7244	+		RSAU_001880
2011379.0	0.86	-1.01	0.257	0.624	-	gcp	RSAU_001882
2011819.0	1.81	-0.24	0.7857	0.9889	-	gcp	RSAU_001882
2014373.0	0.53	-1.15	0.1672	0.5985			
2015345.0	10.11	0.02	0.9833	0.9896	+	ilvD	RSAU_001886
2016475.0	0.56	1.53	0.0824	0.5985	+	ilvB	RSAU_001887
2017160.0	0.72	-0.23	0.7684	0.9889	+	ilvB	RSAU_001887
2020859.0	2.14	1.72	0.0506	0.5815	+	leuA	RSAU_001890
2021812.0	0.99	-0.09	0.909	0.9889	+	leuB	RSAU_001891
2022705.0	1.35	-0.66	0.4546	0.8474	+	leuC	RSAU_001892
2025331.0	1.65	-0.68	0.4376	0.8302			
2026230.0	2.03	-1.96	0.0269	0.4279	+	putative transposase	RSAU_001895
2026565.0	7.88	-0.05	0.9535	0.9889	+	putative transposase	RSAU_001895
2026567.0	5.96	-0.1	0.8923	0.9889	+	putative transposase	RSAU_001895
2028063.0	0.5	1.28	0.1358	0.5985	-		RSAU_001898
2028209.0	0.32	0.98	0.2303	0.5985	-		RSAU_001898
2029056.0	0.67	0.43	0.6214	0.9445	-		RSAU_001898
2029265.0	19.1	-0.98	0.2676	0.6368	-		RSAU_001898
2029266.0	0.41	-0.22	0.7855	0.9889	-		RSAU_001898
2032191.0	0.43	-0.1	0.9048	0.9889	-		RSAU_001899
2032214.0	0.26	0.96	0.2392	0.5985	-		RSAU_001899
2033104.0	0.6	-0.49	0.545	0.9042			
2033786.0	0.53	-1.15	0.1672	0.5985	-		RSAU_001902
2034320.0	0.82	-1.32	0.1186	0.5985	-	tex	RSAU_001903
2039651.0	2.29	-0.85	0.3312	0.7244			
2042049.0	1.49	-0.7	0.4322	0.8251	-		RSAU_001912
2042668.0	0.87	-0.57	0.47	0.8553	-		RSAU_001913
2043146.0	3.35	0.62	0.4008	0.8008	-		RSAU_001913
2044110.0	15.56	-1.04	0.1616	0.5985	-		RSAU_001914
2046387.0	0.34	0.4	0.6432	0.9572	-	kdpB	RSAU_001916
2050784.0	1.22	-0.72	0.417	0.8128	+	kdpD	RSAU_001918
2050807.0	0.47	-0.13	0.8717	0.9889	+	kdpD	RSAU_001918
2051283.0	5.47	-0.25	0.774	0.9889	+	kdpD	RSAU_001918
2053981.0	0.7	-1.69	0.0558	0.5815	-		RSAU_001920
2054331.0	80.96	-0.5	0.4442	0.8371	-		RSAU_001920
2054332.0	0.36	-0.19	0.8176	0.9889	-		RSAU_001920
2062434.0	0.77	-1.33	0.1183	0.5985			
2062533.0	1.06	-1.47	0.0873	0.5985			
2062634.0	0.53	-1.15	0.1672	0.5985			
2062675.0	0.47	-0.13	0.8717	0.9889			
2064001.0	0.67	1.33	0.1211	0.5985			
2068301.0	1.18	-0.09	0.9235	0.9889			
2070953.0	9.52	-1.52	0.0887	0.5985	-	murAA	RSAU_001938
2070954.0	0.9	-0.16	0.8499	0.9889	-	murAA	RSAU_001938
2071460.0	1.8	1.36	0.1079	0.5985	-		RSAU_001939
2077270.0	0.41	-0.22	0.7855	0.9889	-	atpF	RSAU_001945
2080410.0	0.2	0.02	0.9822	0.9889	-	upp	RSAU_001950
2081536.0	0.43	-0.1	0.9048	0.9889	-	glyA	RSAU_001951
2081546.0	0.79	-0.16	0.8562	0.9889	-	glyA	RSAU_001951
2081547.0	0.47	-0.13	0.8717	0.9889	-	glyA	RSAU_001951
2081554.0	1.0	-0.77	0.375	0.7781	-	glyA	RSAU_001951
2081556.0	15.57	-0.65	0.4534	0.8474	-	glyA	RSAU_001951
2081559.0	0.43	-0.1	0.9048	0.9889	-	glyA	RSAU_001951
2081567.0	0.96	-0.76	0.3808	0.785	-	glyA	RSAU_001951
2081571.0	1.2	-0.89	0.3069	0.6932	-	glyA	RSAU_001951
2081588.0	0.53	-1.15	0.1672	0.5985	-	glyA	RSAU_001951
2081610.0	0.67	-0.36	0.6483	0.9604	-	glyA	RSAU_001951
2081628.0	0.85	-0.71	0.4167	0.8128	-	glyA	RSAU_001951
2081631.0	2.6	-1.0	0.2621	0.6341	-	glyA	RSAU_001951
2081637.0	0.96	-1.2	0.1765	0.5985	-	glyA	RSAU_001951
2081638.0	2.88	-0.13	0.884	0.9889	-	glyA	RSAU_001951
2081679.0	1.43	-0.74	0.4055	0.8012	-	glyA	RSAU_001951
2081680.0	0.32	0.98	0.2303	0.5985	-	glyA	RSAU_001951
2081682.0	1.02	-1.01	0.2563	0.6231	-	glyA	RSAU_001951
2082558.0	2.16	-0.22	0.8044	0.9889	-		RSAU_001952
2093115.0	0.37	-1.09	0.1867	0.5985	-	fbaA	RSAU_001963
2093116.0	29.07	-0.5	0.3958	0.797	-	fbaA	RSAU_001963
2093117.0	0.9	-1.71	0.0533	0.5815	-	fbaA	RSAU_001963
2093775.0	0.5	1.28	0.1358	0.5985	-	fbaA	RSAU_001963
2094002.0	0.47	-0.13	0.8717	0.9889			
2094299.0	0.43	-0.1	0.9048	0.9889	+		RSAU_001964
2094484.0	0.37	-1.09	0.1867	0.5985	+		RSAU_001964
2096574.0	12.19	-0.44	0.5399	0.9042			
2096876.0	484.3	1.42	0.101	0.5985	-	rpoE	RSAU_001966
2097152.0	0.5	-1.46	0.0938	0.5985	-	rpoE	RSAU_001966
2097182.0	15.45	0.12	0.8488	0.9889	-	rpoE	RSAU_001966
2097217.0	0.79	-1.12	0.2074	0.5985	-	rpoE	RSAU_001966
2097665.0	0.67	0.51	0.5685	0.9207	-	blt	RSAU_001967
2100170.0	0.43	-0.1	0.9048	0.9889	-		RSAU_001969
2100171.0	10.94	0.13	0.8623	0.9889	-		RSAU_001969
2106139.0	0.38	1.17	0.1692	0.5985	-	deoC2	RSAU_001975
2107220.0	2.74	-0.45	0.6051	0.9402	+	deoD2	RSAU_001976
2107534.0	0.2	0.02	0.9822	0.9889	+	deoD2	RSAU_001976
2112488.0	1.11	-0.97	0.2704	0.6395	-	ma1	RSAU_001980
2113393.0	0.91	-0.66	0.4579	0.8493	-		RSAU_001981
2114759.0	0.8	0.71	0.3818	0.7853	+	czrB	RSAU_001983

2116860.0	0.96	-0.76	0.3808	0.785			
2117588.0	1.27	0.99	0.2665	0.6354	-		RSAU_001985
2117688.0	1.73	-0.75	0.3902	0.7916			
2118585.0	0.46	-1.31	0.1257	0.5985	+		RSAU_001986
2118920.0	4.69	-0.08	0.9315	0.9889	+		RSAU_001986
2118922.0	6.27	-0.39	0.5931	0.9382	+		RSAU_001986
2120741.0	5.06	0.47	0.5446	0.9042			
2122515.0	0.53	-1.15	0.1672	0.5985	-		RSAU_001989
2126497.0	1.61	-0.8	0.369	0.7723			
2126499.0	3.17	1.03	0.2272	0.5985			
2126500.0	0.76	0.61	0.49	0.8774			
2126531.0	3.83	-2.27	0.0081	0.2044			
2126593.0	0.2	0.02	0.9822	0.9889	+	mtlF	RSAU_001992
2132391.0	1.12	-0.41	0.6409	0.9554	-	fmtB	RSAU_001996
2132392.0	140.68	-0.9	0.2636	0.6351	-	fmtB	RSAU_001996
2132393.0	1.25	0.2	0.8142	0.9889	-	fmtB	RSAU_001996
2132734.0	0.66	-1.51	0.0823	0.5985	-	fmtB	RSAU_001996
2132977.0	1.02	-1.41	0.0987	0.5985	-	fmtB	RSAU_001996
2138493.0	0.53	1.28	0.1367	0.5985	-	fmtB	RSAU_001996
2139223.0	0.82	-1.32	0.1186	0.5985	-	fmtB	RSAU_001996
2139511.0	0.6	0.2	0.798	0.9889	-	fmtB	RSAU_001996
2141696.0	0.36	-0.19	0.8176	0.9889	-		RSAU_001998
2144168.0	1.55	-0.1	0.9124	0.9889			
2144363.0	0.31	0.98	0.2331	0.5985	-		RSAU_002002
2144828.0	0.58	1.53	0.0821	0.5985	-		RSAU_002007
2144939.0	0.26	0.96	0.2392	0.5985	-		RSAU_002008
2145234.0	0.5	1.28	0.1358	0.5985	-		RSAU_002008
2145380.0	0.32	0.98	0.2303	0.5985	-		RSAU_002008
2146227.0	0.89	0.47	0.5905	0.9372	-		RSAU_002008
2146436.0	18.94	-1.02	0.2454	0.6089	-		RSAU_002008
2146437.0	0.41	-0.22	0.7855	0.9889	-		RSAU_002008
2147289.0	0.26	0.96	0.2392	0.5985	-		RSAU_002008
2148279.0	0.52	0.1	0.902	0.9889	-		RSAU_002009
2149265.0	0.43	1.17	0.1679	0.5985	-		RSAU_002009
2151756.0	1.06	-0.81	0.3228	0.7152	-		RSAU_002011
2151893.0	0.41	-0.22	0.7855	0.9889	-		RSAU_002011
2152234.0	2.63	0.18	0.8209	0.9889	-		RSAU_002011
2155109.0	12.1	0.32	0.5875	0.9341	-		RSAU_002013
2155696.0	0.36	-0.19	0.8176	0.9889	-		RSAU_002014
2157338.0	1.08	1.4	0.1029	0.5985	-		RSAU_002016
2158383.0	4.62	-1.42	0.1023	0.5985			
2159670.0	0.69	-0.52	0.5174	0.9024	-		RSAU_002018
2160373.0	1.95	0.42	0.6228	0.9445	-	htsC	RSAU_002019
2166341.0	0.78	0.51	0.5627	0.9148	-		RSAU_002024
2174191.0	0.41	-0.22	0.7855	0.9889			
2184258.0	0.32	0.32	0.6918	0.9852			
2186805.0	1.1	-1.4	0.1	0.5985	-		RSAU_002043
2188373.0	0.48	0.07	0.9354	0.9889			
2190759.0	0.41	-1.31	0.1267	0.5985	+	hysA2	RSAU_002045
2191249.0	0.48	0.07	0.9354	0.9889	-		RSAU_002046
2192324.0	1.1	0.17	0.8464	0.9889	+		RSAU_002047
2193448.0	6.91	0.07	0.9211	0.9889			
2193475.0	0.43	-0.1	0.9048	0.9889			
2196524.0	0.53	-1.15	0.1672	0.5985			
2201981.0	0.7	0.91	0.3043	0.6915	-		RSAU_002056
2207034.0	0.54	0.16	0.8538	0.9889	-	infA	RSAU_002064
2210000.0	0.42	-0.19	0.8115	0.9889	-	rpsE	RSAU_002069
2218993.0	0.74	-0.29	0.741	0.9889	+		RSAU_002088
2218995.0	2.31	1.4	0.0932	0.5985	+		RSAU_002088
2219163.0	0.7	0.91	0.3043	0.6915	+		RSAU_002088
2219746.0	1.11	0.04	0.9619	0.9889	-		RSAU_002089
2220424.0	0.49	1.17	0.167	0.5985	-		RSAU_002089
2221738.0	3.47	0.54	0.5267	0.9042	-	topB	RSAU_002090
2221739.0	2.33	-0.24	0.7824	0.9889	-	topB	RSAU_002090
2222408.0	0.2	0.02	0.9822	0.9889	-	topB	RSAU_002090
2225362.0	0.37	-1.09	0.1867	0.5985			
2226221.0	0.42	-0.19	0.8115	0.9889	-		RSAU_002093
2231335.0	1.26	-0.2	0.8231	0.9889	-	femX	RSAU_002097
2231696.0	6.3	1.27	0.1142	0.5985	-	femX	RSAU_002097
2234835.0	0.32	0.98	0.2303	0.5985	+		RSAU_002100
2240334.0	0.2	0.02	0.9822	0.9889	-	moeA	RSAU_002107
2240491.0	0.38	-0.16	0.8442	0.9889	-	moeA	RSAU_002107
2241445.0	0.36	-0.19	0.8176	0.9889	-	moaB	RSAU_002109
2243535.0	2.39	-0.91	0.2924	0.6724	-	modB	RSAU_002112
2250743.0	3.01	-0.54	0.5458	0.9042	-		RSAU_002119
2250797.0	1.2	-0.65	0.454	0.8474	-		RSAU_002119
2251688.0	0.47	-0.13	0.8717	0.9889	-		RSAU_002120
2251954.0	0.38	-0.16	0.8442	0.9889	-		RSAU_002120
2256495.0	1.01	-0.49	0.5467	0.9042	+	ureG	RSAU_002126
2256998.0	12.12	-2.09	0.0175	0.3406	+	ureD	RSAU_002127
2258617.0	3.9	-1.1	0.204	0.5985			
2260458.0	0.36	-0.19	0.8176	0.9889	-		RSAU_002131
2265193.0	2.53	0.4	0.6269	0.9445	-		RSAU_002134
2266219.0	1.38	-0.34	0.7037	0.9889			
2266499.0	7.56	-0.36	0.6004	0.9402	+		RSAU_002135
2267624.0	6.21	-0.73	0.3933	0.7937			
2267699.0	0.2	0.02	0.9822	0.9889			

2268981.0	0.2	0.02	0.9822	0.9889			
2269056.0	0.36	-0.19	0.8176	0.9889	-		RSAU_002138
2269547.0	1.74	-0.2	0.8159	0.9889			
2269681.0	7.35	-1.61	0.0701	0.5985	-		RSAU_002139
2270155.0	1.91	-0.43	0.6145	0.9442	-		RSAU_002141
2270393.0	10.55	1.04	0.0709	0.5985	-		RSAU_002141
2270412.0	0.2	0.02	0.9822	0.9889	-		RSAU_002141
2270575.0	1.36	0.11	0.902	0.9889			
2271415.0	0.37	-0.43	0.6051	0.9402	-		RSAU_002142
2271416.0	0.26	0.96	0.2392	0.5985	-		RSAU_002142
2272767.0	0.22	0.04	0.9554	0.9889	-		RSAU_002143
2273311.0	0.48	-0.5	0.5479	0.9042			
2280131.0	8.98	-0.24	0.7784	0.9889	-		RSAU_002148
2282581.0	1.31	-1.08	0.2216	0.5985			
2282582.0	1.36	0.95	0.2723	0.6409			
2283833.0	4.94	-0.43	0.6309	0.9471	+		RSAU_002152
2284746.0	0.36	-0.19	0.8176	0.9889	-		RSAU_002153
2287418.0	1.29	0.1	0.8976	0.9889	-		RSAU_002156
2291324.0	14.88	0.61	0.2484	0.6118			
2291517.0	0.8	0.71	0.3818	0.7853			
2291977.0	8.31	-0.08	0.9271	0.9889	+		RSAU_002160
2291978.0	17.07	-0.32	0.713	0.9889	+		RSAU_002160
2293298.0	0.9	-1.71	0.0533	0.5815	-		RSAU_002162
2294011.0	0.2	0.02	0.9822	0.9889	-		RSAU_002162
2296471.0	0.71	-0.48	0.5476	0.9042	-		RSAU_002164
2301033.0	3.81	1.46	0.1013	0.5985			
2301367.0	1.34	-0.68	0.4321	0.8251	+		RSAU_002168
2303469.0	0.56	0.59	0.4672	0.8527			
2305067.0	0.53	-1.15	0.1672	0.5985	-	rpiA	RSAU_002171
2305804.0	0.85	-0.61	0.4405	0.8319			
2305805.0	264.65	0.63	0.1247	0.5985			
2305806.0	3.75	0.59	0.4625	0.8493			
2306255.0	0.26	0.96	0.2392	0.5985	+		RSAU_002172
2307310.0	7.13	0.7	0.42	0.8128	-	galM	RSAU_002173
2308636.0	0.73	-0.67	0.4196	0.8128	-		RSAU_002175
2310976.0	6.75	3.11	4.0E-4	0.034	-		RSAU_002177
2310977.0	2.9	0.88	0.3105	0.6982	-		RSAU_002177
2311991.0	4.82	-0.07	0.9386	0.9889	+		RSAU_002178
2312713.0	36.41	-0.75	0.2288	0.5985	+	gltS	RSAU_002179
2312714.0	0.38	-0.16	0.8442	0.9889	+	gltS	RSAU_002179
2315600.0	44.66	-2.87	1.0E-4	0.0102	-		RSAU_002181
2317106.0	7.36	-0.08	0.9267	0.9889	-		RSAU_002184
2317656.0	13.97	-2.66	3.0E-4	0.0256	-		RSAU_002184
2320809.0	2.64	2.05	0.021	0.3773	-		RSAU_002186
2321094.0	0.42	-0.19	0.8115	0.9889	-		RSAU_002187
2322216.0	0.36	-0.19	0.8176	0.9889	+		RSAU_002188
2323278.0	0.32	0.98	0.2303	0.5985	-	tcaB	RSAU_002189
2323285.0	1.83	0.56	0.5209	0.903	-	tcaB	RSAU_002189
2323287.0	2.7	0.22	0.7886	0.9889	-	tcaB	RSAU_002189
2323292.0	1.63	0.97	0.2779	0.6485	-	tcaB	RSAU_002189
2323331.0	0.37	-1.09	0.1867	0.5985	-	tcaB	RSAU_002189
2323370.0	0.27	0.1	0.8977	0.9889	-	tcaB	RSAU_002189
2323436.0	1.19	-1.07	0.223	0.5985	-	tcaB	RSAU_002189
2323474.0	0.65	-0.64	0.4606	0.8493	-	tcaB	RSAU_002189
2323849.0	5.17	-2.42	0.0049	0.1553			
2324193.0	0.36	0.36	0.6599	0.9656	-	tcaA	RSAU_002190
2324479.0	1.88	-1.52	0.0783	0.5985	-	tcaA	RSAU_002190
2324945.0	0.9	-1.27	0.1534	0.5985	-	tcaA	RSAU_002190
2326733.0	0.98	0.34	0.664	0.9701	+		RSAU_002192
2326754.0	2.24	-0.74	0.4061	0.8012	+		RSAU_002192
2327941.0	0.37	-0.43	0.6051	0.9402	-		RSAU_002193
2327942.0	0.26	0.96	0.2392	0.5985	-		RSAU_002193
2330327.0	1.84	0.69	0.3771	0.7816	+		RSAU_002196
2332108.0	0.86	0.65	0.4621	0.8493	+		RSAU_002197
2332884.0	1.42	0.84	0.3448	0.7425	+		RSAU_002199
2332984.0	0.32	0.98	0.2303	0.5985	+		RSAU_002199
2335787.0	0.36	-0.19	0.8176	0.9889	+		RSAU_002202
2340059.0	0.77	-1.33	0.1183	0.5985	+		RSAU_002205
2340765.0	0.26	0.96	0.2392	0.5985	+		RSAU_002205
2344776.0	0.32	0.98	0.2303	0.5985	-		RSAU_002210
2345256.0	0.37	-1.09	0.1867	0.5985	-		RSAU_002210
2345764.0	1.27	0.31	0.7193	0.9889	-		RSAU_002210
2347420.0	2.1	-1.18	0.1725	0.5985	-		RSAU_002212
2348270.0	0.6	-0.49	0.545	0.9042	+		RSAU_002213
2350033.0	0.46	-1.31	0.1257	0.5985	-	scrA	RSAU_002215
2350307.0	51.07	0.67	0.3232	0.7152	-	scrA	RSAU_002215
2350308.0	0.36	-0.19	0.8176	0.9889	-	scrA	RSAU_002215
2352161.0	4.23	-1.22	0.1343	0.5985		ssr42	
2352229.0	59.68	-1.36	0.1039	0.5985		ssr42	
2352274.0	42.24	0.76	0.3148	0.7037		ssr42	
2352952.0	0.38	-0.16	0.8442	0.9889		ssr42	
2353023.0	11.19	-0.99	0.0923	0.5985		ssr42	
2353024.0	2022.04	-1.69	0.0040	0.1465		ssr42	
2353025.0	14.82	-1.03	0.1555	0.5985		ssr42	
2353046.0	0.37	-0.43	0.6051	0.9402			
2353057.0	0.66	-1.31	0.1224	0.5985			
2353062.0	1.37	-1.9	0.0321	0.4751			

2353280.0	0.54	-1.45	0.0941	0.5985			
2353281.0	3.66	-0.53	0.4882	0.8755			
2353282.0	867.55	-0.87	0.0459	0.5692			
2353283.0	10.71	-0.32	0.6807	0.981			
2353284.0	6.57	-1.93	0.0142	0.2953			
2353319.0	0.46	-1.31	0.1257	0.5985	+	rsp	RSAU_002217
2353323.0	6.61	-0.64	0.3878	0.79	+	rsp	RSAU_002217
2353324.0	1212.95	-0.93	0.0077	0.2032	+	rsp	RSAU_002217
2353325.0	12.97	0.32	0.6468	0.9604	+	rsp	RSAU_002217
2353331.0	1.24	-1.95	0.0282	0.4415	+	rsp	RSAU_002217
2353358.0	2.0	-1.66	0.0493	0.5815	+	rsp	RSAU_002217
2353364.0	0.75	-1.67	0.0572	0.5815	+	rsp	RSAU_002217
2353367.0	0.89	-0.25	0.7811	0.9889	+	rsp	RSAU_002217
2353378.0	243.12	1.23	0.1575	0.5985	+	rsp	RSAU_002217
2353379.0	3.43	0.87	0.2628	0.6349	+	rsp	RSAU_002217
2353388.0	3.17	-3.06	5.0E-4	0.036	+	rsp	RSAU_002217
2353394.0	41.95	1.47	0.0922	0.5985	+	rsp	RSAU_002217
2353428.0	0.55	0.22	0.798	0.9889	+	rsp	RSAU_002217
2353431.0	520.12	-0.64	0.3599	0.7631	+	rsp	RSAU_002217
2353432.0	44994.83	-1.18	0.0151	0.306	+	rsp	RSAU_002217
2353433.0	169.76	-0.08	0.9009	0.9889	+	rsp	RSAU_002217
2353434.0	0.77	-1.33	0.1183	0.5985	+	rsp	RSAU_002217
2353435.0	163.58	-0.26	0.7074	0.9889	+	rsp	RSAU_002217
2353436.0	16896.23	-0.92	0.0354	0.5014	+	rsp	RSAU_002217
2353437.0	44.76	-0.64	0.3355	0.7311	+	rsp	RSAU_002217
2353438.0	0.81	-0.19	0.8277	0.9889	+	rsp	RSAU_002217
2353440.0	15.58	-0.55	0.4741	0.8606	+	rsp	RSAU_002217
2353442.0	3.82	-0.55	0.4922	0.8774	+	rsp	RSAU_002217
2353450.0	0.84	-0.43	0.626	0.9445	+	rsp	RSAU_002217
2353454.0	0.36	-0.15	0.8534	0.9889	+	rsp	RSAU_002217
2353470.0	2.3	-1.11	0.1736	0.5985	+	rsp	RSAU_002217
2353475.0	1.11	-0.5	0.5714	0.9216	+	rsp	RSAU_002217
2353525.0	0.27	0.1	0.8977	0.9889	+	rsp	RSAU_002217
2353573.0	0.7	-1.69	0.0558	0.5815	+	rsp	RSAU_002217
2353586.0	0.33	-1.08	0.1895	0.5985	+	rsp	RSAU_002217
2353592.0	0.44	-0.3	0.7187	0.9889	+	rsp	RSAU_002217
2353595.0	1.7	-2.47	0.0053	0.164	+	rsp	RSAU_002217
2353657.0	0.82	-1.11	0.214	0.5985	+	rsp	RSAU_002217
2353666.0	0.32	0.32	0.6918	0.9852	+	rsp	RSAU_002217
2353667.0	136.21	0.96	0.2528	0.6186	+	rsp	RSAU_002217
2353672.0	0.88	-1.69	0.0543	0.5815	+	rsp	RSAU_002217
2353681.0	76.79	-0.68	0.1965	0.5985	+	rsp	RSAU_002217
2353682.0	0.69	-0.81	0.3591	0.7631	+	rsp	RSAU_002217
2353685.0	7.72	0.1	0.905	0.9889	+	rsp	RSAU_002217
2353767.0	172.6	1.48	0.095	0.5985	+	rsp	RSAU_002217
2353768.0	3.11	0.64	0.392	0.7926	+	rsp	RSAU_002217
2353769.0	0.46	-1.31	0.1257	0.5985	+	rsp	RSAU_002217
2353808.0	2.41	-0.9	0.2762	0.6469	+	rsp	RSAU_002217
2353946.0	2.29	-2.29	0.0078	0.2032	+	rsp	RSAU_002217
2353976.0	1.79	-2.52	0.0045	0.1486	+	rsp	RSAU_002217
2353985.0	1.62	-1.91	0.0293	0.444	+	rsp	RSAU_002217
2354077.0	0.58	-1.56	0.0751	0.5985	+	rsp	RSAU_002217
2354116.0	0.37	-1.09	0.1867	0.5985	+	rsp	RSAU_002217
2354134.0	0.46	-1.31	0.1257	0.5985	+	rsp	RSAU_002217
2354156.0	4.03	-2.08	0.0189	0.3608	+	rsp	RSAU_002217
2354171.0	1.25	-1.66	0.0605	0.5873	+	rsp	RSAU_002217
2354173.0	7.61	-2.32	0.0018	0.092	+	rsp	RSAU_002217
2354215.0	0.54	-1.45	0.0941	0.5985	+	rsp	RSAU_002217
2354245.0	0.46	-1.31	0.1257	0.5985	+	rsp	RSAU_002217
2354362.0	135.03	1.04	0.1962	0.5985	+	rsp	RSAU_002217
2354398.0	0.53	-0.4	0.6304	0.9471	+	rsp	RSAU_002217
2354417.0	0.63	-1.55	0.0762	0.5985	+	rsp	RSAU_002217
2354452.0	2.26	-2.15	0.0144	0.296	+	rsp	RSAU_002217
2354455.0	0.2	0.02	0.9822	0.9889	+	rsp	RSAU_002217
2354484.0	39.44	1.59	0.0738	0.5985	+	rsp	RSAU_002217
2354486.0	1.64	-2.34	0.0087	0.2085	+	rsp	RSAU_002217
2354531.0	0.37	-1.09	0.1867	0.5985	+	rsp	RSAU_002217
2354560.0	0.96	-2.05	0.0213	0.3773	+	rsp	RSAU_002217
2354601.0	0.96	-2.05	0.0213	0.3773	+	rsp	RSAU_002217
2354603.0	2.91	-1.75	0.0334	0.4796	+	rsp	RSAU_002217
2354688.0	1.03	-1.09	0.2182	0.5985	+	rsp	RSAU_002217
2354729.0	0.54	-1.45	0.0941	0.5985	+	rsp	RSAU_002217
2354778.0	2.68	-1.81	0.0362	0.5052	+	rsp	RSAU_002217
2354804.0	3.83	-1.71	0.0431	0.5604	+	rsp	RSAU_002217
2354823.0	3.1	0.52	0.54	0.9042	+	rsp	RSAU_002217
2354824.0	364.86	-0.86	0.1085	0.5985	+	rsp	RSAU_002217
2354825.0	2.75	-1.1	0.1808	0.5985	+	rsp	RSAU_002217
2354828.0	0.92	-1.19	0.1809	0.5985	+	rsp	RSAU_002217
2354839.0	0.53	0.02	0.9779	0.9889	+	rsp	RSAU_002217
2354856.0	3.16	-2.82	0.0014	0.0772	+	rsp	RSAU_002217
2354858.0	1.24	-2.23	0.0121	0.2598	+	rsp	RSAU_002217
2354895.0	9.25	0.44	0.5901	0.9372	+	rsp	RSAU_002217
2354896.0	8517.83	0.01	0.988	0.9932	+	rsp	RSAU_002217
2354897.0	2600.51	-0.97	0.0691	0.5985	+	rsp	RSAU_002217
2354898.0	29.63	-0.57	0.4163	0.8128	+	rsp	RSAU_002217
2354950.0	6.48	-2.58	0.0019	0.092	+	rsp	RSAU_002217
2354953.0	78.87	1.26	0.142	0.5985	+	rsp	RSAU_002217

2354970.0	1.24	-1.15	0.1934	0.5985	+	rsp	RSAU_002217
2354991.0	2.08	-2.14	0.0127	0.2704	+	rsp	RSAU_002217
2355019.0	2.75	-2.25	0.0097	0.2224	+	rsp	RSAU_002217
2355023.0	211.46	1.18	0.1704	0.5985	+	rsp	RSAU_002217
2355024.0	3.36	1.41	0.0965	0.5985	+	rsp	RSAU_002217
2355068.0	0.8	-1.66	0.0586	0.5815	+	rsp	RSAU_002217
2355072.0	1.04	-2.12	0.0172	0.3387	+	rsp	RSAU_002217
2355076.0	0.54	-1.45	0.0941	0.5985	+	rsp	RSAU_002217
2355136.0	0.72	1.66	0.0605	0.5873	+	rsp	RSAU_002217
2355137.0	227.86	1.49	0.0178	0.3443	+	rsp	RSAU_002217
2355138.0	2.53	1.34	0.0949	0.5985	+	rsp	RSAU_002217
2355178.0	0.46	-1.31	0.1257	0.5985	+	rsp	RSAU_002217
2355267.0	1.16	-1.59	0.0724	0.5985	+	rsp	RSAU_002217
2355271.0	0.56	-0.43	0.6266	0.9445	+	rsp	RSAU_002217
2355272.0	0.37	-1.09	0.1867	0.5985	+	rsp	RSAU_002217
2355295.0	1.36	-1.27	0.153	0.5985	+	rsp	RSAU_002217
2355386.0	150.63	-0.8	0.2633	0.6351	+	rsp	RSAU_002217
2355387.0	15828.25	-1.46	0.0	9.0E-4	+	rsp	RSAU_002217
2355388.0	90.05	-0.95	0.2033	0.5985	+	rsp	RSAU_002217
2355389.0	0.63	-1.55	0.0762	0.5985	+	rsp	RSAU_002217
2355457.0	0.92	0.6	0.4919	0.8774			
2355477.0	10.05	0.6	0.4991	0.8864			
2356893.0	0.72	-0.23	0.7684	0.9889	-		RSAU_002220
2356918.0	0.2	0.02	0.9822	0.9889	-		RSAU_002220
2356995.0	0.36	-0.19	0.8176	0.9889	-		RSAU_002220
2357462.0	0.41	-0.22	0.7855	0.9889	-		RSAU_002221
2357487.0	2.98	-0.26	0.7559	0.9889	-		RSAU_002221
2357547.0	0.36	0.36	0.6599	0.9656	-		RSAU_002221
2357597.0	0.98	-0.49	0.5667	0.9185	-		RSAU_002221
2357619.0	7.97	-1.72	0.0534	0.5815	-		RSAU_002221
2358089.0	3.25	-1.22	0.163	0.5985	-		RSAU_002221
2358327.0	10.16	1.02	0.0829	0.5985	-		RSAU_002221
2358346.0	0.43	0.05	0.9531	0.9889	-		RSAU_002221
2358378.0	2.01	-2.56	0.0040	0.1465	-		RSAU_002221
2358506.0	6.66	-0.38	0.6591	0.9656	-		RSAU_002221
2360844.0	0.75	-1.03	0.2467	0.6106			
2362563.0	1.12	0.39	0.6092	0.9442	-	rT	RSAU_002226
2364528.0	0.53	-1.15	0.1672	0.5985	+		RSAU_002227
2368318.0	0.84	-1.7	0.0529	0.5815	-	rI	RSAU_002232
2369603.0	6.37	-2.46	0.0016	0.0829	-	rH	RSAU_002234
2370018.0	0.65	0.16	0.8432	0.9889	-	rH	RSAU_002234
2371611.0	7.57	0.8	0.2832	0.656	-	rG	RSAU_002235
2371987.0	15.48	1.11	0.1643	0.5985	-	rG	RSAU_002235
2372719.0	1.0	-0.77	0.375	0.7781	-	rG	RSAU_002235
2372724.0	0.53	-1.15	0.1672	0.5985	-	rG	RSAU_002235
2375259.0	0.34	0.4	0.6432	0.9572	-		RSAU_002236
2375646.0	1.58	-1.72	0.0514	0.5815	-		RSAU_002236
2375656.0	4.43	-0.66	0.4376	0.8302	-	nirD	RSAU_002237
2375658.0	1.7	1.08	0.2189	0.5985	-	nirD	RSAU_002237
2379497.0	0.27	0.1	0.8977	0.9889	-		RSAU_002240
2380050.0	1.43	0.28	0.742	0.9889			
2380914.0	0.46	-0.55	0.512	0.9024	-		RSAU_002241
2380935.0	0.31	0.98	0.2331	0.5985	-		RSAU_002241
2382215.0	2.83	0.05	0.9568	0.9889			
2383789.0	0.87	-0.57	0.47	0.8553	-		RSAU_002244
2387987.0	0.42	-0.19	0.8115	0.9889	-		RSAU_002250
2390601.0	0.6	-0.49	0.545	0.9042	-		RSAU_002253
2392012.0	6.52	0.6	0.4053	0.8012	-	gpmA	RSAU_002255
2392744.0	1.21	-0.45	0.6135	0.9442			
2392926.0	0.26	0.96	0.2392	0.5985	-		RSAU_002256
2393661.0	0.37	-1.09	0.1867	0.5985			
2396652.0	0.22	0.04	0.9554	0.9889	+	hlgA	RSAU_002258
2396732.0	0.39	1.17	0.1684	0.5985	+	hlgA	RSAU_002258
2398833.0	14.51	1.13	0.1675	0.5985	+	hlgB	RSAU_002260
2400269.0	2.01	0.2	0.8193	0.9889	-	bioW	RSAU_002262
2401642.0	0.61	-0.15	0.8618	0.9889	-	bioF	RSAU_002263
2402743.0	17.04	-0.19	0.7044	0.9889	-	bioB	RSAU_002264
2403110.0	0.41	-0.22	0.7855	0.9889	-	bioA	RSAU_002265
2404378.0	2.93	-0.66	0.4598	0.8493	-	bioD	RSAU_002266
2404557.0	1.16	-0.31	0.7244	0.9889	-	bioD	RSAU_002266
2404558.0	0.51	-0.49	0.5791	0.9253	-	bioD	RSAU_002266
2406736.0	0.2	0.02	0.9822	0.9889	-		RSAU_002268
2409178.0	0.22	0.04	0.9554	0.9889			
2414732.0	1.05	-0.06	0.9486	0.9889	+		RSAU_002276
2415415.0	0.33	-1.08	0.1895	0.5985	-		RSAU_002277
2415583.0	1.07	-1.01	0.2501	0.6134	-		RSAU_002277
2420049.0	0.62	0.42	0.6365	0.9532	-		RSAU_002280
2421201.0	0.46	-1.31	0.1257	0.5985	-		RSAU_002280
2424087.0	1.05	-0.5	0.5148	0.9024	-		RSAU_002282
2426890.0	6.23	-2.15	0.0158	0.3165	-		RSAU_002284
2426891.0	0.53	-1.15	0.1672	0.5985	-		RSAU_002284
2431306.0	0.26	0.96	0.2392	0.5985			
2431362.0	0.51	0.69	0.4358	0.8295			
2432214.0	7.44	1.38	0.1034	0.5985	-		RSAU_002289
2437458.0	2.78	0.45	0.5544	0.9111			
2437506.0	6.8	-2.74	0.0012	0.0672			
2438832.0	0.42	-0.19	0.8115	0.9889	-		RSAU_002294

2439641.0	0.69	-0.52	0.5174	0.9024	-	pepA2	RSAU_002295
2440739.0	8.23	-0.67	0.4357	0.8295			
2444896.0	0.82	-0.44	0.6163	0.9445			
2445576.0	0.41	0.46	0.6005	0.9402	-		RSAU_002300
2446183.0	0.38	1.17	0.1692	0.5985	-		RSAU_002300
2447614.0	0.38	1.17	0.1692	0.5985	-	opp1D	RSAU_002302
2448461.0	0.87	-1.19	0.1801	0.5985	-	opp1C	RSAU_002303
2451152.0	0.42	-0.19	0.8115	0.9889	-	opp1A	RSAU_002305
2453848.0	0.26	0.96	0.2392	0.5985	-		RSAU_002308
2454340.0	3.36	1.41	0.0965	0.5985			
2456193.0	0.38	-0.16	0.8442	0.9889	-		RSAU_002310
2456572.0	0.51	-0.41	0.6403	0.9553	-		RSAU_002310
2456680.0	0.51	-0.49	0.5791	0.9253			
2458507.0	0.26	0.96	0.2392	0.5985			
2458746.0	2.09	0.11	0.9058	0.9889	-		RSAU_002312
2461136.0	0.2	0.02	0.9822	0.9889			
2463227.0	3.48	-0.77	0.3746	0.7781			
2469244.0	2.62	0.37	0.628	0.9445			
2469805.0	1.25	-0.71	0.4146	0.8128	-		RSAU_002326
2469909.0	2.99	-0.66	0.4582	0.8493			
2470806.0	1.95	-1.92	0.0298	0.4483	+		RSAU_002327
2471141.0	7.0	-0.07	0.9354	0.9889	+		RSAU_002327
2471143.0	6.27	-0.39	0.5931	0.9382	+		RSAU_002327
2472333.0	0.36	-0.19	0.8176	0.9889			
2473338.0	0.48	0.07	0.9354	0.9889			
2475184.0	3.94	-1.61	0.0366	0.5052	-		RSAU_002332
2478422.0	0.41	-0.22	0.7855	0.9889	+		RSAU_002334
2479723.0	0.98	-0.4	0.6551	0.9656			
2479841.0	0.26	0.96	0.2392	0.5985			
2481432.0	0.6	-0.49	0.545	0.9042	-		RSAU_002338
2481455.0	0.72	-0.54	0.5336	0.9042	-		RSAU_002338
2483137.0	1.06	-0.8	0.3688	0.7723	-	galU	RSAU_002339
2486710.0	0.74	1.32	0.1232	0.5985			
2487266.0	0.32	0.98	0.2303	0.5985	-	fnbA	RSAU_002341
2493490.0	0.94	1.39	0.1066	0.5985	-	gntK	RSAU_002343
2493491.0	0.84	0.27	0.7243	0.9889	-	gntK	RSAU_002343
2496706.0	2.09	0.31	0.7103	0.9889			
2497759.0	1.14	-1.65	0.0587	0.5815	-		RSAU_002348
2501910.0	1.89	1.57	0.0707	0.5985	+		RSAU_002350
2502403.0	0.71	-1.62	0.0653	0.5985			
2502627.0	8.74	-0.58	0.5033	0.8913	+		RSAU_002351
2502762.0	6.77	0.82	0.2779	0.6485	+		RSAU_002351
2503645.0	0.2	0.02	0.9822	0.9889			
2503720.0	0.36	-0.19	0.8176	0.9889	-		RSAU_002352
2504214.0	1.74	-0.2	0.8159	0.9889	-		RSAU_002353
2504348.0	7.03	-1.69	0.0586	0.5815	-		RSAU_002354
2504822.0	1.91	-0.43	0.6145	0.9442	-		RSAU_002356
2505060.0	10.42	1.07	0.0671	0.5985	-		RSAU_002356
2505079.0	0.2	0.02	0.9822	0.9889	-		RSAU_002356
2505242.0	1.08	0.37	0.678	0.98			
2505986.0	0.53	-1.15	0.1672	0.5985			
2509344.0	0.26	0.96	0.2392	0.5985	+		RSAU_002358
2509608.0	0.6	0.2	0.798	0.9889			
2511926.0	8.49	-1.08	0.1856	0.5985			
2513786.0	8.77	0.73	0.3599	0.7631	-	frp	RSAU_002364
2515480.0	2.07	-0.49	0.5799	0.9258			
2515590.0	14.44	-0.57	0.5135	0.9024			
2518450.0	10.74	-0.29	0.6755	0.9797	-	srtA	RSAU_002369
2520286.0	0.41	-0.22	0.7855	0.9889	-	sdaAA	RSAU_002372
2524525.0	1.13	-1.03	0.2378	0.5985	+		RSAU_002375
2526198.0	0.85	-0.61	0.4405	0.8319	-		RSAU_002378
2526962.0	0.44	0.49	0.5479	0.9042	-	glcB	RSAU_002379
2527353.0	5.88	-2.92	7.0E-4	0.0473	-	glcB	RSAU_002379
2529026.0	0.38	-0.16	0.8442	0.9889			
2530425.0	0.53	1.28	0.1367	0.5985	-	cidC	RSAU_002380
2531260.0	0.39	1.17	0.1684	0.5985	-		RSAU_002381
2534194.0	0.33	-1.08	0.1895	0.5985	+	ssaA4	RSAU_002384
2534239.0	1.31	0.05	0.9532	0.9889	+	ssaA4	RSAU_002384
2534435.0	1.85	0.84	0.3451	0.7425	+	ssaA4	RSAU_002384
2534718.0	0.37	-1.09	0.1867	0.5985	-	mvaA	RSAU_002385
2537661.0	0.43	-0.1	0.9048	0.9889	-		RSAU_002387
2537662.0	40.2	-0.61	0.2012	0.5985	-		RSAU_002387
2537802.0	0.42	-0.19	0.8115	0.9889	-		RSAU_002387
2537803.0	122.05	-0.26	0.6926	0.9855	-		RSAU_002387
2537804.0	0.9	-0.24	0.7792	0.9889	-		RSAU_002387
2538352.0	1.34	-0.31	0.6809	0.981			
2539809.0	0.36	-0.19	0.8176	0.9889	+	clpL	RSAU_002389
2539962.0	33.05	-0.84	0.242	0.6016	+	clpL	RSAU_002389
2539963.0	1.13	-0.87	0.3211	0.7152	+	clpL	RSAU_002389
2541364.0	0.47	-0.13	0.8717	0.9889	+	clpL	RSAU_002389
2543042.0	1.73	-0.01	0.9947	0.9974	-	feoB1	RSAU_002391
2543449.0	3.07	-0.67	0.4429	0.8356	-	feoB1	RSAU_002391
2543675.0	0.76	-0.19	0.8108	0.9889	-	feoA	RSAU_002392
2544062.0	0.7	0.19	0.8104	0.9889			
2554919.0	0.26	0.96	0.2392	0.5985	-		RSAU_002401
2555486.0	18.4	0.78	0.3233	0.7152	-		RSAU_002401
2556112.0	0.33	-1.08	0.1895	0.5985			

2558696.0	1.11	1.08	0.2191	0.5985	-		RSAU_002404
2558697.0	339.12	0.79	0.0443	0.5626	-		RSAU_002404
2558698.0	4.31	0.62	0.4278	0.8209	-		RSAU_002404
2559117.0	2.44	-1.88	0.0288	0.4415	-		RSAU_002404
2560489.0	0.2	0.02	0.9822	0.9889	-		RSAU_002405
2561557.0	2.47	1.12	0.1869	0.5985	-		RSAU_002406
2561558.0	4.62	1.07	0.176	0.5985	-		RSAU_002406
2561798.0	1.87	-1.19	0.1799	0.5985			
2563968.0	0.38	1.17	0.1692	0.5985	-		RSAU_002408
2563969.0	0.46	0.66	0.4528	0.8474	-		RSAU_002408
2564723.0	0.38	-0.16	0.8442	0.9889	-		RSAU_002408
2564752.0	2.66	1.17	0.1884	0.5985	-		RSAU_002408
2565439.0	0.41	-0.22	0.7855	0.9889			
2566865.0	0.32	0.98	0.2303	0.5985	-	isaA	RSAU_002410
2566875.0	0.89	1.9	0.0332	0.4796			
2567559.0	1.61	-0.59	0.4909	0.8774	-		RSAU_002411
2567916.0	0.77	-1.33	0.1183	0.5985	-		RSAU_002411
2568494.0	0.72	0.4	0.6224	0.9445	-		RSAU_002411
2568795.0	0.6	-0.49	0.545	0.9042			
2570219.0	0.2	0.02	0.9822	0.9889			
2572866.0	0.49	1.17	0.167	0.5985	+		RSAU_002418
2575907.0	1.11	0.87	0.3265	0.7205	-	cobW	RSAU_002423
2576824.0	1.35	0.63	0.4672	0.8527			
2576839.0	0.26	0.96	0.2392	0.5985	-	feoB	RSAU_002424
2576944.0	0.37	-1.09	0.1867	0.5985	-	feoB	RSAU_002424
2577147.0	1.3	-1.44	0.1071	0.5985	-	feoB	RSAU_002424
2580906.0	1.06	-1.48	0.0863	0.5985	-		RSAU_002429
2584695.0	0.53	-1.15	0.1672	0.5985			
2585229.0	1.27	0.34	0.7017	0.9889			
2585593.0	1.39	0.45	0.557	0.9121	-		RSAU_002434
2590958.0	2.23	0.86	0.273	0.6418	-	panC	RSAU_002439
2591984.0	0.32	0.98	0.2303	0.5985	+	panE	RSAU_002441
2593695.0	1.26	-0.56	0.4844	0.8717			
2598175.0	13.39	-0.53	0.5441	0.9042	-		RSAU_002445
2598467.0	4.39	2.67	0.0027	0.1128			
2598538.0	3.71	-1.0	0.165	0.5985			
2600881.0	15.98	0.66	0.4379	0.8302	-	mqo2	RSAU_002448
2601942.0	7.68	-1.02	0.1377	0.5985			
2602860.0	0.2	0.02	0.9822	0.9889	-		RSAU_002449
2602861.0	27.92	-0.24	0.7854	0.9889	-		RSAU_002449
2603416.0	0.65	-0.64	0.4606	0.8493	-		RSAU_002449
2603417.0	1.41	-0.64	0.4579	0.8493	-		RSAU_002449
2605374.0	0.87	1.55	0.0766	0.5985			
2605405.0	0.53	-1.15	0.1672	0.5985			
2605421.0	1.33	-1.29	0.1472	0.5985			
2605631.0	1.1	-0.3	0.7251	0.9889	-	cdh	RSAU_002452
2611881.0	0.73	-0.9	0.3102	0.6982	-	cudT	RSAU_002456
2615825.0	0.2	0.02	0.9822	0.9889	-		RSAU_002459
2616610.0	1.94	-1.5	0.0871	0.5985	-		RSAU_002459
2618807.0	0.96	-2.05	0.0213	0.3773	-	cysJ	RSAU_002461
2621173.0	3.76	-1.49	0.0927	0.5985	-		RSAU_002463
2621586.0	0.53	0.02	0.9779	0.9889			
2622532.0	0.86	-0.99	0.2666	0.6354	-		RSAU_002465
2623440.0	0.31	0.98	0.2331	0.5985	-		RSAU_002465
2623441.0	5.25	-0.05	0.9474	0.9889	-		RSAU_002465
2623442.0	3.73	0.72	0.3665	0.7714	-		RSAU_002465
2625802.0	0.95	-1.41	0.0992	0.5985	-		RSAU_002467
2630103.0	0.22	0.04	0.9554	0.9889	-	estA	RSAU_002472
2633936.0	0.27	0.1	0.8977	0.9889	-	arcR	RSAU_002474
2634322.0	0.32	0.32	0.6918	0.9852	-	arcC	RSAU_002475
2637057.0	5.77	0.2	0.8192	0.9889	-	arcB2	RSAU_002477
2643636.0	0.2	0.02	0.9822	0.9889	+		RSAU_002483
2649620.0	5.08	-0.02	0.9808	0.9889	-		RSAU_002486
2651542.0	0.36	-0.19	0.8176	0.9889	-		RSAU_002486
2652348.0	0.41	-0.22	0.7855	0.9889	+		RSAU_002487
2653448.0	0.39	1.17	0.1684	0.5985	+		RSAU_002487
2653630.0	0.89	1.61	0.0668	0.5985	+		RSAU_002487
2660419.0	3.68	0.21	0.8108	0.9889	-	secA2	RSAU_002492
2665905.0	4.77	-0.07	0.9325	0.9889	-	asp1	RSAU_002495
2665944.0	1.39	-1.44	0.092	0.5985	-	asp1	RSAU_002495
2667950.0	0.38	1.17	0.1692	0.5985	-	sraP	RSAU_002497
2668046.0	7.0	-0.36	0.6818	0.9811	-	sraP	RSAU_002497
2669336.0	4.53	-0.85	0.3208	0.7152	-	sraP	RSAU_002497
2670672.0	0.37	-1.09	0.1867	0.5985	-	sraP	RSAU_002497
2672292.0	0.31	0.98	0.2331	0.5985	-	sraP	RSAU_002497
2672787.0	0.42	-0.19	0.8115	0.9889	-	sraP	RSAU_002497
2672989.0	0.33	-1.08	0.1895	0.5985	-	sraP	RSAU_002497
2676078.0	0.37	-0.43	0.6051	0.9402	+		RSAU_002499
2678091.0	0.69	0.1	0.9093	0.9889	+		RSAU_002501
2678276.0	2.31	0.27	0.7441	0.9889	+		RSAU_002501
2678810.0	0.38	-0.16	0.8442	0.9889	+		RSAU_002502
2680790.0	1.86	0.32	0.663	0.9693	-		RSAU_002504
2684654.0	0.69	-0.52	0.5174	0.9024			
2686911.0	1.5	-0.19	0.829	0.9889	+	icaA	RSAU_002511
2689120.0	0.75	0.97	0.2716	0.6407	+	icaC	RSAU_002513
2692668.0	0.2	0.02	0.9822	0.9889	-		RSAU_002515
2695145.0	3.41	-1.73	0.0518	0.5815	-	hisA	RSAU_002519

2695730.0	0.74	-0.27	0.7596	0.9889	-	hisH	RSAU_002520
2696769.0	2.95	0.87	0.2648	0.6354	-	hisC1	RSAU_002522
2698015.0	1.43	0.0	0.9958	0.9974	-	hisD	RSAU_002523
2698062.0	1.09	-0.68	0.388	0.79	-	hisD	RSAU_002523
2701355.0	1.29	-0.67	0.4453	0.8384	-		RSAU_002526
2702898.0	0.71	-0.48	0.5476	0.9042	-		RSAU_002528
2706246.0	2.13	1.11	0.2029	0.5985	-		RSAU_002531
2708766.0	0.77	-0.08	0.9287	0.9889	+		RSAU_002534
2710121.0	0.66	-1.31	0.1224	0.5985	+	pcp	RSAU_002535
2713370.0	0.67	-0.36	0.6844	0.9841	-	c	RSAU_002539
2713479.0	0.26	0.96	0.2392	0.5985	-	c	RSAU_002539
2714939.0	0.62	-0.45	0.5761	0.9244	-	c	RSAU_002539
2718016.0	0.66	0.38	0.668	0.9723	-	rarD	RSAU_002541
2719231.0	8.75	1.3	0.0691	0.5985	+		RSAU_002542
2719232.0	624.91	1.33	0.0023	0.1022	+		RSAU_002542
2719233.0	1.96	0.67	0.4187	0.8128	+		RSAU_002542
2720367.0	0.43	-0.1	0.9048	0.9889	+	nixA	RSAU_002543
2727122.0	0.98	-0.63	0.4213	0.8128	+		RSAU_002552
2728542.0	4.03	1.04	0.2393	0.5985			
2729164.0	2.27	0.35	0.6699	0.9742	-		RSAU_002555
2731704.0	4.99	0.18	0.8388	0.9889	-	rsmG	RSAU_002558
2736255.0	12.0	1.9	0.0286	0.4415			

Bibliography

[1] F. D. Lowy. Staphylococcus aureus infections. *N Engl J Med*, 1998.

[2] A. Ogston. Micrococcus poisoning. *J Anat Physiol*, 17(Pt 1):24–58, 1882. Ogston, A eng England J Anat Physiol. 1882 Oct;17(Pt 1):24-58.

[3] S. T. COWAN, C. SHAW, and R. E. WILLIAMS. Type strain for staphylococcus aureus rosenbach. *J Gen Microbiol*, 10(1): 174–176, Feb 1954.

[4] L Senn, P Basset, I Nahimana, G Zanetti, and DS Blanc. Which anatomical sites should be sampled for screening of methicillin-resistant staphylococcus aureus carriage by culture or by rapid pcr test? *Clinical Microbiology and Infection*, 18 (2):E31–E33, 2012.

[5] Wolfgang Witte. Community-acquired methicillin-resistant staphylococcus aureus: what do we need to know? *Clinical Microbiology and Infection*, 15(s7):17–25, 2009.

[6] J. A. Kluytmans, J. W. Mouton, E. P. Ijzerman, C. M. Vandenbroucke-Grauls, A. W. Maat, J. H. Wagenvoort, and H. A. Verbrugh. Nasal carriage of staphylococcus aureus as a major risk factor for wound infections after cardiac surgery. *J Infect Dis*, 171 (1):216–9, 1995.

[7] W. C. Noble, H. A. Valkenburg, and C. H. Wolters. Carriage of staphylococcus aureus in random samples of a normal population. *J Hyg (Lond)*, 65(4):567–73, 1967.

[8] V. L. Yu, A. Goetz, M. Wagener, P. B. Smith, J. D. Rihs, J. Hanchett, and J. J. Zuravleff. Staphylococcus aureus nasal carriage and infection in patients on hemodialysis. efficacy of antibiotic prophylaxis. *N Engl J Med*, 315(2):91–6, 1986.

[9] C. von Eiff, K. Becker, K. Machka, H. Stammer, and G. Peters. Nasal carriage as a source of staphylococcus aureus bacteremia. study group. *N Engl J Med*, 344(1):11–6, 2001.

[10] C. U. Tuazon, A. Perez, T. Kishaba, and J. N. Sheagren. Staphylococcus aureus among insulin-injecting diabetic patients. an increased carrier rate. *JAMA*, 231(12):1272, 1975.

[11] Lona Mody, Carol A Kauffman, Susan Donabedian, Marcus Zervos, and Suzanne F Bradley. Epidemiology of staphylococcus aureus colonization in nursing home residents. *Clinical Infectious Diseases*, 46(9):1368–1373, 2008.

[12] D. S. Berman, S. Schaefler, M. S. Simberkoff, and J. J. Rahal. Staphylococcus aureus colonization in intravenous drug abusers, dialysis patients, and diabetics. *J Infect Dis*, 155(4):829–31, 1987.

[13] M. Miller, C. Cespedes, P. Vavagiakis, R. S. Klein, and F. D. Lowy. Staphylococcus aureus colonization in a community sample of hiv-infected and hiv-uninfected drug users. *Eur J Clin Microbiol Infect Dis*, 22(8):463–9, 2003.

[14] REO Williams. Healthy carriage of staphylococcus aureus: its prevalence and importance. *Bacteriological reviews*, 27(1):56, 1963.

[15] Alex van Belkum, Nelianne J Verkaik, Corné P de Vogel, Hélène A Boelens, Jeroen Verveer, Jan L Nouwen, Henri A Verbrugh, and Heiman FL Wertheim. Reclassification of staphylococcus aureus nasal carriage types. *Journal of Infectious Diseases*, 199(12):1820–1826, 2009.

[16] T Khanna, R Friendship, C Dewey, and JS Weese. Methicillin resistant staphylococcus aureus colonization in pigs and pig farmers. *Veterinary microbiology*, 128(3):298–303, 2008.

[17] Marina Morgan. Methicillin-resistant staphylococcus aureus and animals: zoonosis or humanosis? *Journal of Antimicrobial Chemotherapy*, 62(6):1181–1187, 2008.

[18] Henrik Hasman, Arshnee Moodley, Luca Guardabassi, M Stegger, RL Skov, and Frank Møller Aarestrup. Spa type distribution in staphylococcus aureus originating from pigs, cattle and poultry. *Veterinary microbiology*, 141(3):326–331, 2010.

[19] Beth A Hanselman, Steve A Kruth, Joyce Rousseau, Donald E Low, Barbara M Willey, Allison McGeer, and J Scott Weese. Methicillin-resistant staphylococcus aureus colonization in veterinary personnel. *Emerging infectious diseases*, 12(12):1933, 2006.

[20] Christopher Weidenmaier, Christiane Goerke, and Christiane Wolz. Staphylococcus aureus determinants for nasal colonization. *Trends in microbiology*, 20(5):243–250, 2012.

[21] Pietro Speziale, Giampiero Pietrocola, Simonetta Rindi, Maria Provenzano, Giulio Provenza, Antonella Di Poto, Livia Visai, and Carla Renata Arciola. Structural and functional role of staphylococcus aureus surface components recognizing adhesive matrix molecules of the host. *Future microbiology*, 4(10):1337–1352, 2009.

[22] JUE Sollid, AS Furberg, AM Hanssen, and M Johannessen. Staphylococcus aureus: determinants of human carriage. *Infection, Genetics and Evolution*, 21:531–541, 2014.

[23] Robertino M Mera, Jose A Suaya, Heather Amrine-Madsen, Cosmina S Hogea, Linda A Miller, Emily P Lu, Daniel F Sahm, Patrick O'Hara, and Camilo J Acosta. Increasing role of staphylococcus aureus and community-acquired methicillin-resistant staphylococcus aureus infections in the united states: a 10-year trend of replacement and expansion. *Microbial Drug Resistance*, 17(2):321–328, 2011.

[24] F. R. Deleo, M. Otto, B. N. Kreiswirth, and H. F. Chambers. Community-associated meticillin-resistant staphylococcus aureus. *Lancet*, 375(9725):1557–68, 2010.

[25] Martha Iwamoto, Yi Mu, Ruth Lynfield, Sandra N Bulens, Joelle Nadle, Deborah Aragon, Susan Petit, Susan M Ray, Lee H Harrison, Ghinwa Dumyati, et al. Trends in invasive methicillin-resistant staphylococcus aureus infections. *Pediatrics*, 132 (4):e817–e824, 2013.

[26] Scott K Fridkin, Jeffrey C Hageman, Melissa Morrison, Laurie Thomson Sanza, Kathryn Como-Sabetti, John A Jernigan, Kathleen Harriman, Lee H Harrison, Ruth Lynfield, and Monica M Farley. Methicillin-resistant staphylococcus aureus disease in three communities. *New England Journal of Medicine*, 352(14):1436–1444, 2005.

[27] Jose R Mediavilla, Liang Chen, Barun Mathema, and Barry N Kreiswirth. Global epidemiology of community-associated methicillin resistant staphylococcus aureus (ca-mrsa). *Current opinion in microbiology*, 15(5):588–595, 2012.

[28] B. Shopsin, M. Gomez, S. O. Montgomery, D. H. Smith, M. Waddington, D. E. Dodge, D. A. Bost, M. Riehman, S. Naidich, and B. N. Kreiswirth. Evaluation of protein a gene polymorphic region dna sequencing for typing of staphylococcus aureus strains. *J Clin Microbiol*, 1999.

[29] Marie Hallin, Alexander W Friedrich, and Marc J Struelens. spa typing for epidemiological surveillance of staphylococcus aureus. In *Molecular Epidemiology of Microorganisms*, pages 189–202. Springer, 2009.

[30] Y Katayama, T Ito, and K Hiramatsu. A new class of genetic element, staphylococcus cassette chromosome mec, encodes methicillin resistance in staphylococcus aureus. *Antimicrobial Agents and Chemotherapy*, 44(6):1549–1555, 2000.

[31] International Working Group on the Classification of Staphylococcal Cassette Chromosome Elements (IWG-SCC et al. Classification of staphylococcal cassette chromosome mec (sccmec): guidelines for reporting novel sccmec elements. *Antimicrobial Agents and Chemotherapy*, 53(12):4961–4967, 2009.

[32] Keiichi Hiramatsu, Longzhu Cui, Makoto Kuroda, and Teruyo Ito. The emergence and evolution of methicillin-resistant staphylococcus aureus. *Trends in microbiology*, 9(10):486–493, 2001.

[33] Teruyo Ito, Kyoko Kuwahara-Arai, Yuki Katayama, Yuki Uehara, Xiao Han, Yoko Kondo, and Keiichi Hiramatsu. Staphylococcal cassette chromosome mec (scc mec) analysis of mrsa. *Methicillin-Resistant Staphylococcus Aureus (MRSA) Protocols*, pages 131–148, 2014.

[34] Martin CJ Maiden, Jane A Bygraves, Edward Feil, Giovanna Morelli, Joanne E Russell, Rachel Urwin, Qing Zhang, Jiaji Zhou, Kerstin Zurth, Dominique A Caugant, et al. Multilocus sequence typing: a portable approach to the identification of clones within populations of pathogenic microorganisms. *Proceedings of the National Academy of Sciences*, 95(6):3140–3145, 1998.

[35] Mark C Enright, Nicholas PJ Day, Catrin E Davies, Sharon J Peacock, and Brian G Spratt. Multilocus sequence typing for characterization of methicillin-resistant and methicillin-susceptible clones ofstaphylococcus aureus. *Journal of clinical microbiology*, 38(3):1008–1015, 2000.

[36] Fred C Tenover, Robert D Arbeit, Richard V Goering, Patricia A Mickelsen, Barbara E Murray, David H Persing, and Bala Swaminathan. Interpreting chromosomal dna restriction patterns produced by pulsed-field gel electrophoresis: criteria for bacterial strain typing. *Journal of clinical microbiology*, 33(9):2233, 1995.

[37] Joana Rolo, Maria Miragaia, Agata Turlej-Rogacka, Joanna Empel, Ons Bouchami, Nuno A Faria, Ana Tavares, Waleria Hryniewicz, Ad C Fluit, Hermínia De Lencastre, et al. High genetic diversity among community-associated staphylococcus aureus in europe: results from a multicenter study. *PLoS One*, 7(4):e34768, 2012.

[38] Robert S Daum. Skin and soft-tissue infections caused by methicillin-resistant staphylococcus aureus. *New England Journal of Medicine*, 357(4):380–390, 2007.

[39] John J. Engemann, Yehuda Carmeli, Sara E. Cosgrove, Vance G. Fowler, Melissa Z. Bronstein, Sharon L. Trivette, Jane P. Briggs, Daniel J. Sexton, and Keith S. Kaye. Adverse clinical and economic outcomes attributable to methicillin resistance among patients with staphylococcus aureus surgical site infection. *Clin Infect Dis*, 36(5):592–598, Mar 2003.

[40] R. Bunikowski, M. E. Mielke, H. Skarabis, M. Worm, I. Anagnostopoulos, G. Kolde, U. Wahn, and H. Renz. Evidence for a disease-promoting effect of staphylococcus aureus-derived exotoxins in atopic dermatitis. *J Allergy Clin Immunol*, 105(4): 814–819, Apr 2000.

[41] James E Cassat, Neal D Hammer, J. Preston Campbell, Meredith A Benson, Daniel S Perrien, Lara N Mrak, Mark S Smeltzer, Victor J Torres, and Eric P Skaar. A secreted bacterial protease tailors the staphylococcus aureus virulence repertoire to modulate bone remodeling during osteomyelitis. *Cell Host & Microbe*, 13(6):759–772, 2013.

[42] Mark E. Shirtliff and Jon T. Mader. Acute septic arthritis. *Clin Microbiol Rev*, 15(4):527–544, Oct 2002.

[43] G. R. Corey. Staphylococcus aureus bloodstream infections: definitions and treatment. *Clin Infect Dis*, 48 Suppl 4:S254–9, 2009.

[44] B. C. Hartman, J. Leedom, W. P. Lewis, and P. Weintraub. Postsurgical toxic shock syndrome: report of a case in which full syndrome manifestations were aborted by early recognition and therapy. *J Am Osteopath Assoc*, 84(4):356–9, 1984.

[45] Martin E Stryjewski and Henry F Chambers. Skin and soft-tissue infections caused by community-acquired methicillin-resistant staphylococcus aureus. *Clinical Infectious Diseases*, 46(Supplement 5):S368–S377, 2008.

[46] Fei-Fei Gu, Qi Hou, Hai-Hui Yang, Yue-Qiu Zhu, Xiao-Kui Guo, Yu-Xing Ni, and Li-Zhong Han. Characterization of staphylococcus aureus isolated from non-native patients with skin and soft tissue infections in shanghai. *PloS one*, 10(4):e0123557, 2015.

[47] Y. Nakamura, J. Oscherwitz, K. B. Cease, S. M. Chan, R. Munoz-Planillo, M. Hasegawa, A. E. Villaruz, G. Y. Cheung, M. J. McGavin, J. B. Travers, M. Otto, N. Inohara, and G. Nunez. Staphylococcus delta-toxin induces allergic skin disease by activating mast cells. *Nature*, 503(7476):397–401, 2013.

[48] Hilmar Wisplinghoff, Harald Seifert, Sandra M Tallent, Tammy Bischoff, Richard P Wenzel, and Michael B Edmond. Nosocomial bloodstream infections in pediatric patients in united states hospitals: epidemiology, clinical features and susceptibilities. *The Pediatric infectious disease journal*, 22(8):686–691, 2003.

[49] Daniel P. Lew and Francis A. Waldvogel. Osteomyelitis. *Lancet*, 364(9431):369–379, 2004.

[50] Werner Zimmerli, Andrej Trampuz, and Peter E. Ochsner. Prosthetic-joint infections. *N Engl J Med*, 351(16):1645–1654, Oct 2004.

[51] Christopher H. Goss and Marianne S. Muhlebach. Review: Staphylococcus aureus and mrsa in cystic fibrosis. *J Cyst Fibros*, 10(5):298–306, Sep 2011.

[52] M. C. McElroy, H. R. Harty, G. E. Hosford, G. M. Boylan, J. F. Pittet, and T. J. Foster. Alpha-toxin damages the air-blood barrier of the lung in a rat model of staphylococcus aureus-induced pneumonia. *Infect Immun*, 67(10):5541–4, 1999.

[53] J. Bubeck Wardenburg, T. Bae, M. Otto, F. R. Deleo, and O. Schneewind. Poring over pores: alpha-hemolysin and panton-valentine leukocidin in staphylococcus aureus pneumonia. *Nat Med*, 13(12):1405–6, 2007.

[54] John K McCormick, Jeremy M Yarwood, and Patrick M Schlievert. Toxic shock syndrome and bacterial superantigens: an update. *Annual Reviews in Microbiology*, 55(1):77–104, 2001.

[55] M. S. Bergdoll, B. A. Crass, R. F. Reiser, R. N. Robbins, and J. P. Davis. A new staphylococcal enterotoxin, enterotoxin f, associated with toxic-shock-syndrome staphylococcus aureus isolates. *Lancet*, 1(8228):1017–21, 1981.

[56] Adam R Spaulding, Wilmara Salgado-Pabón, Petra L Kohler, Alexander R Horswill, Donald YM Leung, and Patrick M Schlievert. Staphylococcal and streptococcal superantigen exotoxins. *Clinical microbiology reviews*, 26(3):422–447, 2013.

[57] Christine Heilmann. Adhesion mechanisms of staphylococci. In *Bacterial Adhesion*, pages 105–123. Springer, 2011.

[58] Jon Beckwith. The sec-dependent pathway. *Research in microbiology*, 164(6):497–504, 2013.

[59] William Wiley Navarre and Olaf Schneewind. Proteolytic cleavage and cell wall anchoring at the lpxtg motif of surface proteins in gram-positive bacteria. *Molecular microbiology*, 14(1):115–121, 1994.

[60] Sarkis K Mazmanian, Gwen Liu, Hung Ton-That, and Olaf Schneewind. Staphylococcus aureus sortase, an enzyme that anchors surface proteins to the cell wall. *Science*, 285(5428):760–763, 1999.

[61] Gerald D Shockman and JF Barren. Structure, function, and assembly of cell walls of gram-positive bacteria. *Annual Reviews in Microbiology*, 37(1):501–527, 1983.

[62] Jean-Marie Ghuysen and Jack L Strominger. Structure of the cell wall of staphylococcus aureus, strain copenhagen. ii. separation and structure of disaccharides. *Biochemistry*, 2(5):1119–1125, 1963.

[63] J Me Ghuysen, DJ Tipper, Claire H Birge, and JL Strominger. Structure of the cell wall of staphylococcus aureus strain copenhagen. vi. the soluble glycopeptide and its sequential degradation by peptidases*. *Biochemistry*, 4(10):2245–2254, 1965.

[64] Sjef J De Kimpe, Muralitharan Kengatharan, Christoph Thiemermann, and John R Vane. The cell wall components peptidoglycan and lipoteichoic acid from staphylococcus aureus act in synergy to cause shock and multiple organ failure. *Proceedings of the National Academy of Sciences*, 92(22):10359–10363, 1995.

[65] Ralf Schwandner, Roman Dziarski, Holger Wesche, Mike Rothe, and Carsten J Kirschning. Peptidoglycan-and lipoteichoic acid-induced cell activation is mediated by toll-like receptor 2. *Journal of Biological Chemistry*, 274(25):17406–17409, 1999.

[66] Wenchang Yuan, Qiwen Hu, Hang Cheng, Weilong Shang, Nan Liu, Ziyu Hua, Junmin Zhu, Zhen Hu, Jizhen Yuan, Xia Zhang, et al. Cell wall thickening is associated with adaptive resistance to amikacin in methicillin-resistant staphylococcus aureus clinical isolates. *Journal of Antimicrobial Chemotherapy*, page dks522, 2013.

[67] Longzhu Cui, Xiaoxue Ma, Katsuhiro Sato, Keiko Okuma, Fred C Tenover, Elsa M Mamizuka, Curtis G Gemmell, Mi-Na Kim, Marie-Cecile Ploy, N El Solh, et al. Cell wall thickening is a common feature of vancomycin resistance in staphylococcus aureus. *Journal of clinical microbiology*, 41(1):5–14, 2003.

[68] Stephanie Brown, John P Santa Maria Jr, and Suzanne Walker. Wall teichoic acids of gram-positive bacteria. *Annual review of microbiology*, 67, 2013.

[69] Jonathan G Swoboda, Jennifer Campbell, Timothy C Meredith, and Suzanne Walker. Wall teichoic acid function, biosynthesis, and inhibition. *Chembiochem*, 11(1):35–45, 2010.

[70] Nathalie T Reichmann and Angelika Gründling. Location, synthesis and function of glycolipids and polyglycerolphosphate lipoteichoic acid in gram-positive bacteria of the phylum firmicutes. *FEMS microbiology letters*, 319(2):97–105, 2011.

[71] A. Grundling and O. Schneewind. Genes required for glycolipid synthesis and lipoteichoic acid anchoring in staphylococcus aureus. *J Bacteriol*, 189(6):2521–30, 2007.

[72] A. Grundling and O. Schneewind. Synthesis of glycerol phosphate lipoteichoic acid in staphylococcus aureus. *Proc Natl Acad Sci U S A*, 104(20):8478–83, 2007.

[73] Iris Fedtke, Diana Mader, Thomas Kohler, Hermann Moll, Graeme Nicholson, Raja Biswas, Katja Henseler, Friedrich Götz, Ulrich Zähringer, and Andreas Peschel. A staphylococcus aureus ypfp mutant with strongly reduced lipoteichoic acid (lta) content: Lta governs bacterial surface properties and autolysin activity. *Molecular microbiology*, 65(4):1078–1091, 2007.

[74] Tamsin R Sheen, Celia M Ebrahimi, Ida H Hiemstra, Steven B Barlow, Andreas Peschel, and Kelly S Doran. Penetration of the blood–brain barrier by staphylococcus aureus: contribution of membrane-anchored lipoteichoic acid. *Journal of Molecular Medicine*, 88(6):633–639, 2010.

[75] Nathalie T Reichmann, Carolina Piçarra Cassona, João M Monteiro, Amy L Bottomley, Rebecca M Corrigan, Simon J Foster, Mariana G Pinho, and Angelika Gründling. Differential localization of lta synthesis proteins and their interaction with the cell division machinery in staphylococcus aureus. *Molecular microbiology*, 92(2):273–286, 2014.

[76] L Vincent Collins, Sascha A Kristian, Christopher Weidenmaier, Marion Faigle, Kok PM van Kessel, Jos AG van Strijp, Friedrich Götz, Birgid Neumeister, and Andreas Peschel. Staphylococcus aureus strains lacking d-alanine modifications of teichoic acids are highly susceptible to human neutrophil killing and are virulence attenuated in mice. *Journal of Infectious Diseases*, 186(2):214–219, 2002.

[77] Timothy J Foster and Magnus Höök. Surface protein adhesins of staphylococcus aureus. *Trends in microbiology*, 6(12): 484–488, 1998.

[78] Timothy J Foster, Joan A Geoghegan, Vannakambadi K Ganesh, and Magnus Höök. Adhesion, invasion and evasion: the many functions of the surface proteins of staphylococcus aureus. *Nature Reviews Microbiology*, 12(1):49–62, 2014.

[79] J. Deisenhofer. Crystallographic refinement and atomic models of a human fc fragment and its complex with fragment b of protein a from staphylococcus aureus at 2.9- and 2.8-a resolution. *Biochemistry*, 20(9):2361–70, 1981. Deisenhofer, J eng Biochemistry. 1981 Apr 28;20(9):2361-70.

[80] Lena Cedergren, Roland Andersson, Birger Jansson, Mathias Uhlén, and Björn Nilsson. Mutational analysis of the interaction between staphylococcal protein a and human igg1. *Protein engineering*, 6(4):441–448, 1993.

[81] M. Graille, E. A. Stura, A. L. Corper, B. J. Sutton, M. J. Taussig, J. B. Charbonnier, and G. J. Silverman. Crystal structure of a staphylococcus aureus protein a domain complexed with the fab fragment of a human igm antibody: structural basis for recognition of b-cell receptors and superantigen activity. *Proc Natl Acad Sci U S A*, 97(10):5399–404, 2000.

[82] AH Patel, P Nowlan, ED Weavers, and T Foster. Virulence of protein a-deficient and alpha-toxin-deficient mutants of staphylococcus aureus isolated by allele replacement. *Infection and Immunity*, 55(12):3103–3110, 1987.

[83] M. I. Gomez, A. Lee, B. Reddy, A. Muir, G. Soong, A. Pitt, A. Cheung, and A. Prince. Staphylococcus aureus protein a induces airway epithelial inflammatory responses by activating tnfr1. *Nat Med*, 10(8):842–8, 2004.

[84] G. Soong, F. J. Martin, J. Chun, T. S. Cohen, D. S. Ahn, and A. Prince. Staphylococcus aureus protein a mediates invasion across airway epithelial cells through activation of rhoa gtpase signaling and proteolytic activity. *Journal of Biological Chemistry*, 286(41):35891–35898, 2011.

[85] B. Sinha, P. P. Francois, O. Nusse, M. Foti, O. M. Hartford, P. Vaudaux, T. J. Foster, D. P. Lew, M. Herrmann, and K. H. Krause. Fibronectin-binding protein acts as staphylococcus aureus invasin via fibronectin bridging to integrin alpha5beta1. *Cell Microbiol*, 1(2):101–17, 1999.

[86] Richard J. Bingham, Enrique Rudiño-Piñera, Nicola A G. Meenan, Ulrich Schwarz-Linek, Johan P. Turkenburg, Magnus Höök, Elspeth F. Garman, and Jennifer R. Potts. Crystal structures of fibronectin-binding sites from staphylococcus aureus fnbpa in complex with fibronectin domains. *Proc Natl Acad Sci U S A*, 105(34):12254–12258, Aug 2008.

[87] Christine Heilmann, Silke Niemann, Bhanu Sinha, Mathias Herrmann, Beate E. Kehrel, and Georg Peters. Staphylococcus aureus fibronectin-binding protein (fnbp)-mediated adherence to platelets, and aggregation of platelets induced by fnbpa but not by fnbpb. *J Infect Dis*, 190(2):321–329, Jul 2004.

[88] J. M. Patti, T. Bremell, D. Krajewska-Pietrasik, A. Abdelnour, A. Tarkowski, C. Ryden, and M. Hook. The staphylococcus aureus collagen adhesin is a virulence determinant in experimental septic arthritis. *Infect Immun*, 62(1):152–61, 1994.

[89] Yinong Zong, Yi Xu, Xiaowen Liang, Douglas R. Keene, Agneta Höök, Shivasankarappa Gurusiddappa, Magnus Höök, and Sthanam V L. Narayana. A 'collagen hug' model for staphylococcus aureus cna binding to collagen. *EMBO J*, 24(24):4224–4236, Dec 2005.

[90] M. G. Thomas, S. Peacock, S. Daenke, and A. R. Berendt. Adhesion of staphylococcus aureus to collagen is not a major virulence determinant for septic arthritis, osteomyelitis, or endocarditis. *J Infect Dis*, 179(1):291–293, Jan 1999.

[91] M. O. Elasri, J. R. Thomas, R. A. Skinner, J. S. Blevins, K. E. Beenken, C. L. Nelson, and M. S. Smeltzer. Staphylococcus aureus collagen adhesin contributes to the pathogenesis of osteomyelitis. *Bone*, 30(1):275–280, Jan 2002.

[92] M. N. Rhem, E. M. Lech, J. M. Patti, D. McDevitt, M. Höök, D. B. Jones, and K. R. Wilhelmus. The collagen-binding adhesin is a virulence factor in staphylococcus aureus keratitis. *Infect Immun*, 68(6):3776–3779, Jun 2000.

[93] S. A. Hienz, T. Schennings, A. Heimdahl, and J. I. Flock. Collagen binding of staphylococcus aureus is a virulence factor in experimental endocarditis. *J Infect Dis*, 174(1):83–88, Jul 1996.

[94] Vannakambadi K. Ganesh, Jose J. Rivera, Emanuel Smeds, Ya-Ping Ko, M Gabriela Bowden, Elisabeth R. Wann, Shivasankarappa Gurusiddappa, J Ross Fitzgerald, and Magnus Höök. A structural model of the staphylococcus aureus clfa-fibrinogen interaction opens new avenues for the design of anti-staphylococcal therapeutics. *PLoS Pathog*, 4(11):e1000226, Nov 2008.

[95] Louise M. O'Brien, Evelyn J. Walsh, Ruth C. Massey, Sharon J. Peacock, and Timothy J. Foster. Staphylococcus aureus clumping factor b (clfb) promotes adherence to human type i cytokeratin 10: implications for nasal colonization. *Cell Microbiol*, 4(11):759–770, Nov 2002.

[96] Evelyn J. Walsh, Helen Miajlovic, Oleg V. Gorkun, and Timothy J. Foster. Identification of the staphylococcus aureus mscramm clumping factor b (clfb) binding site in the alphac-domain of human fibrinogen. *Microbiology*, 154(Pt 2):550–558, Feb 2008.

[97] Heiman F L. Wertheim, Evelyn Walsh, Roos Choudhurry, Damian C. Melles, Hélène A M. Boelens, Helen Miajlovic, Henri A. Verbrugh, Timothy Foster, and Alex van Belkum. Key role for clumping factor b in staphylococcus aureus nasal colonization of humans. *PLoS Med*, 5(1):e17, Jan 2008.

[98] Michelle E. Mulcahy, Joan A. Geoghegan, Ian R. Monk, Kate M. O'Keeffe, Evelyn J. Walsh, Timothy J. Foster, and Rachel M. McLoughlin. Nasal colonisation by staphylococcus aureus depends upon clumping factor b binding to the squamous epithelial cell envelope protein loricrin. *PLoS Pathog*, 8(12):e1003092, Dec 2012.

[99] Huanle Liu, Jingnan Lv, Xiuqin Qi, Yu Ding, Dan Li, Longhua Hu, Liangxing Wang, and Fangyou Yu. The carriage of the serine-aspartate repeat protein-encoding sdr genes among staphylococcus aureus lineages. *Braz J Infect Dis*, 19(5):498–502, 2015.

[100] Hs Tung, B. Guss, U. Hellman, L. Persson, K. Rubin, and C. Rydén. A bone sialoprotein-binding protein from staphylococcus aureus: a member of the staphylococcal sdr family. *Biochem J*, 345 Pt 3:611–619, Feb 2000.

[101] Artur Sabat, Damian C. Melles, Gayane Martirosian, Hajo Grundmann, Alex van Belkum, and Waleria Hryniewicz. Distribution of the serine-aspartate repeat protein-encoding sdr genes among nasal-carriage and invasive staphylococcus aureus strains. *J Clin Microbiol*, 44(3):1135–1138, Mar 2006.

[102] Rainer Friedrich, Peter Panizzi, Pablo Fuentes-Prior, Klaus Richter, Ingrid Verhamme, Patricia J. Anderson, Shun-Ichiro Kawabata, Robert Huber, Wolfram Bode, and Paul E. Bock. Staphylocoagulase is a prototype for the mechanism of cofactor-induced zymogen activation. *Nature*, 425(6957):535–539, Oct 2003.

[103] Triantafyllos Chavakis, K Wiechmann, KT Preissner, and M Herrmann. Staphylococcus aureus interactions with the endothelium. *Thromb Haemost*, 94:278–285, 2005.

[104] W. H. Sperber and S. R. Tatini. Interpretation of the tube coagulase test for identification of staphylococcus aureus. *Appl Microbiol*, 29(4):502–505, Apr 1975.

[105] E. J. Smith, L. Visai, S. W. Kerrigan, P. Speziale, and T. J. Foster. The sbi protein is a multifunctional immune evasion factor of staphylococcus aureus. *Infection and Immunity*, 79(9):3801–3809, 2011.

[106] Katrin Haupt, Michael Reuter, Jean van den Elsen, Julia Burman, Steffi Hälbich, Julia Richter, Christine Skerka, and Peter F. Zipfel. The staphylococcus aureus protein sbi acts as a complement inhibitor and forms a tripartite complex with host complement factor h and c3b. *PLoS Pathog*, 4(12):e1000250, Dec 2008.

[107] Neal D. Hammer and Eric P. Skaar. Molecular mechanisms of staphylococcus aureus iron acquisition. *Annu Rev Microbiol*, 65:129–147, 2011.

[108] Sarkis K. Mazmanian, Eric P. Skaar, Andrew H. Gaspar, Munir Humayun, Piotr Gornicki, Joanna Jelenska, Andrzej Joachmiak, Dominique M. Missiakas, and Olaf Schneewind. Passage of heme-iron across the envelope of staphylococcus aureus. *Science*, 299(5608):906–909, Feb 2003.

[109] K. Krishna Kumar, D. A. Jacques, G. Pishchany, T. Caradoc-Davies, T. Spirig, G. R. Malmirchegini, D. B. Langley, C. F. Dickson, J. P. Mackay, R. T. Clubb, E. P. Skaar, J. M. Guss, and D. A. Gell. Structural basis for hemoglobin capture by staphylococcus aureus cell-surface protein, isdh. *Journal of Biological Chemistry*, 286(44):38439–38447, 2011.

[110] C. F. Dickson, K. Krishna Kumar, D. A. Jacques, G. R. Malmirchegini, T. Spirig, J. P. Mackay, R. T. Clubb, J. M. Guss, and D. A. Gell. Structure of the hemoglobin-isdh complex reveals the molecular basis of iron capture by staphylococcus aureus. *Journal of Biological Chemistry*, 2014.

[111] S. R. Clarke, R. Mohamed, L. Bian, A. F. Routh, J. F. Kokai-Kun, J. J. Mond, A. Tarkowski, and S. J. Foster. The staphylococcus aureus surface protein isda mediates resistance to innate defenses of human skin. *Cell Host Microbe*, 1(3):199–212, 2007.

[112] A. M. Palazzolo-Ballance, M. L. Reniere, K. R. Braughton, D. E. Sturdevant, M. Otto, B. N. Kreiswirth, E. P. Skaar, and F. R. DeLeo. Neutrophil microbicides induce a pathogen survival response in community-associated methicillin-resistant staphylococcus aureus. *J Immunol*, 180(1):500–9, 2008.

[113] F. A. Kapral and M. M. Miller. Product of staphylococcus aureus responsible for the scalded-skin syndrome. *Infect Immun*, 4(5):541–5, 1971. Kapral, F A Miller, M M eng Infect Immun. 1971 Nov;4(5):541-5.

[114] J. Bubeck Wardenburg, T. Bae, M. Otto, F. R. Deleo, and O. Schneewind. Poring over pores: alpha-hemolysin and panton-valentine leukocidin in staphylococcus aureus pneumonia. *Nat Med*, 13(12):1405–6, 2007.

[115] S. Bhakdi and J. Tranum-Jensen. Alpha-toxin of staphylococcus aureus. *Microbiol Rev*, 55(4):733–51, 1991.

[116] S. Bhakdi, R. Fussle, and J. Tranum-Jensen. Staphylococcal alpha-toxin: oligomerization of hydrophilic monomers to form amphiphilic hexamers induced through contact with deoxycholate detergent micelles. *Proc Natl Acad Sci U S A*, 78(9): 5475–9, 1981.

[117] A. Valeva, R. Schnabel, I. Walev, F. Boukhallouk, S. Bhakdi, and M. Palmer. Membrane insertion of the heptameric staphylococcal alpha-toxin pore. a domino-like structural transition that is allosterically modulated by the target cell membrane. *J Biol Chem*, 276(18):14835–41, 2001.

[118] NORBERT Suttorp and EIMO Habben. Effect of staphylococcal alpha-toxin on intracellular ca2+ in polymorphonuclear leukocytes. *Infection and immunity*, 56(9):2228–2234, 1988.

[119] A. Hildebrand, M. Pohl, and S. Bhakdi. Staphylococcus aureus alpha-toxin. dual mechanism of binding to target cells. *J Biol Chem*, 266(26):17195–200, 1991. Hildebrand, A Pohl, M Bhakdi, S eng J Biol Chem. 1991 Sep 15;266(26):17195-200.

[120] Georgia A. Wilke and Juliane Bubeck Wardenburg. Role of a disintegrin and metalloprotease 10 in staphylococcus aureus alpha-hemolysin-mediated cellular injury. *Proc Natl Acad Sci U S A*, 107(30):13473–13478, Jul 2010.

[121] Gisela von Hoven, Amable J. Rivas, Claudia Neukirch, Stefan Klein, Christian Hamm, Qianqian Qin, Martina Meyenburg, Sabine Füser, Paul Saftig, Nadja Hellmann, Rolf Postina, and Matthias Husmann. Dissecting the role of adam10 as a mediator of s. aureus α-toxin action. *Biochem J*, May 2016.

[122] Sebastian Virreira Winter, Arturo Zychlinsky, and Bart W Bardoel. Genome-wide crispr screen reveals novel host factors required for staphylococcus aureus α-hemolysin-mediated toxicity. *Scientific reports*, 6, 2016.

[123] Ichiro Inoshima, Naoko Inoshima, Georgia A. Wilke, Michael E. Powers, Karen M. Frank, Yang Wang, and Juliane Bubeck Wardenburg. A staphylococcus aureus pore-forming toxin subverts the activity of adam10 to cause lethal infection in mice. *Nature Medicine*, 17(10):1310–1314, 2011.

[124] Taylor S Cohen, Jamese J Hilliard, Omari Jones-Nelson, Ashley E Keller, Terrence OíDay, Christine Tkaczyk, Antonio DiGiandomenico, Melissa Hamilton, Mark Pelletier, Qun Wang, et al. Staphylococcus aureus α toxin potentiates opportunistic bacterial lung infections. *Science translational medicine*, 8(329):329ra31–329ra31, 2016.

[125] Oliver Goldmann, Lorena Tuchscherr, Manfred Rohde, and Eva Medina. α-hemolysin enhances staphylococcus aureus internalization and survival within mast cells by modulating the expression of β1 integrin. *Cellular microbiology*, 2016.

[126] A. L. Dumont and V. J. Torres. Cell targeting by the staphylococcus aureus pore-forming toxins: it's not just about lipids. *Trends Microbiol*, 22(1):21–7, 2014.

[127] François Vandenesch, G Lina, and Thomas Henry. Staphylococcus aureus hemolysins, bi-component leukocidins, and cytolytic peptides: a redundant arsenal of membrane-damaging virulence factors? *The Staphylococci and staphylococcal pathogenesis*, page 80, 2012.

[128] Rich Olson, Hirofumi Nariya, Kenji Yokota, Yoshiyuki Kamio, and Eric Gouaux. Crystal structure of staphylococcal lukf delineates conformational changes accompanying formation of a transmembrane channel. *Nature Structural & Molecular Biology*, 6(2):134–140, 1999.

[129] Naoko Morinaga, Yuriko Kaihou, and Masatoshi Noda. Purification, cloning and characterization of variant luke-lukd with strong leukocidal activity of staphylococcal bi-component leukotoxin family. *Microbiology and immunology*, 47(1):81–90, 2003.

[130] Jun Kaneko, Toshiko Ozawa, Toshio Tomita, and Yoshiyuki Kamio. Sequential binding of staphylococcal y-hemolysin to human erythrocytes and complex formation of the hemolysin on the cell surfaceÜ. *Bioscience, biotechnology, and biochemistry*, 61(5):846–851, 1997.

[131] T. Tomita and Y. Kamio. Molecular biology of the pore-forming cytolysins from staphylococcus aureus, alpha- and gamma-hemolysins and leukocidin. *Biosci Biotechnol Biochem*, 61(4):565–72, 1997. Tomita, T Kamio, Y eng JAPAN Biosci Biotechnol Biochem. 1997 Apr;61(4):565-72.

[132] N. Malachowa, A. R. Whitney, S. D. Kobayashi, D. E. Sturdevant, A. D. Kennedy, K. R. Braughton, D. W. Shabb, B. A. Diep, H. F. Chambers, M. Otto, and F. R. DeLeo. Global changes in staphylococcus aureus gene expression in human blood. *PLoS One*, 6(4):e18617, 2011.

[133] I. M. Nilsson, O. Hartford, T. Foster, and A. Tarkowski. Alpha-toxin and gamma-toxin jointly promote staphylococcus aureus virulence in murine septic arthritis. *Infect Immun*, 67(3):1045–9, 1999. Nilsson, I M Hartford, O Foster, T Tarkowski, A eng Wellcome Trust/United Kingdom Infect Immun. 1999 Mar;67(3):1045-9.

[134] A. L. Dumont, P. Yoong, X. Liu, C. J. Day, N. M. Chumbler, D. B. James, 3rd Alonzo, F., N. J. Bode, D. B. Lacy, M. P. Jennings, and V. J. Torres. Identification of a crucial residue required for staphylococcus aureus lukab cytotoxicity and receptor recognition. *Infect Immun*, 2013.

[135] A. L. Dumont, T. K. Nygaard, R. L. Watkins, A. Smith, L. Kozhaya, B. N. Kreiswirth, B. Shopsin, D. Unutmaz, J. M. Voyich, and V. J. Torres. Characterization of a new cytotoxin that contributes to staphylococcus aureus pathogenesis. *Mol Microbiol*, 79 (3):814–25, 2011.

[136] A. L. DuMont, P. Yoong, C. J. Day, 3rd Alonzo, F., W. H. McDonald, M. P. Jennings, and V. J. Torres. Staphylococcus aureus lukab cytotoxin kills human neutrophils by targeting the cd11b subunit of the integrin mac-1. *Proc Natl Acad Sci U S A*, 110 (26):10794–9, 2013.

[137] A. L. DuMont, P. Yoong, B. G. Surewaard, M. A. Benson, R. Nijland, J. A. van Strijp, and V. J. Torres. Staphylococcus aureus elaborates leukocidin ab to mediate escape from within human neutrophils. *Infect Immun*, 81(5):1830–41, 2013.

[138] Jason H Melehani, David BA James, Ashley L DuMont, Victor J Torres, and Joseph A Duncan. Staphylococcus aureus leukocidin a/b (lukab) kills human monocytes via host nlrp3 and asc when extracellular, but not intracellular. *PLoS Pathog*, 11 (6):e1004970, 2015.

[139] B. Loffler, M. Hussain, M. Grundmeier, M. Bruck, D. Holzinger, G. Varga, J. Roth, B. C. Kahl, R. A. Proctor, and G. Peters. Staphylococcus aureus panton-valentine leukocidin is a very potent cytotoxic factor for human neutrophils. *PLoS Pathog*, 6(1):e1000715, 2010.

[140] M. Labandeira-Rey, F. Couzon, S. Boisset, E. L. Brown, M. Bes, Y. Benito, E. M. Barbu, V. Vazquez, M. Hook, J. Etienne, F. Vandenesch, and M. G. Bowden. Staphylococcus aureus panton-valentine leukocidin causes necrotizing pneumonia. *Science*, 315(5815):1130–3, 2007.

[141] Dirk Holzinger, Laura Gieldon, Vijayashree Mysore, Nadine Nippe, Debra J Taxman, Joseph A Duncan, Peter M Broglie, Kristina Marketon, Judith Austermann, Thomas Vogl, et al. Staphylococcus aureus panton-valentine leukocidin induces an inflammatory response in human phagocytes via the nlrp3 inflammasome. *Journal of leukocyte biology*, 92(5):1069–1081, 2012.

[142] Ching Wen Tseng, Juan Carlos Biancotti, Bethany L Berg, David Gate, Stacey L Kolar, Sabrina Müller, Maria D Rodriguez, Kavon Rezai-Zadeh, Xuemo Fan, David O Beenhouwer, et al. Increased susceptibility of humanized nsg mice to panton-valentine leukocidin and staphylococcus aureus skin infection. *PLoS Pathog*, 11(11):e1005292, 2015.

[143] P. D. Ward and W. H. Turner. Identification of staphylococcal panton-valentine leukocidin as a potent dermonecrotic toxin. *Infect Immun*, 28(2):393–7, 1980. Ward, P D Turner, W H eng Infect Immun. 1980 May;28(2):393-7.

[144] A. Gravet, D. A. Colin, D. Keller, R. Girardot, H. Monteil, and G. Prevost. Characterization of a novel structural member, luke-lukd, of the bi-component staphylococcal leucotoxins family. *FEBS Lett*, 436(2):202–8, 1998.

[145] 3rd Alonzo, F., L. Kozhaya, S. A. Rawlings, T. Reyes-Robles, A. L. DuMont, D. G. Myszka, N. R. Landau, D. Unutmaz, and V. J. Torres. Ccr5 is a receptor for staphylococcus aureus leukotoxin ed. *Nature*, 493(7430):51–5, 2013.

[146] A. Peschel and M. Otto. Phenol-soluble modulins and staphylococcal infection. *Nat Rev Microbiol*, 11(10):667–73, 2013.

[147] M. Otto. Basis of virulence in community-associated methicillin-resistant staphylococcus aureus. *Annu Rev Microbiol*, 64: 143–62, 2010. Otto, Michael eng Annu Rev Microbiol. 2010;64:143-62. doi: 10.1146/annurev.micro.112408.134309.

[148] R. Wang, K. R. Braughton, D. Kretschmer, T. H. Bach, S. Y. Queck, M. Li, A. D. Kennedy, D. W. Dorward, S. J. Klebanoff, A. Peschel, F. R. DeLeo, and M. Otto. Identification of novel cytolytic peptides as key virulence determinants for community-associated mrsa. *Nat Med*, 13(12):1510–4, 2007.

[149] S. S. Chatterjee, H. S. Joo, A. C. Duong, T. D. Dieringer, V. Y. Tan, Y. Song, E. R. Fischer, G. Y. Cheung, M. Li, and M. Otto. Essential staphylococcus aureus toxin export system. *Nat Med*, 19(3):364–7, 2013.

[150] D. Kretschmer, A. K. Gleske, M. Rautenberg, R. Wang, M. Koberle, E. Bohn, T. Schoneberg, M. J. Rabiet, F. Boulay, S. J. Klebanoff, K. A. van Kessel, J. A. van Strijp, M. Otto, and A. Peschel. Human formyl peptide receptor 2 senses highly pathogenic staphylococcus aureus. *Cell Host Microbe*, 7(6):463–73, 2010.

[151] Dennis Hanzelmann, Hwang-Soo Joo, Mirita Franz-Wachtel, Tobias Hertlein, Stefan Stevanovic, Boris Macek, Christiane Wolz, Friedrich Götz, Michael Otto, Dorothee Kretschmer, et al. Toll-like receptor 2 activation depends on lipopeptide shedding by bacterial surfactants. *Nature Communications*, 7, 2016.

[152] D. W. Scheifele, G. L. Bjornson, R. A. Dyer, and J. E. Dimmick. Delta-like toxin produced by coagulase-negative staphylococci is associated with neonatal necrotizing enterocolitis. *Infect Immun*, 55(9):2268–73, 1987. Scheifele, D W Bjornson, G L Dyer, R A Dimmick, J E eng Infect Immun. 1987 Sep;55(9):2268-73.

[153] M. Grosz, J. Kolter, K. Paprotka, A. C. Winkler, D. Schafer, S. S. Chatterjee, T. Geiger, C. Wolz, K. Ohlsen, M. Otto, T. Rudel, B. Sinha, and M. Fraunholz. Cytoplasmic replication of staphylococcus aureus upon phagosomal escape triggered by phenol-soluble modulin alpha. *Cell Microbiol*, 16(4):451–65, 2014.

[154] M. Huseby, K. Shi, C. K. Brown, J. Digre, F. Mengistu, K. S. Seo, G. A. Bohach, P. M. Schlievert, D. H. Ohlendorf, and C. A. Earhart. Structure and biological activities of beta toxin from staphylococcus aureus. *J Bacteriol*, 189(23):8719–26, 2007.

[155] I. Walev, U. Weller, S. Strauch, T. Foster, and S. Bhakdi. Selective killing of human monocytes and cytokine release provoked by sphingomyelinase (beta-toxin) of staphylococcus aureus. *Infect Immun*, 64(8):2974–9, 1996.

[156] Medora J Huseby, Andrew C Kruse, Jeff Digre, Petra L Kohler, Jillian A Vocke, Ethan E Mann, Kenneth W Bayles, Gregory A Bohach, Patrick M Schlievert, Douglas H Ohlendorf, et al. Beta toxin catalyzes formation of nucleoprotein matrix in staphylococcal biofilms. *Proceedings of the National Academy of Sciences*, 107(32):14407–14412, 2010.

[157] Carla JC de Haas, Karin Ellen Veldkamp, Andreas Peschel, Floor Weerkamp, Willem JB Van Wamel, Erik CJM Heezius, Miriam JJG Poppelier, Kok PM Van Kessel, and Jos AG van Strijp. Chemotaxis inhibitory protein of staphylococcus aureus, a bacterial antiinflammatory agent. *The Journal of experimental medicine*, 199(5):687–695, 2004.

[158] B. Postma, M. J. Poppelier, J. C. van Galen, E. R. Prossnitz, J. A. van Strijp, C. J. de Haas, and K. P. van Kessel. Chemotaxis inhibitory protein of staphylococcus aureus binds specifically to the c5a and formylated peptide receptor. *J Immunol*, 172 (11):6994–7001, 2004.

[159] A. J. Laarman, G. Mijnheer, J. M. Mootz, W. J. van Rooijen, M. Ruyken, C. L. Malone, E. C. Heezius, R. Ward, G. Milligan, J. A. van Strijp, C. J. de Haas, A. R. Horswill, K. P. van Kessel, and S. H. Rooijakkers. Staphylococcus aureus staphopain a inhibits cxcr2-dependent neutrophil activation and chemotaxis. *EMBO J*, 31(17):3607–19, 2012.

[160] D. Shortle. A genetic system for analysis of staphylococcal nuclease. *Gene*, 22(2-3):181–9, 1983.

[161] V. Thammavongsa, D. M. Missiakas, and O. Schneewind. Staphylococcus aureus degrades neutrophil extracellular traps to promote immune cell death. *Science*, 342(6160):863–6, 2013.

[162] A. L. Cheung, A. S. Bayer, G. Zhang, H. Gresham, and Y. Q. Xiong. Regulation of virulence determinants in vitro and in vivo in staphylococcus aureus. *FEMS Immunol Med Microbiol*, 40(1):1–9, 2004.

[163] Ambrose L Cheung, Koren A Nishina, Maria Pilar Trotonda, and Sandeep Tamber. The sara protein family of staphylococcus aureus. *The international journal of biochemistry & cell biology*, 40(3):355–361, 2008.

[164] P Recsei, B Kreiswirth, M O'reilly, PM Schlievert, A Gruss, and RP Novick. Regulation of exoprotein gene expression in staphylococcus aureus by agr. *Molecular and General Genetics MGG*, 202(1):58–61, 1986.

[165] H. L. Peng, R. P. Novick, B. Kreiswirth, J. Kornblum, and P. Schlievert. Cloning, characterization, and sequencing of an accessory gene regulator (agr) in staphylococcus aureus. *J Bacteriol*, 170(9):4365–72, 1988.

[166] L. Janzon and S. Arvidson. The role of the delta-lysin gene (hld) in the regulation of virulence genes by the accessory gene regulator (agr) in staphylococcus aureus. *EMBO J*, 9(5):1391–9, 1990.

[167] Richard P Novick. Autoinduction and signal transduction in the regulation of staphylococcal virulence. *Molecular microbiology*, 48(6):1429–1449, 2003.

[168] J. M. Yarwood, D. J. Bartels, E. M. Volper, and E. P. Greenberg. Quorum sensing in staphylococcus aureus biofilms. *J Bacteriol*, 186(6):1838–50, 2004.

[169] L. Zhang and G. Ji. Identification of a staphylococcal agrb segment(s) responsible for group-specific processing of agrd by gene swapping. *J Bacteriol*, 186(20):6706–13, 2004.

[170] Matthew Thoendel and Alexander R Horswill. Identification of staphylococcus aureus agrd residues required for autoinducing peptide biosynthesis. *Journal of Biological Chemistry*, 284(33):21828–21838, 2009.

[171] Edward Geisinger, Tom W Muir, and Richard P Novick. Agr receptor mutants reveal distinct modes of inhibition by staphylococcal autoinducing peptides. *Proceedings of the National Academy of Sciences*, 106(4):1216–1221, 2009.

[172] David J Sidote, Christopher M Barbieri, Ti Wu, and Ann M Stock. Structure of the staphylococcus aureus agra lyttr domain bound to dna reveals a beta fold with an unusual mode of binding. *Structure*, 16(5):727–735, 2008.

[173] Anastasia N Nikolskaya and Michael Y Galperin. A novel type of conserved dna-binding domain in the transcriptional regulators of the algr/agra/lytr family. *Nucleic acids research*, 30(11):2453–2459, 2002.

[174] Kalagiri Rajasree, Aneesa Fasim, and Balasubramanian Gopal. Conformational features of the staphylococcus aureus agra-promoter interactions rationalize quorum-sensing triggered gene expression. *Biochemistry and Biophysics Reports*, 6:124–134, 2016.

[175] Richard P Novick, HF Ross, SJ Projan, J Kornblum, B Kreiswirth, and S Moghazeh. Synthesis of staphylococcal virulence factors is controlled by a regulatory rna molecule. *The EMBO journal*, 12(10):3967, 1993.

[176] E. Morfeldt, D. Taylor, A. von Gabain, and S. Arvidson. Activation of alpha-toxin translation in staphylococcus aureus by the trans-encoded antisense rna, rnaiii. *EMBO J*, 14(18):4569–77, 1995. Morfeldt, E Taylor, D von Gabain, A Arvidson, S eng ENGLAND EMBO J. 1995 Sep 15;14(18):4569-77.

[177] Ravi Kr Gupta, Thanh T Luong, and Chia Y Lee. Rnaiii of the staphylococcus aureus agr system activates global regulator mgra by stabilizing mrna. *Proceedings of the National Academy of Sciences*, 112(45):14036–14041, 2015.

[178] S. Y. Queck, M. Jameson-Lee, A. E. Villaruz, T. H. Bach, B. A. Khan, D. E. Sturdevant, S. M. Ricklefs, M. Li, and M. Otto. Rnaiii-independent target gene control by the agr quorum-sensing system: insight into the evolution of virulence regulation in staphylococcus aureus. *Mol Cell*, 32(1):150–8, 2008.

[179] Lindsey Shaw, Ewa Golonka, Jan Potempa, and Simon J Foster. The role and regulation of the extracellular proteases of staphylococcus aureus. *Microbiology*, 150(1):217–228, 2004.

[180] Clément Chevalier, Sandrine Boisset, Cédric Romilly, Benoit Masquida, Pierre Fechter, Thomas Geissmann, François Vandenesch, and Pascale Romby. Staphylococcus aureus rnaiii binds to two distant regions of coa mrna to arrest translation and promote mrna degradation. *PLoS Pathog*, 6(3):e1000809, 2010.

[181] Sandrine Boisset, Thomas Geissmann, Eric Huntzinger, Pierre Fechter, Nadia Bendridi, Maria Possedko, Clément Chevalier, Anne Catherine Helfer, Yvonne Benito, Alain Jacquier, et al. Staphylococcus aureus rnaiii coordinately represses the synthesis of virulence factors and the transcription regulator rot by an antisense mechanism. *Genes & development*, 21(11): 1353–1366, 2007.

[182] Svetlana Chabelskaya, Valérie Bordeau, and Brice Felden. Dual rna regulatory control of a staphylococcus aureus virulence factor. *Nucleic acids research*, 42(8):4847–4858, 2014.

[183] Karen E Beenken, Lara N Mrak, Linda M Griffin, Agnieszka K Zielinska, Lindsey N Shaw, Kelly C Rice, Alexander R Horswill, Kenneth W Bayles, and Mark S Smeltzer. Epistatic relationships between sara and agr in staphylococcus aureus biofilm formation. 2010.

[184] A. Abdelnour, S. Arvidson, T. Bremell, C. Ryden, and A. Tarkowski. The accessory gene regulator (agr) controls staphylococcus aureus virulence in a murine arthritis model. *Infect Immun*, 61(9):3879–85, 1993. Abdelnour, A Arvidson, S Bremell, T Ryden, C Tarkowski, A eng Infect Immun. 1993 Sep;61(9):3879-85.

[185] A. L. Cheung, K. J. Eberhardt, E. Chung, M. R. Yeaman, P. M. Sullam, M. Ramos, and A. S. Bayer. Diminished virulence of a sar-/agr- mutant of staphylococcus aureus in the rabbit model of endocarditis. *J Clin Invest*, 94(5):1815–22, 1994.

[186] A. F. Gillaspy, S. G. Hickmon, R. A. Skinner, J. R. Thomas, C. L. Nelson, and M. S. Smeltzer. Role of the accessory gene regulator (agr) in pathogenesis of staphylococcal osteomyelitis. *Infect Immun*, 63(9):3373–80, 1995. Gillaspy, A F Hickmon, S G Skinner, R A Thomas, J R Nelson, C L Smeltzer, M S eng Infect Immun. 1995 Sep;63(9):3373-80.

[187] Ana T Giraudo, Aldo Calzolari, Angel A Cataldi, Cristina Bogni, and Rosa Nagel. The sae locus of staphylococcus aureus encodes a two-component regulatory system. *FEMS microbiology letters*, 177(1):15–22, 1999.

[188] Andrea Steinhuber, Christiane Goerke, Manfred G Bayer, Gerd Döring, and Christiane Wolz. Molecular architecture of the regulatory locus sae of staphylococcus aureus and its impact on expression of virulence factors. *Journal of bacteriology*, 185 (21):6278–6286, 2003.

[189] T. Geiger, C. Goerke, M. Mainiero, D. Kraus, and C. Wolz. The virulence regulator sae of staphylococcus aureus: promoter activities and response to phagocytosis-related signals. *J Bacteriol*, 190(10):3419–28, 2008.

[190] Fei Sun, Chunling Li, Dowon Jeong, Changmo Sohn, Chuan He, and Taeok Bae. In the staphylococcus aureus two-component system sae, the response regulator saer binds to a direct repeat sequence and dna binding requires phosphorylation by the sensor kinase saes. *Journal of bacteriology*, 192(8):2111–2127, 2010.

[191] Do-Won Jeong, Hoonsik Cho, Marcus B Jones, Kenneth Shatzkes, Fei Sun, Quanjiang Ji, Qian Liu, Scott N Peterson, Chuan He, and Taeok Bae. The auxiliary protein complex saepq activates the phosphatase activity of sensor kinase saes in the saers two-component system of staphylococcus aureus. *Molecular microbiology*, 86(2):331–348, 2012.

[192] Caralyn E Flack, Oliwia W Zurek, Delisha D Meishery, Kyler B Pallister, Cheryl L Malone, Alexander R Horswill, and Jovanka M Voyich. Differential regulation of staphylococcal virulence by the sensor kinase saes in response to neutrophil-derived stimuli. *Proceedings of the National Academy of Sciences*, 111(19):E2037–E2045, 2014.

[193] Lara N Mrak, Agnieszka K Zielinska, Karen E Beenken, Ian N Mrak, Danielle N Atwood, Linda M Griffin, Chia Y Lee, and Mark S Smeltzer. saers and sara act synergistically to repress protease production and promote biofilm formation in staphylococcus aureus. *PloS one*, 7(6):e38453, 2012.

[194] Yingfang Liu, Adhar C Manna, Cheol-Ho Pan, Irina A Kriksunov, Daniel J Thiel, Ambrose L Cheung, and Gongyi Zhang. Structural and function analyses of the global regulatory protein sara from staphylococcusaureus. *Proceedings of the National Academy of Sciences of the United States of America*, 103(7):2392–2397, 2006.

[195] M. G. Bayer, J. H. Heinrichs, and A. L. Cheung. The molecular architecture of the sar locus in staphylococcus aureus. *J Bacteriol*, 178(15):4563–70, 1996.

[196] A. C. Manna, M. G. Bayer, and A. L. Cheung. Transcriptional analysis of different promoters in the sar locus in staphylococcus aureus. *J Bacteriol*, 180(15):3828–36, 1998.

[197] P áM Dunman, E Murphy, S Haney, D Palacios, G Tucker-Kellogg, S Wu, EL Brown, RJ Zagursky, D Shlaes, and SJ Projan. Transcription profiling-based identification ofstaphylococcus aureus genes regulated by the agrand/or sara loci. *Journal of bacteriology*, 183(24):7341–7353, 2001.

[198] Karen E Beenken, Jon S Blevins, and Mark S Smeltzer. Mutation of sara in staphylococcus aureus limits biofilm formation. *Infection and Immunity*, 71(7):4206–4211, 2003.

[199] Y. Liu, A. Manna, R. Li, W. E. Martin, R. C. Murphy, A. L. Cheung, and G. Zhang. Crystal structure of the sarr protein from staphylococcus aureus. *Proc Natl Acad Sci U S A*, 98(12):6877–82, 2001.

[200] A. Manna and A. L. Cheung. Characterization of sarr, a modulator of sar expression in staphylococcus aureus. *Infect Immun*, 69(2):885–96, 2001.

[201] Adhar C. Manna and Ambrose L. Cheung. Transcriptional regulation of the agr locus and the identification of dna binding residues of the global regulatory protein sarr in staphylococcus aureus. *Molecular Microbiology*, 60(5):1289–1301, 2006.

[202] Dindo Reyes, Diego O Andrey, Antoinette Monod, William L Kelley, Gongyi Zhang, and Ambrose L Cheung. Coordinated regulation by agra, sara, and sarr to control agr expression in staphylococcus aureus. *Journal of bacteriology*, 193(21):6020–6031, 2011.

[203] A. C. Manna, S. S. Ingavale, M. Maloney, W. van Wamel, and A. L. Cheung. Identification of sarv (sa2062), a new transcriptional regulator, is repressed by sara and mgra (sa0641) and involved in the regulation of autolysis in staphylococcus aureus. *J Bacteriol*, 186(16):5267–80, 2004.

[204] Adhar C Manna and Ambrose L Cheung. Expression of sarx, a negative regulator of agr and exoprotein synthesis, is activated by mgra in staphylococcus aureus. *Journal of bacteriology*, 188(12):4288–4299, 2006.

[205] B Said-Salim, PM Dunman, FM McAleese, D Macapagal, E Murphy, PJ McNamara, S Arvidson, TJ Foster, SJ Projan, and BN Kreiswirth. Global regulation of staphylococcus aureus genes by rot. *Journal of bacteriology*, 185(2):610–619, 2003.

[206] Edward Geisinger, Rajan P Adhikari, Ruzhong Jin, Hope F Ross, and Richard P Novick. Inhibition of rot translation by rnaiii, a key feature of agr function. *Molecular microbiology*, 61(4):1038–1048, 2006.

[207] Susham Ingavale, Willem van Wamel, Thanh T Luong, Chia Y Lee, and Ambrose L Cheung. Rat/mgra, a regulator of autolysis, is a regulator of virulence genes in staphylococcus aureus. *Infection and immunity*, 73(3):1423–1431, 2005.

[208] Thanh T Luong, Paul M Dunman, Ellen Murphy, Steven J Projan, and Chia Y Lee. Transcription profiling of the mgra regulon in staphylococcus aureus. *Journal of bacteriology*, 188(5):1899–1910, 2006.

[209] Peng R Chen, Taeok Bae, Wade A Williams, Erica M Duguid, Phoebe A Rice, Olaf Schneewind, and Chuan He. An oxidation-sensing mechanism is used by the global regulator mgra in staphylococcus aureus. *Nature chemical biology*, 2(11):591–595, 2006.

[210] Chikara Kaito, Daisuke Morishita, Yasuhiko Matsumoto, Kenji Kurokawa, and Kazuhisa Sekimizu. Novel dna binding protein sarz contributes to virulence in staphylococcus aureus. *Molecular microbiology*, 62(6):1601–1617, 2006.

[211] B. Sinha, P. Francois, Y. A. Que, M. Hussain, C. Heilmann, P. Moreillon, D. Lew, K. H. Krause, G. Peters, and M. Herrmann. Heterologously expressed staphylococcus aureus fibronectin-binding proteins are sufficient for invasion of host cells. *Infect Immun*, 68(12):6871–6878, Dec 2000.

[212] F. Agerer, A. Michel, K. Ohlsen, and C. R. Hauck. Integrin-mediated invasion of staphylococcus aureus into human cells requires src family protein-tyrosine kinases. *J Biol Chem*, 278(43):42524–31, 2003. Agerer, Franziska Michel, Antje Ohlsen, Knut Hauck, Christof R eng J Biol Chem. 2003 Oct 24;278(43):42524-31. Epub 2003 Jul 31.

[213] B. Sinha and M. Fraunholz. Staphylococcus aureus host cell invasion and post-invasion events. *Int J Med Microbiol*, 300 (2-3):170–5, 2010.

[214] Marta Zapotoczna, Zala Jevnikar, Helen Miajlovic, Janko Kos, and Timothy J Foster. Iron-regulated surface determinant b (isdb) promotes staphylococcus aureus adherence to and internalization by non-phagocytic human cells. *Cellular microbiology*, 15(6):1026–1041, 2013.

[215] Stefanie Baur, Maren Rautenberg, Manuela Faulstich, Timo Grau, Yannik Severin, Clemens Unger, Wolfgang H Hoffmann, Thomas Rudel, Ingo B Autenrieth, and Christopher Weidenmaier. A nasal epithelial receptor for staphylococcus aureus wta governs adhesion to epithelial cells and modulates nasal colonization. *PLoS Pathog*, 10(5):e1004089, 2014.

[216] Hattie D Gresham, Jon H Lowrance, Tony E Caver, Bridget S Wilson, Ambrose L Cheung, and Frederik P Lindberg. Survival of staphylococcus aureus inside neutrophils contributes to infection. *The Journal of Immunology*, 164(7):3713–3722, 2000.

[217] Malgorzata Kubica, Krzysztof Guzik, Joanna Koziel, Miroslaw Zarebski, Walter Richter, Barbara Gajkowska, Anna Golda, Agnieszka Maciag-Gudowska, Klaudia Brix, Les Shaw, et al. A potential new pathway for staphylococcus aureus dissemination: the silent survival of s. aureus phagocytosed by human monocyte-derived macrophages. *PLoS One*, 3(1):e1409, 2008.

[218] DJ Hess, MJ Henry-Stanley, EA Erickson, and CL Wells. Intracellular survival of staphylococcus aureus within cultured enterocytes. *Journal of Surgical Research*, 114(1):42–49, 2003.

[219] Grace Soong, Franklin Paulino, Sarah Wachtel, Dane Parker, Matthew Wickersham, Dongni Zhang, Armand Brown, Christine Lauren, Margaret Dowd, Emily West, et al. Methicillin-resistant staphylococcus aureus adaptation to human keratinocytes. *mBio*, 6(2):e00289–15, 2015.

[220] Richard A Proctor, Christof Von Eiff, Barbara C Kahl, Karsten Becker, Peter McNamara, Mathias Herrmann, and Georg Peters. Small colony variants: a pathogenic form of bacteria that facilitates persistent and recurrent infections. *Nature Reviews Microbiology*, 4(4):295–305, 2006.

[221] Lorena Tuchscherr, Eva Medina, Muzaffar Hussain, Wolfgang Völker, Vanessa Heitmann, Silke Niemann, Dirk Holzinger, Johannes Roth, Richard A Proctor, Karsten Becker, et al. Staphylococcus aureus phenotype switching: an effective bacterial strategy to escape host immune response and establish a chronic infection. *EMBO molecular medicine*, 3(3):129–141, 2011.

[222] Richard A Proctor, André Kriegeskorte, Barbara C Kahl, Karsten Becker, Bettina Löffler, and Georg Peters. Staphylococcus aureus small colony variants (scvs): a road map for the metabolic pathways involved in persistent infections. *Host-adapted metabolism and its regulation in Bacterial Pathogens*, 2015.

[223] Ronald S Flannagan, Bryan Heit, and David E Heinrichs. Intracellular replication of staphylococcus aureus in mature phagolysosomes in macrophages precedes host cell death, and bacterial escape and dissemination. *Cellular Microbiology*, 2015.

[224] Lisa Münzenmayer, Tobias Geiger, Ellen Daiber, Berit Schulte, Stella E Autenrieth, Martin Fraunholz, and Christiane Wolz. Influence of sae-regulated and agr-regulated factors on the escape of staphylococcus aureus from human macrophages. *Cellular microbiology*, 2016.

[225] K. W. Bayles, C. A. Wesson, L. E. Liou, L. K. Fox, G. A. Bohach, and W. R. Trumble. Intracellular staphylococcus aureus escapes the endosome and induces apoptosis in epithelial cells. *Infect Immun*, 66(1):336–42, 1998. Bayles, K W Wesson, C A Liou, L E Fox, L K Bohach, G A Trumble, W R eng AI28401/AI/NIAID NIH HHS/ R29-AI38901/AI/NIAID NIH HHS/ Infect Immun. 1998 Jan;66(1):336-42.

[226] T. M. Jarry and A. L. Cheung. Staphylococcus aureus escapes more efficiently from the phagosome of a cystic fibrosis bronchial epithelial cell line than from its normal counterpart. *Infection and Immunity*, 74(5):2568–2577, 2006.

[227] B. Giese, S. Dittmann, K. Paprotka, K. Levin, A. Weltrowski, D. Biehler, T. T. Lam, B. Sinha, and M. J. Fraunholz. Staphylococcal alpha-toxin is not sufficient to mediate escape from phagolysosomes in upper-airway epithelial cells. *Infection and Immunity*, 77(9):3611–3625, 2009.

[228] Bernd Giese, Frithjof Glowinski, Kerstin Paprotka, Silvia Dittmann, Tobias Steiner, Bhanu Sinha, and Martin J. Fraunholz. Expression of Œ¥-toxin by staphylococcus aureus mediates escape from phago-endosomes of human epithelial and endothelial cells in the presence of Œ-toxin. *Cellular Microbiology*, 13(2):316–329, 2011.

[229] S. N. A. Qazi, E. Counil, J. Morrissey, C. E. D. Rees, A. Cockayne, K. Winzer, W. C. Chan, P. Williams, and P. J. Hill. agr expression precedes escape of internalized staphylococcus aureus from the host endosome. *Infection and Immunity*, 69 (11):7074–7082, 2001.

[230] Martin Fraunholz and Bhanu Sinha. Intracellular staphylococcus aureus: live-in and let die. *The Staphylococci and staphylococcal pathogenesis*, page 116, 2012.

[231] S. N. A. Qazi, S. E. Harrison, T. Self, P. Williams, and P. J. Hill. Real-time monitoring of intracellular staphylococcus aureus replication. *Journal of Bacteriology*, 186(4):1065–1077, 2004.

[232] Christian Garzoni, Patrice Francois, Antoine Huyghe, Sabine Couzinet, Caroline Tapparel, Yvan Charbonnier, Adriana Renzoni, Sacha Lucchini, Daniel P Lew, Pierre Vaudaux, et al. A global view of staphylococcus aureus whole genome expression upon internalization in human epithelial cells. *BMC genomics*, 8(1):1, 2007.

[233] Dorte Frees, Arnaud Chastanet, Saara Qazi, Karen Sørensen, Philip Hill, Tarek Msadek, and Hanne Ingmer. Clp atpases are required for stress tolerance, intracellular replication and biofilm formation in staphylococcus aureus. *Molecular microbiology*, 54(5):1445–1462, 2004.

[234] Raul A Almeida, Karl R Matthews, Eduardo Cifrian, Albert J Guidry, and Stephen P Oliver. Staphylococcus aureus invasion of bovine mammary epithelial cells. *Journal of Dairy Science*, 79(6):1021–1026, 1996.

[235] Y. Y. Pang, J. Schwartz, M. Thoendel, L. W. Ackermann, A. R. Horswill, and W. M. Nauseef. agr-dependent interactions of staphylococcus aureus usa300 with human polymorphonuclear neutrophils. *J Innate Immun*, 2(6):546–59, 2010. Pang, Yun Yun Schwartz, Jamie Thoendel, Matthew Ackermann, Laynez W Horswill, Alexander R Nauseef, William M eng R01 AI078921/AI/NIAID NIH HHS/ R01 AI07958/AI/NIAID NIH HHS/ T32 AI 7511/AI/NIAID NIH HHS/ Research Support, N.I.H., Extramural Research Support, U.S. Gov't, Non-P.H.S. Switzerland 2010/09/11 06:00 J Innate Immun. 2010;2(6):546-59. doi: 10.1159/000319855. Epub 2010 Sep 10.

[236] H. Bantel. alpha-toxin is a mediator of staphylococcus aureus-induced cell death and activates caspases via the intrinsic death pathway independently of death receptor signaling. *The Journal of Cell Biology*, 155(4):637–648, 2001.

[237] B. Haslinger, K. Strangfeld, G. Peters, K. Schulze-Osthoff, and B. Sinha. Staphylococcus aureus alpha-toxin induces apoptosis in peripheral blood mononuclear cells: role of endogenous tumour necrosis factor-alpha and the mitochondrial death pathway. *Cell Microbiol*, 5(10):729–41, 2003.

[238] F. Essmann, H. Bantel, G. Totzke, I. H. Engels, B. Sinha, K. Schulze-Osthoff, and R. U. Janicke. Staphylococcus aureus alpha-toxin-induced cell death: predominant necrosis despite apoptotic caspase activation. *Cell Death Differ*, 10(11):1260–72, 2003. Essmann, F Bantel, H Totzke, G Engels, I H Sinha, B Schulze-Osthoff, K Janicke, R U eng England Cell Death Differ. 2003 Nov;10(11):1260-72.

[239] A. Denes, G. Lopez-Castejon, and D. Brough. Caspase-1: is il-1 just the tip of the iceberg? *Cell Death Dis*, 3:e338, 2012. Denes, A Lopez-Castejon, G Brough, D eng England Cell Death Dis. 2012 Jul 5;3:e338. doi: 10.1038/cddis.2012.86.

[240] Tamara Reyes-Robles, Francis Alonzo, Lina Kozhaya, D Borden Lacy, Derya Unutmaz, and Victor J Torres. Staphylococcus aureus leukotoxin ed targets the chemokine receptors cxcr1 and cxcr2 to kill leukocytes and promote infection. *Cell host & microbe*, 14(4):453–459, 2013.

[241] A. N. Spaan, B. G. Surewaard, R. Nijland, and J. A. van Strijp. Neutrophils versus staphylococcus aureus: a biological tug of war. *Annu Rev Microbiol*, 67:629–50, 2013.

[242] Anne-Laure Genestier, Marie-Cécile Michallet, Gilles Prévost, Gregory Bellot, Lara Chalabreysse, Simone Peyrol, Françoise Thivolet, Jerome Etienne, Gérard Lina, François M. Vallette, François Vandenesch, and Laurent Genestier. Staphylococcus aureus panton-valentine leukocidin directly targets mitochondria and induces bax-independent apoptosis of human neutrophils. *Journal of Clinical Investigation*, 115(11):3117–3127, 2005.

[243] Michael S. Gilmore, Bas G. J. Surewaard, Reindert Nijland, András N. Spaan, John A. W. Kruijtzer, Carla J. C. de Haas, and Jos A. G. van Strijp. Inactivation of staphylococcal phenol soluble modulins by serum lipoprotein particles. *PLoS Pathogens*, 8 (3):e1002606, 2012.

[244] T. Geiger, P. Francois, M. Liebeke, M. Fraunholz, C. Goerke, B. Krismer, J. Schrenzel, M. Lalk, and C. Wolz. The stringent response of staphylococcus aureus and its impact on survival after phagocytosis through the induction of intracellular psms expression. *PLoS Pathog*, 8(11):e1003016, 2012.

[245] M. Fraunholz, J. Bernhardt, J. Schuldes, R. Daniel, M. Hecker, and B. Sinha. Complete genome sequence of staphylococcus aureus 6850, a highly cytotoxic and clinically virulent methicillin-sensitive strain with distant relatedness to prototype strains. *Genome Announc*, 1(5), 2013. Fraunholz, Martin Bernhardt, Jorg Schuldes, Jorg Daniel, Rolf Hecker, Michael Sinha, Bhanu eng 2013/09/28 06:00 Genome Announc. 2013 Sep 26;1(5). pii: e00775-13. doi: 10.1128/genomeA.00775-13.

[246] M. Li, K. Rigby, Y. Lai, V. Nair, A. Peschel, B. Schittek, and M. Otto. Staphylococcus aureus mutant screen reveals interaction of the human antimicrobial peptide dermcidin with membrane phospholipids. *Antimicrob Agents Chemother*, 53(10):4200–10, 2009. Li, Min Rigby, Kevin Lai, Yuping Nair, Vinod Peschel, Andreas Schittek, Birgit Otto, Michael Antimicrob Agents Chemother. 2009 Oct;53(10):4200-10. Epub 2009 Jul 13.

[247] Sébastien Rodrigue, Arne C Materna, Sonia C Timberlake, Matthew C Blackburn, Rex R Malmstrom, Eric J Alm, and Sallie W Chisholm. Unlocking short read sequencing for metagenomics. *PLoS One*, 5(7):e11840, 2010.

[248] Sue C Geller, Jeff P Gregg, Paul Hagerman, and David M Rocke. Transformation and normalization of oligonucleotide microarray data. *Bioinformatics*, 19(14):1817–1823, 2003.

[249] Christiane Wolz, Tobias Geiger, and Christiane Goerke. The synthesis and function of the alarmone (p) ppgpp in firmicutes. *International Journal of Medical Microbiology*, 300(2):142–147, 2010.

[250] C Ster, M Allard, S Boulanger, M Lamontagne Boulet, J Mulhbacher, DA Lafontaine, E Marsault, P Lacasse, and F Malouin. Experimental treatment of staphylococcus aureus bovine intramammary infection using a guanine riboswitch ligand analog. *Journal of dairy science*, 96(2):1000–1008, 2013.

[251] Eric M Kofoed, Donghong Yan, Anand K Katakam, Mike Reichelt, Baiwei Lin, Janice Kim, Summer Park, Shailesh Date, Min Xu, Cary Austin, et al. De novo guanine biosynthesis, but not the riboswitch-regulated purine salvage pathway, is required for staphylococcus aureus infection in vivo. *Journal of bacteriology*, pages JB–00051, 2016.

[252] Martin Gering and R Brückner. Transcriptional regulation of the sucrase gene of staphylococcus xylosus by the repressor scrr. *Journal of bacteriology*, 178(2):462–469, 1996.

[253] Chunyan Hu, Ning Xiong, Yong Zhang, Simon Rayner, and Shiyun Chen. Functional characterization of lipase in the pathogenesis of staphylococcus aureus. *Biochemical and biophysical research communications*, 419(4):617–620, 2012.

[254] Stuart M Ingleston, Gary J Sharples, and Robert G Lloyd. The acidic pin of ruva modulates holliday junction binding and processing by the ruvabc resolvasome. *The EMBO journal*, 19(22):6266–6274, 2000.

[255] J. M. Morrison, E. W. Miller, M. A. Benson, 3rd Alonzo, F., P. Yoong, V. J. Torres, S. H. Hinrichs, and P. M. Dunman. Characterization of ssr42, a novel virulence factor regulatory rna that contributes to the pathogenesis of a staphylococcus aureus usa300 representative. *J Bacteriol*, 194(11):2924–38, 2012.

[256] M. G. Lei, D. Cue, C. M. Roux, P. M. Dunman, and C. Y. Lee. Rsp inhibits attachment and biofilm formation by repressing fnba in staphylococcus aureus mw2. *J Bacteriol*, 193(19):5231–41, 2011.

[257] Silvija N Coulter, William R Schwan, Eva YW Ng, Michael H Langhorne, Heather D Ritchie, Shannon Westbrock-Wadman, Wendy O Hufnagle, Kim R Folger, Arnold S Bayer, and C Kendall Stover. Staphylococcus aureus genetic loci impacting growth and survival in multiple infection environments. *Molecular microbiology*, 30(2):393–404, 1998.

[258] Vilasack Thammavongsa, Dominique M Missiakas, and Olaf Schneewind. Staphylococcus aureus degrades neutrophil extracellular traps to promote immune cell death. *Science*, 342(6160):863–866, 2013.

[259] K. Paprotka, B. Giese, and M. J. Fraunholz. Codon-improved fluorescent proteins in investigation of staphylococcus aureus host pathogen interactions. *J Microbiol Methods*, 83(1):82–6, 2010.

[260] Zhong Wang, Mark Gerstein, and Michael Snyder. Rna-seq: a revolutionary tool for transcriptomics. *Nature reviews genetics*, 10(1):57–63, 2009.

[261] M. I. Love, W. Huber, and S. Anders. Moderated estimation of fold change and dispersion for rna-seq data with deseq2. *Genome Biol*, 15(12):550, 2014. Love, Michael I Huber, Wolfgang Anders, Simon eng 5T32CA009337-33/CA/NCI NIH HHS/ Research Support, N.I.H., Extramural Research Support, Non-U.S. Gov't England 2014/12/18 06:00 Genome Biol. 2014;15(12):550.

[262] Sudip Das, Claudia Lindemann, Bernadette C Young, Julius Muller, Babett Österreich, Nicola Ternette, Ann-Cathrin Winkler, Kerstin Paprotka, Richard Reinhardt, Konrad U Förstner, et al. Natural mutations in a staphylococcus aureus virulence regulator attenuate cytotoxicity but permit bacteremia and abscess formation. *Proceedings of the National Academy of Sciences*, 113(22):E3101–E3110, 2016.

[263] V. Nagarajan and M. O. Elasri. Sammd: Staphylococcus aureus microarray meta-database. *BMC Genomics*, 8:351, 2007.

[264] Wook Chang, David A Small, Freshteh Toghrol, and William E Bentley. Global transcriptome analysis of staphylococcus aureus response to hydrogen peroxide. *Journal of bacteriology*, 188(4):1648–1659, 2006.

[265] Kazuya Morikawa, Ryosuke L Ohniwa, Joongbaek Kim, Atsushi Maruyama, Toshiko Ohta, and Kunio Takeyasu. Bacterial nucleoid dynamics: oxidative stress response in staphylococcus aureus. *Genes to cells*, 11(4):409–423, 2006.

[266] Oscar Aparicio, Joseph V Geisberg, Edward Sekinger, Annie Yang, Zarmik Moqtaderi, and Kevin Struhl. Chromatin immunoprecipitation for determining the association of proteins with specific genomic sequences in vivo. *Current protocols in molecular biology*, pages 21–3, 2005.

[267] C. J. Kristich, V. T. Nguyen, T. Le, A. M. T. Barnes, S. Grindle, and G. M. Dunny. Development and use of an efficient system for random mariner transposon mutagenesis to identify novel genetic determinants of biofilm formation in the core enterococcus faecalis genome. *Applied and Environmental Microbiology*, 74(11):3377–3386, 2008.

[268] Yuhua Chang, Weimin Gu, Nils Fischer, and Lynne McLandsborough. Identification of genes involved in listeria monocytogenes biofilm formation by mariner-based transposon mutagenesis. *Applied Microbiology and Biotechnology*, 93(5): 2051–2062, 2011.

[269] J. Ashour and M. K. Hondalus. Phenotypic mutants of the intracellular actinomycete rhodococcusequi created by in vivo himar1 transposon mutagenesis. *Journal of Bacteriology*, 185(8):2644–2652, 2003.

[270] T. M. Maier, R. Pechous, M. Casey, T. C. Zahrt, and D. W. Frank. In vivo himar1-based transposon mutagenesis of francisella tularensis. *Applied and Environmental Microbiology*, 72(3):1878–1885, 2006.

[271] Michael Hensel, Jacqueline E Shea, Colin Gleeson, Michael D Jones, et al. Simultaneous identification of bacterial virulence genes by negative selection. *Science*, 269(5222):400, 1995.

[272] Tim van Opijnen and Andrew Camilli. Transposon insertion sequencing: a new tool for systems-level analysis of microorganisms. *Nature Reviews Microbiology*, 11(7):435–442, 2013.

[273] J. D. Gawronski, S. M. Wong, G. Giannoukos, D. V. Ward, and B. J. Akerley. Tracking insertion mutants within libraries by deep sequencing and a genome-wide screen for haemophilus genes required in the lung. *Proc Natl Acad Sci U S A*, 106(38): 16422–7, 2009.

[274] Gemma C Langridge, Minh-Duy Phan, Daniel J Turner, Timothy T Perkins, Leopold Parts, Jana Haase, Ian Charles, Duncan J Maskell, Sarah E Peters, Gordon Dougan, et al. Simultaneous assay of every salmonella typhi gene using one million transposon mutants. *Genome research*, 19(12):2308–2316, 2009.

[275] Andrew L Goodman, Nathan P McNulty, Yue Zhao, Douglas Leip, Robi D Mitra, Catherine A Lozupone, Rob Knight, and Jeffrey I Gordon. Identifying genetic determinants needed to establish a human gut symbiont in its habitat. *Cell host & microbe*, 6(3):279–289, 2009.

[276] Tim van Opijnen, Kip L. Bodi, and Andrew Camilli. Tn-seq: high-throughput parallel sequencing for fitness and genetic interaction studies in microorganisms. *Nature Methods*, 6(10):767–772, 2009.

[277] D. J. Lampe, B. J. Akerley, E. J. Rubin, J. J. Mekalanos, and H. M. Robertson. Hyperactive transposase mutants of the himar1 mariner transposon. *Proc Natl Acad Sci U S A*, 96(20):11428–33, 1999.

[278] David J Lampe, Theresa E Grant, and Hugh M Robertson. Factors affecting transposition of the himar1 mariner transposon in vitro. *Genetics*, 149(1):179–187, 1998.

[279] Martín Muñoz-López and José L García-Pérez. Dna transposons: nature and applications in genomics. *Current genomics*, 11(2):115–128, 2010.

[280] T. Bae, A. K. Banger, A. Wallace, E. M. Glass, F. Aslund, O. Schneewind, and D. M. Missiakas. Staphylococcus aureus virulence genes identified by bursa aurealis mutagenesis and nematode killing. *Proceedings of the National Academy of Sciences*, 101 (33):12312–12317, 2004.

[281] Jérôme Mulhbacher, Eric Brouillette, Marianne Allard, Louis-Charles Fortier, François Malouin, and Daniel A Lafontaine. Novel riboswitch ligand analogs as selective inhibitors of guanine-related metabolic pathways. *PLoS Pathog*, 6(4):e1000865, 2010.

[282] Yang Zhang, Mariya Morar, and Steven E Ealick. Structural biology of the purine biosynthetic pathway. *Cellular and molecular life sciences*, 65(23):3699–3724, 2008.

[283] Roy R. Chaudhuri, Andrew G. Allen, Paul J. Owen, Gil Shalom, Karl Stone, Marcus Harrison, Timothy A. Burgis, Michael Lockyer, Jorge Garcia-Lara, Simon J. Foster, Stephen J. Pleasance, Sarah E. Peters, Duncan J. Maskell, and Ian G. Charles. Comprehensive identification of essential staphylococcus aureus genes using transposon-mediated differential hybridisation (tmdh). *BMC Genomics*, 10(1):291, 2009.

[284] P. D. Fey, J. L. Endres, V. K. Yajjala, T. J. Widhelm, R. J. Boissy, J. L. Bose, and K. W. Bayles. A genetic resource for rapid and comprehensive phenotype screening of nonessential staphylococcus aureus genes. *mBio*, 4(1):e00537–12–e00537–12, 2013.

[285] John A McDonald and William N Kelley. Lesch-nyhan syndrome: altered kinetic properties of mutant enzyme. *Science*, 171 (3972):689–691, 1971.

[286] Michael D Valentino, Lucy Foulston, Ama Sadaka, Veronica N Kos, Regis A Villet, John Santa Maria, David W Lazinski, Andrew Camilli, Suzanne Walker, David C Hooper, et al. Genes contributing to staphylococcus aureus fitness in abscess- and infection-related ecologies. *MBio*, 5(5):e01729–14, 2014.

[287] Rebecca Yee, Peng Cui, Wanliang Shi, Jie Feng, and Ying Zhang. Genetic screen reveals the role of purine metabolism in staphylococcus aureus persistence to rifampicin. *Antibiotics*, 4(4):627–642, 2015.

[288] Patrick Ebner, Janina Rinker, Minh Thu Nguyen, Peter Popella, Mulugeta Nega, Arif Luqman, Birgit Schittek, Moreno Di Marco, Stefan Stevanovic, and Friedrich Götz. Excreted cytoplasmic proteins contribute to pathogenicity in staphylococcus aureus. *Infection and immunity*, 84(6):1672–1681, 2016.

[289] Junko K Akada, Mutsunori Shirai, Hiroaki Takeuchi, Masataka Tsuda, and Teruko Nakazawa. Identification of the urease operon in helicobacter pylori and its control by mrna decay in response to ph. *Molecular microbiology*, 36(5):1071–1084, 2000.

[290] Wenwei Lin, Vanessa Mathys, Emily Lei Yin Ang, Vanessa Hui Qi Koh, Julia María Martínez Gómez, Michelle Lay Teng Ang, Siti Zarina Zainul Rahim, Mai Ping Tan, Kevin Pethe, and Sylvie Alonso. Urease activity represents an alternative pathway for mycobacterium tuberculosis nitrogen metabolism. *Infection and immunity*, 80(8):2771–2779, 2012.

[291] Mike Hasenberg, Sabine Stegemann-Koniszewski, and Matthias Gunzer. Cellular immune reactions in the lung. *Immunological reviews*, 251(1):189–214, 2013.

[292] Yukihiro Kabeya, Hiromitsu Nakanishi, Kenji Suzuki, Takanari Ichikawa, Youichi Kondou, Minami Matsui, and Shin-ya Miyagishima. The ylmg protein has a conserved function related to the distribution of nucleoids in chloroplasts and cyanobacteria. *BMC plant biology*, 10(1):1, 2010.

[293] Morgan A Wyatt, Wenliang Wang, Christelle M Roux, Federico C Beasley, David E Heinrichs, Paul M Dunman, and Nathan A Magarvey. Staphylococcus aureus nonribosomal peptide secondary metabolites regulate virulence. *Science*, 329(5989): 294–296, 2010.

[294] Fei Sun, Hoonsik Cho, Do-Won Jeong, Chunling Li, Chuan He, and Taeok Bae. Aureusimines in staphylococcus aureus are not involved in virulence. *PloS one*, 5(12):e15703, 2010.

[295] Sebastian Blaettner, Sudip Das, Thomas Rudel, and Martin J. Fraunholz. A non-ribosomally synthesized dipeptide is required for efficient phagosomal escape, intracellular survival and virulence of staphylococcus aureus. 3001Forthcoming.

[296] Maria-Trinidad Gallegos, Robert Schleif, Amos Bairoch, Kay Hofmann, and Juan L Ramos. Arac/xyls family of transcriptional regulators. *Microbiology and Molecular Biology Reviews*, 61(4):393–410, 1997.

[297] Jose Antonio Ibarra, Ernesto Pérez-Rueda, Ronan K. Carroll, and Lindsey N. Shaw. Global analysis of transcriptional regulators in staphylococcus aureus. *BMC Genomics*, 14(1):126, 2013.

[298] D. Cue, M. G. Lei, T. T. Luong, L. Kuechenmeister, P. M. Dunman, S. O'Donnell, S. Rowe, J. P. O'Gara, and C. Y. Lee. Rbf promotes biofilm formation by staphylococcus aureus via repression of icar, a negative regulator of icaadbc. *J Bacteriol*, 191 (20):6363–73, 2009.

[299] Sebastian Blaettner, Sudip Das, Thomas Rudel, and Martin J. Fraunholz. A non-ribosomally synthesized dipeptide is required for efficient phagosomal escape, intracellular survival and virulence of staphylococcus aureus. 3001Forthcoming.

[300] Tianming Li, Lei He, Yan Song, Amer E Villaruz, Hwang-Soo Joo, Qian Liu, Yuanjun Zhu, Yanan Wang, Juanxiu Qin, Michael Otto, et al. Arac-type regulator rsp adapts staphylococcus aureus gene expression to acute infection. *Infection and immunity*, 84(3):723–734, 2016.

[301] Sudip Das, Claudia Lindemann, Bernadette C. Young, Julius Muller, Babett Österreich, Nicola Ternette, Ann-Cathrin Winkler, Kerstin Paprotka, Richard Reinhardt, Konrad U. Förstner, Elizabeth Allen, Amy Flaxman, Yuko Yamaguchi, Christine S. Rollier, Pauline van Diemen, Sebastian Blättner, Christian W. Remmele, Martina Selle, Marcus Dittrich, Tobias Müller, Jörg Vogel, Knut Ohlsen, Derrick W. Crook, Ruth Massey, Daniel J. Wilson, Thomas Rudel, David H. Wyllie, and Martin J. Fraunholz. Natural mutations in a staphylococcus aureus virulence regulator attenuate cytotoxicity but permit bacteremia and abscess formation. *Proceedings of the National Academy of Sciences*, 2016.

[302] Corbette Roberts, Kelsi L Anderson, Ellen Murphy, Steven J Projan, William Mounts, Barry Hurlburt, Mark Smeltzer, Ross Overbeek, Terrence Disz, and Paul M Dunman. Characterizing the effect of the staphylococcus aureus virulence factor regulator, sara, on log-phase mrna half-lives. *Journal of bacteriology*, 188(7):2593–2603, 2006.

[303] B. Haslinger-Loffler, B. C. Kahl, M. Grundmeier, K. Strangfeld, B. Wagner, U. Fischer, A. L. Cheung, G. Peters, K. Schulze-Osthoff, and B. Sinha. Multiple virulence factors are required for staphylococcus aureus-induced apoptosis in endothelial cells. *Cell Microbiol*, 7(8):1087–97, 2005.

[304] Iwona Konieczna, Paulina Zarnowiec, Marek Kwinkowski, Beata Kolesinska, Justyna Fraczyk, Zbigniew Kaminski, and Wieslaw Kaca. Bacterial urease and its role in long-lasting human diseases. *Current Protein and Peptide Science*, 13(8): 789–806, 2012.

[305] Erlend Bore, Solveig Langsrud, Øyvind Langsrud, Tone Mari Rode, and Askild Holck. Acid-shock responses in staphylococcus aureus investigated by global gene expression analysis. *Microbiology*, 153(7):2289–2303, 2007.

[306] Camiel Lambert Christiaan Wielders. The dissemination among staphylococcus aureus of the staphylococcal chromosome cassette mec (sccmec) which confers multiresistance. *Utrecht University Repository*, 2002.

[307] Cosimo Fuda, Dusan Hesek, Mijoon Lee, Werner Heilmayer, Rodger Novak, Sergei B Vakulenko, and Shahriar Mobashery. Mechanistic basis for the action of new cephalosporin antibiotics effective against methicillin-and vancomycin-resistant staphylococcus aureus. *Journal of Biological Chemistry*, 281(15):10035–10041, 2006.

[308] Longzhu Cui, Jian-Qi Lian, Hui-min Neoh, Ethel Reyes, and Keiichi Hiramatsu. Dna microarray-based identification of genes associated with glycopeptide resistance in staphylococcus aureus. *Antimicrobial agents and chemotherapy*, 49(8): 3404–3413, 2005.

[309] Cheryl YM Okumura and Victor Nizet. Subterfuge and sabotage: evasion of host innate defenses by invasive gram-positive bacterial pathogens. *Annual review of microbiology*, 68:439, 2014.

[310] Nicole Lemmens, Willem van Wamel, Susan Snijders, Alan J Lesse, Howard Faden, and Alex van Belkum. Genomic comparisons of usa300 staphylococcus aureus colonizating the nose and rectum of children with skin abscesses. *Microbial pathogenesis*, 50(3):192–199, 2011.

[311] Ryan P Lamers, Jason W Stinnett, Gowrishankar Muthukrishnan, Christopher L Parkinson, and Alexander M Cole. Evolutionary analyses of staphylococcus aureus identify genetic relationships between nasal carriage and clinical isolates. *PLoS One*, 6(1):e16426, 2011.

[312] B. C. Young, T. Golubchik, E. M. Batty, R. Fung, H. Larner-Svensson, A. A. Votintseva, R. R. Miller, H. Godwin, K. Knox, R. G. Everitt, Z. Iqbal, A. J. Rimmer, M. Cule, C. L. Ip, X. Didelot, R. M. Harding, P. Donnelly, T. E. Peto, D. W. Crook, R. Bowden, and D. J. Wilson. Evolutionary dynamics of staphylococcus aureus during progression from carriage to disease. *Proc Natl Acad Sci U S A*, 109(12):4550–5, 2012.

[313] Maisem Laabei, Anne-Catrin Uhlemann, Franklin D Lowy, Eloise D Austin, Maho Yokoyama, Khadija Ouadi, Edward Feil, Harry A Thorpe, Barnabas Williams, Mark Perkins, et al. Evolutionary trade-offs underlie the multi-faceted virulence of staphylococcus aureus. *PLoS Biol*, 13(9):e1002229, 2015.

[314] Tanya Golubchik, Elizabeth M Batty, Ruth R Miller, Helen Farr, Bernadette C Young, Hanna Larner-Svensson, Rowena Fung, Heather Godwin, Kyle Knox, Antonina Votintseva, et al. Within-host evolution of staphylococcus aureus during asymptomatic carriage. *PLoS One*, 8(5):e61319, 2013.

[315] Joanna Koziel, Agnieszka Maciag-Gudowska, Tomasz Mikolajczyk, Malgorzata Bzowska, Daniel E Sturdevant, Adeline R Whitney, Lindsey N Shaw, Frank R DeLeo, and Jan Potempa. Phagocytosis of staphylococcus aureus by macrophages exerts cytoprotective effects manifested by the upregulation of antiapoptotic factors. *PLoS One*, 4(4):e5210, 2009.

[316] Douglas A Drevets. Dissemination of listeria monocytogenesby infected phagocytes. *Infection and immunity*, 67(7):3512–3517, 1999.

[317] J Muse Davis and Lalita Ramakrishnan. The role of the granuloma in expansion and dissemination of early tuberculous infection. *Cell*, 136(1):37–49, 2009.

[318] Guy E. Thwaites and Vanya Gant. Are bloodstream leukocytes trojan horses for the metastasis of staphylococcus aureus? *Nature Reviews Microbiology*, 9(3):215–222, 2011.

[319] E Velasco, R Byington, CAS Martins, M Schirmer, LM C Dias, and VMSC Gonçalves. Comparative study of clinical characteristics of neutropenic and non-neutropenic adult cancer patients with bloodstream infections. *European Journal of Clinical Microbiology and Infectious Diseases*, 25(1):1–7, 2006.

[320] Kenneth L Bost, Warren K Ramp, Natalie C Nicholson, Jennifer L Bento, Ian Marriott, and Michael C Hudson. Staphylococcus aureus infection of mouse or human osteoblasts induces high levels of interleukin-6 and interleukin-12 production. *Journal of Infectious Diseases*, 180(6):1912–1920, 1999.

[321] Annalisa D'Andrea, Manthrasalam Rengaraju, Nicholas M Valiante, J Chehimi, M Kubin, M Aste, SH Chan, M Kobayashi, D Young, and E Nickbarg. Production of natural killer cell stimulatory factor (interleukin 12) by peripheral blood mononuclear cells. *The Journal of experimental medicine*, 176(5):1387–1398, 1992.

[322] Giorgio Trinchieri. Interleukin-12 and the regulation of innate resistance and adaptive immunity. *Nature Reviews Immunology*, 3(2):133–146, 2003.

[323] Jaklien C Leemans, Margriet JBM Vervoordeldonk, Sandrine Florquin, Kok P van Kessel, and Tom van der Poll. Differential role of interleukin-6 in lung inflammation induced by lipoteichoic acid and peptidoglycan from staphylococcus aureus. *American journal of respiratory and critical care medicine*, 165(10):1445–1450, 2002.

[324] Iñigo Lasa, Alejandro Toledo-Arana, Alexander Dobin, Maite Villanueva, Igor Ruiz de los Mozos, Marta Vergara-Irigaray, Víctor Segura, Delphine Fagegaltier, José R Penadés, Jaione Valle, et al. Genome-wide antisense transcription drives mrna processing in bacteria. *Proceedings of the National Academy of Sciences*, 108(50):20172–20177, 2011.

[325] T. Bae and O. Schneewind. Allelic replacement in staphylococcus aureus with inducible counter-selection. *Plasmid*, 55(1):58–63, 2006.

[326] Christian W Remmele, Yibo Xian, Marco Albrecht, Michaela Faulstich, Martin Fraunholz, Elisabeth Heinrichs, Marcus T Dittrich, Tobias Müller, Richard Reinhardt, and Thomas Rudel. Transcriptional landscape and essential genes of neisseria gonorrhoeae. *Nucleic acids research*, 42(16):10579–10595, 2014.

[327] Marcel Martin. Cutadapt removes adapter sequences from high-throughput sequencing reads. *EMBnet. journal*, 17(1): pp–10, 2011.

[328] Ben Langmead and Steven L Salzberg. Fast gapped-read alignment with bowtie 2. *Nature methods*, 9(4):357–359, 2012.

[329] George E Moore and Linda K Woods. Culture media for human cellsórpmi 1603, rpmi 1634, rpmi 1640 and gem 1717. *Methods in Cell Science*, 3(1):503–509, 1977.

[330] K. Hattar, U. Sibelius, A. Bickenbach, E. Csernok, W. Seeger, and F. Grimminger. Subthreshold concentrations of anti-proteinase 3 antibodies (c-anca) specifically prime human neutrophils for fmlp-induced leukotriene synthesis and chemotaxis. *J Leukoc Biol*, 69(1):89–97, 2001.

[331] Douglas Hanahan. Studies on transformation of escherichia coli with plasmids. *Journal of molecular biology*, 166(4):557–580, 1983.

[332] Monica Riley, Takashi Abe, Martha B Arnaud, Mary KB Berlyn, Frederick R Blattner, Roy R Chaudhuri, Jeremy D Glasner, Takashi Horiuchi, Ingrid M Keseler, Takehide Kosuge, et al. Escherichia coli k-12: a cooperatively developed annotation snapshot—2005. *Nucleic acids research*, 34(1):1–9, 2006.

[333] Seth G Grant, Joel Jessee, Fredric R Bloom, and Douglas Hanahan. Differential plasmid rescue from transgenic mouse dnas into escherichia coli methylation-restriction mutants. *Proceedings of the National Academy of Sciences*, 87(12):4645–4649, 1990.

[334] Tim Durfee, Richard Nelson, Schuyler Baldwin, Guy Plunkett, Valerie Burland, Bob Mau, Joseph F Petrosino, Xiang Qin, Donna M Muzny, Mulu Ayele, et al. The complete genome sequence of escherichia coli dh10b: insights into the biology of a laboratory workhorse. *Journal of bacteriology*, 190(7):2597–2606, 2008.

[335] B. N. Kreiswirth, S. Lofdahl, M. J. Betley, M. O'Reilly, P. M. Schlievert, M. S. Bergdoll, and R. P. Novick. The toxic shock syndrome exotoxin structural gene is not detectably transmitted by a prophage. *Nature*, 305(5936):709–12, 1983.

[336] B. A. Diep, S. R. Gill, R. F. Chang, T. H. Phan, J. H. Chen, M. G. Davidson, F. Lin, J. Lin, H. A. Carleton, E. F. Mongodin, G. F. Sensabaugh, and F. Perdreau-Remington. Complete genome sequence of usa300, an epidemic clone of community-acquired meticillin-resistant staphylococcus aureus. *Lancet*, 367(9512):731–9, 2006.

[337] B. R. Boles, M. Thoendel, A. J. Roth, and A. R. Horswill. Identification of genes involved in polysaccharide-independent staphylococcus aureus biofilm formation. *PLoS One*, 5(4):e10146, 2010.

[338] J. M. Vann and R. A. Proctor. Ingestion of staphylococcus aureus by bovine endothelial cells results in time- and inoculum-dependent damage to endothelial cell monolayers. *Infect Immun*, 55(9):2155–63, 1987.

[339] Markus Fischer, Ilka Haase, Evelyn Simmeth, Günther Gerisch, and Annette Müller-Taubenberger. A brilliant monomeric red fluorescent protein to visualize cytoskeleton dynamics in dictyostelium. *FEBS letters*, 577(1-2):227–232, 2004.

Abbreviations & Symbols

λ	Wavelength
a	Amplitude
a.a	**a**mino **a**cid/s
BSA	**B**ovine **S**erum **A**lbumin
CFUs	**C**olony-**f**orming **U**nits
DMEM	**D**ulbecco's **M**odified **E**agle's **M**edium
DPBS	**D**ulbecco's **P**hosphate **B**uffered **S**aline
GFP	**G**reen **F**luorescent **P**rotein
HBSS	**H**ank's **B**alanced **S**alt **S**olution
hMDMs	**h**uman **M**onocyte-**D**erived **M**acrophage**s**
hPMNs	**h**uman **P**oly**M**orphonuclear **N**eutrophil**s**
LB	**L**uria **B**ertani
MLST	**M**ulti-**L**ocus **S**equence **T**yping
mRFP	**m**onomeric **R**ed **F**luorescent **P**rotein
MRSA	**M**ethicillin-**r**esistant ***S**taphylococcus **a**ureus*
MSCRAMM	**M**icrobial **S**urface **C**omponent **R**ecognizing **A**dhesive **M**atrix **M**olecule
MSSA	**M**ethicillin-**s**ensitive ***S**taphylococcus **a**ureus*
NB	**N**utrient **B**roth
NIM	**N**eutrophil **I**nfection **M**edium
nt	**n**ucleo**t**ide/s
OD	**O**ptical **D**ensity
PBMCs	**P**eripheral **B**lood **M**ononuclear **C**ell**s**
PBS	**P**hosphate **B**uffered **S**aline
PCR	**P**olymerase **C**hain **R**eaction
PE	**P**hyco**e**rythrin
RBC	**R**ed **B**lood **C**ell
rpm	**r**evolutions **p**er **m**inute
RPMI	**R**oswell **P**ark **M**emorial **I**nstitute
RQ	**R**elative **Q**uantification
SEM	**S**tandard **E**rror of **M**ean
t	Time
TSA	**T**ryptic **S**oy **A**gar
TSB	**T**ryptic **S**oy **B**roth
VRSA	**V**ancomycin-**r**esistant ***S**taphylococcus **a**ureus*

Abbreviations and symbols are sorted in alphanumeric order

Affidavit

I hereby confirm that my thesis entitled 'Genome-wide identification of virulence-associated genes in *Staphylococcus aureus* using Transposon insertion-site deep sequencing' is the result of my own work. I did not receive any help or support from commercial consultants. All sources and / or materials applied are listed and specified in the thesis.

Furthermore, I also confirm that this thesis has not yet been submitted as part of another examination process neither in identical or similar form.

Würzburg, 2016 Signature

Eidesstattliche Erklärung

Hiermit erkläre ich an Eides statt, die Dissertation 'Genomweite Identifizierung Virulenz-assoziierter Gene in *Staphylococcus aureus* mittels Transposon-Sequenzierung' eigenständig, d.h. insbesondere selbstandig und ohne Hilfe eines kommerziellen Promotionsberaters, angefertigt und keine anderen als die von mir angegebenen Quellen und Hilfsmittel verwendet zu haben.

Ich erkläre außerdem, dass die Dissertation weder in gleicher noch in ähnlicher Form bereits in einem anderen Prüfungsverfahren vorgelegen hat.

Würzburg, 2016 Unterschrift

Acknowledgements

I would like to extend my sincere gratitude towards my primary supervisor Prof. Dr. Thomas Rudel, for providing me with this opportunity to successfully conduct my doctoral research at the Chair of Microbiology, University of Würzburg. His supervision and inputs at crucial instances helped me grow as a scientist.

I am much obliged to my co-supervisors, Prof. Dr. Bhanu Sinha and PD Dr. Knut Ohlsen, for their excellent guidance and being part of my doctoral thesis committee.

I would also like to thank Prof. Dr. Thomas Dandekar for chairing the doctoral thesis committee.

Special thanks to our very own leader of the *Staphylococcus* research group, Dr. Martin Fraunholz whose contribution, guidance and help is immeasurable.

I also want to extend my gratitude towards the Graduate School of Life Sciences, University of Würzburg for letting me be part of a vibrant and structured doctoral program. The funding body DFG SFB TRR34 for the exciting project possibility.

I would like to convey my sincere gratitude towards all present and former fellow members of the *Staphylococcus* research group. Mrs. Kerstin Paprotka, Dr. Ann-Cathrin Winkler, Dr. Magdalena Grosz, Mr. Sebastian Blättner, Ms. Jessica Horn, Ms. Kathrin Stelzner, Ms. Michaela Groma and Ms. Adriana Moldovan for an excellent working environment and all their support.

I am extremely thankful to all my collaborators in Würzburg or away, for making research possible and smooth. In Würzburg; Dr. Babett Österreich and Ms. Martina Selle from IMIB, Würzburg. Prof. Dr. Alma Zernecke and Mrs. Melanie Schott from Institute for Experimental Biomedicine, Würzburg. Natarajaswamy Kalleda and Dr. Andreas Beilhack from ZEMM, Würzburg. Prof. Dr. Jörg Vogel and Dr. Konrad Förstner from IMIB, Würzburg. Dr. Alexander Keller from DNA-ANALYTIK, Biocenter, Würzburg. Mrs. Rosemarie Bott from Chair of Human Genetics, Würzburg. Dr. Tobias Müller, Dr. Dr. Marcus Dittrich and Mr. Christian Remmele from Chair of Bioinformatics, Würzburg. Prof. Dr. Stefan Gaubatz from Biocenter, Würzburg.

Outside Würzburg; Prof. Dr. Richard Reinhardt and Dr. Bruno Huettel from Max Planck Genome Centre, Cologne. Prof. Dr. Eva Medina and Dr. Sarah Horst from HZI, Braunschweig. Prof. Dr. Daniel Wilson, Dr. David Wyllie and Claudia Lindemann from Nuffield Department of Medicine, University of Oxford, UK.

I am indebted to my family - my father, Late Dr. Debkrishna Das, who has been a beacon of light in my life's path and the continuous driving force behind every accomplishment. My mother, Mrs. Kusum Behera, whose nurture and support is unmatched. My elder sister, Ms. Sunanda Das, for all her love and support.

I shall be ever grateful to my best friends, Mr. Soumava Bera and Mr. Sounak Dutta and my girlfriend Ms. Linda Raupach for the immense support and joys through thick & thins of my personal and professional life.

I want to extend special thanks to my dearest friends Sheetal, Maria, Jo-Ana, Claudia, Oliver, Roy,

Sebastian, Arnab, Tanmay, Dennis for all their love and support, and for someway or the other inspiring me.

Lastly, a shout out goes to the former and present members of the entire Chair of Microbiology and those who in anyway have contributed to my knowledge, experiments and extended their help...